KINGSTON UNIVERSITY

Conducting Elastomer Blends

Kok Chong Yong

A thesis submitted in partial fulfilment of the requirements of Kingston University for the degree of Doctor of Philosophy

A PhD degree research project carried out in collaboration with the Tun Abdul Razak Research Centre, Brickendonbury, Hertford, Hertfordshire, U.K.

MATERIALS RESEARCH GROUP
SCHOOL OF PHARMACY AND CHEMISTRY
FACULTY OF SCIENCE
KINGSTON UNIVERSITY
PENRHYN ROAD
KINGSTON-UPON-THAMES
SURREY
KT1 2EE

July 2007

THE FOLLOWING HAVE NOT BEEN COPIED ON INSTRUCTION FROM THE UNIVERSITY

Figure 1.1	page 9
Figure 1.2	page 9
Figure 1.3	page 11
Figure 1.4	page 14
Figure 1.5	page 17
Figure 1.12	page 33
Figure 4.3	page 114

Abstract

There are many existing and developing commercial applications for electrically-conductive elastomeric blends. These have been based on carbon black or metal fillers, or more recently conducting polymer powders, incorporated into natural or synthetic rubbers. A number of polyaniline-rubber blends, often with poor electrical conductivities have been reported in the literature. Interest was found in this project to improve the compatibility, mechanical and electrical properties of this type of blend through different mixing methods (i.e. solution and thermo-mechanical) with more systematic mixing procedures and better optimised mixing conditions.

Poly(butadiene-*co*-acrylonitrile) rubber [NBR] and polyaniline dodecylbenzenesulfonate [PAni.DBSA] were chosen for study as blends in the present work, because their solubility parameters were calculated to be compatible (NBR with 48.2 wt% of acrylonitrile content had the best compatibility with PAni.DBSA) and also because the polymers were thermally stable and readily available. No literature work was found relating to the electrical properties of natural rubber-PAni.DBSA blend. Therefore, epoxidised natural rubber (with 50 mole% of epoxide level) was also selected in this work in order to investigate a novel usage of this natural resource.

Non-vulcanised NBR-PAni.DBSA and non-vulcanised ENR-PAni.DBSA blends with useful electrical conductivities (up to about 10^{-2} and 10^{-3}S.cm^{-1} respectively) were successfully prepared by solution mixing for the first time in this work. Peroxide-vulcanised NBR-PAni.DBSA blends with similar electrical conductivities (up to x 10^{-2}S.cm^{-1}) were also successfully prepared for the first time by thermo-mechanical mixing (with an internal mixer). The conductivities of all these blends were much higher than those of comparable materials reported in the literature due to the reasonably good compatibility between the two polymers and the high mixing efficiency of the two chosen mixing methods (i.e. solution and thermo-mechanical mixing). The electrical conductivities of the peroxide-

vulcanised blends were found to be unaffected by the presence of dicumyl peroxide vulcanising agent.

The FT-IR spectra of both non-vulcanised and peroxide-vulcanised NBR-PAni.DBSA blends (either prepared by solution or thermo-mechanical mixing) resembled a superposition of the spectra of the constituent materials. However, some notable peak shifts were observed, providing evidence of the bonding interaction between the two polymers. For ENR-PAni.DBSA blends, the ring opening of ENR with increasing PAni.DBSA content was successfully quantified by NMR and FT-IR spectroscopic (based on the intensities of all spectroscopy bands assigned to the functional groups relating to ENR ring opening).

The non-vulcanised and peroxide-vulcanised NBR-PAni.DBSA blends with up to 30 wt% of PAni.DBSA, (produced either by solution or thermo-mechanical mixing) showed the largest temperature shifts for their thermal events in both the sub- and above-ambient temperature DSC thermograms, strengthening the evidence of interaction between the two polymers. Progressive glass transition temperature (Tg) shifts with increasing PAni.DBSA content were observed for the ENR-PAni.DBSA blends from both the sub- and the above-ambient temperature DSC thermograms, supporting the proposition that there was further ring opening of the ENR.

Optical and electron micrographs of all NBR- and ENR-PAni.DBSA blends showed that the higher the content of PAni.DBSA, the greater the phase separation (dark-green regions with larger proportion of PAni.DBSA) between the rubber and conductive filler. However, the thermo-mechanically mixed NBR-PAni.DBSA blends (made by high temperature-processing, ~140°C), produced more well-blended regions (seen as rubber-rich pale-green regions) between the two polymers, even with a high level of PAni.DBSA content, i.e. ≥40 wt%. Transmission electron micrographs of all NBR- and ENR-PAni.DBSA blends prepared in this work revealed numerous small PAni.DBSA particles (of colloidal dimensions, 50-1000nm), which were also likely to have contributed to the electrical conductivities of all these blends (especially for those that were below their percolation thresholds).

The effect of PAni.DBSA polymer chain alignment on the peroxide-vulcanised NBR-PAni.DBSA blends prepared by thermo-mechanical mixing was also studied in this work. It was found that both the mechanical properties (i.e. tensile properties and tear strength) and the electrical conductivities of the blends were enhanced, when they were strained along the orientation axis of elongated PAni.DBSA polymer chains (the orientation tended to be parallel to the flow direction when the blends were passing through a two roll-mill). Both FT-IR spectroscopy and optical microscopy successfully revealed a higher level of inter-chain interaction among the elongated PAni.DBSA particles for the blends strained along this particular orientation axis. All the peroxide-vulcanised blends also exhibited a good historical memory in terms of their electrical conductivities (99% retention of the original non-strained sample's value) during the multi-cycles of strain loading and unloading. This was attributed to the high proportion of well-blended regions in all the blends prepared by thermo-mechanical mixing.

Acknowledgements

The journey of getting this PhD degree award was a "roller-coaster" for me. It was definitely won't be able to achieve my dream without the help from all these very kind peoples and they are:

1. Malaysia Rubber Board - thanks for funding this postgraduate study and kindly granted me with the sabbatical leave.
2. Professor Peter J. Foot - thanks for the brilliant supervision and continuous guidance throughout the entire journey. You have made my dream comes true.
3. Dr. Huda Morgan, Dr. Stuart Cook and Dr. Andrew J. Tinker - thanks for all the very kind advices, supports and assistances to me.
4. All the technicians and scientists from both Kingston University and Tun Abdul Razak Research Centre who helped me in some of the experimental parts.

I would also like to take this opportunity to thank my parents and family for their invaluable supports.

Table of Contents

List of Abbreviations & Symbols

Abbreviation/Symbol

A	Infrared spectroscopy peak absorbance
ACN	Acrylonitrile
BR	Poly(isobutylene-*co*-isoprene)
BS	British Standards
C	Concentration
CB	Carbon black
CR	Polychloroprene
D	Dimension/dimensional
DBSA	Dodecylbenzenesulfonic acid
DC	Direct current
DCP	Dicumyl peroxide
DSC	Differential scanning calorimetric
δ_p	Solubility parameter for polymer
δ_s	Solubility parameter for solvent
E	Activation energy
EB%	Elongation percentage at break
EB	Polyaniline emeraldine base
ENR	Epoxidised natural rubber
EPDM	Poly(ethylene-*co*-propylene-*co*-diene)
EVA	Poly(ethylene-*co*-vinyl acetate)
f	Volume fraction
f_p	Volume fraction at percolation threshold
F	Molar attraction constants
FT-IR	Fourier transform-infrared
GPR	General purpose reagents
H	High-hardness test
IRHD	International Rubber Hardness Degrees
L	Low-hardness test
M	Micro-hardness test
MAH	Maleic anhydride
N	Normal hardness test
NBR	Poly(butadiene-*co*-acrylonitrile)

Abbreviation/Symbol

NMR	Nuclear magnetic resonance
NR	Natural rubber
OM	Optical microscope/microscopy
p	Probability
p_c	Occupancy probability at percolation threshold
PAni	Polyaniline
PAni.DBSA	Dodecylbenzenesulfonic acid doped polyaniline
PAni.HCl	Hydrochloric acid doped polyaniline
PAni.p-TSA	p-toluene sulfonic acid doped polyaniline
PBN	α-phenyl-*N*-*tert*-butylnitrone
ρ	Density
p.h.r.	Parts per hundred rubber
p.p.m.	Parts per million
Ppy	Polypyrrole
PS	Polystyrene
PTFE	Polytetrafluoroethylene
PVC	Polyvinyl chloride
R	Correlation coefficient
r.p.m.	Rounds per minute
SBS	Poly(butadiene-*co*-styrene)
SEM	Scanning electron microscope/microscopy
SMR	Standard Malaysian Rubber
t	Critical exponent
TARRC	Tun Abdul Razak Research Centre (Hertford, U.K.)
TEM	Transmission electron microscope/microscopy
Tg	Glass transition temperature
TGA	Thermo-gravimetric analysis
THF	Tetrahydrofuran
TPBSA	Tetrapropylbenzenesulfonic acid
V	Volume
XPS	X-ray photoelectron spectroscopy
wt%	Weight percentage
W	Weight
σ	Electrical conductivity

Chapter 1: Introduction

1.1 Terminology

Elastomers are polymer materials which have rubber-like properties and are widely known as electrical insulators. Elastomers can be either natural or synthetic rubbers (most of the commercially available synthetic rubbers are co-polymers). Different types of elastomers and their molecular structures [1] are shown in Table 1.1.

Table 1.1: Elastomers and Their Molecular Structures

Name	Chemical Name	Molecular Structure
Natural Rubber/ NR	Cis-1,4-polyisoprene	$[-CH_2-C(CH_3)=CH-CH_2-]_n$
Polybutadiene	Polybutadiene	$[-CH_2-CH=CH-CH_2-]_n$
Styrene Butadiene Rubber/ SBR	Poly(butadiene-*co*-styrene)	$[(-CH_2-CH=CH-CH_2-)_x(-CH_2-CH(C_6H_5)-)_y]_n$
Nitrile Rubber/ NBR	Poly(butadiene-*co*-acrylonitrile)	$[(-CH_2-CH=CH-CH_2-)_x(-CH_2-CH(CN)-)_y]_n$
Butyl Rubber/ BR	Poly(isobutylene-*co*-isoprene)	$[(-CH_2-C(CH_3)_2-)_x(-CH_2-C(CH_3)=CH-CH_2-)_y]_n$
EPR/EPDM	Poly(ethylene-*co*-propylene-*co*-diene)	$[-(-CH_2-CH_2-)_{37}(-CH_2-CH(CH_3)-)_{13}\text{-diene-}]_n$
Neoprene	Polychloroprene	$[-CH_2-C(Cl)=CH-CH_2-]_n$
Silicone	Polydimethylsiloxane	$[-Si(CH_3)_2-O-]_n$
Thiokol	Polyalkylenesulfide	$[-CH_2-CH_2-S_{2\text{-}4}-]_n$
Urethane	Polyester or polyether urethanes	$HO[-P\text{-}OCONHRNHCOO-]_nP\text{-}OH$
EVA	Poly(ethylene-*co*-vinyl acetate)	$[(-CH_2-CH_2-)_x(-CH_2-CH(C{=}O{-}CH_3)-)]$

Intrinsically electrical conductive polymers are also called 'organic synthetic metals' [2] and examples include polyacetylene [3-4], polyphenylenes [5-7], polypyrroles [8], polythiophenes [9-12], poly(phenylenevinylene) [13-14], polyanilines [15-21], polypyridine and ladder-structured polyquinoxalines [22]. The key feature of the intrinsic electrically conductive polymers is the presence of conjugated bonds with π-electrons delocalised along the polymer chains [23]. In their undoped form, the polymers are either insulating or weakly semi-conductive. The polymers are converted into electrically conductive or doped forms via oxidation or reduction reactions which form delocalised charge carriers.

1.2 Electrically Conductive Elastomers

1.2.1 Historical and Principal Uses of Conventional Electrically Conductive Elastomers

Conventional electrical conductive polymer blends can be prepared using either an elastomeric [24-34] or a hard thermoplastic host [35-49] with conventional conductive fillers, i.e. carbon blacks or metallic fillers depending on the application of their final products.

Conductive elastomers were not of major interest until about 1930, when several patents described the use of conductive compounds for the prevention of corona discharge in cables [50]. The early workers employed mostly large quantities of graphite, coarse carbon blacks or even powdered metals in order to produce electrical conductivity, and the resulting elastomers had very poor physical properties. The introduction of acetylene black and later, other black-coloured conducting polymers led to production of some elastomers having mechanical properties nearly equal to those of electrically insulating elastomers (except that is not yet possible to produce a very soft highly electrically conductive elastomer [50]) and the application of the coarser fillers has been discontinued. The use of furnace blacks in place of channel blacks has led to most carbon black filled-elastomers being antistatic since the Second World War [50].

A major use of conventional electrically conductive elastomers is to dissipate the electrostatic charges which are developed whenever two dissimilar surfaces are separated either with or without rubbing. Interest in the use of conductive elastomers for antistatic purposes appears to have developed in the late 1930s, when the surgical world became worried about the frequency of explosions in operating theatres (due to static electricity). Effective development of antistatic elastomer hospital goods did not take place until after 1945 [50]. Antistatic materials have been used in many situations where explosive vapours, liquids or powders are being handled; also for vehicle and aircraft tyres, where static charges, generated by the tyres or acquired in flight, are conducted to earth through the tyres. For antistatic purposes, electrically conductive elastomers have also been used to make products, e.g. conveyor belting, hose, anchor coats of carpet backings, aircraft escape chutes, pipe expansion joints and electrical systems in explosives factories.

Since 1940, the application of electrically conductive elastomers for heating purposes has been the subject of numerous patents, and conductive silicone rubber blends were the most popular chosen materials [50]. Probably the most successful application has been for ceiling heating [51]. Electrically heated conductive hand wear has also been designed for military use [51].

Conventional electrically conductive elastomers have been used in the field of making electronic devices in order to reduce their size, for the last two decades [51]. Electronic parts, e.g. connectors, switches, thermostats, integrated circuit chips mounting and gaskets of electromagnetic interference screens, are made with conductive elastomers. There are also a number of specific cable applications of conventional conducting elastomers, i.e. cable RFI screens, terminators and splice housings.

Electrically conductive elastomers have been applied in order to replace metallic conductors because soft materials have the advantages of flexibility and the ability to absorb mechanical shock. In addition, soft polymer conductors have the following advantages over metals [50]:

i. Ease of shaping
ii. Low density
iii. Wide range of electrical conductivities
iv. Low thermal conductivity
v. Corrosion resistance

1.2.2 Novel Electrically Conductive Elastomers

Novel electrically conductive polymer blends are non-carbon black and non-metallic particles filled-polymer blends. They should ideally be blends of an elastomeric [36, 45, 47-49, 52-67] or a thermoplastic host [68-84] with an intrinsic electrically conductive polymer filler.

Conventional electrically conductive elastomers have some very significant disadvantages compared with novel electrically conductive elastomers. Carbon fillers have limited applications in order to produce electrically conductive elastomers because they are relatively poor conductors, providing a shielding effectiveness of 40-50dB only with about 40 weight percentage (wt %) of loaded filler [85]. Carbon black-filled elastomers have high percolation thresholds for conductivity, and the conductivity values are not higher than about 10^{-8}S.cm^{-1} [86]. Metal powders have high densities, and so weight fractions of 60% are often needed to achieve shielding effectiveness [85]. Oxidation of the metal surface can also reduce the effective conductivity of the composite [87]. Other conductive fillers such as metal coated fibres are also of limited use, due to their complicated preparation [85].

According to Yamaguchi [88], electric resistance increased permanently after several cycles of strain applied for carbon-black filled-natural rubber and carbon black- filled synthetic rubber test specimens. As reported by Sau [89] for blends of ethylene-propylene-diene rubber (EPDM), acrylonitrile-butadiene rubber (NBR) and silicone rubber respectively with carbon black as conductive filler, the conductivities were decreased by increasing the degree of compression. All these

observations were attributed to the destruction of conductive carbon black networks.

Intrinsically conductive polymers and their "buckytubes" which lead to the formation of microtubules instead of spheres [90-91] may help to overcome the above-mentioned problems. By stretching the intrinsic electrically conductive polymer alone, an increase of the polymer's conductivity along the orientation axis could be observed [92-95].

Some intrinsically conductive polymers have poor stability [23], and many have poor mechanical properties [96] and higher cost than commodity polymers [85]. An easy and effective method to overcome the problems is by preparing composite materials containing the intrinsic electrically conductive polymer as fillers dispersed in an elastomeric or thermoplastic matrix. To disperse a conductive polymer in an elastomeric insulating matrix, one can use either mechanical mixing [52-54, 86, 97-99], solution mixing [55-62, 95, 98], an electrochemical method [63-66] or *in situ* polymerisation [67].

Novel electrically conductive elastomers are expected to have a combination of good electrical properties of the intrinsically conductive polymers with good mechanical properties of elastomers. They should be considered for more sophisticated applications, e.g. electronic sensors (odour or DNA detectors) [58, 100], superior corrosion-inhibiting protecting coatings or paints [101], gas separation membranes [1,102-103] and electromagnetic interference (EMI) shielding. Novel electrically conductive elastomers are also expected to have good processability and could potentially be processed with the conventional elastomer processing-machines, e.g. injection moulder, internal mixer and single or twin screw extruder.

1.3 Literature Review

Summaries of some interesting works related to intrinsic electrically conductive polymer-filled elastomers prepared by using the four different methods, i.e. mechanical mixing, solution mixing, electrochemical intergrowth or *in situ* polymerisation, are shown below:-

i. Intrinsic electrically conductive polymer-filled elastomers prepared by mechanical mixing.

a. Leyva [52] reported that blends of SBS and PAni.DBSA were prepared by using Berstoff two-roll mill (60°C for 10 minutes, 15 and 20 r.p.m.) and Haake internal mixer (130°C, 60 r.p.m. for 12 minutes) respectively. It was observed that the blend reached an electrical conductivity of 1 $S.cm^{-1}$ with around 33 wt% of PAni.DBSA in the blend. The conductivity was also enhanced when the blend was formed at higher temperature under intensive mixing in a Haake internal mixer (about 6 orders of magnitude higher than that of a blend prepared with a two-roll mill). It was reported that highly crosslinked blend was prepared by using Haake internal mixer at higher temperature. Through X-ray photoelectron spectroscopy analysis (XPS), it was observed that the degree of doping for PAni by DBSA was increased (about 82-90%) by melt-processing the PAni.DBSA inside the SBS matrix with a Haake internal mixer. It was also reported that the mechanical properties of the prepared blend (tensile strength, 0.5MPa and elongation at break, 60% for blend with 33 wt% of added PAni.DBSA) were much poorer than those of pure SBS (tensile strength, 21.0MPa and elongation at break, 5200%).

b. As reported by Faez [53], blends of EPDM with different proportions of PAni.DBSA were prepared in a counter-rotating cam rotor internal mixer, coupled with a Haake rheometer. Blends were crosslinked with either

phenolic resin (SP-1045) or electron beam irradiation. The blend of EPDM-PAni.DBSA (64 wt% NBR:30 wt% PAni.DBSA) crosslinked with 6 wt% phenolic resin showed an electrical conductivity of 8 x 10^{-7}S.cm^{-1}, and a blend of EPDM-PAni.DBSA (70 wt% NBR:30 wt% PAni.DBSA) crosslinked by 75kGy electron beam showed electrical conductivity of 20 x 10^{-7}S.cm^{-1}. It was observed that tension at break for all blends increased with PAni.DBSA loading until 30 wt% and the tension dropped beyond a 30 wt% concentration. It was also observed that elongation at break values for all blends decreased with increasing PAni.DBSA loading. It was concluded that the electron beam irradiation crosslinking method is not affected by the presence of acid necessary for doping PAni. So electron beam irradiation might be a good alternative to conventional chemical agents to crosslink elastomer-intrinsic electrically conductive polymer blends.

c. Helaly [54] prepared blends of Standard Malaysian Rubber (SMR-20 grade) with polyaniline emeraldine base by using a two-roll mill in order to study the efficiency of polyaniline against PBN (α-phenyl-*N-tert*-butylnitrone, a synthetic antioxidant) as a thermal ageing resistance-antioxidant for SMR-20. The rheometric properties of prepared blends were determined using a Monsanto oscillating disc rheometer. The compounded blends were vulcanised by a ZnO/stearic acid system in a hydraulic press at 142°C. The mechanical properties (tensile strength, elongation at break and modulus at 200% elongation) were determined according to ASTM methods. It was found that polyaniline only had a slight effect on the maximum torque, minimum torque and cure rate index of cured SMR-20. It was also reported that SMR-20 vulcanizates containing polyaniline showed lower tensile values than that of PBN. It was concluded that the efficiency of polyaniline as an antioxidant for SMR-20 was lower than that of PBN.

d. As reported by Vallim [86], 100 p.h.r. of NBR with 29 wt% (NBR29) or 45 wt% (NBR45) acrylonitrile content were blended with 50 p.h.r. and 100

p.h.r of PAni.HCl, PAni.DBSA (dodecylbenzenesulfonic acid salt), PAni.TBSA (tetrapropylbenzenesulfonic acid salt) and PAni.TSA respectively by using a two roll-mill at 50°C. These blends were also vulcanized with sulphur at 150°C in a hot press. In their work, blends with NBR29 presented lower surface conductivities (10^{-12} and 10^{-10}S, 50 and 100 p.h.r of different acid doped PAni respectively) compared to NBR45 blends (10^{-11} and 10^{-9}S, 50 and 100 p.h.r. of different acid doped PAni respectively) with the same acid doped PAni (see Figure 1.1). They concluded that high PAni content increased the conductivity of NBR by four orders of magnitude (10^{-8}S.cm^{-1}); however, the blends of NBR-PAni had mechanical properties close to those of crude PAni and was hard and brittle. Increasing addition of PAni also lowered the crosslinking degree of NBR. The NBR45 (with 45 wt% of acrylonitrile content) seems to be more compatible with doped PAni than NBR29 (with 29 wt% acrylonitrile content).

e. As reported by Davies [97], SBS copolymer was blended with PAni.DBSA (which was reported to have electrical conductivity, σ about 5 to 10S.cm^{-1} and particle size, about 20μm) by using Brabender internal mixer. The prepared blends achieved electrical conductivity (see Figure 1.2) as high as 2S.cm^{-1} at a loading of 50 wt% dodecylbenzenesulfonic acid doped polyaniline (PAni.DBSA). Meanwhile, at a loading of 5 wt% of PAni.DBSA, the blend achieved an electrical conductivity of about 10^{-4}S.cm^{-1}. Unfortunately, the mechanical properties of the prepared blend were not assessed, but it was concluded that it was able to be extruded.

Figure 1.1: Surface Conductivity as a Function of Applied Potential. (a, b) NBR29; (c, d) NBR45 containing (a, c) 50 p.h.r. or (b, d) 100 p.h.r. of PAni; (■) NBR-PAni.TBSA; (○) NBR-PAni.DBSA; (Δ) NBR-PAni.TSA; (▼) NBR-PAni.HCl (Figure reproduced from Reference 86)

Figure 1.2: Conductivity vs. Composition for a SBS-PAni.DBSA Blend (Figure reproduced from Reference 97)

f. Polychloroprene (CR) was blended by Pinho [98] with hydrochloric acid doped polyaniline (PAni.HCl) and p-toluene sulfonic acid doped polyaniline (PAni.p-TSA) respectively by using a two-roll mill at 50°C and a rotor speed of 15 r.p.m. These blends showed conductivity only at compositions of CR/PAni.HCl or PAni.p-TSA = 50:50 wt%. Those with PAni.HCl, and PAni.p-TSA presented volume conductivity values of 10^{-9} and 10^{-10}S.cm^{-1} respectively. A CR-PAni base blend was also prepared by using a two-roll mill. The blend was exposed to HCl vapour for 8 hours and the conductivity reached 10^{-8}S.cm^{-1}. It can be said that the CR-doped PAni composites prepared in this work might have high elastomer and conducting polymer phase segregation because of the chosen mechanical mixing method.

g. Faez [99] reported the preparation of blends of EPDM and PAni doped with p-toluenesulfonic acid (PAni.p-TSA) in a twin screw, co-rotating internal mixer coupled to a Haake rheometer. Crosslinking agent (dicumyl peroxide) was also added to the system in order to vulcanize the EPDM. It was observed that with content of PAni.p-TSA at 30 or higher p.h.r. (parts per hundred rubber), it would induce degradation processes of the crosslinking agent and hence reduce the crosslinking level of the EPDM. It was reported that by keeping all other variables constant ([PAni.p-TSA]/[peroxide] = 10 and rotor speed = 50 r.p.m.), the blends prepared at 80°C and 150°C had conductivities of magnitude 10^{-8} and 10^{-6} S.cm^{-1} respectively. The relative increase of the degradation of EPDM at 470°C and the new weight losses which were observed by thermo-gravimetric analysis (TGA), suggested that a higher PAni.p-TSA content in the blend would induce greater phase separation between EPDM and PAni.p-TSA. The same observation was made through scanning electron microscopy (SEM) and optical microscopy (OM) analysis for the EPDM with various parts of PAni.p-TSA (1-50 p.h.r.). It was reported that PAni.p-TSA could act as a reinforcing agent for the blend (with added content, less than 30 p.h.r.) before the blend lost its elastomeric behaviour. It was also observed that a

low percolation threshold for the blend was reached with only 1 p.h.r. of added PAni.p-TSA. It was concluded that by changing the content of added PAni.p-TSA and controlling the mixing parameters, it would be possible to produce vulcanized elastomeric conductive (10^{-9} – 10^{-6} $S.cm^{-1}$, see Figure 1.3) EPDM- PAni.p-TSA blends.

Figure 1.3: Variation of the Logarithm of the Electrical Conductivity (Log σ) of EPDM-PAni.p-TSA Blends as a Function of PAni.p-TSA Concentration (Figure reproduced from Reference 99)

ii. Intrinsic electrically conductive polymer-filled elastomers prepared by solution mixing.

a. Radhakrishnan [55] prepared blends of styrene-butadiene copolymer with polypyrrole (SBS-PPy) through indirect solution mixing. SBS was dissolved in tetrahydrofuran (THF) and different amounts of initiator [anhydrous ferric chloride ($FeCl_3$)] were then added to the solution. The solvent, THF was evaporated and the resulting film was exposed to saturated pyrrole vapour for 20 hours. The resulting blend was shown to have a phase-segregated morphology by using IR spectroscopy and it was believed that PPy

deposition took place preferentially at the butadiene domains. The electrical resistance of SBS-PPy with 25 wt% $FeCl_3$ was reported to be about 10^4 to 10^5ohm.cm. The electrical resistivity of SBS-PPy blend was low at and above room temperature (26°C) and decreased sharply below room temperature (≤ 10°C). The electrical resistivity of SBS-PPy also increased with extension and decreased with compression. It was concluded that the SBS-PPy blend and SBS-carbon black blend have similar electrical conductivity behaviour during extension and compression with the only difference that SBS-PPy blend was more piezo-sensitive compared to SBS-carbon black blend.

b. Zheng [56] reported that EVA copolymers [with 20 wt% (EVA20) and 70 wt% (EVA70) of vinyl acetate units] could be blended respectively with N-octadecylated PAni [Pani-18] (60 alkyl side chains have been substituted onto 100 aniline units) and N-dodecylated PAni [PAni-12] (70 alkyl side chains substitution) by using the shared solvent, toluene. All the prepared blends were post-doped with methanesulfonic acid before sent for characterization (infrared spectra/FTIR analysis, differential scanning calorimeter/DSC, microscopic observation and x-ray diffraction analysis). Electrical properties for all the prepared blends were studied and analysed by using percolation theory. For the doped PAni-18/EVA20 blend, the lowest observed sharp percolation transition from an insulating state to conducting state was at about 2 wt% of doped PAni-18 and for doped PAni-12/EVA20 blend, the observed percolation threshold from an insulating state to semi-conducting state ($10^{-6}S.cm^{-1}$) was at about 8 wt% of doped PAni-12. Meanwhile for the PAni-18/EVA70 blend, the observed percolation threshold was at about 12-20 wt% of doped PAni-18. The conductivity also showed a second jump to final saturation as the content of PAni-12 was increased from 60 wt% to 80 wt% in PAni-12/EVA20 blends and that of PAni-18 was increased from 60 wt% to 80 wt% in PAni-18/EVA70 blends. It was concluded that the percolation thresholds for all

the prepared blends were sensitive to the morphological structure. Their threshold values were lowered by the enhancement of homogeneity of the dispersion of electrically conductive phase in the elastomeric matrix, although the absolute values of bulk conductivity were rather low.

c. Gospodinova [57] blended a copolymer of EVA with 11 mole% of vinyl acetate units with PAni-DBSA by using solution mixing (with shared solvent, xylene). The prepared blends were characterised by electron microscopy, i.e. TEM and SEM. The electrical conductivity measurements were also performed by the conventional four-probe technique. It was observed that the blends prepared by using a colloidal form of PAni-DBSA had the low percolation thresholds for electrical conductivity (0.5-1.0 wt% PAni-DBSA). Blends prepared by using PAni-DBSA (dried form and re-dispersed in xylene) had higher percolation thresholds (2.5-5.0 wt% PAni-DBSA) in terms of electrical conductivity. It was also reported that for all blends, high conductivity (up to 10^{-2} $S.cm^{-1}$) was achieved at reasonably low PAni-DBSA content, about 10 wt% (see Figure 1.4).

d. Cataldo [58] prepared blends of polybutadiene rubber with camphorsulphonic acid doped PAni by using the shared solvent, chloroform. Films of the composite were cast by evaporation of the solvent. Only small focus was given to the electrical properties of the resulting blend (it was reported that the surface electrical resistance was about 20kΩ). A lot of effort was given in this work in order to prove the resulting composite was well-blended through solution mixing.

Figure 1.4: Electrical Conductivity vs. PAni Content obtained by: (1) Aniline Polymerisation in the Presence of HCl; (2) Aniline Polymerisation in the Presence of DBSA; (3) Mixing of Colloidal PAni Dispersion synthesised in the Presence of DBSA Solution (Figure reproduced from Reference 57)

e. Leyva [59] reported that blends of SBS and PAni.DBSA were produced from solution by using a shared solvent, toluene. The mixed solutions were magnetically stirred for 24 hours at room temperature or submitted to ultrasonic vibration (50W and 60kHz) for 1 hour. Films were prepared through casting by evaporating the solvent from blend solutions at room temperature for 24 hours. The electrical properties of the resulting blends were analysed using percolation theory. Blends prepared by magnetic stirring presented a percolation threshold of 2.2 wt% of PAni.DBSA and exponent value of 3.6. Meanwhile, blends prepared by the ultrasonic method had a larger critical volume fraction, 3.8 wt% of PAni.DBSA and a lower exponent value of 2.2. This behaviour indicated that more homogeneous blends were obtained by ultrasonic mixing and disrupted the formation of continuous (connected) paths of conductive polymer inside the isolating matrix. So, blends prepared by ultrasonication were reported to have lower electrical conductivity. However, the evidence as provided in this paper is not too convincing to the reader, especially the evidence of reason for low percolation threshold for some prepared blends. For example, the authors tried to explain the formation of microtubules in some

low PAni.DBSA loaded blends (which was claimed to be the reason for low percolation threshold) through some SEM micrographs, and unfortunately, they look rather more like the structures of crystallisation or other morphological features.

f. Work as reported by Carone [60] is actually an early part of the same work published as Reference [95]. In this early part, focus was given to material characterisations (infrared spectroscopy, nuclear magnetic resonance spectroscopy and ultraviolet-visible spectroscopy) of the prepared PEUAPAN (grafted copolymers of amidated polyurethane with polyaniline emeraldine base) and PEUASPAN (grafted copolymers of amidated polyurethane with sulfonated polyaniline). It was concluded that the maximum proportion of amidation for PEUAPAN should be 60% and for PEUASPAN 20%. The PEUASPAN was assumed to be less amidated than PEUAPAN because SPAN was used in the acidic form.

g. Domenech [61] reported that blends of maleic anhydride (MAH) grafted EPDM and PAni.DBSA were prepared through indirect solution blending. Chloroform was used as solvent for EPDM and 0.5 wt% MAH grafted EPDM and xylene was used as solvent for 1.9 wt.% MAH grafted EPDM. Different amounts of oxidant [$(NH_4)_2S_2O_8$] and HDBSA solution were then added to the rubber solutions. Films were cast and exposed to the aniline monomer saturated atmosphere for 24 hours. The main focus in this work was given to material characterisations (DSC, thermogravimetric analysis/TGA and IR spectroscopy analysis). It was concluded that the presence of MAH had promoted the homogeneity of the resulting blends. The EPDM-PAni.DBSA blend was also reported to be electro-active and had relative electrical conductivities around 10^{-3}S.cm^{-1}.

h. Schmidt [62] reported that blends of EPDM (ethylene/propylene ratio: 73/27, diene content: 5 wt%) or EPDM-g-MAH (grafted with 1.9 wt% of

maleic anhydride) with PAni.DBSA were prepared. EPDM was dissolved in chloroform, and meanwhile, EPDM-g-MAH and PAni.DBSA were dissolved in ρ-xylene respectively. Different proportions of PAni.DBSA (4.8% to 69%) and crosslinking agent, i.e., phenolic resin (pre-dissolved in ρ-xylene) were also added to the blend solution in order to study the effects on thermal stability by using thermogravimetric analysis (TGA) and Fourier–transform infrared spectroscopy (FTIR). The TGA results showed more than one stage of degradation (the second stage with temperature range, 380-520°C was observed to be most significant) for both pure PAni.DBSA and EPDM-PAni.DBSA blends. In the second stage of degradation, the bound dopant, PAni.DBSA as well as EPDM were degraded simultaneously. The activation energy (*E*) for crosslinked blends was reported to be in the range of 180-250kJ.mol^{-1}, higher values than those determined for pure components and non-crosslinked blends (in the range of 150-210kJ.mol^{-1}). The effects of adding PAni.DBSA and maleated EPDM were relatively insignificant in terms of the determined E values. The mechanism of degradation of both systems was concluded to be associated with random scission of the polymer chains. The FTIR spectra for the crosslinked EPDM-PAni.DBSA blends showed absorption bands associated with saturated and unsaturated hydrocarbons, water, carbon dioxide and nitrogen containing compounds.

i. As reported by Carone [95], PEUAPAN and PEUASPAN were chemically synthesized by using the shared solvent, *N*-methyl-2-pyrrolidone (NMP). When PEUAPAN and PEUASPAN were HCl doped, their electrical conductivity ($<10^{-14}\Omega^{-1}.cm^{-1}$) increased by many orders of magnitude, reaching values of (6.1±0.6) x10^{-3} and (1.5±0.6) x$10^{-3}\Omega^{-1}.cm^{-1}$ respectively. By stretching these grafted copolymer films, their conductivities measured along their deformation direction were increased. At a strain of 30% the conductivity increase was 1.5-fold for PEUAPAN and threefold for PEUASPAN. The Young's moduli of these grafted copolymers were

increased (9.8MPa for PEUAPAN and 3.5MPa for PEUASPAN) compared to polyurethane (1.1MPa). However, the tensile strengths (2.5MPa for PEUAPAN and 0.9MPa for PEUASPAN) were decreased compared to polyurethane (4.6MPa). Carone found the grafted copolymers to be flexible and self-supporting.

j. As reported by Pinho [98], the CR was solution-blended with PAni.HCl powder in shared solvent, chloroform. CR-PAni emeraldine base (EB) blends were obtained by using solvents, i.e. chloroform and NMP respectively. These CR-EB blends were doped by dipping in a 1M HCl aqueous solution for 48 hours or by exposing to HCl vapour for 8 hours. In general, the CR-doped or un-doped polyaniline blends prepared by using chloroform solution had higher bulk conductivity values than the same blends prepared by using NMP solution. The bulk conductivity values for CR-PAni.HCl blends prepared either by direct solution blending with PAni.HCl powder ($4 \times 10^{-4} S.cm^{-1}$, see Figure 1.5) or post-doped with HCl solution ($4 \times 10^{-4} S.cm^{-1}$) or HCl vapour ($2 \times 10^{-4} S.cm^{-1}$) were reported to be quite similar.

Figure 1.5: Effect of the PAni.HCl Content on the Electrical Conductivity of CR-PAni.HCl Blends prepared by a Solution Process (Figure reproduced from Reference 98)

iii. Intrinsic electrically conductive polymer-filled elastomers prepared by electrochemical methods of polymerisation.

a. Tassi [63] reported that uniform and homogenous films [believed to be a graft copolymer of polyaniline and nitrile rubber (29% acrylonitrile : 71% butadiene)] had been obtained through potentiodynamic (potential was cycled from 0 to 2.0V at scanning rate of $20mVs^{-1}$ up to a constant peak current) and potentiostatic synthesis (at 1.5, 1.3, 1.0, 0.8, 0.7 and 0.6 V respectively). 0.1M of aniline solution, 0.1M of $(C_4H_9)_4NBF_4$, 1.0M of CF_3COOH and two platinum electrodes (one coated with nitrile rubber) were used in their work. The resulting films were reported to be insoluble in toluene or chloroform. It was assumed that the aniline cation radicals attacked the C=C bond of rubber, attaching themselves on the rubber chain and simultaneously creating new free radicals. The new radicals would either react with other aniline cation radicals or initiate crosslinking. Unfortunately, there were no mechanical or electrical properties reported in this work.

b. Naoi [64] reported that polypyrrole (PPy) films grown with the aid of an NBR-precoated platinum electrode by using electro-polymerization method was found to have a highly enhanced anion doping-undoping process because of its oriented grown structure. In the preparation of this material (Pt/NBR/PPy), the NBR film, an insulator and soluble in electrolyte solution of acetonitrile (AN)/LiClO4, played the role of a host polymer that would regulate the growth of PPy film in the direction perpendicular to the substrate plane. The PPy film grew through the fine channels etched by the penetration of the electrolyte into the NBR film during electro-polymerization. The basic electrode kinetic properties of the Pt/NBR/PPy electrode were investigated by contrasting them with a PPy film grown in a straightforward way on a Pt substrate (Pt/PPy). Potential step and ac impedance measurements for these electrodes evidenced that a

Pt/NBR/PPy electrode showed faster anion doping process than a Pt/PPy electrode. Inspection by scanning electron microscopy (SEM) revealed that a PPy film grown directly on Pt substrate had a rather compact structure. In contrast, a PPy film formed with the aid of NBR had rough, porous and perpendicularly oriented structure, indicative of the special history of the formation procedure. It was concluded that the Pt/NBR/PPy electrode had a good potential to be utilized as a cathode active material for a rechargeable lithium battery because of its advantageous electrochemical properties.

c. Zoppi [65] reported that films of NBR (29% of acrylonitrile content) with Poly (3-methyl-thiophene) [P3MeT] were prepared through potentiostatic synthesis (at 1.70, 1.85 and 1.95V wrt Ag/AgCl reference) and galvanostatic synthesis at $4mA.cm^{-2}$ using different current coulombic charges (4.8, 7.2 and $9.6C.cm^{-2}$) or constant charge with different current densities (2.0, 4.0 and $8.0mA.cm^{-2}$) respectively. The Pt working electrode was coated with a 100μm thick NBR. It was reported that the galvanostatically prepared composite films showed a lower ohmic drop resistance (100Ω, at $4.0mA.cm^{-2}$ for 20 minutes) and higher diffusion coefficient ($2 \times 10^{-8}cm^2.s^{-1}$) of BF_4^- ions (tetrabutylammonium tetrafluoroborate was used as the electrolyte) than those prepared potentiostatically (with an ohmic drop resistance of 125Ω for films obtained at 1.70V for 5 minutes, and a diffusion coefficient of BF_4^- ions, 3×10^{-9} $cm^2.s^{-1}$). The measured electrical conductivity of the films was reported to be $0.2S.cm^{-1}$.

d. Yigit [66] reported that composites of SMR-polythiophene had been prepared by electrochemical polymerisation of thiophene onto SMR-coated platinum electrode at a constant potential of +1.8V versus Ag/Ag^+ ($10^{-2}M$) reference electrode. The resulting composite reached a high electrical conductivity (of the order of $10^{-1}S.cm^{-1}$), but only with 80 wt% of

polythiophene loading. However, some chain scission was also reported to occur, leading to the degradation of the SMR at this high level of polythiophene loading.

iv. Intrinsic electrically conductive polymer-filled elastomers prepared by using *in situ* polymerisation.

a. Soares [67] reported the preparation of NBR-PAni.DBSA blends by *in situ* polymerisation of aniline in the presence of NBR (with shared solvent, toluene). The blends reached an electrical conductivity of about 10^{-2}S.cm^{-1} with 48 wt% of PAni.DBSA. It was found that the prepared blends had homogeneous morphology with the presence of microtubules (as studied by scanning electron microscope), higher viscosity and higher amount of insoluble material.

In the present project, preparation of NBR-PAni.DBSA blends by direct solution mixing and at high temperatures with an internal mixer (thermo-mechanical method) was carried out since these methods had never been used before for NBR-PAni.DBSA blends. This high product-yielding modern thermo-mechanical mixing technique is believed to have a better potential of production scale upgrading for actual industrial applications, whereas solution mixing can ensure maximum homogeneity with low thermal degradation.

1.4 Main Raw Materials for the Preparation of Elastomer-Intrinsically Conductive Polymer Blends

1.4.1 Selection Criteria for Main Raw Materials

Selection criteria for the optimum type of elastomer and intrinsically conductive polymer are listed as follows:

i. Selection criteria for elastomer:

- High chemical attack resistance to oil, acid and alkaline attack
- Ease of vulcanisation by using sulphur or sulphurless method
- High compatibility with the selected intrinsically conductive polymer
- Good supply and commercially available

ii. Selection criteria for type of intrinsic electrically conductive polymer

- Ease and reasonable cost of synthesis
- High thermal and chemical stability
- Good processability; can be dissolved by using common organic solvents
- Good electrical conductivity
- High compatibility with the selected elastomer
- Good supply and commercially available

In this project, polybutadiene-acrylonitrile copolymer (NBR) was selected partly because of its widely known high chemical attack resistance [1, 64, 86]. NBR can be vulcanised by using conventional sulphur or sulphurless system [1]. Vulcanised NBR shows a low swelling degree with organic solvents [1, 86]. NBR manufacturers are available worldwide, e.g. Bayer and Nippon Zeon. By solubility parameter calculation in this project, it was predicted that NBR would have quite good compatibility with conductive polymers, especially polyaniline (PAni), when its acrylonitrile content is relatively high.

Epoxidised natural rubber (ENR) was also chosen as an elastomeric host in one part of this work due to the interest of the research project sponsor, i.e. the Malaysian Rubber Board, to promote and enhance some potential novel usages of natural rubber.

PAni based elastomer blends have been the subject of intensive research and development for a number of years [52-67, 95, 97-99]. Special interest has been focused on PAni, since the monomer (aniline) is relatively inexpensive, the polymerisation process is straightforward and it proceeds with a high yield [104-105]. When PAni is doped with sulfonated organic acids containing large alkyl groups (long flexible chains), e.g. dodecylbenzenesulfonic acid (DBSA) or p-toluenesulfonic acid (p-TSA), it becomes highly electrically conductive and soluble in many organic solvents [106]. According to Poussin et al [106], the p-TSA doped PAni reached the measured conductivity at about 16S.cm^{-1}. It was also reported that undoped PAni (emeraldine base), hydrochloric acid (HCl) doped PAni, p-TSA doped PAni and DBSA doped PAni were stable at least to about 200°C, 100°C, 260-300°C and 260°C respectively [106]. Hence, NBR (with high resistance to chemical attack) is an appropriate partner for blending with strong acid doped PAni. Different types of doped PAni are also commercially available (one of the main manufacturers is PANIPOL Oy, Finland).

1.4.2 Polybutadiene-Acrylonitrile Copolymer (NBR)

The copolymer of polybutadiene and acrylonitrile has been known as nitrile butyl rubber (NBR) because of its elastomeric properties. The first literature reference to NBR is found in a French patent issued in 1931 [1]. NBR is defined as a copolymer of butadiene and an unsaturated nitrile. The majority of grades of NBR (structure illustrated in Figure 1.6) which are available today are made by copolymerising the monomers of butadiene and acrylonitrile. Since the molecular weights of these two monomers are nearly equal, their proportions by weight are practically the same as their molar proportions. NBR is available in several grades of oil resistance based on the acrylonitrile content (18 to 50 wt %).

Figure 1.6: Example of NBR Molecular Structure

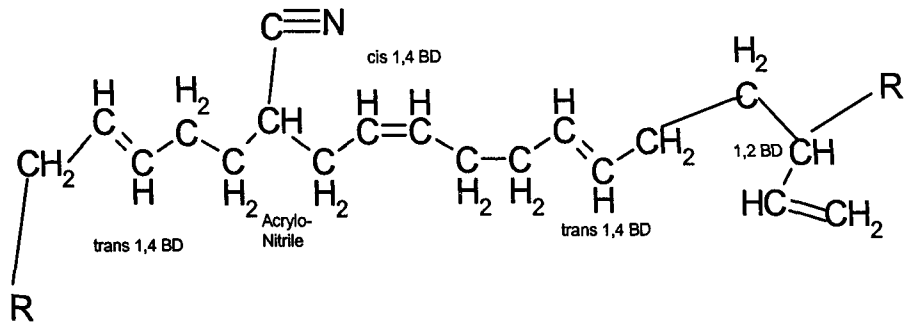

The important property trends which are influenced by acrylonitrile content are summarized in Table 1.2. The oil resistance of an NBR vulcanizate is determined by two primary factors; firstly, the proportion of acrylonitrile in a copolymer and secondly, the chemical nature of the oil or fuel in question. Other relevant factors include added softeners, pigments, state of cure, degree of crosslinking, polymerisation temperature and homogeneity of the copolymer.

Table 1.2: Property Trends Influenced by Percentages of Acrylonitrile in the NBR Copolymer

Properties	*%Acrylonitrile, 18%⟷50%*
Oil Resistance Improves	→
Fuel Resistance Increases	→
Tensile Strength Increases	→
Hardness Increases	→
Abrasion Resistance Improves	→
Gas Impermeability Increases	→
Heat Resistance Increases	→
Low Temperature Resistance Increases	←
Resilience Increases	←
Plasticizer Compatibility Increases	←

NBR is reported to have poor compatibility with natural rubber and good compatibility with SBS. Since NBR is an unsaturated copolymer, it can be

vulcanized by using sulphur (the higher the acrylonitrile content, the less sulphur is required for proper cure), peroxide, e.g., dicumyl peroxide (for excellent heat ageing resistance), phenolic resin (similar approach as peroxide-vulcanisation) or electron beam irradiation (chemical-free vulcanisation method).

1.4.3 Epoxidised Natural Rubber (ENR)

Natural rubber was first reacted with a peroxyacid in 1922 and although the structure of the product was not elucidated, epoxidation must have occurred [107]. Since then, numeral papers have been published on the preparation and properties of epoxidised natural rubber (ENR). Different types of reaction conditions were applied, and the products variously described as hard thermoplastic [108-110] to soft rubber [111-113]. The purpose of epoxidation of natural rubber or other saturated polymers is to increase its solvent resistance and improve wear resistance and mechanical properties [114-115]. However, some publications have reported a reduction in tensile strength [116-117]. A number of works related to epoxidised lattices have also been carried out [115, 118-119].

In the 1970's, there was renewed interest in the chemical modification of NR to produce other polymer materials, as a result of the oil crisis. Epoxidation was an attractive route because of the simple reaction procedure; the reaction can be carried out in the latex phase, and a relatively low cost reagent is involved. The chemistry of epoxidation of natural rubber is well-established [120-122] and it is known that secondary ring-opening reactions of the initially formed epoxide group can occur [123]. Two distinct types of ring-opened products are obtained depending principally on two different conditions [112], i.e. the *trans* diol (at high acidic condition) [124] and the five-membered cyclic or furan (at high epoxidation level) [111, 125]. Detailed mechanisms of ENR ring-opening were discussed in Section 3.3.2.

ENR was commercialised in 1991 by Kumpulan Guthrie Berhad, Malaysia in two different grades of epoxide content, i.e. 25 and 50 mole% [126]. They have

a unique set of properties offering high strength, due to their ability to undergo strain crystallisation, along with increased glass transition temperatures (with every mole% increase in the epoxidation level, the transition temperature increases by 0.93°C [126]) and solubility parameters (each 1 mole% epoxidation raises the solubility parameter by approximately $0.031(MJ.m^{-3})^{0.5}$ [126]). These properties are reflected in vulcanisates with increased oil resistance, enhanced adhesive properties, a high degree of damping and reduced gas permeation.

Specific interactions, via epoxide groups, result in a high degree of reinforcement by silica fillers, without the need for coupling agents. Functional group interactions also result in ENR forming compatible blends with a range of chlorine-containing polymers, e.g. polyvinyl chloride (PVC) and chlorinated polyethylene. Reactions between the epoxide groups in ENR and reactive groups on other polymers (e.g. carboxylated nitrile rubber) result in 'self-vulcanising [127-129]' blends.

ENR has found commercial applications in a wide range of areas, e.g. their hysteresis properties are utilised in both mechanical and acoustic damping devices and in speciality shoe soles to give high wet grip. ENR grades are used in the construction of composite conveyor belts because of their adhesive properties and the combination of high strength and low resilience of ENR based conveyor belts are advantageous under severe service conditions.

1.4.4 Intrinsic Electrically Conductive Polymers

1.4.4.1 Electronic Conduction of Polymers

Some loosely held electrons can be found from the "backbones" of intrinsic electrically conductive polymers [130], and the conductivity of these polymers occurs from a state of relative oxidation or reduction. In these states, the polymer itself can gain (for reduction) or lose (for oxidation) electrons in its structure [131]. Counter ions from the solution can go into the polymer to create electrostatic neutrality when the polymer is consequently becomes electronically charged.

These counter ions are often referred to as dopants. However, it is noted that this is not doping in the sense of inorganic semiconductors, attributed to the fact that the dopant can provide charge carriers. The charge carriers are generated chemically by removing electrons from, or adding to, the delocalised π-system of the conducting polymers.

Let us considering the polymer in terms of a semiconductor and using the band structure model [132], oxidation of the polymer results in the loss of an electron and imparts a new electronic energy state. Removal of one electron from a π bond leaves the remaining electron in a partly localised orbital – different in energy from the valence and conduction bands. This polymer will behave as a heavily doped semiconductor attributed to that these bands are above the valence band [133].

One double bond is broken by oxidising of the polymer (see Figure 1.7). As a result, a paired radical and positive charge on the polymer chain (known as a polaron) will be created. The polarons can convert to bipolarons when their concentration gets high enough for them to interact with each other. This is because the radical-cations can spread out through the neighbouring π structure, i.e. across about 8 bond lengths, and achieve contact with another radical cation. A new π bond is created with the combination of these two radicals (one from each polaron). However, this bond is more stable than the two radical-cations one. A bipolaron will be the final product, which is more stable than two polarons at the same distance apart and it may also have greater mobility when an electric field is applied.

The columbic repulsion of positively charged polarons can prevent the radicals from combining and subsequently forming a bipolaron at the low oxidation level. In contrast, the concentration of polarons will increase and they will become close enough to each other in order to create bipolarons when the oxidation level is increased. The positive charges will achieve high mobility along the chain when the radical components of polarons have combined to form a new π bond, and the result is a highly intrinsic electrically conductive polymer.

Figure 1.7: Formation of bipolaron in polyacetylene

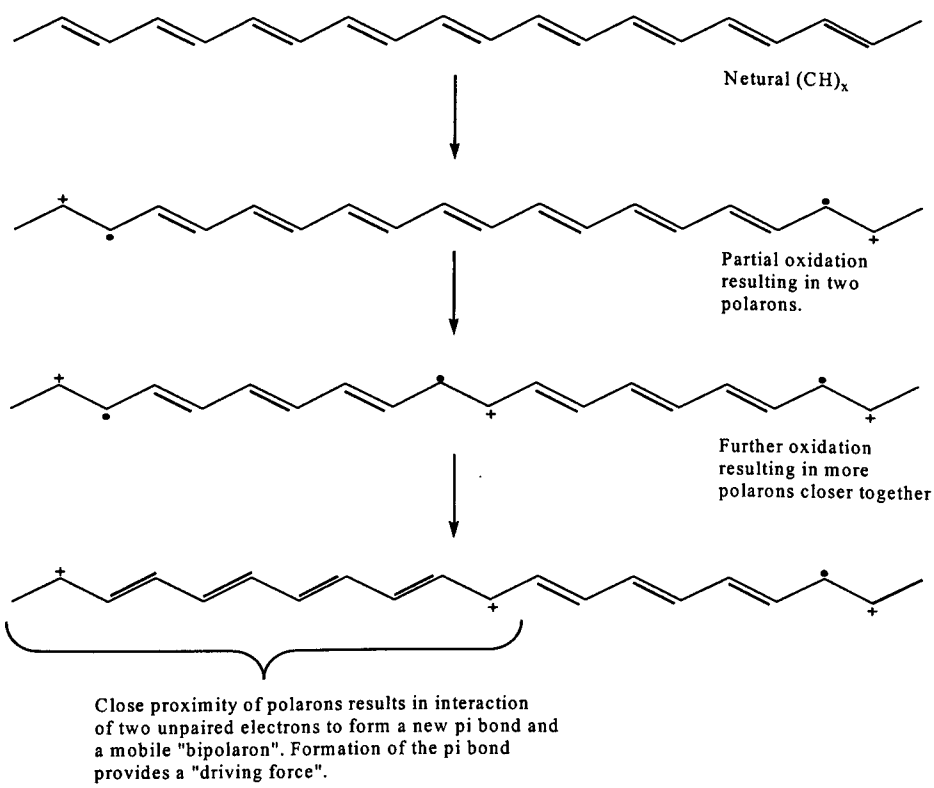

1.4.4.2 Polyaniline (PAni)

PAni is the oldest known synthetic organic polymer [105]. It can be obtained generally by using two methods, i.e. the chemical or electrochemical oxidative and emulsion polymerisation of monomer (aniline) in acidic media. PAni is a base with good thermal stability, and can be transformed into an intrinsically conductive polymer by doping with acids (pH < 4).

PAni can exist in various forms (with different colours), i.e. a fully reduced form (leucoemeraldine, see Figure 1.8), fully oxidised form (pernigraniline, see Figure 1.9) and partially oxidised base form (emeraldine base or EB, see Figure 1.10) [105]. EB is the ideal form of PAni to be utilised in terms of good electrical properties [2, 134]. The chemical structure of EB contains both benzoid (-NH-) and quinoid (-N=) pairs. The smallest repeat unit of PAni can be illustrated as a structure containing four benzene rings (see Figure 1.11).

Figure 1.8: Structure of fully reduced form of polyaniline (leucoemeraldine)

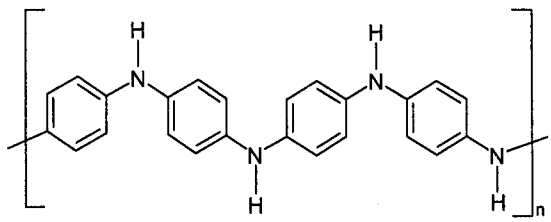

Figure 1.9: Structure of fully oxidised form of polyaniline (pernigraniline)

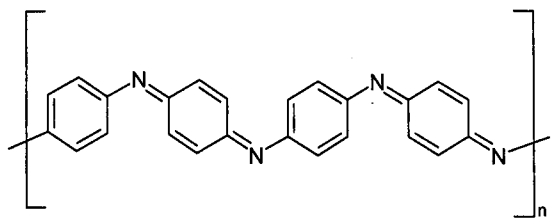

Figure 1.10: Structure of polyaniline emeraldine base

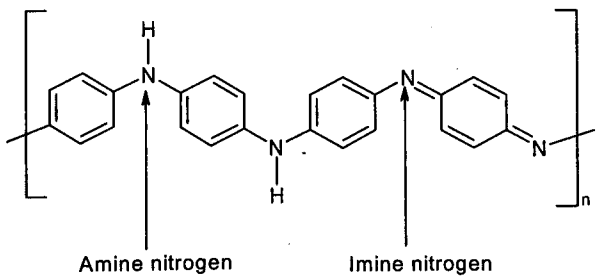

Figure 1.11: Molecular Structure of Polyaniline Smallest Repeat Unit

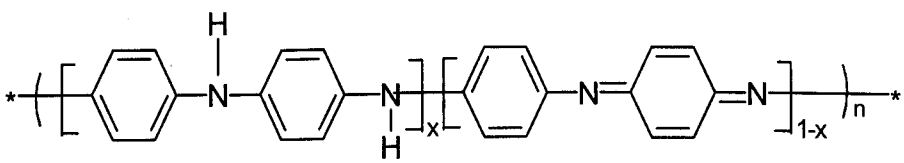

The electrical properties of PAni are controlled by two parameters [134-136], i.e. the oxidation level and the protonation level. EB can be produced in salt form by treating with acid (pH<4). The degree of protonation can be altered through variation of the pH of the acid medium, i.e. acid with lower pH value will result in a higher level of protonation. The maximum doping level occurs when half of the nitrogen sites on the polymer chain are protonated.

EB can be a good electrical conductor because of the possibility of charge combination and its delocalisation amongst the possible resonance forms of its structure. When it is treated with a protonic acid, the imine nitrogen atoms are preferentially protonated [137], resulting in the formation of a completely symmetrical polymer. As a result, a highly conjugated π system with identical monomer units would exist and lead the polymer to have excellent electrical conductivity [138]. The conjugation at the same time also leads the polymer to have strong visible absorption (causing a dark-green colour).

Most of the emeraldine salts were also found to be insoluble and non-processable. However, there are some methods can be used in order to improve the solubility and processability of EB. Poussin et al [106] reported that EB can be doped with sulfonated organic acids containing large alkyl groups (long flexible chains), e.g. dodecylbenzenesulfonic acid (DBSA) or p-toluenesulfonic acid (p-TSA) and the resulting sulfonic acid-doped-PAni had good solubility in some of the common solvents, e.g. THF and chloroform. Treatment of protonated PAni with aqueous alkali will lead to de-protonation and the insoluble EB form can be regenerated. The processability of an intrinsically electrical conductive polymer could be improved by incorporating appropriate substituents on the main 'backbone' of the polymer [139-141]. Kathirgamanathan et al [141] prepared copolymers of poly(*m*-methylaniline) and poly(*m*-ethylaniline) by using the oxidative polymerisation method. Both of the copolymers behaved like thermoplastics, which could be processed using the compression moulding technique.

1.5 Phase Mixing and Percolation Theory in Electrical Conductive Blends

1.5.1 Solubility Parameter Theory

Solubility can be determined by direct measurement, correlations with other physical parameters, or indirect calculations. For polymers (especially with low polarity molecules), the ease of mixing can be predicted by simply checking that the two solubility parameters, δ_p (solubility parameter for polymer) and δ_s (solubility parameter for solvent) are very similar. The solubility parameters of solvents, δ_s can usually be determined directly by various methods [104, 142]. The solubility parameters of polymers can only be determined indirectly.

Since the heats of vaporisation of polymers are not measurable, the values of δ_p must be determined by using different methods [142]. The group contribution approach [143-145] is the most popular method, where the values of assigned numbers to each group in the involved polymer repeat unit need to be totalled. The numbers are called molar attraction constants and they are obtained semi-empirically. In this project, this method was applied because it is the most straightforward one (does not involve any laboratory work).

The molar attraction constants, F have the SI unit of $(J.m^3)^{0.5}.mol^{-1}$. The various F terms are listed for each group, under the heading F_i, and if there are two identical groups in the polymer repeat unit, the F value for the group is doubled. The solubility parameter of a polymer, δ_p $[(MJ.m^{-3})^{0.5}]$, can be calculated by using Equation 1.1.

$$\delta_p = \left[\frac{\rho \times \sum F_i}{M_0}\right] \qquad \text{(Equation 1.1)}$$

where; ρ is density of polymer $[kg.m^{-3}]$, M_0 is the formula weight of the polymer repeat unit $[kg.mol^{-1}]$ and ΣF_i is sum of all groups' molar attraction constants in polymer repeat unit $[(J.m^3)^{0.5}.mol^{-1}]$. Molar attraction constants, F_i, of some common groups may be found in the literature [142-145]. Solubility parameter

values for some of the elastomers and common solvents (see Table 1.3 and 1.4 for some compiled values) can be obtained directly from the literature [2, 142, 146-147].

Table 1.3: Values of Solubility Parameter for Some Common Elastomers

Elastomers	Solubility Parameters $(MJ.m^{-3})^{0.5}$
Butadiene/Acrylonitrile Copolymer (wt/wt%)	
82/18	17.7-19.0
75/25	18.9-19.4
70/30	19.2-20.3
60/40	19.9-21.4
Butadiene/Styrene Copolymer (wt/wt%)	
96/4	16.5-16.6
87.5/12.5	16.6-17.6
85/15	17.2-17.5
71.5/28.5	16.6-17.5
60/40	17.5-17.8
Butyl Rubber	15.8-16.5
Chlorinated Rubber	19.2
Natural Rubber	16.2-17.1
Polychloroprene	15.2-19.2
Epoxidised Natural Rubber (mole% epoxide)	
26	17.4
48	18.2
71	18.6
Silicone Rubber (polydimethyl)	15.0

Table 1.4: Values of Solubility Parameter for Some Common Solvents

Solvents	Solubility Parameters $(MJ.m^{-3})^{0.5}$
Vinyl chloride	16.0
Diisopropyl ketone	16.4
Turpentine	16.6
Dichloropropane-2,2	16.8
Dichlorofluoromethane (Freon 21)	17.0
Dipentene	17.4
Butyl bromide (normal)	17.8
Xylene	18.0
Toluene	18.2
Dichloroethylene (cis-1,2/trans-1,2*)	18.6/18.4*
Chloroform	19.0
Tetrahydrofuran (THF)	19.0
Acetone	20.3
Aniline	21.1
Pyridine	21.9

It is also worthwhile to note that compatibility between two polymers (e.g. an elastomer and a conductive polymer) can be improved if they have a strong capability to form inter-component hydrogen bonding. A hydrogen bond is a special type of attractive interaction (perhaps a variation of a dipole-dipole bond) that exists between an electronegative atom and a hydrogen atom bonded to another electronegative atom. Hydrogen bonds can occur between molecules (intermolecularly), or within different parts of a single molecule (intramolecularly). The typical hydrogen bond is stronger than van der Waals forces, but weaker than covalent or ionic bonds. A compatibiliser, which is usually a hydrogen bond donor (e.g. hydroquinone, 4-hydroxybenzoic acid and terephthalic acid), can be used in order to enhance the capability of forming hydrogen bonds between the mixing components.

1.5.2 Percolation Theory in Electrical Conductive Blends

Percolation theory is a general mathematical theory of connectivity and transport in geometrically complex systems [148-149]. Let us consider a square grid and randomly occupy sites on this grid with a probability (p) [149]. It is found that there are mostly isolated occupied sites with occasional pairs of neighbouring sites that are both occupied for p with small values. When the neighbouring sites are both occupied, a cluster can be formed. More isolated clusters will exist (some clusters grow and some merge), as the occupancy p increases. As a result, the clusters on the whole site get larger (see Figure 1.12). One cluster will then dominate and become infinitely large at a particular value of the occupancy probability ($p_1 < 1.0$). The other clusters become absorbed into this one above the p_1. When the value of p reaches 1.0, every site will be occupied.

Figure 1.12: Formation of Clusters in A Square Grid with Different Occupancy Probability (p) Values (Figure reproduced from Reference 149)

In these figures, the different colours simply indicate the different clusters and have no other significance. At one particular value of the occupancy probability, a very interesting phenomenon happens; where one cluster will suddenly become infinitely large. The cluster is called as the spanning cluster as it spans the entire lattice. This sudden onset of a spanning cluster occurs at a particular value of the occupancy probability known as the percolation threshold (p_c) and this is the fundamental characteristic of percolation theory. The exact value of the threshold depends on which kind of grid is used and the dimensionality of the grid [148-149].

Sudden changes like this are very common in the studies of physics. For example, a magnet will lose its magnetisation at a particular temperature (i.e. the Curie Temperature) when heated [149]. These phenomenons are known as phase transitions (or critical phenomena) in general and the percolation threshold is just one of the examples. As a result, many of the properties close to this transition can be described in very simple terms. The infinite (or spanning) cluster is not including all occupied sites. Let us consider at the probability that an occupied site is in the infinite cluster ($P(p)$), then the value must be zero below the percolation threshold (since there is no spanning cluster). Simple analytical terms [148-149] are used to describe the phenomenons that occur above the threshold:

$$P(p) \sim (p-p_c)^{\beta} \; ; \; p > p_c$$

where; lower case p is the occupancy probability and upper case P is the fraction of occupied sites belonging to the percolating cluster. This is known as a power law or scaling law and the exponent, β is known as a critical exponent. It is entirely independent of the kind of lattice being studied and it only depends on the dimensionality of space (i.e. 2D or 3D) [148-149]. This is said as the universality and also an important aspect of percolation theory. Generally, it means that the large scale behaviour of these systems can be described by relatively simple mathematical relationships which are entirely independent of the small scale construction [148-149]. This powerful concept can be applied to study and

understand the behaviour of a very wide range of systems without needing to consider the detailed local structure. The percolation threshold itself is not universal, but the scaling laws and critical exponents are.

In terms of an electrically conductive blend, it is assumed that the occupied sites are conductive fillers, the empty sites represent insulators (e.g. elastomers), and that electrical current can flow between nearest neighbour conductor sites. The conductor sites will either isolate or form small clusters of nearest neighbour sites at low concentration p. Two conductor sites will be categorised to the same cluster if they are connected by a path of nearest neighbour conductor sites, and a current can flow between them. A conducting path connecting opposite edges of the lattice does not exist at low p values and as a result, the mixture is an insulator. On the other side, many conduction paths between opposite edges will be created at large p values, where electrical current can flow, and the mixture becomes a conductor. Therefore, a threshold concentration (p_c) must exist at some concentration in between, where for the first time electrical current can percolate from one edge to the other. In this case, we will have an insulator below p_c and a conductor above p_c. The percolation threshold or the "critical concentration" will be the concentration at threshold.

1.6 Project Objective & Aims

NBR-PAni.DBSA blends with poor electrical conductivities have been prepared by previous work [86]. Interest was found in order to improve the compatibility and electrical conductivities of this type of blend through different mixing methods (i.e. solution and thermo-mechanical) with more systematic mixing procedures and better optimised mixing conditions. No literature works have been reported relating to the study of electrical properties of natural rubber-PAni.DBSA blends.

The main objective for this PhD research degree project was to study the preparation of good compatible and highly electrically conductive blends by using various types of elastomer (i.e. different grades of NBR and ENR) as the host

matrix and an intrinsic electrically conductive polymer (i.e. PAni.DBSA) as the conductive filler, through solution mixing (for the fundamental study, i.e. compatibility of the mixing components) and thermo-mechanical mixing (for larger scale application purpose). Various tasks were carried out during the project in order to achieve the main objectives and they are stated below:-

i. Investigation of the compatibility between different types of elastomer (e.g. different grades of NBR and ENR) and conductive polymers (e.g. PAni.DBSA) by comparing their solubility parameter values.
ii. Synthesis of different forms of polyaniline, i.e. the undoped one (PAni emeraldine base) and the sulfonic acid-doped one (PAni.DBSA).
iii. Study of preparation of non-vulcanised elastomer-intrinsic electrically conductive polymer blends (i.e. NBR-PAni.DBSA and ENR-PAni.DBSA) by solution mixing.
iv. Study of preparation of vulcanised elastomer-intrinsic electrically conductive polymer blends (i.e. NBR-PAni.DBSA) by thermo-mechanical mixing (with an internal mixer). The effect of a vulcanising agent (i.e. dicumyl peroxide) on the electrical and mechanical properties of these vulcanised blends was also investigated.
v. Characterisation of the main raw materials (i.e. different grades of NBR, ENR and PAni.DBSA) and both non-vulcanised and vulcanised elastomer-conductive polymer blends by using elemental analysis, electromagnetic spectroscopy (i.e. NMR and FT-IR) and thermal analysis (i.e. DSC). Chemical interactions between two of the mixing components were also investigated by using same spectroscopic and thermal analysis method.
vi. Morphological and phase separation study of all the solution and thermo-mechanical mixed elastomer-conductive polymer blends by optical and transmission electron microscopy.
vii. Measurement of electrical properties, i.e. direct current (DC) conductivity for main raw materials (i.e. different grades of NBR, ENR and PAni.DBSA) and both of the non-vulcanised and vulcanised elastomer-conductive

polymer blends prepared by solution and thermo-mechanical mixing respectively. Electrical properties of all these blends were derived in terms of percolation theory and were correlated with the results of their microscopy studies.

viii. Study of mechanical properties (i.e. tensile properties, tear strength, hardness, compression set and tension set) of the main raw materials (i.e. NBR and PAni.DBSA) and vulcanised elastomer-conductive polymer blends (i.e. NBR-PAni.DBSA blends) prepared via thermo-mechanical mixing. Mechanical properties of all these blends were also correlated with the results of their microscopy studies.

This PhD research degree project was generally divided into three major parts, i.e.:

i. Study of non-vulcanised nitrile rubber (as elastomeric host)-polyaniline dodecylbenzenesulfonate (as conductive filler) blends prepared by solution mixing.
ii. Study of non-vulcanised epoxidised natural rubber (as elastomeric host)-polyaniline dodecylbenzenesulfonate (as conductive filler) blends prepared by solution mixing.
iii. Study of peroxide-vulcanised nitrile rubber (as elastomeric host)-polyaniline dodecylbenzenesulfonate (as conductive filler) blends by thermo-mechanical mixing (i.e. with an internal mixer).

References

1. Morton, M. *Rubber Technology (2nd Edition)*. New York: Van Nostrand Reinhold Company, pp.16-17, (1973).
2. Morgan, H., Foot, P. J. S. and Brooks, N. W. *J. Mater. Sci.,* **36**, 5369 (2001).
3. Ito, T., Shirakawa, H. and Ikeda, S. *J. Polym. Sci., Polym. Chem. Educ.,* **12**, 11 (1974).

4. Shirakawa, H. *Handbook of Conducting Polymers (2nd Edition).* New York: Marcel Dekker, pp.197, (1998).

5. Kovacic, P. and Jones, M. B. *Chem. Rev.,* **87(2)**, 357 (1987).

6. Brown, C. E., Kovacic, P., Wilkie, C. A., Kinsinger, J. A., Hein, R. E., Yaniger, S. I. and Cody Jr., R. B. *J. Polym. Sci., Polym. Chem. Educ.,* **24(2)**, 255 (1986).

7. Schluter, A. D. *Handbook of Conducting Polymers (2nd Edition).* New York: Marcel Dekker, pp. 209-224, (1998).

8. Diaz, A. F. and Hall, B. *IBM J. Res. Dev.,* **27**, 342 (1983).

9. Roncali, J. *Chem. Rev.*, **92**, 711 (1992).

10. Waltman, R. J., Bargon, J. and Diaz, A. F. *J. Phys. Chem.*, **87**, 1459 (1983).

11. Baughman, R. H. *Chem. Rev.*, **82**, 209 (1982).

12. Sato, M., Tanaka, S. and Kaeriyama, K. *J. Chem. Soc., Chem. Commun.,* 873 (1986).

13. Gagnon, D. R., Capistran, J. D., Karasz, F. E. and Lenz, R. W. *Polym. Bull.,* **12**, 293 (1984).

14. Takassi, M. A., Chen, W., Niziurski, R. E., Cava, M. P. and Metzger, R. M. *Synthetic Met.,* **36(1)**, 55 (1990).

15. Chiang, J. C. and MacDiarmid, A. G., *Synthetic Met.*, **13**, 193 (1986).

16. Yue, J. and Epstein, A. J. *J. Am. Chem. Soc.*, **112**, 2800 (1990).

17. Angelopoulos, M., Asturias, G. E., Ermer, S. P., Ray, A., Scherr, E. and MacDiarmid, A. G. *Mol. Cryst. Liq. Cryst.*, **160**, 151 (1988).

18. Yue, J., Epstein, A. J. and MacDiarmid, A. G. *Mol. Cryst. Liq. Cryst.*, **189**, 255 (1990).

19. MacDiarmid, A. G., Chiang, J.-C., Richter, A. E., Somasiri, N. L. D. and Epstein, A. J. *Conducting Polymers: Special Applications: Proceeding of the Workshop held at Sintra, Portugal, July 28-31, 1986.* Dordrecht: Lancaster Reidel, pp. 105-120, (1987).

20. Tan, K. L., Tan, B. T. G., Khor, S. H., Neoh, K. G. and Kang, E. T. *J. Phys. Chem. Solids*, **52(5)**, 673 (1991).

21. Angelopoulos, M., Ray, A., MacDiarmid, A. G. and Epstein, A. J. *Synthetic Met.,* **21**, 21 (1987) .

22. Yamamoto, T., Nakamura, T., Fukumoto, H. and Kubota, K. *Chem. Letter,* 502 (2003).

23. Foot, P. J. S. and Kaiser, A. B. *Kirk-Othmer Encyclopaedia of Chemical Technology: Conducting Polymers, Website Version. http://www.mrw.interscience.wiley.com/kirk/articles/elecreyn.a01.html.* New York: John Wiley & Sons Inc., (2004).

24. Luheng, W., Tianhuai, D. and Peng, W. *Sensors and Actuators A: Phys.*, **135(2)**, 587 (2007).

25. Carrillo, A., Martin-Domínguez, I. R., Glossman, D. and Marquez, A. *Sensors and Actuators A: Phys.*, **119(1)**, 157 (2005).

26. Sun, Y., Luo, S., Watkins, K. and Wong, C. P. *Polymer Degrad. Stab.*, **86(2)**, 209(2004).

27. Das, N. C., Chaki, T. K. and Khastgir, D. *Carbon*, **40(6)** 807 (2002).

28. Das, N. C., Khastgir, D., Chaki, T. K. and Chakraborty, A. *Comp. Part A: Appl. Sci. and Manufacturing*, **31(10)**, 1069 (2000).

29. Nasr, G. M., Osman, H. M., Abu-Abdeen, M. and Aboud, A. I. *Polym. Testing*, **18(7)**, 483 (1999).

30. Sau, K. P., Chaki, T. K. and Khastgir, D. *Polymer*, **39(25)**, 6461 (1998).

31. Sau, K. P., Chaki, T. K. and Khastgir, D. *Comp. Part A: Appl. Sci. and Manuf.*, **29(4)**, 363 (1998).

32. Badawy, M. M. and Nasr, G. M. *Polymer Testing*, **16(2)**, 155 (1997).

33. Pramanik, P. K., Khastgir, D. and Saha, T. N. *Composites*, **23(3)**, 183 (1992).

34. Job, A. E., Oliveira, F. A., Alves, N., Giacometti, J. A. and Mattoso, L. H. C. *Synthetic Met.*, **135**, 99 (2003).

35. Dai, K., Xu, X.-B. and Li, Z.-M. *Polymer*, **48(3)**, 849 (2007).

36. Luo, Y., Liu, Y. and Wang, L. *Sensors and Actuators B: Chemical*, **119(2)**, 516 (2006).

37. Clark, A. C., Ho, S. P. and LaBerge, M. *Tribology Int.*, **39(11)**, 1327 (2006).

38. Yui, H., Wu, G., Sano, H., Sumita, M. and Kino, K. *Polymer*, **47(10)**, 3599 (2006).

39. Shaojin, J., Pingkai, J., Zhicheng, Z. and Zhongguang, W. *Radiation Phys. & Chem.*, **75(4)**, 524 (2006).

40. Xu, X.-B., Li, Z.-M., Yang, M.-B., Jiang, S. and Huang, R. *Carbon*, **43(7)**, 1479(2005).

41. Li, Z.-M., Xu, X.-B., Lu, A., Shen, K.-Z., Huang, R. and Yang, M.-B. *Carbon*, **42(2)**, 428 (2004).

42. Chen, J., Iwata, H., Maekawa, Y., Yoshida, M. and Tsubokawa, N. *Radiation Phys. and Chem.*, **67(3)**, 397 (2003).

43. Wycisk, R., Pozniak, R. and Pasternak, A. *J. Electrostatics*, **56(1)**, 55 (2002).

44. Feng, J. and Chan, C.-M. *Polymer*, **41(19)**, 7279 (2000).

45. Luo, Y., Wang, G., Zhang, B. and Zhang, Z. *European Polym. J.*, **34(8)**, 1221 (1998).

46. Hampl, J. and Bouda, V. *Synthetic Met.*, **67(1-3)**, 129 (1994).

47. Li, C., Liang, T., Lu, W., Tang, C., Hu, X., Cao, M. and Liang, J. *Comp. Sci. & Tech.*, **64(13-14)**, 2089 (2004).

48. Omastova, M., Chodak, I. and Pionteck, J. *Synthetic Met.*, **102(1-3)**, 1251 (1999).

49. Andreatta, A. and Smith, P. *Synthetic Met.*, **55(2)**, 1017 (1993).

50. Norman, R. H. *Conductive Rubbers and Plastics*. England: Elsevier, pp. 3-4, (1970).

51. Norman, R. H. *European Rubber J.*, **169**, 20 (1981).

52. Leyva, M. E., Barra, G. M. O, Gorelova, M. M., Soares, B. G. and Sens, M. *J. Appl. Polym. Sci.*, **80(4)**, 626 (2001).

53. Faez, R., Schuster, R. H. and De Paoli, M.-A. *European Polym. J.*, **38(12)**, 2459 (2002).

54. Helaly, F. M., Darwich, W. M. and Abd El-Ghaffar, M.A. *Polym. Degrad. Stabil.*, **64**, 251 (1999).

55. Radhakrishnan, S. and Saini, D. R. *Polym. Int.*, **34**, 111 (1994).

56. Zheng, W., Levon, K., Taka, T., Laasko, J. and Osterholm. J.-E. *J. Polym. Sci. Phys.*, **33**, 1289 (1995).

57. Gospodinova, N., Mokreva, P., Tsanov, T. and Terlemezyan, L. *Polymer*, **38**, 743 (1997).

58. Cataldo, F. and Maltese, P. *Polym. Adv. Technol.,* **12**, 293 (2001).

59. Leyva, M. E., Barra, G. M. O. and Soares, B. G. *Synthetic Met.,* **123**, 443 (2001).

60. Carone, E., D'Ilario, L. and Martinelli, A. *J. Appl. Polym. Sci.,* **83(4),** 857 (2002).

61. Domenech, S. C., Bortoluzzi, J. H., Soldi, V. and Franco, C. V. *J. Appl. Polym. Sci.,* **87**, 535 (2003).

62. Schmidt, V., Domenech, S. C., Soldi, M. S., Pinheiro, E. A. and Soldi, V. *Polym. Degrad. Stabil.*, **83**, 519 (2004).

63. Tassi, E. L. and De Paoli, M.-A. *Polymer*, **33(11)**, 2427 (1992).

64. Naoi, K. and Osaka, T. *J. Electrochem. Soc.,* **134**, 2479 (1987).

65. Zoppi, R. A. and De Paoli, M.-A. *J. Electroanal. Chem.,* **290**, 275 (1990).

66. Yigit, S., Hacaloglu, J., Akbulut, U. and Toppare, L. *Synthetic Met.,* **79**, 11 (1996).

67. Soares, B. G., Amorim, G. S., Souza Jr., F. G., Oliveira, M. G. and Pereira da Silva, J. E. *Synthetic Met.,* **156(2)**, 91 (2006).

68. Castillo-Castro, T. D., Castillo-Ortega, M. M., Villarreal, I., Brown, F., Grijalva, H., Perez-Tello, M., Nuno-Donlucas, S. M. and Puig, J. E. *Comp. Part A: Appl. Sci. and Manufacturing*, **38(2)**, 639 (2007).

69. Ke, Q. and Aoki, K. *J. Colloid and Interface Sci.*, **305(1)**, 40 (2007).

70. Ding, S.-J., Zhang, C.-L., Yang, M., Qu, X.-Z., Lu, Y.-F. and Yang, Z.-Z. *Polymer*, **47(25)**, 8360 (2006).

71. Yoshikawa, H., Hino, T. and Kuramoto, N. *Synthetic Met.*, **156(18)**, 1187 (2006).

72. Bernasik, A., Haberko, J., Wlodarczyk-Miskiewicz, J., Raczkowska, J., Luzny, W., Budkowski, A., Kowalski, K. and Rysz, J. *Synthetic Met.*, **155(3)**, 516 (2005).

73. Martins, C. R. and De Paoli, M.-A. *European Polym. J.*, **41(12)**, 2867 (2005).

74. Shin, J. S., Kim, J. H. and Cheong, I. W. *Synthetic Met.*, **151(3)**, 246 (2005).

75. Gupta, R. K. and Sing,h R. A. *J. Non-Crystalline Solids*, **351(24-26)**, 2022 (2005).

76. Yang, Y., Chu, Y., Yang, F. and Zhang, Y. *Materials Chem. & Phys.*, **92(1)**, 164(2005).

77. Hu, X., Zhang, Y.-Y., Tang, K. and Zou, G.-L. *Synthetic Met.*, **150(1)**, 1 (2005).

78. Segal, E., Tchoudakov, R., Narkis, M., Siegmann, A. and Wei, Y. *Sensors and Actuators B: Chem.*, **104(1)**, 140 (2005).

79. Jousseaume, V., Morsli, M., Bonnet, A. and Lefran,t S. *Optical Materials*, **9(1-4)**, 484 (1998).

80. Fu, Y. and Weiss, R. A. *Synthetic Met.*, **84(1-3)**, 103 (1997).

81. Fu, Y. and Weiss, R. A. *Synthetic Met.*, **84(1-3)**, 129 (1997).

82. Geng, Y.-H., Wang, X.-H., Wang, L.-X., Jing, X.-B. and Wang, F.-S. *Synthetic Met.*, **69(1-3)**, 163 (1995).

83. Ruckenstein, E. and Yang, S. *Synthetic Met.*, **53(3)**, 283 (1993).

84. Fryczkowski, R., Binias, W., Farana, J., Fryczkowska, B. and Wlochowicz, A. *Synthetic Met.*, **145(2-3)**, 195 (2004).

85. Jiang, G., Gilbert, M., Hitt, D. J., Wilcox, G. D. and Balasubramanian, K. *Compos. Part A-Appl. Sci.,* **33**, 745 (2002).

86. Vallim, M. R., Felisberti, M. I. and De Paoli, M.-A. *J. Appl. Polym. Sci.,* **75**, 677 (2000).

87. Bhattacharya, S. K. and Kusy, R. P. *Metal-Filled Polymers: Properties and Applications*. New York: Marcel Dekker, (1986).

88. Yamaguchi, K., Busfield, J. J. C. and Thomas, A. G. *J. Appl. Polym. Sci. Polym. Phys.,* **41**, 2079 (2003).

89. Sau, K. P., Chaki, T. K. and Khastagir, D. *Rubber Chem. Technol.,* **73**, 310 (2000).

90. Balberg, I., Anderson, C. H., Alexander, S. and Wagner, N. *Phys. Rev. B.,* **30(7)**, 3933 (1984).

91. Suzuki, Y. Y., Heeger, A. J. and Pincus, P. *Macromolecules*, **23(21)**, 4730 (1990).

92. Pomfret, S. J., Adams, P. N., Comfort, N. P. and Monkman, A. P. *Polymer*, **41(6)**, 2265 (2000).

93. Abell, L., Pomfret, S. J., Adams, P. N., Middleton, A. C. and Monkman, A. P. *Synthetic Met.,* **84**, 803, (1997).

94. Xie, H.-Q. and Ma, Y.-M. *J. Appl. Polym. Sci.,* **77(10)**, 2156 (2000).

95. Carone, E., D'Ilario, L. and Martinelli, A. *J. Appl. Polym. Sci.,* **86(5)**, 1259 (2002).

96. Laska, J., Zak, K., and Pron, A. *Synthetic Met.,* **84**, 117 (1997).

97. Davies, S. J., Ryan, T. G., Wilde, C. J. and Beyer, G. *Synthetic Met.,* **69**, 209 (1995).

98. Pinho, M. S., Gorelova, M. M., Dezzoti, M., Soares, B. G. and Pertsin, A. J. *J. Appl. Polym. Sci.,* **70**, 1543 (1998).

99. Faez, R., Gazotti, W. A. and De Paoli, M.-A. *Polymer*, **40**, 5497 (1990).

100. http://www.osmetech.com

101. Lu, W.-K., Elsenbaumer, R. L. and Wessling, B. *Synthetic Met.,* **71**, 2163 (1995).

102. Liang, W. and Martin, C. R. *Chem. Mater.,* **3(3)**, 390 (1991).

103. Anderson, M. R., Mattes, B. R., Reiss, H. and Kaner, R. B. *Science*, **252**, 1412 (1991).

104. Narkis, M., Haba, Y., Segal, E., Zilberman, M., Titleman, G. I. and Siegmann, A. *Polym. Adv. Technol.,* **11**, 665 (2000).

105. Syed, A. A. and Dinesan, M. K. *Talanta*, **38**, 815 (1991).

106. Poussin, D., Morgan, H. and Foot, P. J. S. *Polym. Int.,* **52**, 433 (2003).

107. Pummerer, R. and Burkard, P. A. *Ber. Dtcsh. Chem. Ges.*, **55**, 3458 (1992).

108. British Patent 369 716. *Improvement in the Manufacture and Production of Corrosion Products of Rubber*, (1932).

109. Bloomfield, G. F. and Farmer, E. H. *J. Soc. Chem. Ind.*, **53**, 121 (1934).

110. Ng, S. C. and Gan, L. J. *European Polym. J.*, **17**, 1073 (1981).

111. Gelling, I. R. and Smith, J. F. *Controlled Viscosity by Natural Rubber Modification. Proceedings of International Rubber Conference Venice*, (1979).

112. Neth. Patent Application 6 413 160. *Epoxidation of Elastomers*, (1965).

113. Burfield, D., Lim, K.-L. and Law, K.-S. *J. Appl. Polym. Sci.*, **29**, 1661 (1984).

114. Udipi, K. *J. Appl. Polym. Sci.,* **23**, 3301, 3311 (1979).

115. British Patent 1 083 316. *Epoxidation of Elastomers*, (1967).

116. Roux, C. Pautrat, R., Cheritat, R., Ledran, F. and Danijard, J. C. *J. Polym. Sci. Part C*, **16**, 4687 (1969).

117. Colclough, T. *Trans. Instn. Rubb. Ind.*, **38**, 11 (1962).

118. Gonsovskaya, T. B., Ponomare, F. G., Poluektov, P. T. and Khvatova, L. K. *Kauch. Rezina*, **30**, 23 (1971).

119. British Patent 892 361. *Improvements in or relating to an Epoxidation Process and Product*, (1962).

120. Swern, D. *Organic Peroxide, Vol. 2, Chapter 5.* New York: Wiley Interscience, (1971).

121. Plesnicar, B. *Oxidation in Organic Chemistry Vol. 5, Part C, Chapter 3.* pp. 211, (1978).

122. Gelling, I. R. and Porter, M. *Natural Rubber Science and Technology, Chapter 10.* Oxford: Oxford University Press, pp. 359, (1988).

123. Parker, R. E. and Issacs, N. S. *Chem. Rev.*, **59**, 737 (1959).

124. Rosowsky, A. *Heterocyclic Compounds with Three and Four Membered Rings, Part 1.* New York: Interscience Publishers, (1964).

125. Gelling, I. R. *Rubb. Chem. Technol.*, **58**, 86 (1985).

126. Gelling, I. R. *J. Nat. Rubb. Res.,* **6(3)**, 184 (1991).

127. Alex, R., De, P. P. and De, S. K. *J. Polym. Sci.: Part C Polymer Letters*, **27**, 361 (1989).

128. Alex, R., De, P. P. and De, S. K. *Polym. Comm.*, **31**, 118 (1990).

129. Alex, R. De, P. P., Mathew, N. M. and De, S. K. *Plast. Rubb. Processing and Applications*, **15**, 223 (1991).

130. Bredas, J. L. and Sibley, R. *Conjugated Polymers.* Netherlands: Kluwer Academic Publishers, pp. 3, (1991).

131. Bredas, J. L., Chance, R. R. and Silberg, R. *Mol. Cryst. Liq. Cryst.,* **77**, 319 (1981).

132. Grant, P. M. and Batra, I. P. *Synthetic. Met.,* **1**, 193 (1980).

133. Alcacer, L. *Conducting Polymers, Special Applications*. Dordecht, Holland: D. Reidel Publishing Company, pp. 6, (1987).

134. Trivedi, D. C. *Handbook of Organic Conductive Molecules & Polymers, Volume 2, Conductive Polymers: Synthesis and Electrical Properties*. Chichester, England: John Wiley & Sons Ltd., pp. 505-572, (1997).

135. MacDiarmid, A. G. and Chiang, J.-C. *Synthetic Met.,* **13**, 193, (1986).

136. Genies, E. M. and Lapkowski, M. *J. Electroanal. Chem.*, **220(1)**, 67 (1987).

137. MacDiarmid, A. G. *Synthetic Met.,* **125**, 11 (2002).

138. Huang, W.-S., MacDiarmid, A. G. and Epstein, A. J. *J. Chem. Soc., Chem. Commun.,* **23**, 1784 (1987).

139. Bryce, M. R., Chissel, A. D., Kathirgamanathan, P., Parker, D. and Smith, N. R. M. *J. Chem. Soc. Chem. Commun.*, 466 (1987).

140. Bryce, M. R., Chissel, A. D., Smith, N. R. M., Parker, D. and Kathirgamanathan, P. *Synthetic Met.,* **26**, 153 (1988).

141. Kathirgamanathan, P., Adams, P. N., Quill, K. and Underhill, A. E. *J. Mat. Chem.*, **1**, 141 (1991).

142. Orwoll, R. A. *Polymer Handbook, 3rd Edition.* New York: Wiley-Interscience Publication, pp. VII/521-VII/559, (1989).

143. Small, P. A. *J. Appl. Chem.,* **3**, 71 (1953).

144. Hoy, K. L. *J. Paint Technol.,* **42**, 76 (1970).

145. Rudin, A. *The Elements of Polymer Science and Engineering: An Introductory Text for Engineers and Chemists*. New York: Academic Press, (1982).

146. Sheehan, C. J. and Bisio, A. L. *Rubber Chem. Technol.,* **39**, 162 (1966).

147. Bristow, G. M. and Watson, W. F. *Trans. Faraday Soc.,* **54**, 1731 (1958).

148. Stauffer, D. *Introduction to Percolation Theory*. London: Taylor and Francis, (1985).

149. King, B. R., Buldyrev, S. V., Dokholyan, N. V., Havlin, S., Lopez, E., Paul, G. and Stanley, H. E. *Percolation Theory (Website Version)*. http://polymer.bu.edu/hes/articles/kbdhlps02.pdf

Chapter 2: Electrical Conductive Poly(butadiene-*co*-acrylonitrile)-Polyaniline Dodecylbenzenesulfonate [NBR-PAni.DBSA] Blends prepared by Solution Mixing

2.1 Introduction

Reports relating to the study of different types of polyaniline (PAni)-based polymer blend can be found in the literature [1-27]. Different grades of commercially available nitrile rubber (NBR) and in-house synthesized dodecylbenzenesulfonic acid doped-PAni (PAni.DBSA) were selected in this part of work (as the rubber host and intrinsic electrically conductive filler respectively) due to their advantages as discussed in Section 1.4 and the literature [28-29].

Blends of various grades of NBR with PAni have previously been produced by basic mechanical mixing and electrochemical methods only. NBR of 29 wt% [NBR29] and 45 wt% [NBR45] ACN content were blended with PAni.HCl, PAni.DBSA, PAni.TPBSA and PAni.TSA respectively using a two roll-mill [1]. All the blends showed very low conductivities, ranging from only about 10^{-8} to 10^{-12} $S.cm^{-1}$. It was concluded that NBR45 was more compatible with PAni than was NBR29. Some more homogeneous films have been obtained [9] by grafting polyaniline with NBR29 through potentiodynamic or potentiostatic syntheses. The films were insoluble in toluene and in chloroform; they were of quite good quality, but the preparative method was inconvenient for practical purposes.

The aim of this part of the present work was to study electrically conductive blends produced by blending various grades of NBR with different amounts of PAni.DBSA. It was decided to produce blends from solution, which required that both components be soluble in a common solvent. This method has not previously been used to make NBR-based conductive blends. Characterisation of the resulting NBR-PAni.DBSA blends is reported here, using Fourier-transform infrared (FT-IR) spectroscopy, differential scanning calorimetry (DSC), determination of the electrical conductivity of pure polymers and blends and morphological study by optical and electron microscopy. The effects of

acrylonitrile composition on the morphology and electrical properties of the blends were important concerns of these studies.

2.2 Experimental

2.2.1 Chemicals and Raw Materials

Aniline monomer (99 wt%, Sigma-Aldrich), ammonium persulphate [APS] (98 wt%, Sigma-Aldrich), 36.5-38 wt% HCl solution (GPR), anhydrous ferric chloride [$FeCl_3$] (98 wt%, Sigma-Aldrich), 33 wt% ammonia solution (GPR), 70 wt% DBSA solution in 2-propanol (GPR, Sigma-Aldrich), chloroform (GPR), methanol (GPR) and several commercial grades of NBR [Krynac® 27.50, 34.50 and 50.75 (Bayer) and Breon® N41C45 (ZEON Chemicals)]. All grades of NBR were washed with methanol for 24h using Soxhlet extraction in order to remove chemical additives, prior to drying and use for making blends.

2.2.2 Calculation of Solubility Parameter Values for Main Materials

In order to estimate the solubility parameters for all the grades of pure NBR and PAni.DBSA, Equation 1.1 (Chapter 1) and the values of functional group molar attraction constants F_i calculated by Hoy [30] were used.

2.2.3 Stages of Preparation for Elastomer-Intrinsically Conductive Polymer Blends

2.2.3.1 Synthesis of PAni-Emeraldine Base (EB)

PAni.HCl was synthesised by oxidative chemical polymerisation. 50mL of aniline was dissolved in 375mL of 2M HCl and pre-cooled to 1°C. Based on the value of oxidant/monomer initial mole ratio (r) equal to 1.0, the solution of oxidant was prepared by dissolving 125.2g ammonium persulphate (APS) with 276 mL of

2M HCl and pre-cooled to 1°C. The oxidant solution was added gradually to the monomer solution over a period of about 20 minutes, with constant stirring by an overhead stirrer to ensure thorough mixing. The addition of oxidant caused a sudden increase in temperature. A few drops of ferric chloride solution were added to the polymerisation mixture as a catalyst.

The polymerisation mixture was maintained at temperature about 0 to 2°C with constant stirring in an ice bath, while the pH was adjusted to about 0 by adding a small amount of concentrated HCl. The mixture was left for 6h to complete the polymerisation. The mixture was then filtered and washed with 1500mL of 2M hydrochloric acid. The colour of the filtrate was reddish-pink due to the presence of soluble aniline oligomers. The mixture was washed with distilled water until the filtrate was colourless.

To prepare EB, wet PAni.HCl was deprotonated with a five times excess of ammonia (5000mL of ammonia aqueous solution was prepared from 80mL of 33 wt% ammonia) and was stirred for 24h. The resultant mixture was filtered and then washed with distilled water until the filtrate was colourless and no odour of ammonia could be detected. Wet EB was also washed with 750mL of acetone for purification, before being finally dried in a vacuum oven (at 50°C) until constant weight was obtained.

2.2.3.2 Preparation of PAni.DBSA

PAni.DBSA was prepared by protonating the pre-dried EB with aqueous solution of DBSA (prepared directly by using DBSA with 70 wt% solution in 2-propanol) at a molar ratio of EB : DBSA of 1 : 1 for 24h under magnetic stirring. The product was filtered and then washed with small quantities of distilled water (to avoid de-protonation of PAni.DBSA). The residue remained under suction by vacuum pump until cracks in the filter cake started to appear. A further 24h drying of the filter cake was carried out in a vacuum oven at 50°C.

2.2.3.3 Preparation of NBR-PAni.DBSA Blends

NBR-PAni.DBSA blends with following compositions (wt% NBR : wt% PAni.DBSA), 50:50, 60:40, 70:30, 80:20, 90:10, 95:5, 97.5:2.5 and 99:1 were prepared by solution mixing, and chloroform [with δ_s, 19 $(MJ.m^{-3})^{0.5}$] was selected as the shared solvent. In order to reduce the contamination (chemical additives) in raw NBR, 24h methanol washing was performed for each grade by Soxhlet extraction (as shown in Figure 2.1).

Figure 2.1: Setup of Soxhlet Extraction Apparatus

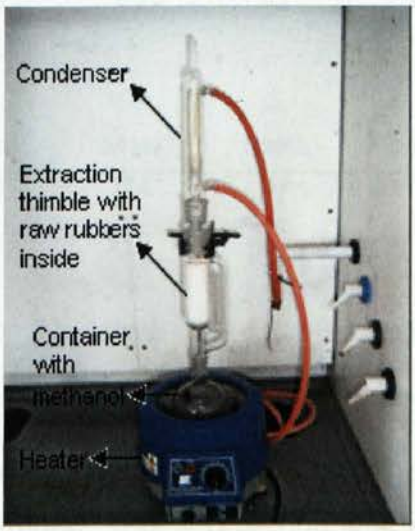

Masterbatch solutions for different grades of methanol-washed NBR and pure PAni.DBSA were prepared, based on the concentration of 0.05g NBR/mL solvent and 0.0167g PAni.DBSA/mL solvent respectively. In order to prepare the masterbatch solutions, each polymer was left to dissolve in chloroform for 36h at room temperature with the aid of a magnetic stirrer. In order to prepare the solution blends, calculated volumes of each polymer masterbatch solution were measured by pipette and were mixed in a conical flask. Each of the prepared blend solutions was also given a 5-minute ultrasonic bath treatment (Fisherbrand F11021 Ultrasonic) in order to enhance its homogeneity (all visually clear). Example formulations for blending different proportions of NBR and PAni.DBSA using the masterbatch solutions are shown in Table 2.1.

Table 2.1: General Formulation for preparing Blends with Different Proportions of NBR and PAni.DBSA by using Masterbatch Solutions

Volume/Weight	Proportion of blend (wt % of NBR : wt % of PAni.DBSA)					
	50:50	60:40	70:30	80:20	90:10	95:5
Volume of added NBR masterbatch solution, mL	4.0	4.0	4.0	4.0	6.0	6.0
Total mass of NBR in g	0.2000	0.2000	0.2000	0.2000	0.3000	0.3000
Volume of added PAni.DBSA masterbatch solution, mL	12.0	8.0	5.2	3.0	2.0	1.0
Total mass of PAni.DBSA in g	0.2000	0.1340	0.0868	0.0501	0.0334	0.0167
Total volume of prepared blend solution, V_{blend}, mL	16.0	12.0	9.2	7.0	8.0	7.0
Total mass of prepared blend in solution, W_{blend}, g	0.40	0.3340	0.2868	0.2501	0.3334	0.3167

The density for each blend with different proportions of NBR and PAni.DBSA was also estimated. This information was needed particularly for the electrical conductivity measurement in order to calculate the thickness of cast films of blend from solution. Equation 2.1 was used to calculate the density of each prepared blend (without solvent).

$$\rho_{blend} = \frac{100}{\left(\frac{a}{x} + \frac{b}{y}\right)} \qquad \text{(Equation 2.1)}$$

where; ρ_{blend} is estimated density of blend [kg.m^{-3}], a is the proportion of NBR [wt%], b is the proportion of PAni.DBSA [wt %], x is the density of each grade of pure NBR [kg.m^{-3}, as provided by manufacturer] and y is the measured density (from a vacuum-pumped pressed pellet) of PAni.DBSA [1134kg.m^{-3}]. Examples of

the calculated values of density for each blend with different proportion of added NBR and PAni.DBSA are shown in Table 2.2.

Table 2.2: Densities of Blends (with Different Proportions of Added NBR and PAni.DBSA) prepared from Masterbatch Solutions

Grade of Added NBR	Proportion of Added Polymers (wt % of NBR : wt % of PAni.DBSA)	Estimated Density of Blend, ρ_{blend} ($kg.m^{-3}$)
NBR Krynac®27.50	50:50	1040.0
($\rho_{NBR\ as\ provided\ by\ manufacturer}$= 960$kg.m^{-3}$)	60:40	1020.0
	70:30	1010.0
	80:20	990.0
	90:10	980.0
	95:5	970.0
NBR Krynac®34.50		
($\rho_{NBR\ as\ provided\ by\ manufacturer}$ = 980$kg.m^{-3}$)	50:50	1050.0
	60:40	1040.0
	70:30	1020.0
	80:20	1010.0
	90:10	1000.0
NBR BreonN41C45	95:5	990.0
($\rho_{NBR\ as\ provided\ by\ manufacturer}$= 1000$kg.m^{-3}$)		
	50:50	1060.0
	60:40	1050.0
	70:30	1040.0
	80:20	1020.0
NBR Krynac®50.75	90:10	1010.0
($\rho_{NBR\ as\ provided\ by\ manufacturer}$ = 1010$kg.m^{-3}$)	95:5	1000.0
	50:50	1070.0
	60:40	1060.0
	70:30	1040.0
	80:20	1030.0
	90:10	1020.0
	95:5	1010.0

2.2.4 Elemental Analysis

Samples of PAni.DBSA prepared as in Section 2.3.2 were submitted to Medac Ltd. for elemental analysis (carbon, hydrogen, nitrogen and sulphur). All these elemental analyses were done by using combustion technique with CE-440 and Carlo Erba analyser for CHN analysis and only Carlo Erba analyser for S

analysis. The uncertainty of CHN and S analyses are ±0.30% absolute and ±0.30% with detection limit <0.10% respectively. The theoretical percentage composition of PAni.DBSA was calculated and was compared with the experimental values (the experimental oxygen percentage in PAni.DBSA was calculated by difference, as is customary) in order to investigate the degree of protonation.

2.2.5 NMR Spectroscopy

NMR spectroscopy analyses (with ^{1}H NMR, Bruker model AC300 and processor, WIN NMR) for different grades of methanol-washed NBR were carried out at Tun Abdul Razak Research Centre (TARRC), Brickendonbury, Hertford in order to compare the actual value with the typical value provided by the manufacturer for acrylonitrile content.

About 5mg of sample was dissolved in d-chloroform before being examined by NMR (with 30° pulse and 6 sec pulse delay). In each case, 4 to 6 portions of the sample were examined. Estimation of the acrylonitrile content was based on integral measurements of the specific peaks assigned for butadiene (1,4 -CH=CH- and 1,2 -CH=CH_2 groups) and acrylonitrile (-CH-C≡N) respectively. The weight percentages of acrylonitrile (wt% ACN) and butadiene (wt% BD) in each sample were calculated by using Equations 2.2 to 2.7 as follows:

$$wt_{1,4\text{-}CH=CH\text{-}} = \{[(\text{Integral } P_{5.8\text{-}5.2\ p.p.m.}) / 2\} \times 54 \qquad \text{(Equation 2.2)}$$

$$wt_{1,2\text{-}CH=CH2} = [(\text{Integral } P_{5.2\text{-}4.8\ p.p.m.})/3] \times 54 \qquad \text{(Equation 2.3)}$$

$$wt_{\text{-}CH\text{-}C\equiv N} = (\text{Integral } P_{3.0\text{-}2.4\ p.p.m.}) \times 53 \qquad \text{(Equation 2.4)}$$

$$wt\%\ ACN = [wt_{\text{-}CH\text{-}C\equiv N} / (wt_{1,4\text{-}CH=CH\text{-}} + wt_{1,2\text{-}CH=CH2} + wt_{\text{-}CH\text{-}C\equiv N})] \times 100 \qquad \text{(Equation 2.5)}$$

$$wt\%\ Cis/Trans\ 1,4BD = [wt_{1,4\text{-}CH=CH\text{-}} / (wt_{1,4\text{-}CH=CH\text{-}} + wt_{1,2\text{-}CH=CH2} + wt_{\text{-}CH\text{-}C\equiv N})] \times 100 \qquad \text{(Equation 2.6)}$$

$$wt\%\ 1,2BD = [wt_{1,2\text{-}CH=CH2} / (wt_{1,4\text{-}CH=CH\text{-}} + wt_{1,2\text{-}CH=CH2} + wt_{\text{-}CH\text{-}C\equiv N})] \times 100 \qquad \text{(Equation 2.7)}$$

where; $wt_{1,4\ -CH=CH-}$ and $wt_{1,2\ -CH=CH2}$ are the relative weights of both functional groups assigned to butadiene, $wt_{-CH-C\equiv N}$ is the weight of functional group assigned to acrylonitrile, $P_{5.8-5.2\ p.p.m.}$, $P_{5.2-4.8\ p.p.m.}$ and $P_{3.0-2.4\ p.p.m.}$ are the areas of peaks assigned to the functional groups, i.e. cis/trans 1,4 -CH=CH-, 1,2 $-CH=CH_2$ and -CH-C≡N respectively, 54 and 53 are relative molecular masses for butadiene and acrylonitrile respectively.

2.2.6 Morphological Studies (Optical Microscopy and TEM)

NBR-PAni.DBSA blends were studied with a Nikon OPTIPHOT-2 optical microscope (magnification 200 times) linked to a computer by a video converter (LINKAM VTO 232) for digital image capture. A small drop of each sample blend solution was put onto a microscope cover-glass and allowed to evaporate to form a thin (3.0μm) transparent film. Blends with 5 wt% of PAni.DBSA (generally below the conductivity threshold) and 10 wt% (generally above the conductivity threshold) were also studied by TEM (with a Philips CM12 microscope at accelerating voltage, 80kV). An ultra-thin sample (150nm) of each blend was obtained for this purpose by sectioning with an RMC MT7000 microtome.

2.2.7 FT-IR Spectroscopy

FT-IR spectroscopy is a measurement technique for collecting IR spectra. Instead of recording the amount of energy absorbed when the frequency of the IR radiation is varied (monochromatic), the IR beam is guided through an interferometer. The essential experiment to obtain an FT-IR spectrum is to obtain an interferogram with and without a sample in the beam and transforming it into the spectrum of the source with sample absorptions and the source without sample absorptions [31]. This can be done by performing a mathematical Fourier transform [31] on the signal data (interferogram) into a spectrum which is identical to that of conventional (dispersive) IR spectroscopy.

IR spectra of PAni.DBSA, all the grades of pure NBR and NBR-PAni.DBSA blends were recorded on a Perkin-Elmer FT-IR Spectrometer PARAGON 100. A small amount of each sample solution was cast onto a KBr window in order to obtain a reasonably thin (3.0μm), transparent film.

2.2.8 Thermal Analysis

DSC is a technique in which the difference in heat flow (power) to a sample (in a pan) and to reference (empty pan) is monitored against time or temperature while the temperature of the sample, in a specified atmosphere, is programmed [32]. There are actually two types of DSC, i.e., power compensated DSC (sample and reference are heated by separated and individual heaters) and heat flux DSC (sample and reference are heated from the same source). The uses of DSC are to investigate the heat capacity, phase changes (T_g, glass transition temperature and T_m, melting point), reactions and calorimetry of the sample.

The PAni.DBSA powder, pure NBR and NBR-PAni.DBSA blend cast films were all characterised by heat flux DSC in this work. Above-ambient temperature (30 to 400°C), a Mettler Toledo DSC822e (heating rate 20°C/minute) was used, and sub-ambient temperature (-60 to 0°C), samples were characterised using a Perkin-Elmer Pyris Diamond DSC (heating rate 10°C/minute). Each sample was sealed in a 40μL aluminium pan and was analysed under N_2 atmosphere. An empty pan was used as the reference. Each thermal analysis was repeated twice, and the error for all of the results is believed to be ±1.5°C.

The onset temperature of the major exotherm was defined as the intersection of tangents drawn to the baseline and major exotherm slope at half height in the above-ambient temperature DSC thermograms. The onset temperature of the glass transition (Tg) was defined as the intersection of tangents drawn to the baseline and major "endotherm" slope at half height in the sub-ambient temperature DSC thermograms.

2.2.9 Electrical Conductivity Measurement

The electrical conductivity values (DC) for all raw materials and blends samples prepared in this work could be calculated from the electrical "resistance" (voltage/current) values measured by the van der Pauw four-probe technique. The van der Pauw method is a commonly used technique [28-29, 33], which characterises a sample of semiconductor material and can be successfully completed with a current source and a voltmeter. In order to use the van der Pauw method, the sample thickness must be much less than the width and length of the sample. In order to reduce errors in the calculations, it is preferable that the sample is symmetrical. There must also be no isolated holes within the sample. The equipment employed in this work was a Keithley 617 programmable electrometer coupled with Keithley 224 programmable current source. The current was passed through one pair of electrodes and the voltage recorded between an adjacent pair of electrodes.

The electrical resistance measurement setup for pure Pani.DBSA pressed pellet, 13mm in diameter, 1.5mm in thickness, prepared by using an evacuated KBr press at 10bars is shown in Figure 2.2. The pellet (assumed homogeneous and of uniform thickness) was placed in a PTFE holder with four metallic contact screws. Three electrical resistance measurements were recorded before the pellet was rotated 90 degrees, and a further three were taken.

Figure 2.2: Electrical Measurement Setup for the Pressed Pure PAni.DBSA Pellet

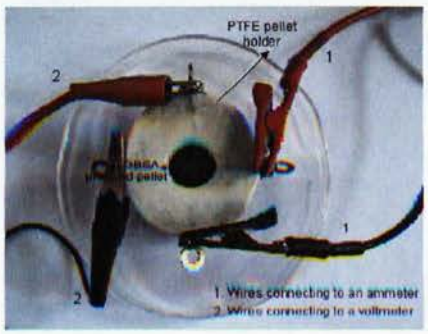

Setup of electrical "resistance" (voltage/current) measurement for the NBR-PAni.DBSA cast film on square microscopic slide ($6.25cm^2$) is shown in Figure 2.3 for 4-probe technique. Fine copper wire, with length about 5cm was stuck to each of the four corners of the cast film on a microscope slide using quick-drying silver paint (Acheson Electrodag 915). Three electrical resistance measurements were also recorded before the cast film was rotated 90 degrees and a further three were taken. 2-probe electrical resistance measurements (as shown in Figure 2.4) were performed for less conductive cast films ($\sigma < 10^{-7}S.cm^{-1}$), e.g. cast films of pure NBR and blends with small amounts of PAni.DBSA, by coating the opposite faces of each cast film with equal widths (5mm) of quick-drying silver paint.

Figure 2.3: Four Probe-Electrical Resistance Measurement Setup for the NBR-PAni.DBSA Cast Films on Microscopic Slide

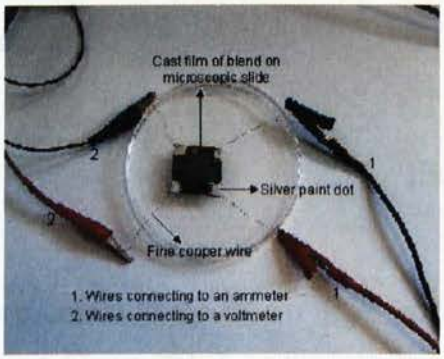

Figure 2.4: Two Probe-Electrical Resistance Measurement Setup for Less Conductive Cast Films on Microscopic Slide

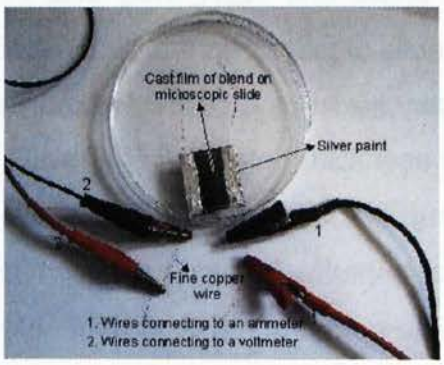

Electrical conductivities as measured by the 4-probe technique were calculated by using the van der Pauw equation (Equation 2.8).

$$\sigma = \frac{2ln2}{(R_1 + R_2)\pi df} \qquad \text{(Equation 2.8)}$$

where; σ is electrical conductivity [S.cm^{-1}], R_1 and R_2 are two average readings of measured "resistance" (voltage/current) for cast blend in its two different contact configurations [Ω], d is thickness of the sample [cm], and f is a geometric factor (approximately 1.00 for symmetrical contacts on circular pellets or square-shaped plaques).

Electrical conductivities as measured by the 2-probe method were calculated by using Equation 2.9.

$$\sigma = \left(\frac{1}{R}\right)\left(\frac{L}{A}\right) \qquad \text{(Equation 2.9)}$$

where; σ is the electrical conductivity [S.cm^{-1}], R is the measured resistance (voltage/current) of the cast blend [Ω], L is the electrode spacing distance [cm] and A is the cross-sectional area [cm^2] of the cast film between the electrodes.

In order to prepare cast films for pure NBR or for NBR-PAni.DBSA blends with thickness about 0.01 cm, pure NBR and blend solutions were dropped respectively (by using pipette) onto the microscopic slide and left for 24h. Each of this cast film was weighed until obtained a constant value in order to make sure all the solvent had gone. Cast films with even thickness were obtained by placing the microscope slide on a smooth and flat surface. Equation 2.10 and 2.11 were respectively applied to estimate the required volumes for pure NBR masterbatch ($V_{NBR\ solution}$) and for NBR-PAni.DBSA blend ($V_{blend\ solution}$) solutions in order to obtain cast films with a thickness of about 0.01cm. The values of estimated $V_{NBR\ solution}$ and $V_{blend\ solution}$ are listed in Table 2.3.

Table 2.3: $V_{NBR\ solution}$ (mL) and $V_{blend\ solution}$ (mL) Values in order to obtain Cast Film with Thickness, 0.01cm

Type of Cast Film *wt% NBR : wt% PAni.DBSA	$V_{NBR\ solution}$ or $V_{blend\ solution}$ (mL)
Pure NBR Krynac®27.50	1.20
Pure NBR Krynac®34.50	1.23
Pure NBR BreonN41C45	1.25
Pure NBR Krynac®50.75	1.26
Blends of Krynac®27.50 with PAni.DBSA	
50:50*	2.60
60:40*	2.30
70:30*	2.02
80:20*	1.73
90:10*	1.47
95:5*	1.34
Blends of Krynac®34.50 with PAni.DBSA	
50:50*	2.63
60:40*	2.34
70:30*	2.05
80:20*	1.77
90:10*	1.50
95:5*	1.37
Blends of BreonN41C45 with PAni.DBSA	
50:50*	2.65
60:40*	2.36
70:30*	2.09
80:20*	1.78
90:10*	1.51
95:5*	1.38
Blends of Krynac®50.75 with PAni.DBSA	
50:50*	2.68
60:40*	2.38
70:30*	2.09
80:20*	1.80
90:10*	1.53
95:5*	1.40

$$V_{NBR\ solution} = 0.0625 \left(\frac{\rho_{NBR}}{C_{NBR}}\right) \qquad \text{(Equation 2.10)}$$

where; $V_{NBR\ solution}$ is the volume required for each grade of pure NBR masterbatch solution [mL], 0.0625 is a constant [mL], ρ_{NBR} is the density of each grade of pure NBR [kg/mL] (as shown in Table 2.2) and C_{NBR} is the concentration of each pure NBR masterbatch solution (0.05g NBR/mL solvent).

$$V_{blend\ solution} = (0.0625 \times \rho_{blend})\left(\frac{V_{blend}}{W_{blend}}\right) \qquad \text{(Equation 2.11)}$$

where; $V_{blend\ solution}$ is the volume required for each blend solution [mL], 0.0625 is a constant [mL], ρ_{blend} is the estimated density of the relevant blend [kg/mL] (as shown in Table 2.2), V_{blend} is the total volume of blend solution with its chosen proportion of added polymers [mL] (as shown in Table 2.1) and W_{blend} is the total weight of prepared blend in solution [kg] (as shown in Table 2.1).

2.3 Results and Discussion

2.3.1 Determination of Solubility Parameter Values for Main Raw Materials

The calculated solubility parameter values for the main raw materials used in this project, i.e. different grades of NBR and pure PAni.DBSA, are summarised in Tables 2.4 and 2.5 respectively. The calculated PAni.DBSA solubility parameter has the same value as reported in literature [29]. It was predicted from the present data that the compatibility between NBR and PAni.DBSA could be enhanced by increasing the acrylonitrile content of NBR, i.e. by using the grades of NBR with high acrylonitrile content, e.g. NBR BreonN41C45 and NBR Krynac®50.75 in order to blend with PAni.DBSA.

Table 2.4: Calculation of Solubility Parameter Values from Molar Attraction Constants for NBR

Smallest repeat unit of NBR:

```
  H H H H H H
  | | | | | |
( -C-C=C-C-C-C- )n
  |       | | |
  H       H H C≡N
```

Molecular Weight of Butadiene = 0.054 kg/mol

Molecular Weight of Acrylonitrile = 0.053 kg/mol

2 possible forms of butadiene (BD), i.e. cis/trans 1,4BD and 1,2BD

Group	F_i $[(J.m^{-3})^{1/2}.m^3]/mol$	Numbers of Group	ΣF_i $[(J.m^{-3})^{1/2}.m^3]/mol$
For Cis/Trans 1,4BD:			
$-CH_2-$	269	2	538
-CH=olefin	249	2	498
			$\Sigma F_i=1036$
For 1,2BD:			
-CH2-	269	1	269
-CH-	176	1	176
=CH2	259	1	259
-CH=	249	1	249
			$\Sigma F_i=953$
For Acrylonitrile:			
$-CH_2-$	269	1	269
>CH-	176	1	176
-CN	725	1	725
			$\Sigma F_i=1170$

Details of Calculation

For Krynac®26, wt % Butadiene : wt % Acrylonitrile= 74:26, density as provided by manufacturer= 960.0kg.m^{-3} :
δ_p = [960.0 (1975.46)/1.861]/ [0.04012+0.01362] = ***19.0 (MJ.m^{-3})$^{1/2}$***

For Krynac®33, wt % Butadiene : wt % Acrylonitrile= 67:33, density as provided by manufacturer= 980.0kg.m^{-3} :
δ_p = [980.0 (2004.14)/1.863]/ [0.03613+0.01754] = ***19.6 (MJ.m^{-3})$^{1/2}$***

For BreonN41C45, wt % Butadiene : wt % Acrylonitrile= 59:41, density as provided by manufacturer= 1000.0kg.m^{-3} :
δ_p = [1000.0 (2030.92)/1.866]/ (0.03164+0.02194) = ***20.3 (MJ.m^{-3})$^{1/2}$***

For Krynac®49, wt % Butadiene : wt % Acrylonitrile= 51:49, density as provided by manufacturer= 1010.0kg.m^{-3} :
δ_p = [1010.0 (2053.93)/1.869]/ (0.02797+0.02555) = ***20.7 (MJ.m^{-3})$^{1/2}$***

Table 2.5: Calculation of Solubility Parameter Values from Molar Attraction Constants for PAni.DBSA

Smallest Repeat Unit of PAni.DBSA:

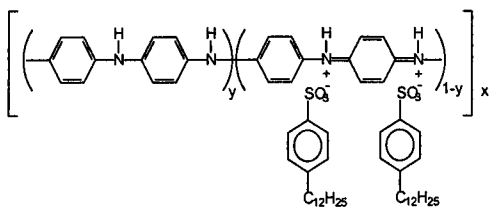

Molecular Weight of Smallest Repeat Unit of PAni.DBSA = 1.014 kg/mol

Group	F_i $[(J.m^{-3})^{1/2}.m^3]/mol$	Numbers of Group	ΣF_i $[(J.m^{-3})^{1/2}.m^3]/mol$
For EB:			
6-member ring	-48	4	-192
-CH=aromatic	240	12	2880
>CH=aromatic	201	6	1206
-NH-	368	2	736
-CH=olefin	249	4	996
>C=olefin	173	2	346
>N-	125	2	250
			ΣF_i=6222
For 2 x DBSA:			
6-member ring	-48	2	-96
-CH=aromatic	240	8	1920
>CH=aromatic	201	4	804
$-CH_2-$	269	22	5918
$-CH_3$	303	2	606
-S-	428	2	856
-O- (epoxide)	360	4	1440
-OH	462	2	924
			ΣF_i=12372

Details of Calculation

Density as measured from pressed pellet (vacuum sucked) of PAni.DBSA powder = 1134.0kg.m^{-3} :

δ_p = [1134.0 (6222 + 12372)]/ (1.014) = ***20.8 (MJ.m^{-3})$^{1/2}$***

2.3.2 Elemental Analysis

The theoretical and experimental percentage composition values for PAni.DBSA used in this project are summarised in Table 2.6. The theoretical formula of PAni.DBSA is $C_{30}H_{39}N_2SO_3$.

The empirical formula from the average found experimental results is $C_{30}H_{37.2}N_{2.3}S_{0.96}O_{3.16}$. The obtained empirical formula is slightly lower in H and in S. This is suggested to be due to traces of water and to the synthesised PAni.DBSA being slightly under-oxidised [29]. The atomic ratio of S to N is about 0.42, i.e. PAni.DBSA used in this project has 42% of protonation.

Table 2.6: The Theoretical and Experimental Molecular Weight Percentage Composition Values for PAni.DBSA

Element	C	H	N	S	O	Total
Theoretical (%)	70.97	7.74	5.51	6.31	9.47	100
Experimental (%), Average	70.40	7.34	6.36	6.00	9.90	100

2.3.3 NMR Spectroscopy

Selected NMR spectra for different grades of methanol-washed NBR are shown in Appendices 2.1 to 2.4. The calculated mean results (with uncertainty about ±2 wt%) are shown in Table 2.7. The acrylonitrile content of each grade of methanol-washed NBR as determined by NMR is consistent with the value quoted by the manufacturer. For grades of NBR with higher acrylonitrile content (BreonN41C45 and Krynac®50.75), the bonds, -CH-C≡N actually occurred in two environments because of increased chances of adjacent acrylonitrile

monomer groups in the co-polymer chain. These give slightly different chemical shifts (2.6 p.p.m. and 2.9 p.p.m.).

Table 2.7: Mean Weight Percentages (wt%) of Acrylonitrile (ACN) and Butadiene (BD) for Different Grades of Methanol-Washed NBR as analysed by NMR Spectroscopy

Grade of NBR	Provided ACN content from Manufacturer, wt%	Detected wt% by NMR Spectroscopy, %		
		ACN	Cis/Trans 1,4 BD	1,2 BD
Krynac®27.50	26	25.7	63.0	11.3
Krynac®34.50	33	33.1	60.4	6.5
BreonN41C45	41	41.4	53.9	4.7
Krynac®50.75	48.5	48.2	49.3	2.5

2.3.4 Morphological Studies (Optical Microscopy and TEM)

All the NBR-PAni.DBSA blends were studied by optical microscopy, but only images of blends containing 5, 20, 30 and 40 wt% of PAni.DBSA prepared with 25.7 and 48.2 ACN wt% rubbers are shown here (Figs. 2.5 and 2.6 respectively). Two visually distinct regions were observed, i.e. pale-green and dark-green.

On increasing the proportion of PAni.DBSA, the area of the dark-green region increases, as would be expected for a classical particulate composite with a metal or graphite filler rather than a polymer blend. There are also some large particles present even at fairly low loadings (e.g. 5 wt%). However, on the basis of the evidence presented below, we believe that there is significant compatibility between the polymers. The 5 wt% blends appear to contain isolated PAni.DBSA particles, and so should be well below the percolation threshold for conductivity;

nevertheless it will be seen below that there is significant residual conductivity in these samples (see Figure 2.14).

Figure 2.5: Optical Micrographs (200 x Magnification) for the Blends of NBR 25.7 ACN wt% and PAni.DBSA. Blends contain, (a) 60 wt% NBR:40 wt% PAni.DBSA, (b) 70 wt% NBR:30 wt% PAni.DBSA, (c) 80 wt% NBR:20 wt% PAni.DBSA and (d) 95 wt% NBR:5 wt% PAni.DBSA

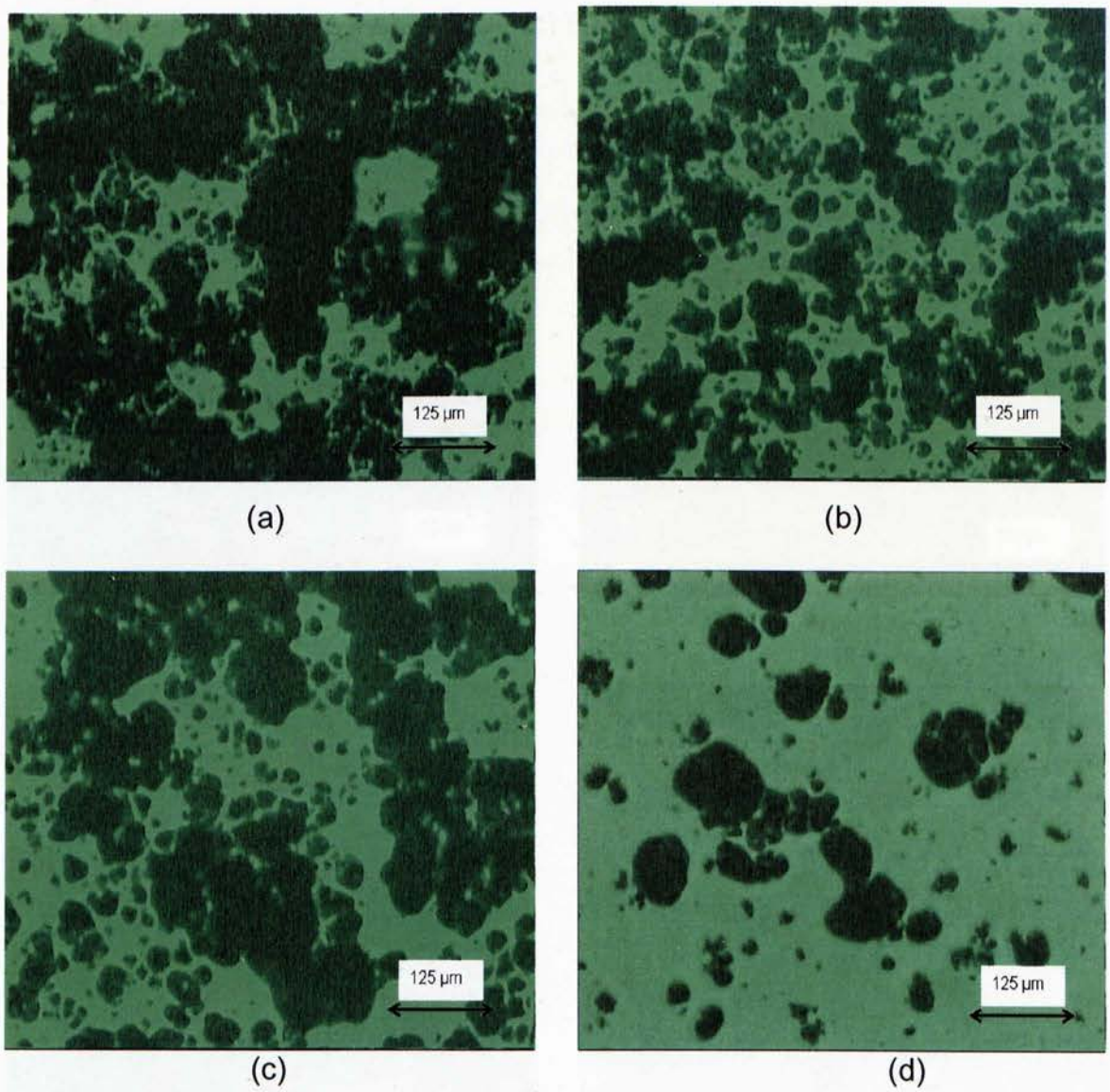

The dark green-regions (rich in PAni.DBSA) are large conductive particles and their agglomerates, resulting from some degree of phase separation. The pale-green regions (rich in NBR) are related to well-blended PAni.DBSA and NBR.

Blends containing NBR with lower ACN contents (25.7 and 33.1 wt%) showed more obvious phase separation than those richer in ACN (41.4 and 48.2 wt%). The two phases also appear to have a larger area of contact in the case of the ACN-rich NBR blends.

Figure 2.6: Optical Micrographs (200 x Magnification) for the Blends of NBR 48.2 ACN wt% and PAni.DBSA. Blends contain, (a) 60 wt% NBR:40 wt% PAni.DBSA, (b) 70 wt% NBR:30 wt% PAni.DBSA, (c) 80 wt% NBR:20 wt% PAni.DBSA and (d) 95 wt% NBR:5 wt% PAni.DBSA

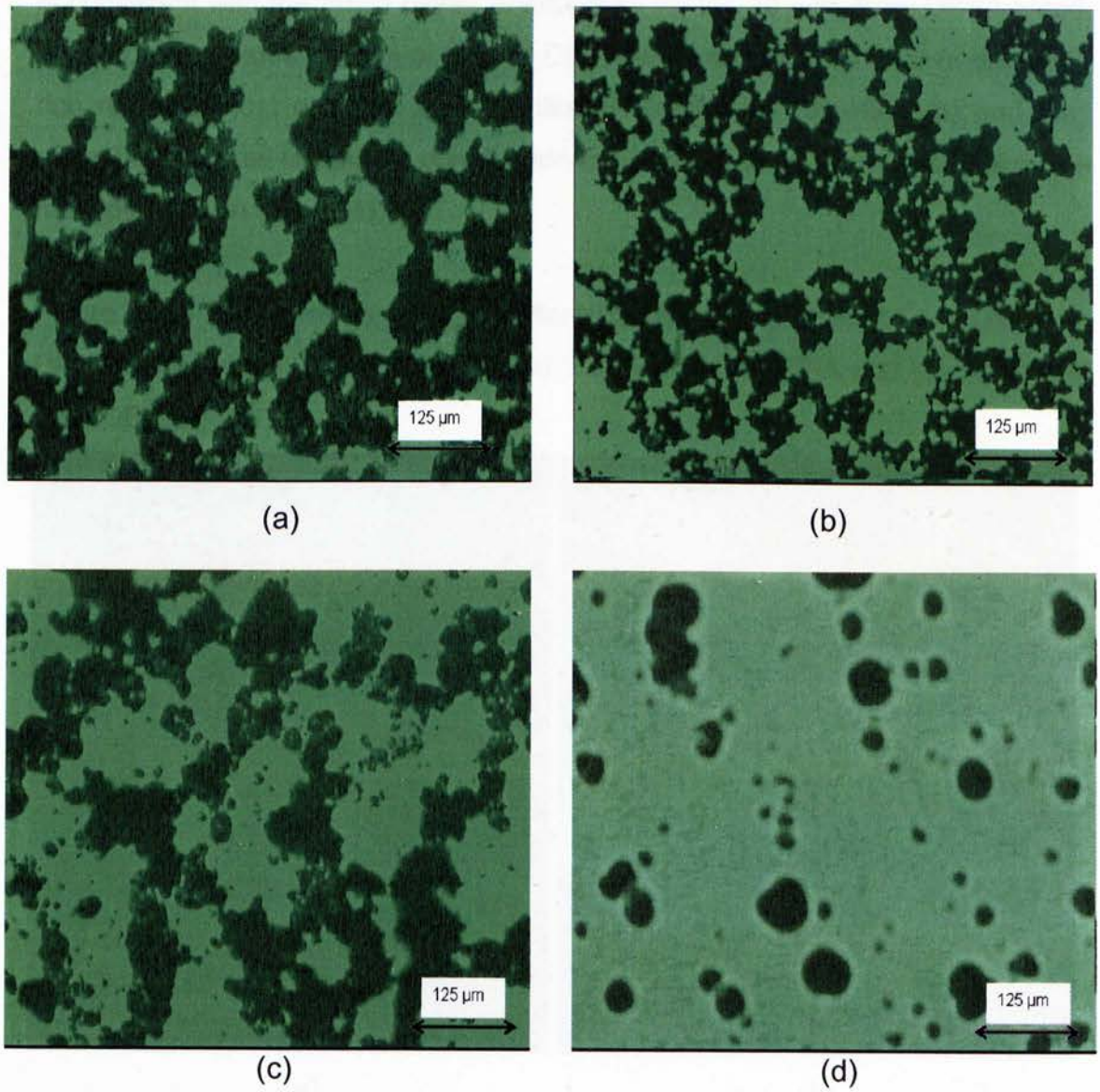

Examples of transmission electron micrographs of blends (5 and 10 wt% PAni.DBSA, prepared with NBR 41.4 ACN wt%) are shown in Fig. 2.7. The darker regions of both TEM micrographs are again related to conductive PAni.DBSA particles in an NBR matrix. Relatively large isolated polyaniline particles are observed in Fig. 2.7(a), which is consistent with the fairly low electrical conductivity of the 5wt% PAni.DBSA blend (see section 2.3.7). In Fig. 2.7(b), the PAni.DBSA particles are starting to cluster or to form conductive pathways, which is consistent with the much higher conductivity for the 10 wt% PAni.DBSA blend. Numerous very small particles of PAni.DBSA were revealed by TEM in the NBR-rich regions; most of these are of colloidal dimensions (50-1000nm) and they might be expected to make a contribution to electrical conductivity even below the main percolation threshold.

Figure 2.7: Transmission Electron Micrographs of the NBR 41.4 ACN wt%-PAni.DBSA Blends. Blends contain, (a) 5 wt% of PAni.DBSA and (b) 10 wt% of PAni.DBSA

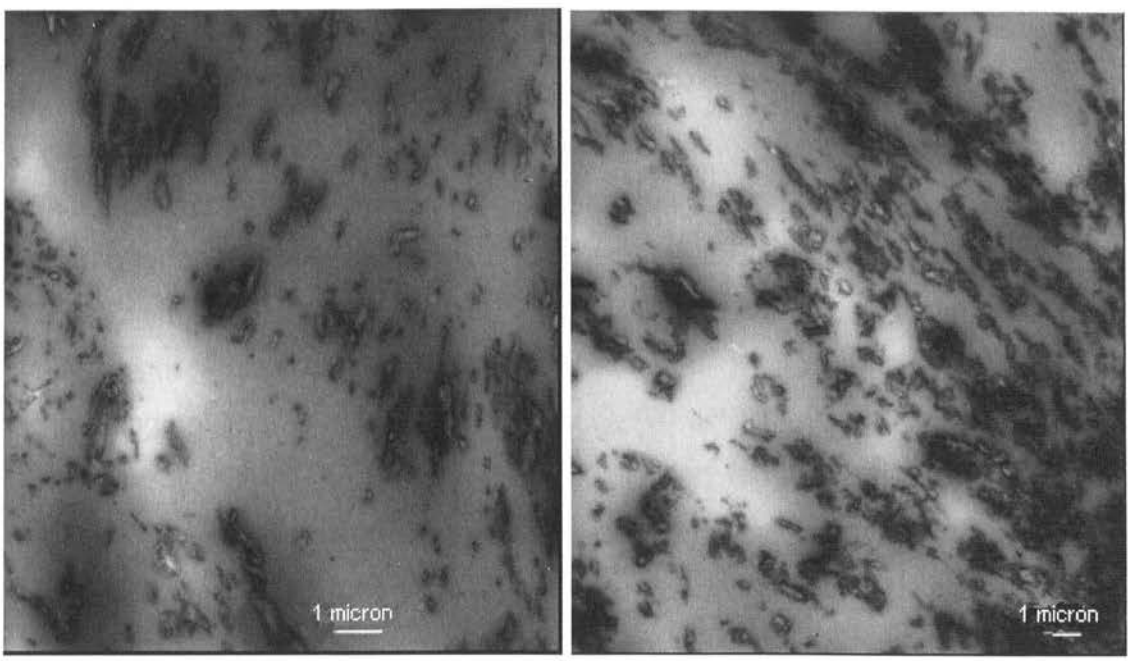

(a) (b)

2.3.5 FT-IR Spectroscopy

Examples of FT-IR spectra for PAni.DBSA, pure NBR 25.7 ACN wt% and their blends (with 10 wt% and 40 wt% of PAni.DBSA) are shown in Fig. 2.8. Examples of FT-IR spectra for PAni.DBSA, pure NBR 48.2 ACN wt% and their blends (with 10 wt% and 40 wt% of PAni.DBSA) are shown in Fig. 2.9.

FT-IR spectra for cast films of all grades of pure NBR show the characteristic absorptions at 2237cm^{-1} (-C≡N stretching), 1630cm^{-1} (C=C stretch) and 1440-1445cm^{-1} (out of plane C-H wagging). The spectrum of PAni.DBSA cast film has characteristic absorptions at 3447cm^{-1} (=N-H stretching), 1559cm^{-1} (N=quinoid=N), 1478cm^{-1} (N-benzoid-N), 1295cm^{-1} (quinoid=N-benzoid), 1240cm^{-1} (C aromatic-N stretching) and 1030cm^{-1} (S=O stretching).

At first sight, the FT-IR spectra of the blend films are merely superpositions of the spectra for both polymers, but detailed examination reveals significant shifts of certain key bands; the mixing of the two blended components may be assessed by studying some of these (Table 2.8). The bands at 3447cm^{-1} (N-H stretching) and 1030cm^{-1} (S=O stretching) are solely attributed to PAni.DBSA, while that at 2237cm^{-1} derives from NBR.

In the spectra of the blends, all these bands have intensities comparable to those for the pure materials, but two large, opposing peak shifts can be observed (a decrease to 3411-3423cm^{-1} for the N-H stretch and an increase to 1080cm^{-1} for the S=O stretch), attributable to changes in the intermolecular interactions. The peak positions for all the dilute blends largely revert to those of the pure conducting polymer at higher concentrations (40 wt% PAni.DBSA and above).

In pure PAni.DBSA, the positively charged N-H hydrogens would have a strong propensity for hydrogen-bonding with the negative sulfonate oxygens, and the infrared frequency changes suggest that this bonding is disrupted by polar interactions with the rubber matrix in the dilute, well-dispersed blends. The larger, more aggregated particles in the concentrated blends (section 3.4) are likely to have much smaller specific surface areas, and therefore strong H-bonding characteristic of bulk PAni.DBSA is again detected in the IR spectra.

Figure 2.8: FT-IR Spectra for PAni.DBSA, Pure NBR 25.7 ACN wt% and Their Blends (with 10 wt% and 40 wt% of added PAni.DBSA). (a) Region 1000cm^{-1} to 1650cm^{-1}, (b) Region 2150cm^{-1} to 2300cm^{-1} and (c) Region 3400cm^{-1} to 3470cm^{-1}

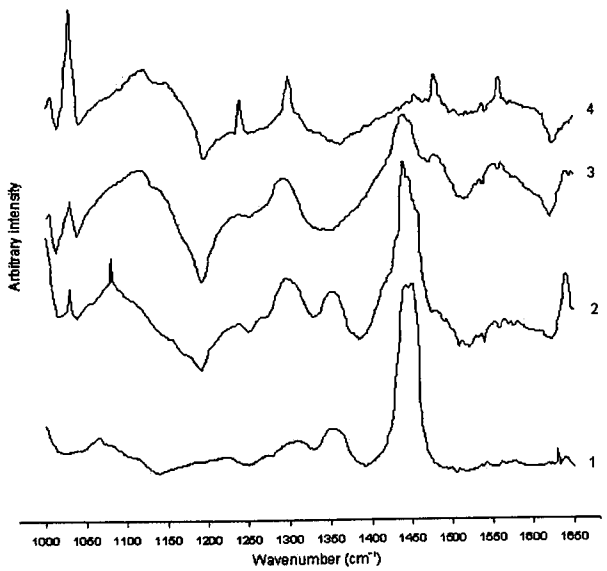

(a)

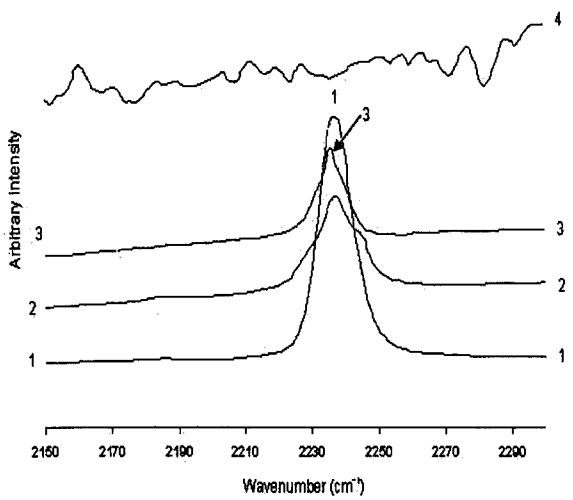

(b)

1-Pure NBR 25.7 ACN wt%

2-Blend with 10 wt% of added PAni.DBSA

3-Blend with 40 wt% of added PAni.DBSA

4-PAni.DBSA

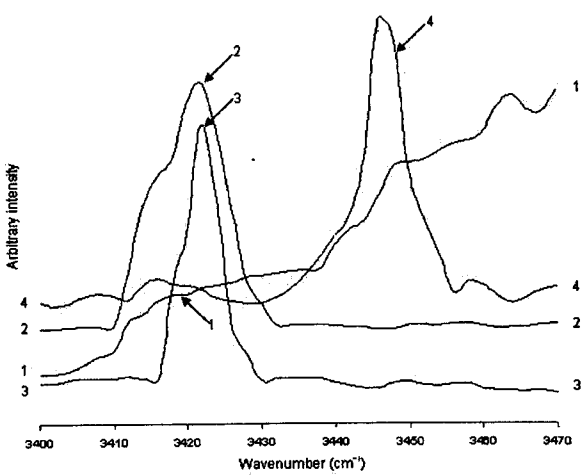

(c)

Figure 2.9: FT-IR Spectra of PAni.DBSA, Pure NBR 48.2 ACN wt% and Their Blends. (a) Region 1000cm^{-1} to 1650cm^{-1}, (b) Region 2150cm^{-1} to 2300cm^{-1} and (c) Region 3400cm^{-1} to 3470cm^{-1}

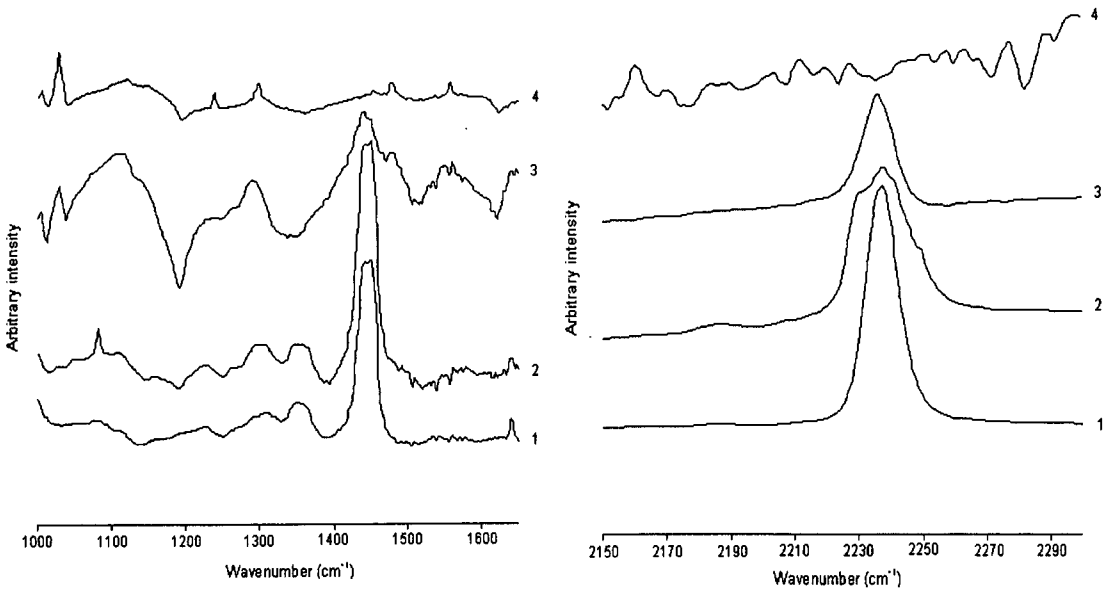

(a) (b)

1-Pure NBR 48.2 ACN wt%

2-Blend with 10 wt% of PAni.DBSA

3-Blend with 40 wt% of PAni.DBSA

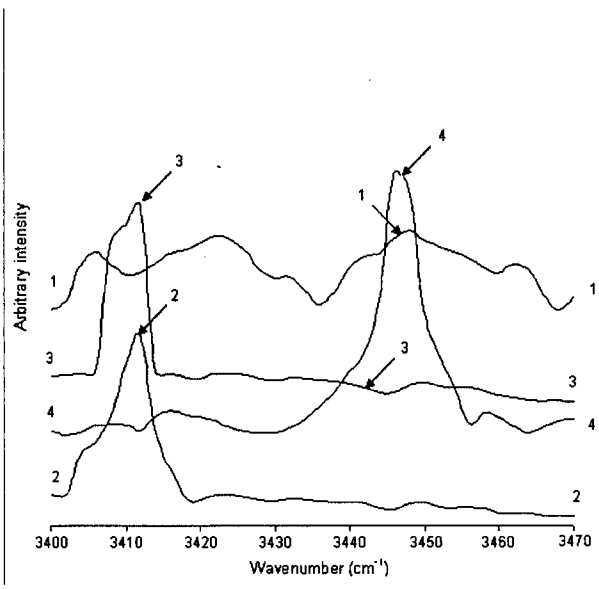

(c)

Table 2.8: Representative IR Absorption Peaks for PAni.DBSA, All Grades of Pure NBR and the Various NBR-PAni.DBSA Blends

Pure material or blend (wt% NBR: wt% PAni.DBSA)	Peak assignment, cm^{-1} Indication of peak intensity: W=weak; M=medium		
	=N-H stretching	S=O stretching	-C≡N stretching
PAni.DBSA	3447W	1030M	-
NBR 25.7 ACN wt%	-	-	2237M
NBR 33.1 ACN wt%	-	-	2237M
NBR 41.4 ACN wt%	-	-	2237M
NBR 48.2 ACN wt%	-	-	2237M
Blends with NBR 25.7 ACN wt%			
90:10	3423W	1030W,1080W	2237W
80:20	3423W	1030W,1080W	2237W
70:30	3419W	1030W,1080W	2237W
60:40	3423W	1030W	2236W
50:50	3440W	1030W	2236W
Blends with NBR 33.1 ACN wt%			
90:10	3417W	1080W	2237W
80:20	3417W	1080W	2237W
70:30	3413W	1080W	2237W
60:40	3423W	1030W	2236W
50:50	3440W	1030W	2236W
Blends with NBR 41.4 ACN wt%			
90:10	3411W	1080W	2237W
80:20	3411W	1080W	2237W
70:30	3407W	1080W	2236W
60:40	3423W	1029W	2236W
50:50	3437W	1029W	2236W
Blends with NBR 48.2 ACN wt%			
90:10	3411W	1081W	2237W
80:20	3411W	1081W	2237W
70:30	3407W	1081W	2236W
60:40	3412W	1029W	2236W
50:50	3437W	1029W	2236W

2.3.6 Thermal Analysis

Figs. 2.10 and 2.11 show examples of the sub-ambient temperature DSC thermograms for two grades of pure NBR (with 25.7 and 48.2 ACN wt%) and their blends with 10 to 50 wt% of PAni.DBSA. (A DSC thermogram for pure PAni.DBSA is not shown here because there were no obvious thermal processes in the low-temperature region). Figs. 2.12 and 2.13 show examples of the above-ambient temperature DSC thermograms for PAni.DBSA, two grades of pure NBR and their blends with 10 to 50 wt% of the conducting polymer.

The calculated mean Tg values for all the pure NBR grades and NBR-PAni.DBSA blends are shown in Table 2.9. The higher acrylonitrile content of NBR produces a higher Tg due to the rigidity of the acrylonitrile blocks in the copolymer [34]. The sub-ambient temperature DSC thermograms of the blends have positive Tg shifts for the NBR component that increase with the proportion of PAni.DBSA up to 30 wt%, and then decrease when 40 wt% or more is added. This would be consistent with the existence of effective dispersion of the conducting polymer at low concentrations, followed by more complete phase separation between the two components at the higher levels of PAni.DBSA.

Table 2.9: The Mean Glass Transition Temperature (Tg) Values for All Grades of Pure NBR and for NBR-PAni.DBSA Blends

Composition (wt% NBR: wt% PAni.DBSA)	Glass transition temperature, °C			
	Blend with NBR 25.7 ACN wt%	Blend with NBR 33.1 CAN wt%	Blend with NBR 41.4 ACN wt%	Blend with NBR 48.2 ACN wt%
Pure NBR	-46	-36	-20	-11
90:10	-46	-35	-19	-8
80:20	-46	-34	-17	-8
70:30	-43	-32	-16	-7
60:40	-45	-34	-18	-8
50:50	-46	-35	-18	-8

All the above-ambient temperature DSC thermograms for the blends show thermal processes that are combinations of events recorded for pure NBR and PAni.DBSA, but the events show some degree of temperature shift relative to the corresponding processes in the pure polymers. As indicated by the data in Table 2.10, all grades of pure NBR were thermally stable up to about 320°C. The PAni.DBSA also had good thermal stability up to about 233°C.

With the caveat that the polymers are approaching the onset of thermal decomposition, some indication of the high-temperature compatibility of PAni.DBSA with NBR in their blends may also be gained from the onset temperatures shown in Table 2.10. For high proportions of PAni.DBSA (40 to 50 wt%), only small shifts in the onset temperature of the major exotherm (w.r.t. that for pure PAni.DBSA) are observed. The blends containing low to moderate amounts of PAni.DBSA (10 to 30 wt%) showed large shifts in the onset temperature of the major exotherm, supporting the other evidence for better mixing in these blends at room temperature and below.

Table 2.10: The Mean Onset Temperature Values of Major Exotherms for the Above-Ambient Temperature DSC Thermograms of PAni.DBSA, Pure NBR and NBR-PAni.DBSA Blends

Composition (wt% NBR: wt% PAni.DBSA)	Onset temperature of major exotherm, °C			
	Blend with NBR 25.7 ACN wt%	Blend with NBR 33.1 ACN wt%	Blend with NBR 41.4 ACN wt%	Blend with NBR 48.2 ACN wt%
Pure NBR	335	330	325	331
90:10	334	324	257	263
80:20	324	323	241	240
70:30	233	232	224	222
60:40	231	239	240	246
50:50	237	237	238	229
PAni.DBSA	233	233	233	233

Figure 2.10: Sub-Ambient Temperature DSC Thermograms for Different Compositions (wt% NBR:wt% PAni.DBSA*) of NBR-PAni.DBSA Blends prepared with Pure NBR 25.7 ACN wt%

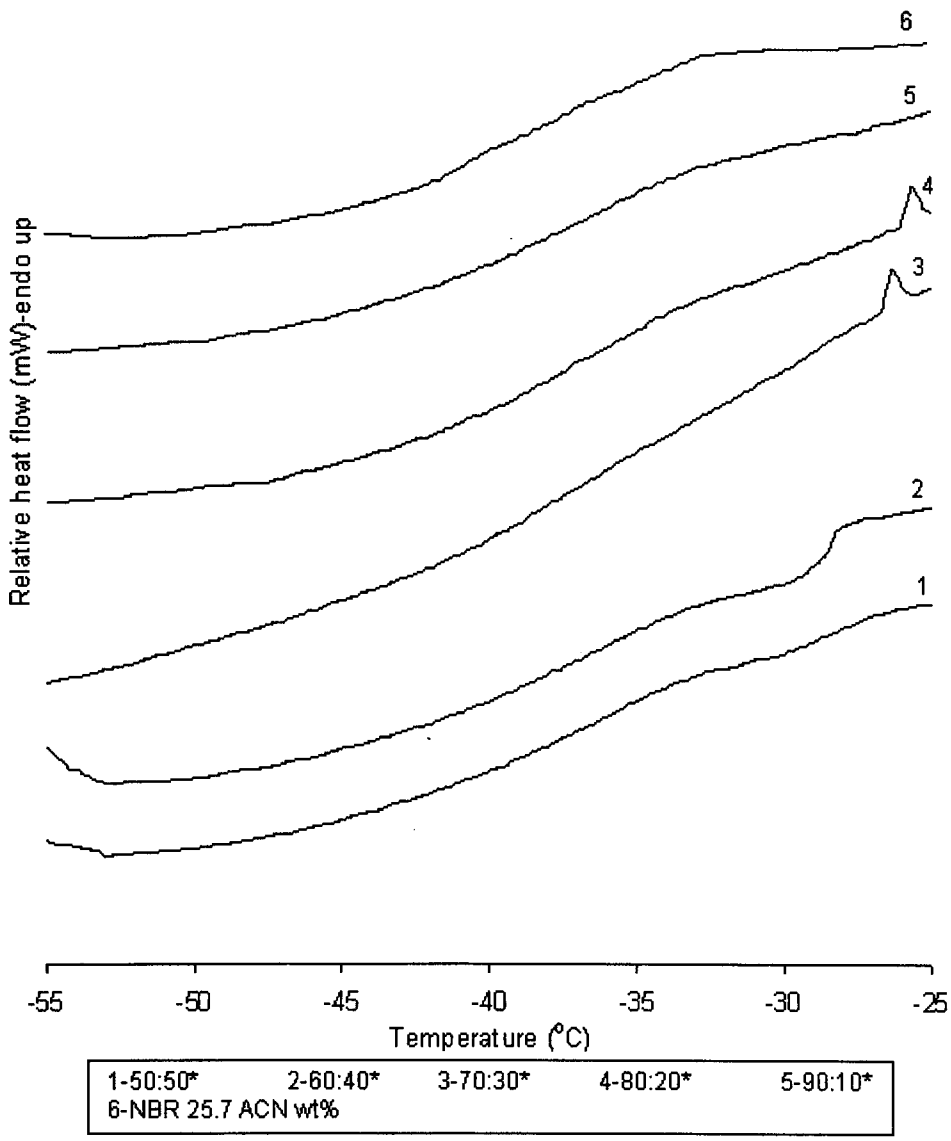

Figure 2.11: Sub-Ambient Temperature DSC Thermograms for NBR-PAni.DBSA Blends of Different Composition (wt% NBR:wt% PAni.DBSA*) prepared with Pure NBR 48.2 ACN wt%

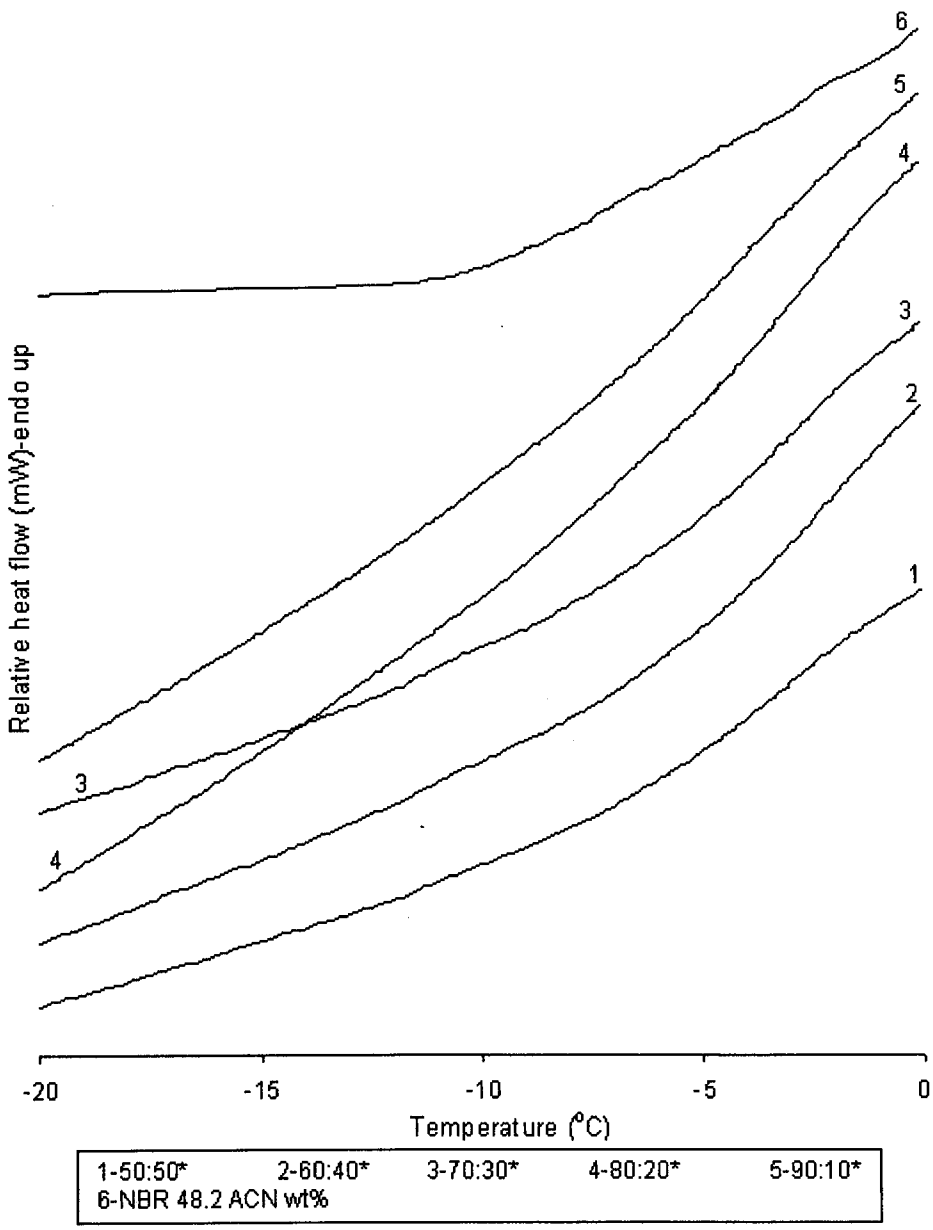

Figure 2.12: Above-Ambient Temperature DSC Thermograms for PAni.DBSA, Pure NBR 25.7 ACN wt% and Different Compositions (wt% NBR: wt% PAni.DBSA*) of Their Blends

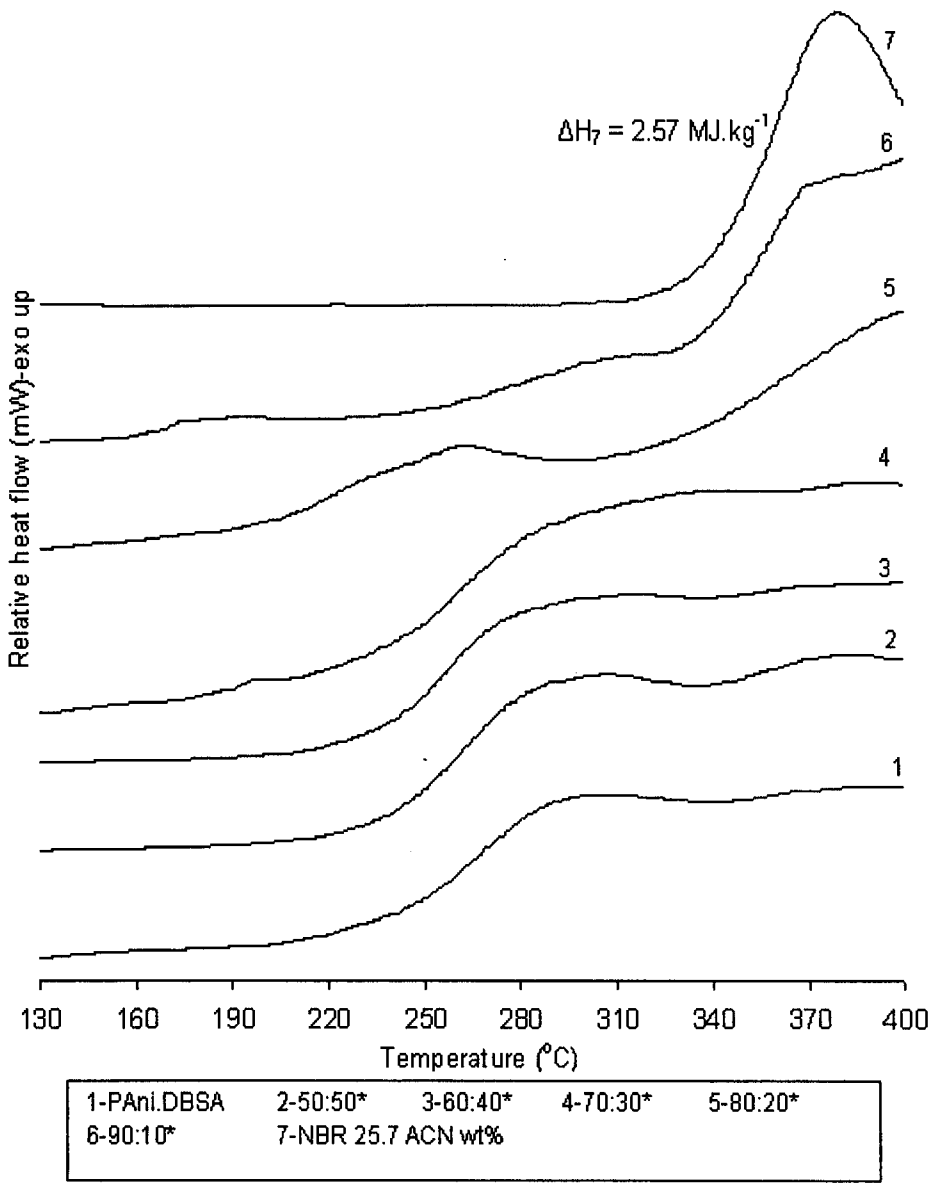

Figure 2.13: Above-Ambient Temperature DSC Thermograms for Pure NBR 48.2 ACN wt% and Different Compositions (wt% NBR:wt% PAni.DBSA*) of NBR-PAni.DBSA Blends prepared with Pure NBR 48.2 ACN wt%

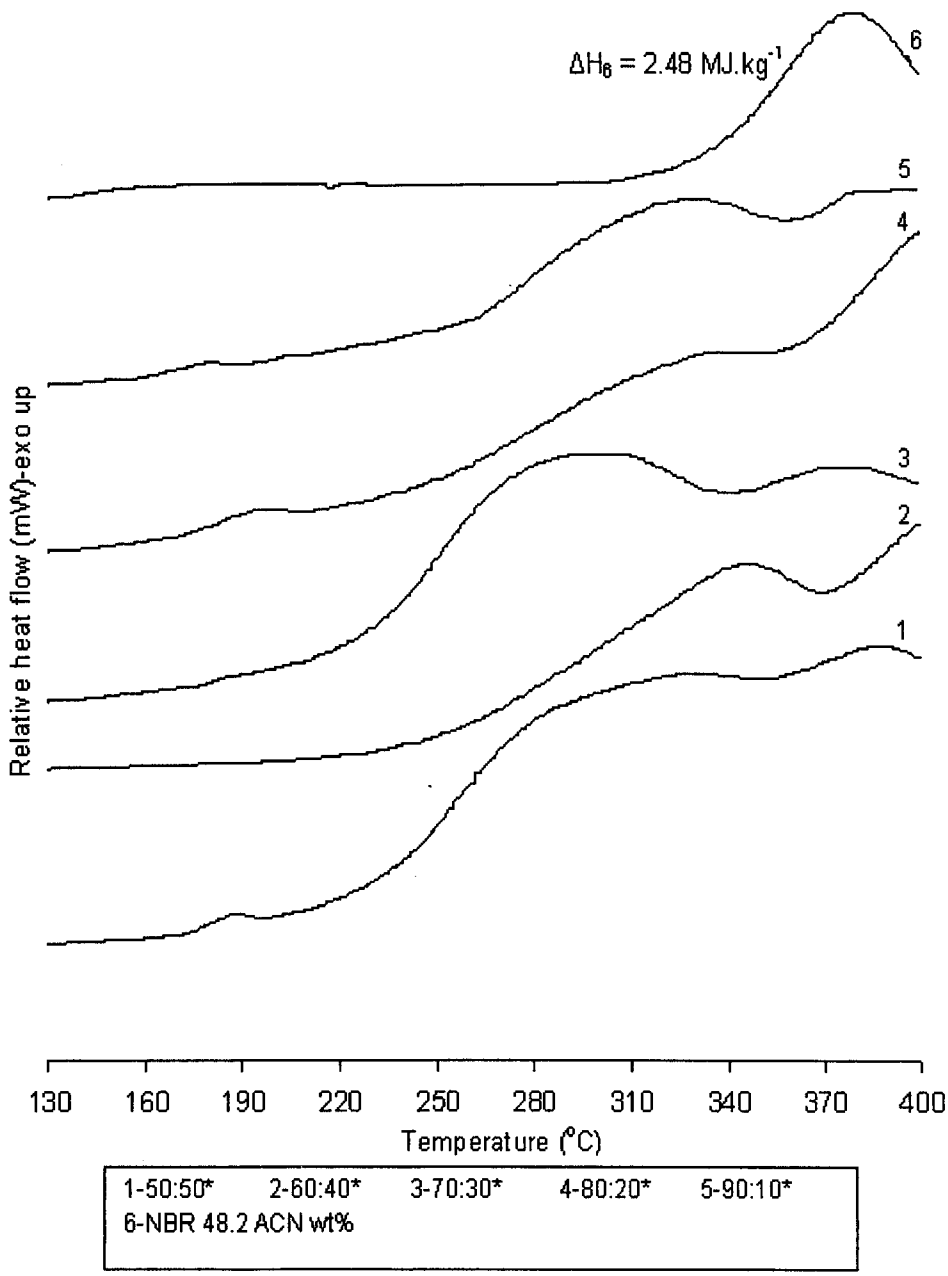

2.3.7 Electrical Conductivity Measurement

The calculated electrical conductivity values for pure PAni.DBSA, the various grades of pure NBR and blends with different proportions of NBR and PAni.DBSA are shown in Fig. 2.14. Clearly all grades of pure NBR are very good electrical insulators, with conductivities in the region of 10^{-14}S.cm^{-1}. The PAni.DBSA used in this project had a reasonably high electrical conductivity of 1.2 ± 0.5S.cm^{-1}, comparable with literature values for pressed pellet samples [28-29]. The pure conducting polymer did not form films very reproducibly, but its film conductivity was nevertheless very high (>100S.cm^{-1}) [35].

Figure 2.14: Electrical Conductivities for the Different Grades of NBR-PAni.DBSA Blends as A Function of PAni.DBSA Content (wt%)

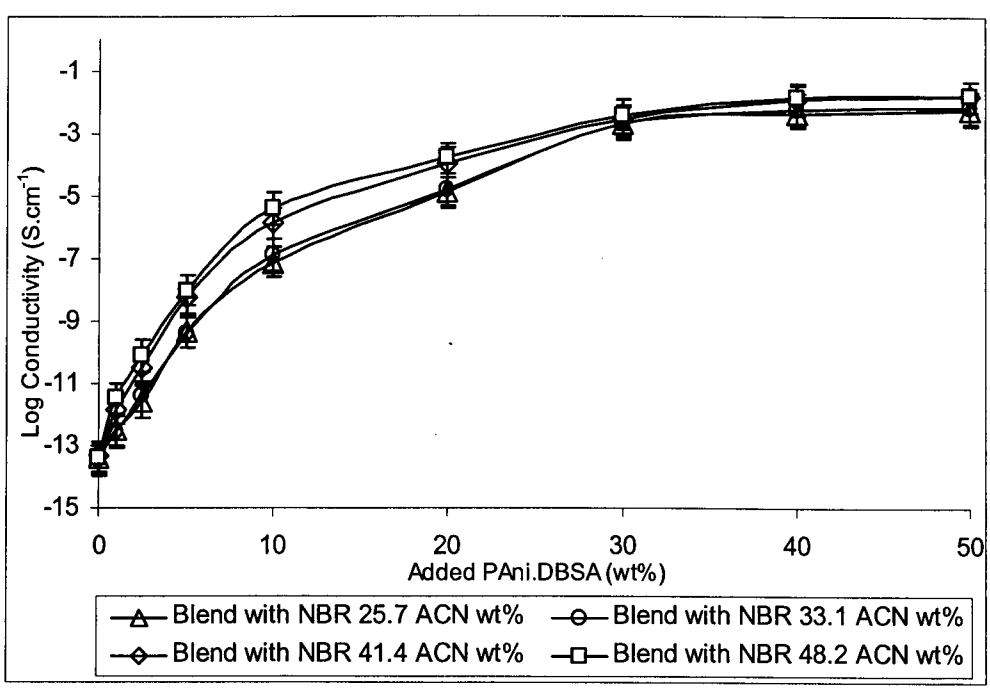

The electrical conductivity of all the blends increased with the proportion of PAni.DBSA, as observed in several studies of PAni.DBSA blends [1, 5, 8, 36-37]; however, the compatibility of the blended polymers was greater in the present work, and the properties of the blends were quite distinctive.

Blends prepared from NBR with higher ACN contents, i.e. 41.4 and 48.2 ACN wt%, had higher electrical conductivities (up to about 10^{-2}S.cm^{-1}) than those prepared with NBR of lower ACN content, i.e. 25.7 and 33.1 wt% (up to about 10^{-3}S.cm^{-1}). Vallim [1] made a similar observation for two NBR-PAni.DBSA blends prepared by basic mechanical mixing. Hence the blends with less phase separation were found to have higher electrical conductivity. This suggests either that the more compatible host material favours the formation of microscopic conductive pathways, or that the well-dispersed PAni.DBSA species within the NBR-rich regions are assisting the process of bulk charge transport.

The conductivity percolation threshold for each family of blends (prepared with same grade of NBR) was estimated by fitting the data from Fig. 2.14 to a simple percolation model as defined by Equation 2.12 [8, 38].

$$\sigma_f = c(f - f_p)^t \qquad \text{(Equation 2.12)}$$

where; c is a constant, t is the critical exponent, f is the volume fraction of the conductive medium and f_p is the volume fraction at the percolation threshold. All the weight fractions referred to above were converted into volume fractions for this analysis. By fitting the data to a plot of log electrical conductivity (σ) versus log (f-f_p), it was possible to estimate the values of t and correlation coefficient (R) for each case (see Figure 2.15). The estimated first stage of electrical conductivity percolation thresholds (in wt% and volume% of PAni.DBSA) are shown in Table 2.11.

Reasonably low electrical conductivity percolation thresholds can evidently be achieved by using NBR with high ACN contents, i.e. 41.4 and 48.2 wt%. All blends also showed a second stage of percolation threshold with higher adding of PAni.DBSA (see Table 2.12) which corresponded to the separated phases, i.e. the dark green regions as shown in optical and electron micrographs.

However, a simple percolation model for conductive particles in an insulating matrix does not fit the data for the dilute polyaniline blends. The very tiny (50-1000nm) particles of PAni.DBSA revealed by TEM microscopy probably

provide the small, but significant conductivity observed in blends having 1-5 wt% loadings of conducting polymer – well below the main percolation threshold. It is proposed that these colloidal-sized particles mediate conductive path formation between the larger particles of PAni.DBSA down to very low loadings.

Table 2.11: First Stage of Electrical Conductivity Percolation Thresholds for Different Grades of NBR-PAni.DBSA Blends

Grade of NBR	Estimated percolation threshold, (wt%/volume% of PAni.DBSA content)	Critical exponent, *t*	Correlation coefficient, *R*
NBR 25.7 ACN wt%	7.5/6.4	4.2	0.98
NBR 33.1 ACN wt%	7.5/6.4	4.1	0.98
NBR 41.4 ACN wt%	6.6/5.8	3.8	0.99
NBR 48.2 ACN wt%	6.0/5.4	3.6	0.99

Table 2.12: Second Stage of Electrical Conductivity Percolation Thresholds for Different Grades of NBR-PAni.DBSA Blends

Grade of NBR	Estimated percolation threshold, (wt%/volume% of PAni.DBSA content)	Critical exponent, *t*	Correlation coefficient, *R*
NBR 25.7 ACN wt%	13.5/11.5	4.5	0.98
NBR 33.1 ACN wt%	13.5/11.5	4.5	0.97
NBR 41.4 ACN wt%	10.0/8.8	1.8	0.96
NBR 48.2 ACN wt%	9.6/8.6	1.8	0.96

Figure 2.15: Log Electrical Conductivity (σ) vs. Log (f-f_p) Charts for Different Grades of Solution Mixed NBR-PAni.DBSA Blends. Blends contain; (a) NBR 25.7 ACN wt%, (b) NBR 33.1 ACN wt%, (c) NBR 41.4 ACN wt% and (d) NBR 48.2 ACN wt%

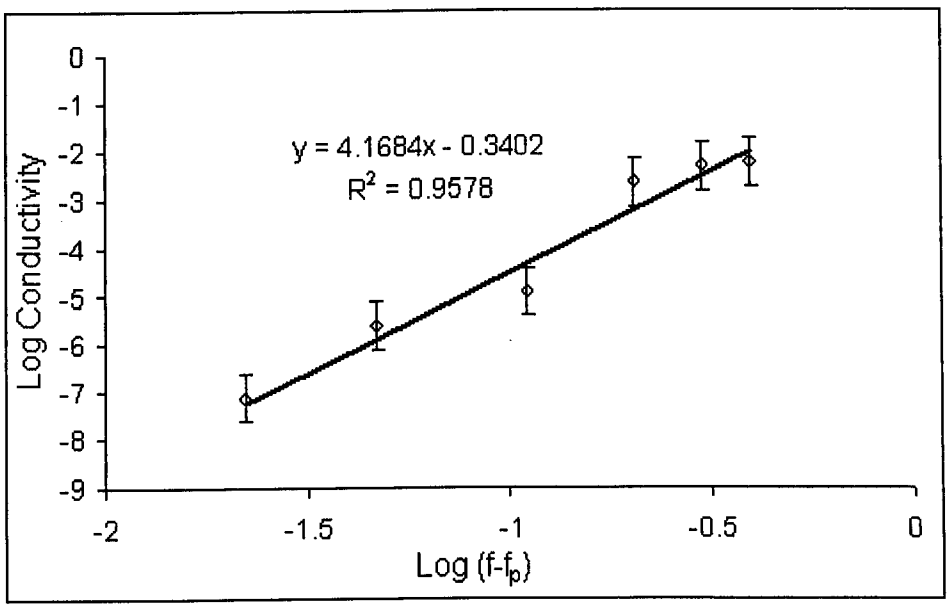

(a)

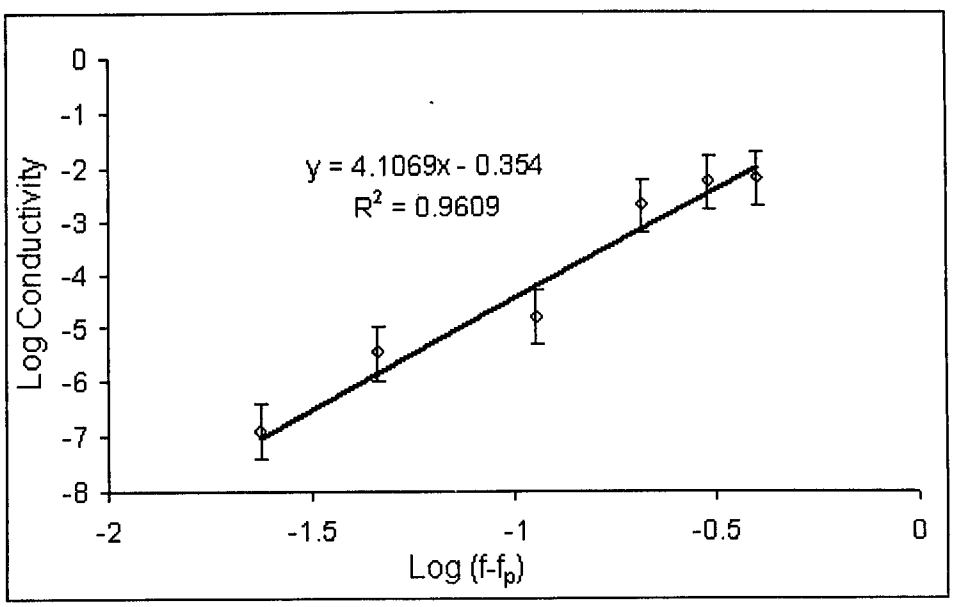

(b)

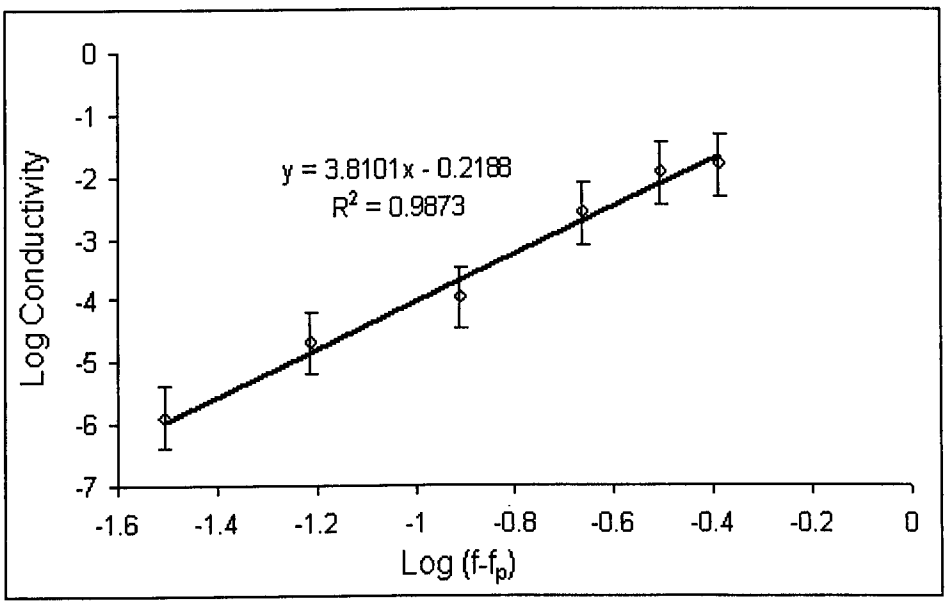
y = 3.8101x - 0.2188
R² = 0.9873
Log Conductivity
Log (f-fp)
0
-1
-2
-3
-4
-5
-6
-7
-1.6
-1.4
-1.2
-1
-0.8
-0.6
-0.4
-0.2
0

(c)

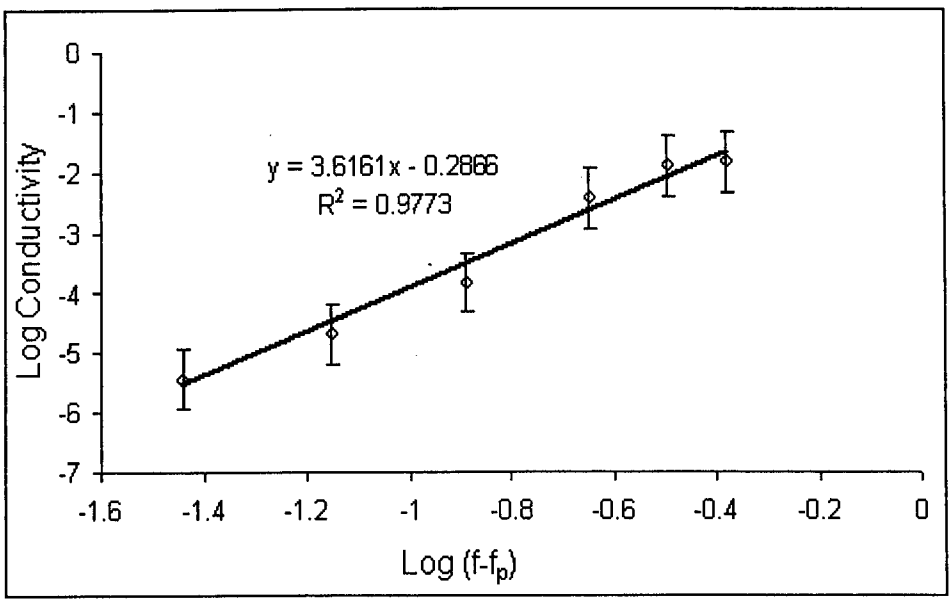
y = 3.6161x - 0.2866
R² = 0.9773
Log Conductivity
Log (f-fp)
0
-1
-2
-3
-4
-5
-6
-7
-1.6
-1.4
-1.2
-1
-0.8
-0.6
-0.4
-0.2
0

(d)

2.4 Conclusion

NBR-PAni.DBSA blends with useful levels of electrical conductivity have been successfully prepared by solution mixing for the first time in this work. The conductivities were much higher than those of comparable materials reported previously [1]. Blends prepared using NBR with the highest ACN content showed the best electrical properties (with an estimated lowest conductivity percolation threshold of 6.0 wt%/5.4 volume% of PAni.DBSA), owing to its reasonably good compatibility with PAni.DBSA.

The FT-IR spectra of pure NBR and PAni.DBSA corresponded well with those reported in the literature [9, 29]. Those for cast films of NBR-PAni.DBSA blends resembled a superposition of the spectra of the pure materials, but some notable peak shifts also provided evidence of the bonding interaction between the two polymers. From the low and high temperature DSC thermograms, NBR-PAni.DBSA blends with the largest temperature shifts for their thermal events (i.e. those containing NBR 48.2 ACN wt%) were also the ones with the best compatibility as indicated by optical and electron microscopy (lower proportion of observed dark-green or PAni.DBSA-rich phase-separated regions).

Publication

1. Yong, K. C., Foot, P. J. S., Morgan, H., Cook, S. and Tinker, A. J. 'Conductive Poly(butadiene-*co*-acrylonitrile)-Polyaniline Dodecylbenzenesulfonate [NBR-PAni.DBSA] Blends prepared in Solution'. *European Polym. J.*, **42(8)**, 1716 (2006).
2. Yong, K. C. et al. 'Conductive Poly(butadiene-*co*-polyacrylonitrile)-Polyaniline Dodecylbenzenesulfonate [NBR-PAni.DBSA] Blends prepared in Solution'. *Proceedings of German Rubber Conference 2006, Nuremberg, Germany*, (3rd-6th July 2006).

References

1. Vallim, M. R., Felisberti, M. I. and De Paoli, M.-A. *J. Appl. Polym. Sci.,* **75**, 677 (2000).

2. Naoi, K. and Osaka, T. *J. Electrochem. Soc.,* **134**, 2479 (1987).

3. Morton, M. *Rubber Technology (2nd Edition).* New York: Van Nostrand Reinhold Company, pp.16-17, (1973).

4. Pinho, M. S., Gorelova, M. M., Dezzoti, M., Soares, B. G. and Pertsin, A. J. *J. Appl. Polym. Sci.,* **70**, 1543 (1998).

5. Leyva, M. E., Barra, G. M. O, Gorelova, M. M., Soares, B. G. and Sens, M. *J. Appl. Polym. Sci.,* **80(4)**, 626 (2001).

6. Radhakrishnan, S. and Saini, D. R. *Polym. Int.,* **34**, 111 (1994).

7. Cataldo, F. and Maltese, P. *Polym. Adv. Technol.,* **12**, 293 (2001).

8. Leyva, M. E., Barra, G. M. O. and Soares, B. G. *Synthetic Met.,* **123**, 443 (2001).

9. Tassi, E. L. and De Paoli, M.-A. *Polymer*, **33(11)**, 2427 (1992).

10. Zoppi, R. A. and De Paoli, M.-A. *J. Electroanal. Chem.,* **290**, 275 (1990).

11. Castillo-Castro, T. D., Castillo-Ortega, M. M., Villarreal, I., Brown F., Grijalva, H., Perez-Tello, M., Nuno-Donlucas, S. M. and Puig, J. E. *Comp. Part A: Appl. Sci. and Manufacturing*, **38(2)**, 639 (2007).

12. Ke, Q. and Aoki, K. *J. Colloid and Interface Sci.*, **305(1)**, 40 (2007).

13. Ding, S.-J., Zhang, C.-L., Yang, M., Qu, X.-Z., Lu, Y.-F. and Yang, Z.-Z. *Polymer*, **47(25)**, 8360 (2006).

14. Yoshikawa, H., Hino, T. and Kuramoto, N. *Synthetic Met.*, **156(18)**, 1187 (2006).

15. Bernasik, A., Haberko, J., Wlodarczyk-Miskiewicz, J., Raczkowska, J., Luzny, W., Budkowski, A., Kowalski, K. and Rysz, J. *Synthetic Met.*, **155(3)**, 516 (2005).

16. Martins, C. R. and De Paoli, M.-A. *European Polym. J.*, **41(12)**, 2867 (2005).

17. Shin, J. S., Kim, J. H. and Cheong, I. W. *Synthetic Met.*, **151(3)**, 246 (2005).

18. Gupta, R. K. and Singh, R. A. *J. Non-Crystalline Solids*, **351(24-26)**, 2022 (2005).

19. Yang, Y., Chu, Y., Yang, F. and Zhang, Y. *Materials Chem. & Phys.*, **92(1)**, 164(2005).

20. Hu, X., Zhang, Y.-Y., Tang, K. and Zou, G.-L. *Synthetic Met.*, **150(1)**, 1 (2005).

21. Segal, E., Tchoudakov, R., Narkis, M., Siegmann, A. and Wei, Y. *Sensors and Actuators B: Chem.*, **104(1)**, 140 (2005).

22. Jousseaume, V., Morsli, M., Bonnet, A. and Lefrant, S. *Optical Materials*, **9(1-4)**, 484 (1998).

23. Fu, Y. and Weiss, R. A. *Synthetic Met.*, **84(1-3)**, 103 (1997).

24. Fu, Y. and Weiss, R. A. *Synthetic Met.*, **84(1-3)**, 129 (1997).

25. Geng, Y.-H., Wang, X.-H., Wang, L.-X., Jing, X.-B. and Wang, F.-S. *Synthetic Met.*, **69(1-3)**, 163 (1995).

26. Ruckenstein, E. and Yang, S. *Synthetic Met.*, **53(3)**, 283 (1993).

27. Fryczkowski, R., Binias, W., Farana, J., Fryczkowska, B. and Wlochowicz, A. *Synthetic Met.*, **145(2-3)**, 195 (2004).

28. Poussin, D., Morgan, H. and Foot, P. J. S. *Polym. Int.,* **52**, 433 (2003).

29. Morgan, H., Foot, P. J. S. and Brooks, N. W. *J. Mater. Sci.,* **36**, 5369 (2001).

30. Hoy, K. L. *J. Paint Technol.,* **42**, 76 (1970).

31. George, B. and McIntyre, P. *Infrared Spectroscopy*. London: John Wiley & Sons, pp. 85-100, (1987).

32. Haines, P. J. *Thermal Methods of Analysis-Principles, Applications and Problems (1st Edition)*. Glasgow: Chapman & Hall, pp. 22-31 & 63-76, (1995).

33. van der Pauw, L. J. *Philips Res. Repts.*, **13**, 1 (1958).

34. Wei, Y., Guang-Way, J., Hsueh, K. F., Scherr, E. M., MacDiarmid, A. G. and Epsteisn, A. J. *Polymer*, **33**, 314 (1992).

35. Morgan, H. and Foot, P. J. S. *Unpublished Report.*

36. Davies, S. J., Ryan, T. G., Wilde, C. J. and Beyer, G. *Synthetic Met.,* **69**, 209 (1995).

37. Gospodinova, N., Mokreva, P., Tsanov, T. and Terlemezyan, L. *Polymer*, **38**, 743 (1997).

38. Stauffer, D. *Introduction to Percolation Theory*, London: Taylor and Francis, (1985).

Chapter 3: Electrical Conductive Epoxidised Natural Rubber-Polyaniline Dodecylbenzenesulfonate [ENR-PAni.DBSA] Blends prepared by Solution Mixing

3.1 Introduction

Numerous types of electrically conductive rubber blend (based on a carbon [1-16] or non-carbon [17-31] conductive filler) have been prepared either through mechanical mixing [1-16, 18-20, 30], solution mixing [17, 19, 21-26, 32, 33], electrochemical intergrowth [27-28, 31] or *in situ* polymerization [29] as discussed in Section 1.3. However, studies [1, 18-29] involving synthetic rubbers [e.g. nitrile rubber, polychloroprene, EPDM, SBS copolymer etc] have become a major interest. Limited literature information is available concerning conductive elastomeric blends based on natural rubbers and intrinsically electrically conductive polymers.

Blends of Standard Malaysian Rubber (SMR-20 grade) with polyaniline were prepared in previous work [30], by using a two-roll mill in order to study the efficiency of polyaniline as an antioxidant against thermal ageing for SMR-20. Some blends of SMR-polythiophene have also been prepared by the electrochemical method [31] and reached a high electrical conductivity (of the order of 10^{-1}S.cm^{-1}), but only with 80 wt% of polythiophene loading.

In this part of the work, epoxidised natural rubber (ENR) was selected for the blending studies described in this chapter because of its good mechanical properties [34] and good predicted compatibility with intrinsically conductive polymers (based on values of solubility parameters found in the literature [26, 34]). Special interest has focused on dodecylbenzenesulfonic acid doped PAni (PAni.DBSA) due to its advantages as discussed in Section 1.4.

The aim of the present work was to study ENR-intrinsically conductive polymer blends made by combining a commercially available grade of ENR with different amounts of PAni.DBSA. Once again, it was decided to produce all of the blends from solution, which required both components to be soluble in a common

shared solvent. This method has successfully been applied for the synthetic rubber-intrinsically conductive polymer blends (Chapter 2), but it had not previously been used for natural rubber-based ones. Characterisation of the resulting blends is reported here, using Fourier-transform infrared (FT-IR) and proton NMR spectroscopy and differential scanning calorimetry (DSC). The electrical conductivities of all the pure polymers and blends were determined, and their morphologies were studied by optical and electron microscopy.

3.2 Experimental

3.2.1 Chemicals and Raw Materials

Aniline monomer (99 wt%, Sigma-Aldrich), ammonium persulphate [APS] (98 wt%, Sigma-Aldrich), 36.5-38 wt% HCl solution (GPR), anhydrous ferric chloride [$FeCl_3$] (98 wt%, Sigma-Aldrich), 33 wt% ammonia solution (GPR), 70 wt% DBSA solution in 2-propanol (GPR, Sigma-Aldrich), chloroform (GPR), methanol (GPR), and ENR (grade ENR 50 with 50 mole% of epoxide level, manufactured by the Malaysian Rubber Board). The raw ENR was washed with methanol for 24h using Soxhlet extraction in order to remove chemical additives.

3.2.2 Solubility Parameter Value Calculations for Main Materials

Equation 1.1 and the values of functional group molar attraction constants F_i calculated by Hoy [35] were used to estimate the solubility parameters for pure ENR 50 and PAni.DBSA.

3.2.3 Synthesis of PAni.DBSA

The same batch of PAni.DBSA synthesised in Chapter 2 was used here. The prepared PAni.DBSA was submitted for elemental analysis and was reported to have a 42% protonation level on the basis of the S:N atomic ratio.

3.2.4 Preparation of ENR-PAni.DBSA Blend

ENR 50-PAni.DBSA blends with the following compositions (wt% ENR 50 : wt% PAni.DBSA) 50:50, 60:40, 70:30, 80:20, 90:10, 95:5, 96:4, 97.5:2.5, 98:2 and 99:1 were prepared by solution mixing, and chloroform [with δ_s, 19.0 $(MJ.m^{-3})^{1/2}$] was selected as the shared solvent. 24h methanol washing was carried out using the Soxhlet extraction apparatus (see Chapter 2: Figure 2.1) in order to reduce the contamination of chemical additives in raw ENR 50.

Table 3.1: General Formulation for preparing Blends with Different Proportions of ENR 50 and PAni.DBSA by using Masterbatch Solutions

Details	Proportion of blend (wt % of ENR 50 : wt % of PAni.DBSA)					
	50:50	60:40	70:30	80:20	90:10	95:5
Volume of added ENR 50 masterbatch solution, mL	10.0	10.0	10.0	10.0	15.0	15.0
Total mass of ENR 50 in g	0.2000	0.2000	0.2000	0.2000	0.3000	0.3000
Volume of added PAni.DBSA master-batch solution, mL	12.0	8.0	5.2	3.0	2.0	1.0
Total mass of PAni.DBSA in g	0.2000	0.1340	0.0868	0.0501	0.0334	0.0167
Total volume of prepared blend solution, V_{blend}, mL	22.0	18.0	15.2	13.0	17.0	16.0
Total mass of prepared blend in solution, W_{blend}, g	0.40	0.3340	0.2868	0.2501	0.3334	0.3167

Masterbatch solutions for methanol-washed ENR 50 and pure PAni.DBSA were prepared, based on the concentration of 0.02g ENR 50/mL solvent and 0.0167g PAni.DBSA/mL solvent respectively. In order to prepare the masterbatch solutions, each polymer was left to dissolve in chloroform for 36h at room temperature with the help of a magnetic stirrer. Example formulations for blending different proportions of ENR 50 and PAni.DBSA by using the masterbatch solutions are shown in Table 3.1.

Calculated volumes of each polymer masterbatch solution were measured by pipette and were mixed in a conical flask in order to prepare the solution blends. Each of the blend solutions was given a 5-minute ultrasonic bath treatment in order to enhance its homogeneity (all visually clear).

The density of each blend with different proportions of added ENR 50 and PAni.DBSA was also estimated. This information was needed particularly in the calculation of electrical conductivity in order to determine the thickness of cast films of blend. Equation 2.1 was used to calculate the density of each of these. Examples of the calculated values of density for each blend with different proportions of added ENR 50 and PAni.DBSA are shown in Table 3.2.

Table 3.2: Densities of Blends (with Different Proportions of ENR 50 and PAni.DBSA) prepared from Masterbatch Solutions

Proportion of Added Polymers (wt % of ENR 50 : wt % of PAni.DBSA)	Estimated Density of Blend, ρ_{blend} ($kg.m^{-3}$)
50:50	1050.0
60:40	1040.0
70:30	1020.0
80:20	1010.0
90:10	990.0
95:5	980.0

3.2.5 NMR Spectroscopy

Samples of pure ENR 50 and ENR-PAni.DBSA blends were studied using a H^1 NMR (Bruker AC300 with processor WIN NMR) in order to investigate the extent of possible ring-opening of the ENR as a result of adding PAni.DBSA. About 5mg of each sample was dissolved in d-chloroform before being examined by NMR (with 30° pulse and 6 sec pulse delay). In each case, 4 to 6 portions of the sample were examined.

3.2.6 Morphological Studies (Optical Microscopy and TEM)

The ENR-PAni.DBSA blends were studied with a Nikon OPTIPHOT-2 optical microscope (200 x magnification) linked to a computer by a video converter (LINKAM VTO 232) for digital image capture. A small drop of each sample blend solution was put onto a microscope cover-glass and allowed to evaporate to form a thin (~3.0μm) transparent film.

Blends with 2.5 wt% (generally below the conductivity threshold) and 5 wt% (generally above the conductivity threshold) of PAni.DBSA were also studied by TEM (with a Philips CM12 microscope at accelerating voltage, 80kV). Some ultra-thin samples (ca. 150nm) of each blend were obtained for this purpose by sectioning with an RMC MT7000 microtome.

3.2.7 FT-IR Spectroscopy

Infra-red spectra of pure ENR 50, PAni.DBSA, and ENR-PAni.DBSA blends were recorded on a Perkin-Elmer FT-IR PARAGON 100 Spectrometer. A small amount of each sample solution was cast onto a KBr window in order to obtain a reasonably thin (3.0μm), transparent film.

3.2.8 Thermal Analysis

Differential scanning calorimetry (DSC) was used to characterise PAni.DBSA powder, pure ENR 50 and all the ENR-PAni.DBSA blend films. Above-ambient temperature (30 to 300°C), a Mettler Toledo DSC822e (heating rate 20°C/minute) was used, and sub-ambient temperature scans (-60 to 0°C) were obtained using a Perkin-Elmer Pyris Diamond DSC (heating rate 50°C/minute). Each sample was sealed in a 40μL aluminium pan and analysed under N_2 atmosphere, with an empty pan as the reference. Each thermal analysis was repeated twice, and the error for all of the results was about ±1.5°C. The definitions described in Section 2.2.8 for the onset temperature of the major exotherm and for the glass transition (Tg) were also applied in this part of work.

3.2.9 Electrical Conductivity Measurement

The dc electrical conductivities of PAni.DBSA, pure ENR 50 and ENR-PAni.DBSA blends were calculated from electrical "resistance" (voltage/current) values measured by 2- or 4-probe techniques. The same measurement equipment, procedures and equations (Equation 2.8-2.11) described in Section 2.2.9 were also used in this part of work.

3.3 Results and Discussion

3.3.1 Solubility Parameter Value Calculations for Main Materials

Chloroform has a solubility parameter of $19.0(MJ.m^{-3})^{1/2}$ [36], and pure ENR 50 was soluble in it. The PAni.DBSA prepared in this work was highly soluble in chloroform, giving dark green solutions. The calculated solubility parameters for the PAni.DBSA and pure ENR 50 (see Table 3.3) used here are 20.8 and $18.4(MJ.m^{-3})^{1/2}$ respectively. All of these calculated values agreed with those reported in the literature [26, 28, 34]. It is predicted that the compatibility

between ENR and PAni.DBSA could be enhanced by increasing the epoxidation level of ENR. Unfortunately, ENR 50 was the only commercial available grade (manufactured by the Malaysian Rubber Board, Malaysia) with the highest level of epoxidation that could be found for this part of work.

Table 3.3: Calculation of Solubility Parameter Values from Molar Attraction Constants for ENR50

Smallest repeat unit of ENR:

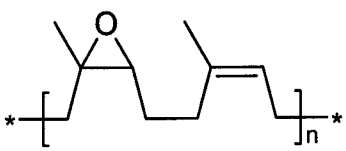

Molecular weight of polyisoprene = 0.053kg/mol
Molecular Weight of epoxidised polyisoprene = 0.069kg/mol

Group	*F_i* $[(J.m^{-3})^{1/2}.m^3]/mol$	*Numbers of Group*	*ΣF_i* $[(J.m^{-3})^{1/2}.m^3]/mol$
For polyisoprene:			
$-CH_2-$	269	2	538
>C=	173	1	173
-CH=	249	1	249
			ΣF_i=960
For epoxidised polyisoprene:			
-CH2-	269	2	538
-CO-	538	1	538
-CH=	249	1	249
			ΣF_i=1325

Details of Calculation

Based on the density of ENR 50= 980.0kg.m^{-3} :

δ_p = [(980.0x1142.5)]/ [0.0265+0.0345] = ***18.35(MJ.m^{-3})$^{1/2}$***

From literature [34], the δ_p for ENR 48 was reported as 18.2(MJ.m^{-3})$^{1/2}$ by using the same calculation method.

3.3.2 NMR Spectroscopy

The calculated results of epoxide level and ring-opening (mole %) for pure ENR 50 and ENR 50-PAni.DBSA blends are summarised in Table 3.4 (see Appendices 3.1 to 3.5 for examples of NMR spectra).

Table 3.4: The Mean Proportions of Epoxide Conversion and Ring-Opening (Mole%) for Pure ENR 50 and ENR 50-PAni.DBSA Blends

Pure material/Blend (wt% ENR 50:wt% PAni.DBSA)	Mole %			
	Epoxide	Furan Group (3.9-3.7 p.p.m.)	'Diol' Group (3.5-3.3 p.p.m.)	Total of Ring Opened (Furan + 'Diol')
Pure ENR 50	47.2	2.1	0.4	2.5
Blends				
95:05	46.4	2.0	1.0	3.0
90:10	43.1	3.5	2.0	5.5
80:20	40.9	1.6	6.1	7.7
70:30	26.3	9.1	14	23.1
60:40	24.6	2.2	21.5	23.7
50:50	21.5	10.6	17.0	27.6

Results from Table 3.4 show a decreasing epoxide content and increasing total of ring-opening. There is quite a lot of variability for the furan group analysis due to the difficulty of inaccurate integration as a result of background noise. It is worth noting the type of ring-opening observed here. When the epoxide ring in ENR opens, it can result in two alternative structures: (1) Ring-opening to form furan groups by joining to the next monomer unit, which will result in peaks assigned to CH-O (in the region of 3.9-3.7 p.p.m.). (2) Ring-opening to form 'diol' groups with CH-OH moieties (assigned to peaks in the region of 3.5-3.3 p.p.m.).

Mechanisms of these two types of ring-opening are shown in Figure 3.1 and 3.2. At high acidic condition, the majority of epoxide groups are isolated and

the main ring-opened products are those expected from simple epoxide chemistry [37] (see Figure 3.1). The final product is normally the *trans* diol, but dehydration of the tertiary alcohol can occur. As the level of epoxidation is increased, the number of adjacent epoxide groups is greater, and a five-membered cyclic ether becomes the major product [38, 39]. This arises from the attack of a ring-opened epoxide on the adjacent epoxide group with the reaction proceeding along the rubber backbone until stopped by a non-epoxide group or steric considerations (see Figure 3.2).

Figure 3.1: Epoxidation of Natural Rubber with A Peroxyacid and Secondary Ring-Opening of Isolated Epoxide Groups

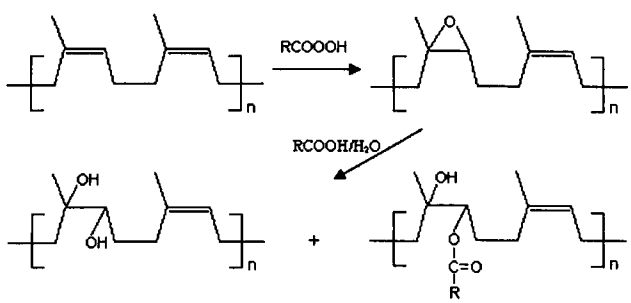

Figure 3.2: Ring-Opening of Adjacent Epoxide Groups to yield Five-Membered Cyclic Ethers

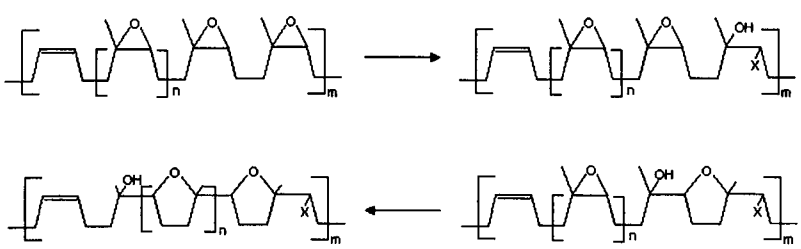

Often both types occur together, with furan tending to predominate when the host rubber has high epoxide content. In these samples there is a predominance of furan formation in both 95:5 and 90:10 blends but in the other cases of higher PAni.DBSA level (i.e. 20-50 wt%), there appears to be a predominance of peaks in the 3.5-3.3 p.p.m. region and hence greater evidence of 'diol' formation. Graphs were plotted for the mole% of epoxide rings (Figure 3.3)

and the mole% of total ring-opening (Figure 3.4) versus the wt% of the PAni.DBSA, and both of them could be fitted (correlation coefficient, ~0.98-0.99) with cubic polynomial equations (as shown in both figures).

Figure 3.3: Chart of the Mole% of ENR Epoxide Ring (Uncertainty, ±2 Mole%) versus the Proportion of PAni.DBSA in the ENR-PAni.DBSA Blends

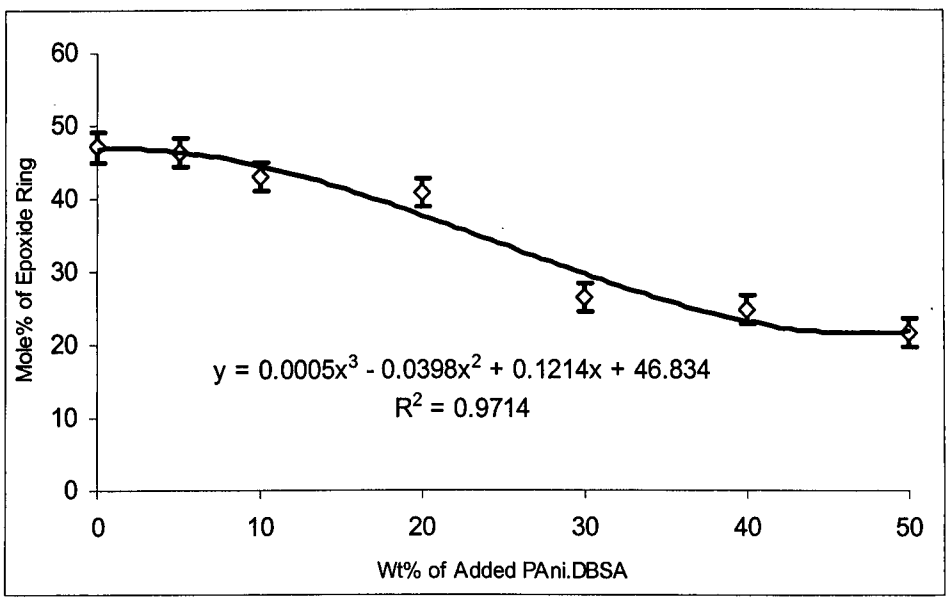

Figure 3.4: Chart of the Mole% of ENR Total Ring-Opening (Uncertainty, ±2 Mole%) versus the Proportion of PAni.DBSA in the ENR-PAni.DBSA Blends

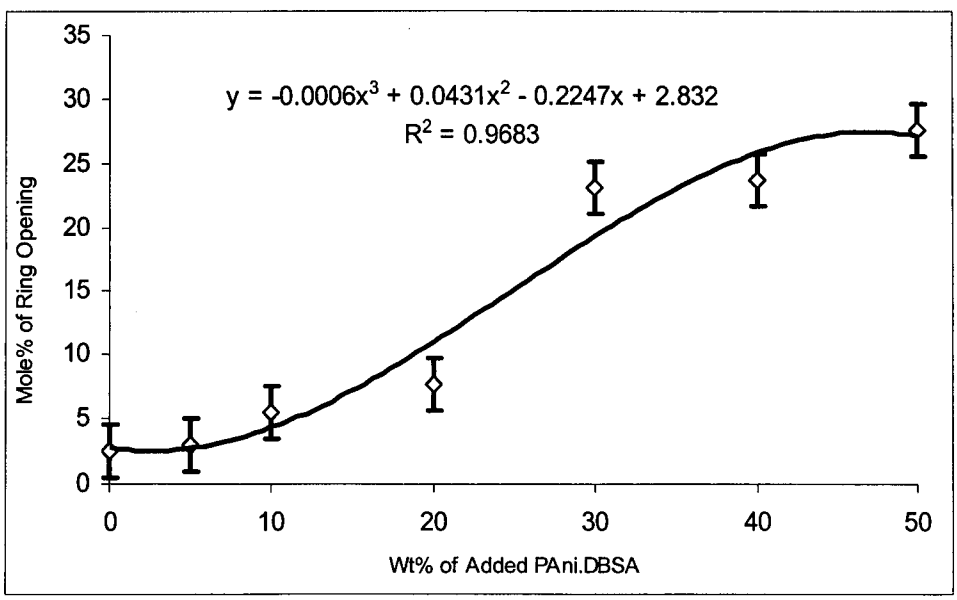

3.3.3 Morphological Studies (Optical Microscopy and TEM)

All the ENR 50-PAni.DBSA blends were studied by optical microscopy, but only images of blends containing 5, 20, 30 and 40 wt% of PAni.DBSA are shown in Figure 3.5.

Figure 3.5: Optical Micrographs (200 x Magnification) for the Blends of ENR 50-PAni.DBSA. Blends contain (a) 60:40 (b) 70:30 (c) 80:20 and (d) 95:5 wt% ENR50:wt% PAni.DBSA

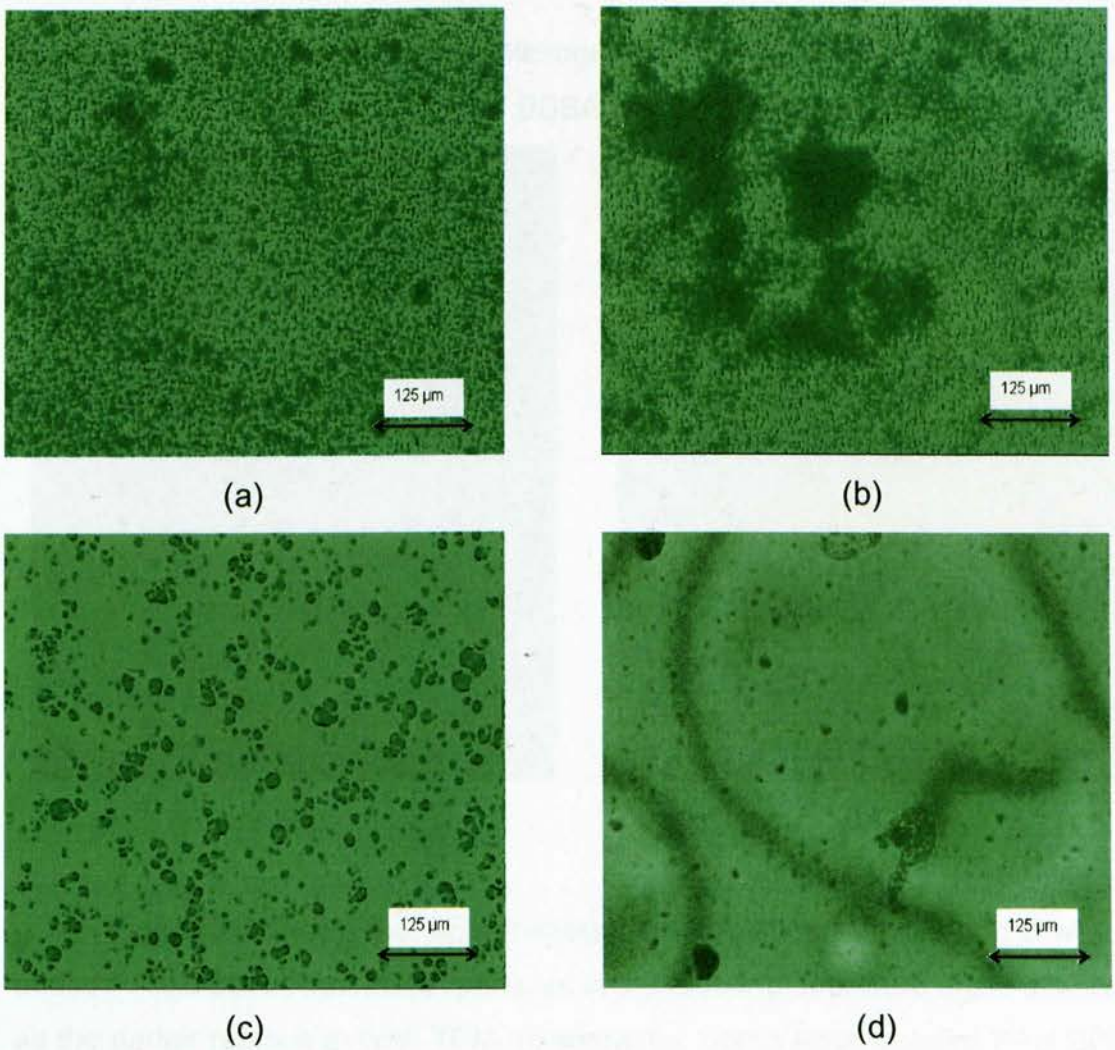

(a) (b) (c) (d)

As for the synthetic rubber based blends (see Section 2.3.4), two different regions were observed, i.e. the regions rich in ENR (pale-green in colour) and the regions rich in PAni.DBSA (dark-green in colour). The dark-green regions

consisted of large conductive particles and their agglomerates, as a result of some degree of phase separation. The pale-green regions were the regions of well-blended PAni.DBSA and ENR. The ENR-PAni.DBSA blends were similar to those in previously-studied NBR-PAni.DBSA blends [Chapter 2] in that the total area of the dark-green region increased with increasing content of PAni.DBSA. For the blend containing ≥30 wt% of PAni.DBSA, some large particles could be found.

Figure 3.6: Transmission Electron Micrographs of the ENR 50-PAni.DBSA Blends. Blends contain, (a) 2.5 wt% of PAni.DBSA and (b) 5 wt% of PAni.DBSA

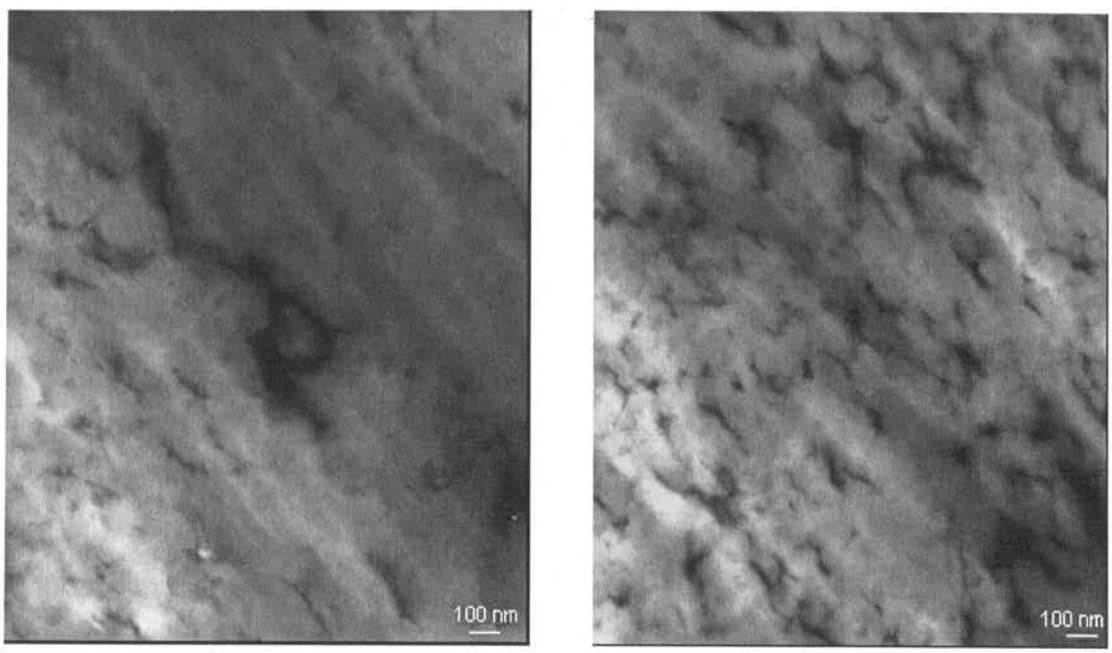

(a) (b)

Figure 3.6 shows the TEM micrographs of blends with 2.5 and 5 wt% of added PAni.DBSA. PAni.DBSA particles in the rubber matrix were again observed as the darker regions in both TEM micrographs. Some large isolated PAni.DBSA particles could be found from Figure 3.6(a) for the ENR blend with 2.5 wt% PAni.DBSA, which also had the relatively low electrical conductivity (shown by Figure 3.13). Some conductive networks were also formed when the PAni.DBSA particles were getting closer to each other [see Figure 3.6(b)] and this was

attributed to the higher loading and better dispersion of PAni.DBSA particles within the ENR host matrix. This is why the 5 wt% PAni.DBSA blend had relatively much higher electrical conductivity (see Figure 3.13). Both of TEM micrographs show some very small particles of PAni.DBSA (in colloidal dimensions, ~20-100nm). These small particles had contributed to the electrical conductivity of the blends since they could also form some small conductive networks (similar to the case of NBR-PAni.DBSA blends studied in Chapter 2).

3.3.4 FT-IR Spectroscopy

Selected regions of the FT-IR spectra for pure PAni.DBSA, pure ENR 50 and their blends with 5 to 50 wt% of PAni.DBSA are shown in Figure 3.7. The FT-IR spectra of pure ENR 50 and all the blends show the characteristic absorptions at 1250cm^{-1} (epoxy ring bond stretching), 875cm^{-1} (C-C of epoxy ring stretching), 796cm^{-1} and 837cm^{-1} (ring deformation), 2859cm^{-1} (C-H stretching vibration of epoxy ring) and 3390cm^{-1} (-OH stretching vibration of 'diol' ring-opening). Some very weak absorptions at 1112cm^{-1} (aliphatic ethers, C-O-C for furan group) were also observed in the FT-IR spectra of pure ENR 50 and all blends.

For the blends with low levels of PAni.DBSA (i.e. ≤20 wt%), there was a predominance of ENR absorption bands in their FT-IR spectra. Meanwhile for the blends with high levels of PAni.DBSA (i.e. ≥30 wt%), their FT-IR spectra exhibited a predominance of PAni.DBSA absorption bands. However through some detailed examination, the intensity of absorptions at 3390cm^{-1} (solely corresponding to the 'diol' ring-opening) for all the blends increased with the amount of added PAni.DBSA. At the same time, the intensity of absorptions at 2859cm^{-1} (solely corresponding to the epoxide ring) decreased with the proportion of PAni.DBSA. The absorbance intensity for each of these peaks is directly related to the changing level of each assigned functional group (since the cast films of all blends had the same thickness). It is proposed that the higher the peak absorbance intensity, the higher the level of each assigned functional group content. All

values of absorbance intensity were based on the local baseline position. Table 3.5 summarises the values of these two sets of characteristic peak absorbances.

Figure 3.7: FT-IR Spectra of PAni.DBSA, Pure ENR 50 and Their Blends (wt% ENR:wt% PAni.DBSA*). (a) 750-1300cm^{-1}, (b) 2800-3100cm^{-1} and (c) 3300-3600cm^{-1}

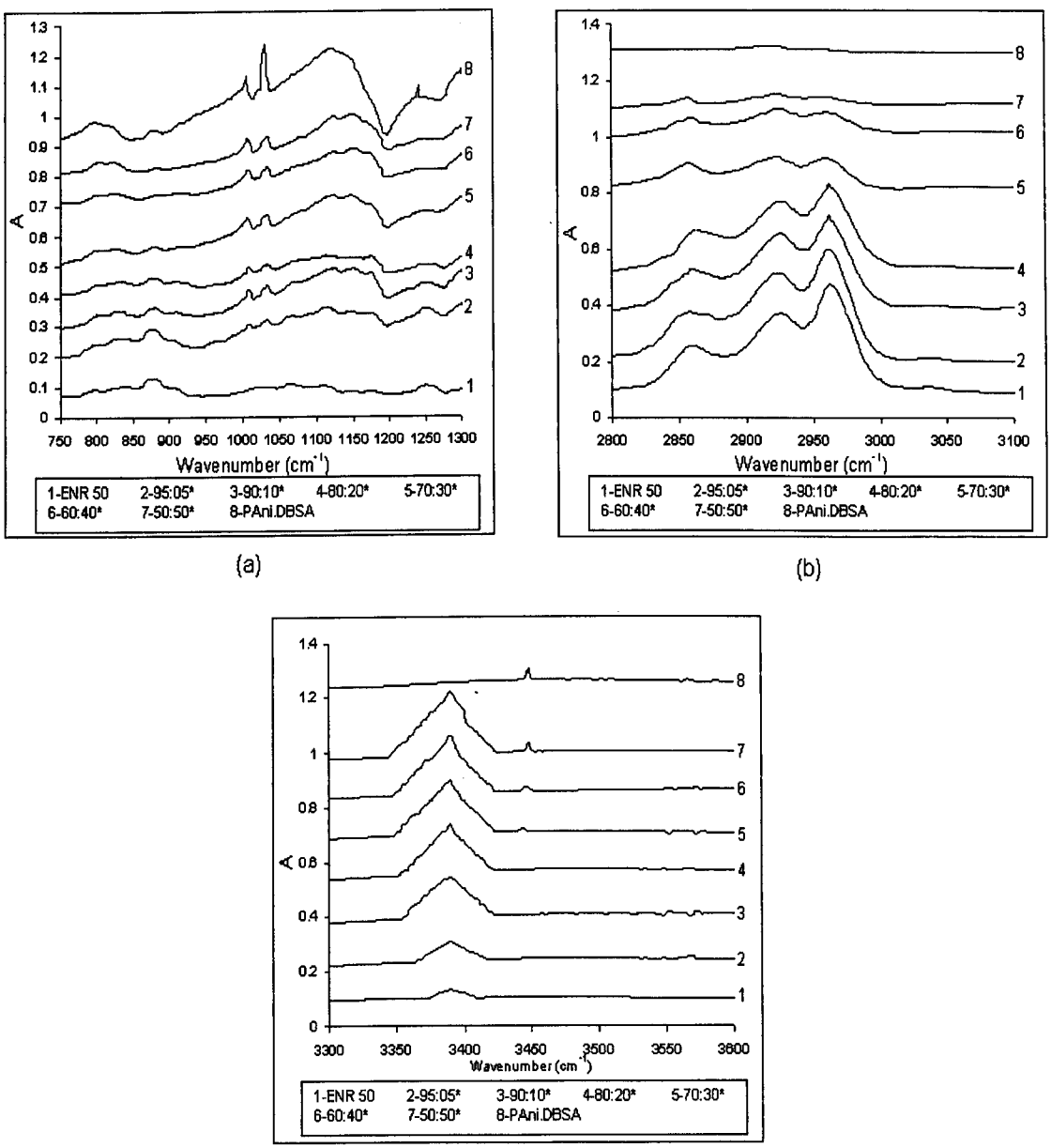

Table 3.5: The FT-IR Spectra Peak Absorbances (A) for Pure ENR 50 and ENR 50-PAni.DBSA Blends at 2859cm^{-1} and 3406cm^{-1}

Composition (wt% ENR : wt% PAni.DBSA*)	Absorbance	
	at 2859cm^{-1}	at 3390cm^{-1}
Pure ENR 50	0.12473	0.03114
Blends		
95:05*	0.12262	0.07784
90:10*	0.11390	0.15568
80:20*	0.10808	0.18483
70:30*	0.06950	0.20546
60:40*	0.06501	0.22112
50:50*	0.05655	0.24011

Figure 3.8: Chart of FT-IR Peak Absorbance, A (Uncertainty, ±0.005) at 2859cm^{-1} versus the wt% of PAni.DBSA in the ENR-PAni.DBSA Blends

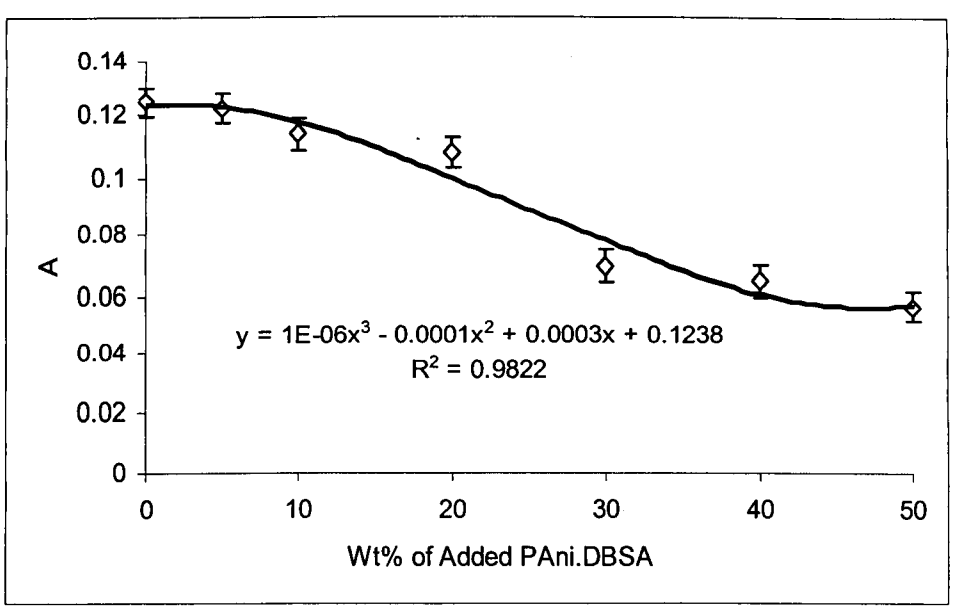

Figure 3.9: Chart of FT-IR Peak Absorbances, A (Uncertainty, ±0.01) at 3390cm^{-1} versus the wt% of PAni.DBSA in the ENR-PAni.DBSA Blends

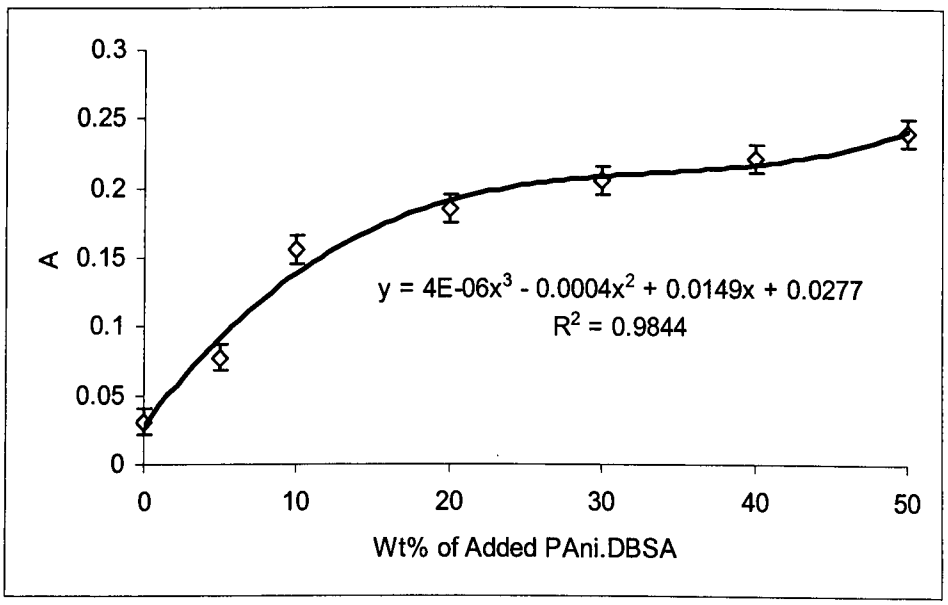

Results from this section are in agreement with those from NMR spectroscopy, where both of them showing that the proportion of 'diol' ring opening increased and the proportion of epoxide ring decreased with the PAni.DBSA loading. Graphs (see Figures 3.8 and 3.9) were plotted for these two characteristic peak absorbance intensities versus the proportion of PAni.DBSA in order to make the comparison quantitatively. It was observed that the values of these two peak absorbance intensities, could again be related by cubic equations (correlation coefficient, ~0.99) as shown in Figures 3.8 and 3.9 respectively.

3.3.5 Thermal Analysis

Figure 3.10 shows the sub-ambient temperature DSC thermograms for pure ENR 50 and its blends with 10 to 50 wt% of PAni.DBSA. (A DSC thermogram for pure PAni.DBSA is again not shown here because there were no obvious thermal events in the low-temperature region). Figure 3.11 shows the above-ambient temperature DSC thermograms for PAni.DBSA, pure ENR 50 and its blends with 10 to 50 wt% of the conducting polymer.

Figure 3.10: Sub-Ambient Temperature DSC Thermograms for Pure ENR 50 and Its Blends (wt% ENR:wt% PAni.DBSA*) with 10 to 50 wt% of PAni.DBSA

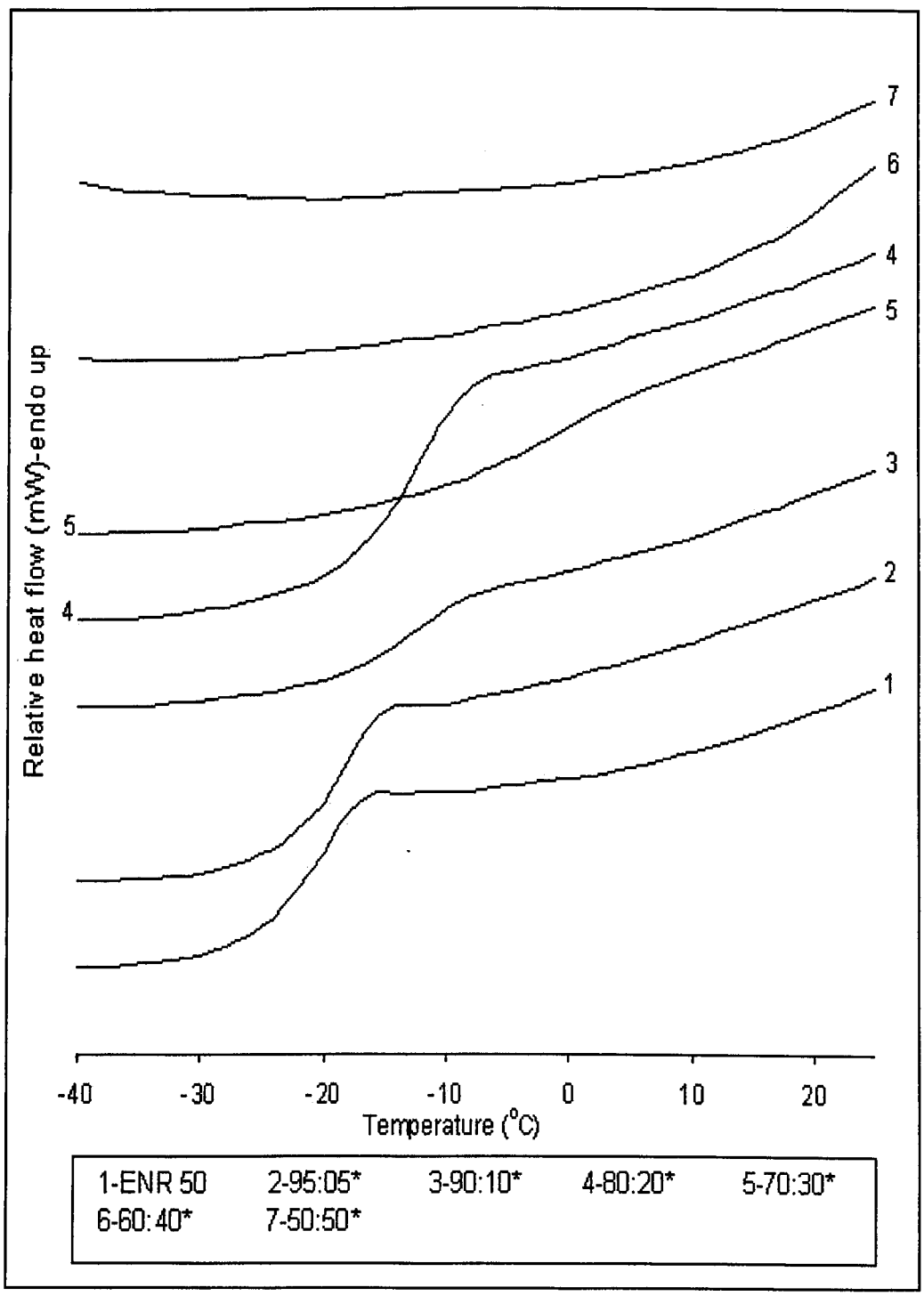

Figure 3.11: Above-Ambient Temperature DSC Thermograms for PAni.DBSA, Pure ENR 50 and Its Blends (wt% ENR:wt% PAni.DBSA*) with 10 to 50 wt% of PAni.DBSA

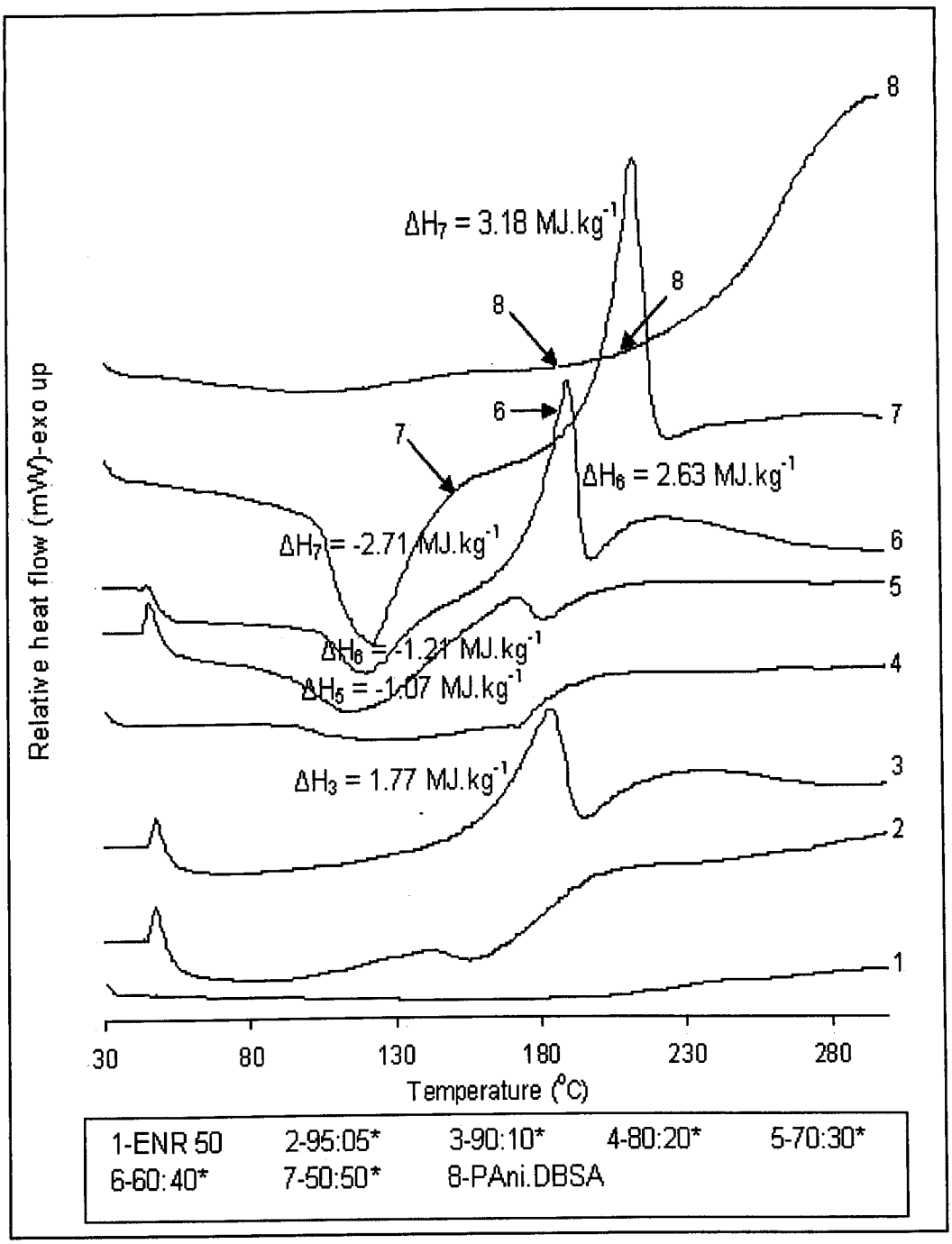

Table 3.6: The Mean Glass Transition Temperature (Tg) Values for Pure ENR 50 and ENR-PAni.DBSA Blends

Pure material/ Blend (wt% ENR : wt% PAni.DBSA)	Glass transition temperature, °C
Pure ENR 50	-26.6
Blends	
95:05	-24.5
90:10	-20.9
80:20	-19.1
70:30	-15.4
60:40	6.0
50:50	6.7

Figure 3.12: Chart of Log Glass Transition Temperature, Tg (Kelvin) versus Log Ring Opening (Mole%) of ENR-PAni.DBSA Blends

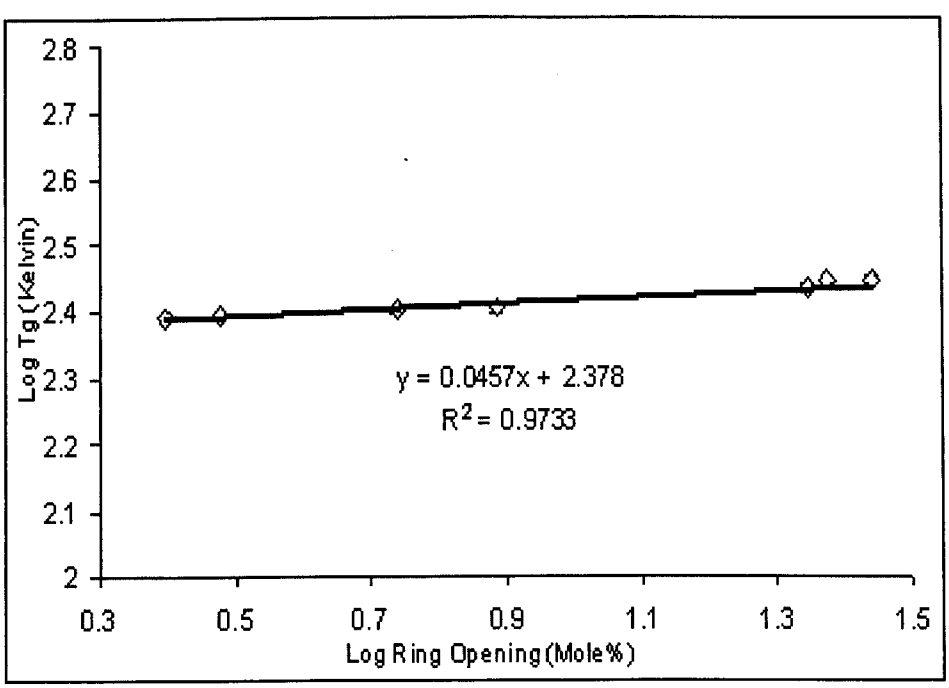

The mean Tg values for the pure ENR 50 and ENR-PAni.DBSA blends are given in Table 3.6. The results show a significant and progressive rise in the Tg values with the proportion of PAni.DBSA. While this may partly be an effect of some phase mixing between the polymers, it also very likely to be the result of ENR ring opening. Ring opened and furanised ENR also has a raised Tg depending on the extent of the ring opening [34]. A log Tg (Kelvin) versus log ring-opening (mole%) chart was plotted in order to compare these two parameters quantitatively (see Figure 3.12). It was found that the log values of these two parameters were linearly related with a slope of 0.0457 and intercept of 2.378 as shown in Figure 3.12.

Table 3.7: The Mean Onset Temperatures of the Exotherm and Endotherm before the Major Exotherm in the Above-Ambient Temperature DSC Thermograms of PAni.DBSA, Pure ENR 50 and ENR-PAni.DBSA Blends

Pure material/ Blend (wt% ENR : wt% PAni.DBSA)	Onset temperature, °C	
	Endotherm	Exotherm
Pure ENR 50	-	206.0
Blends		
95:05	-	162.5
90:10	-	137.0
80:20	94.0	173.0
70:30	92.0	124.0
60:40	106.0	173.0
50:50	104.0	197.0
PAni.DBSA	36.0	234.0

From Table 3.7, pure ENR was thermally stable up to about 206°C. PAni.DBSA also had good thermal stability up to about 233°C. All the above-ambient temperature DSC thermograms for the blends showed thermal processes that were combinations of events observed for pure ENR 50 and PAni.DBSA, but

the events showed some temperature shifts relative to the corresponding processes in the pure polymers (see Table 3.7). The blends with ≤40 wt% of PAni.DBSA showed the largest temperature shifts due to reasonably good compatibility between the two polymers (as shown by the optical micrographs: Figure 3.5). As shown in Figure 3.11, the endothermic event before the major exotherm (corresponding to the total absorbed energy for the ring opening process) increased with increasing loading of PAni.DBSA. It is believed that this was corresponded to the further ring opening (catalysed by the higher concentration of PAni.DBSA) occurred before the major exothermic process (i.e. degradation) of the blend.

3.3.6 Electrical Conductivity Measurement

The calculated electrical conductivity values for the PAni.DBSA, pure ENR 50 and ENR-PAni.DBSA blends are shown by Figure 3.13. Pure ENR 50 is a very good electrical insulator, with a conductivity of about 3.8 x 10^{-16}S.cm^{-1}. The PAni.DBSA used here had an electrical conductivity of 1.2S.cm^{-1}, comparable with values found from literature for amorphous, un-aligned PAni.DBSA [26, 36].

Figure 3.13: Electrical Conductivities for the ENR 50-PAni.DBSA Blends as A Function of PAni.DBSA Content (wt%)

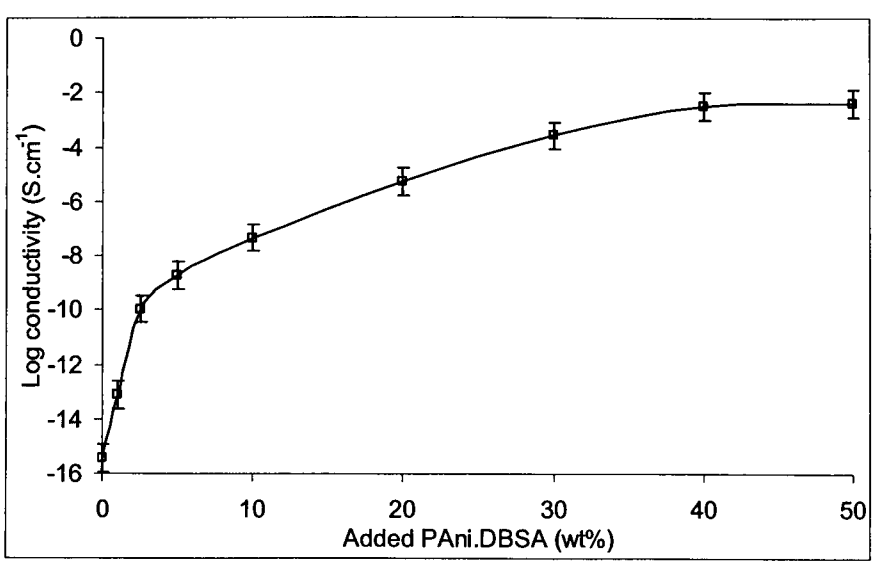

The electrical conductivity of all the blends increased with the proportion of PAni.DBSA, as observed in several studies of PAni.DBSA blends [18, 20, 23, 25-26, 29]. The blends reached an electrical conductivity in the order of 10^{-3} $S.cm^{-1}$ with about 40 wt% of PAni.DBSA loading. The conductivity percolation threshold for all ENR-PAni.DBSA blends was estimated by fitting the data from Figure 3.13 to a percolation model as defined by Equation 2.12 [25, 40]. The values of critical exponent (t) and correlation coefficient (R) for each case were estimated by fitting the data to a plot of log electrical conductivity (σ) versus log (f-f_p) (see Figure 3.14).

Figure 3.14: Log Electrical Conductivity (σ) vs. Log (f-f_p) Chart for Solution Mixed ENR 50-PAni.DBSA Blends; (a) First Stage of Electrical Conductivity Percolation Threshold and (b) Second Stage of Electrical Conductivity Percolation Threshold

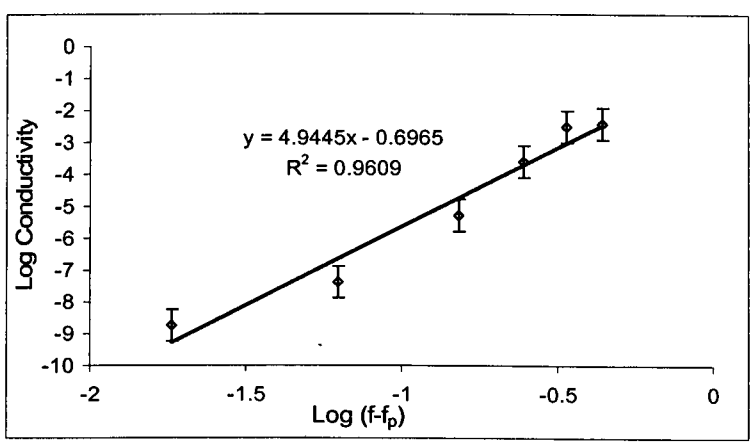

(a)

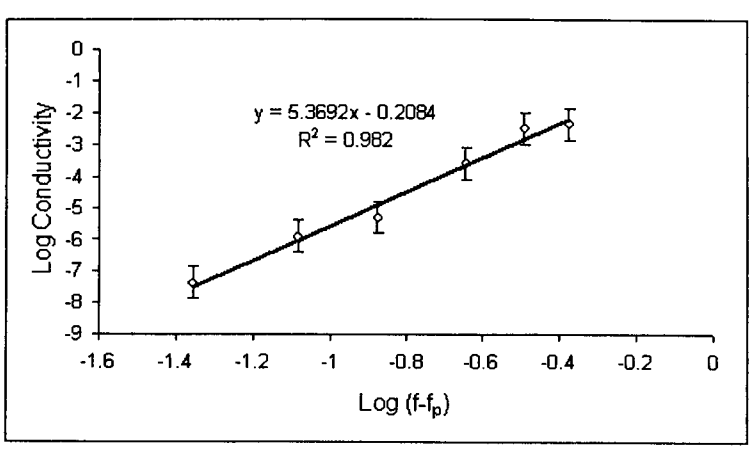

(b)

The estimated first electrical conductivity percolation threshold for the ENR 50-PAni.DBSA blends is 2.9 wt% (or 2.5 volume %) of PAni.DBSA (with t = 4.9 and R = 0.98). A second stage of percolation threshold with about 5 wt% (or 4.4 volume %) of added PAni.DBSA (with t = 5.4 and R = 0.99) was also observed. It corresponded to the separated phases of both polymers, i.e. the dark-coloured regions in the optical and electron micrographs.

A very low threshold value was seen here, for which the conductivity is likely to be contributed by those regions with well dispersed conducting polymer (the pale-green regions of the optical and electron micrographs). The values of t for a classical double-percolation model as described in the literature [40] are in the range between 2 and 4. Here, t as estimated with a value greater than 4 and it is likely to be attributed by some on-going chemical reactions of the blended ENR 50 and PAni.DBSA, e.g. formation of furan and 'diol' group.

3.4 Conclusion

The ENR 50-PAni.DBSA blends prepared in this part of the work had good electrical conductivities, comparable with those of the nitrile rubber-based ones [Chapter 2] due to appreciable compatibility between the two polymers (as shown by the proportion of pale-coloured regions in both optical and electron micrographs). Significant ring-opening of the ENR occurred (as detected by NMR and FT-IR spectroscopy) for blends with a high loading of PAni.DBSA (i.e. 30 wt% or above) and this was attributed to the sensitivity of the epoxide group of the rubber to acidic conditions. A progressive rise in the Tg values and increasing of the endothermic events with the proportion of PAni.DBSA as recorded by low and high temperature DSC thermograms respectively, are also proposed to be the results of ring-opening.

Two stages of electrical percolation threshold were observed for the ENR 50-PAni.DBSA blends, i.e. the first one (2.9 wt%/2.5 volume % of PAni.DBSA) which corresponded to the well-blended regions (pale green in optical

micrographs) and the second one (5 wt%/4.4 volume % of PAni.DBSA) which corresponded to the phase separated regions (dark green in optical micrographs). It has been shown here that the ring opening does not seriously affect the electrical properties of the ENR 50-PAni.DBSA blends. However, it is well known that ring opening of ENR will decrease its elastomeric properties and can ultimately lead to formation of a hard thermoplastic material, called furanised natural rubber [34]. Hence, the tolerable loading of PAni.DBSA is likely to be no more than 30 wt% in practice.

Publication

1. Yong, K. C., Foot, P. J. S., Cook, S. and Tinker, A. J. 'ENR-PAni.DBSA Blends: Production and Properties'. *Polym. Int.*, Manuscript submitted, (2007)

References

1. Job, A. E., Oliveira, F. A., Alves, N., Giacometti, J. A. and Mattoso, L. H. C. *Synthetic Met.*, **135**, 99 (2003).
2. Luheng, W., Tianhuai, D. and Peng, W. *Sensors and Actuators A: Phys.*, **135(2)**, 587 (2007).
3. Carrillo, A., Martín-Domínguez, I. R., Glossman, D. and Marquez, A. *Sensors and Actuators A: Phys.*, **119(1)**, 157 (2005).
4. Sun, Y., Luo, S., Watkins, K. and Wong, C. P. *Polymer Degrad. Stabil.*, **86(2)**, 209(2004).
5. Das, N. C., Chaki, T. K. and Khastgir, D. *Carbon*, **40(6)**, 807 (2002).
6. Das, N. C., Khastgir, D., Chaki, T. K. and Chakraborty, A. *Comp. Part A: Appl. Sci. and Manufacturing*, **31(10)**, 1069 (2000).
7. Nasr, G. M., Osman, H. M., Abu-Abdeen, M. and Aboud, A. I. *Polym. Testing*, **18(7)**, 483 (1999).
8. Sau, K. P., Chaki, T. K. and Khastgir, D. *Polymer*, **39(25)**, 6461 (1998).

9. Sau, K. P., Chaki, T. K. and Khastgir, D. *Comp. Part A: Appl. Sci. and Manuf.*, **29(4)**, 363 (1998).

10. Badawy, M. M. and Nasr, G. M. *Polymer Testing*, **16(2)**, 155 (1997).

11. Pramanik, P. K., Khastgir, D. and Saha, T. N. *Composites*, **23(3)**, 183 (1992).

12. Vallim, M. R., Felisberti, M. I. and De Paoli, M.-A. *J. Appl. Polym. Sci.,* **75**, 677 (2000).

13. Jiang, G., Gilbert, M., Hitt, D. J., Wilcox, G. D. and Balasubramanian, K. *Compos. Part A-Appl. Sci.,* **33**, 745 (2002).

14. Bhattacharya, S. K. and Kusy, R. P. *Metal-Filled Polymers: Properties and Applications.* New York: Marcel Dekker, (1986).

15. Yamaguchi, K., Busfield, J. J. C. and Thomas, A. G. *J. Appl. Polym. Sci. Polym. Phys.,* **41**, 2079 (2003).

16. Sau, K. P., Chaki, T. K. and Khastagir, D. *Rubber Chem. Technol.,* **73**, 310 (2000).

17. Carone, E., D'Ilario, L. and Martinelli, A. *J. Appl. Polym. Sci.,* **86**, 1259 (2002).

18. Davies, S. J., Ryan, T. G., Wilde, C. J. and Beyer, G. *Synthetic Met.,* **69**, 209 (1995).

19. Pinho, M. S., Gorelova, M. M., Dezzoti, M., Soares, B. G. and Pertsin, A. J. *J. Appl. Polym. Sci.,* **70**, 1543 (1998).

20. Leyva, M. E., Barra, G. M. O, Gorelova, M. M., Soares, B. G. and Sens, M. *J. Appl. Polym. Sci.,* **80(4)**, 626 (2001).

21. Radhakrishnan, S. and Saini, D. R. *Polym. Int.,* **34**, 111 (1994).

22. Zheng, W., Levon, K., Taka, T., Laasko, J. and Osterholm, J.-E. *J. Polym. Sci. Phys.,* **33**, 1289 (1995).

23. Gospodinova, N., Mokreva, P., Tsanov, T. and Terlemezyan, L. *Polymer*, **38**, 743 (1997).

24. Cataldo, F. and Maltese, P. *Polym. Adv. Technol.,* **12**, 293 (2001).

25. Leyva, M. E., Barra, G. M. O. and Soares, B. G. *Synthetic Met.,* **123**, 443 (2001).

26. Yong, K. C., Foot, P. J. S., Morgan, H., Cook, S. and Tinker, A. J. *European Polym. J.*, **42(8)**, 1716 (2006).

27. Tassi, E. L. and De Paoli, M.-A. *Polymer*, **33(11)**, 2427 (1992).

28. Zoppi, R. A. and De Paoli, M.-A*J. Electroanal. Chem.*, **290**, 275 (1990).

29. Soares, B. G., Amorim, G. S., Souza Jr., F. G., Oliveira, M. G. and Pereira da Silva, J. E. *Synthetic Met.,* Article in Press (2005).

30. Helaly, F. M., Darwich, W. M. and Abd El-Ghaffar, M.A. *Polym. Degrad. Stabil.,* **64**, 251 (1999).

31. Yigit, S., Hacaloglu, J., Akbulut, U. and Toppare, L. *Synthetic Met.,* **79**, 11 (1996).

32. Domenech, S. C., Bortoluzzi, J. H., Soldi, V. and Franco, C. V. *J. Appl. Polym. Sci.,* **87**, 535 (2003).

33. Schmidt, V., Domenech, S. C., Soldi, M. S., Pinheiro, E. A. and Soldi, V. *Polym. Degrad. Stabil.*, **83**, 519 (2004).

34. Gelling, I. R. *J. Nat. Rubb. Res.,* **6(3)**, 184 (1991).

35. Hoy, K. L. *J. Paint Technol.* **42**, 76 (1970).

36. Poussin, D., Morgan, H. and Foot, P. J. S. *Polym. Int.,* **52**, 433 (2003).

37. Rosowsky, A. *Heterocyclic Compounds with Three and Four Membered Rings, Part 1*. New York: Interscience Publishers, (1964).

38. Gelling, I. R. and Smith, J. F. *Controlled Viscosity by Natural Rubber Modification. Proceedings of International Rubber Conference Venice*, (1979).

39. Gelling, I. R. *Rubb. Chem. Technol.*, **58**, 86 (1985).

40. Stauffer, D. *Introduction to Percolation Theory*, London: Taylor and Francis, (1985).

Chapter 4: Electrical Conductive Peroxide-Vulcanised Poly(butadiene-*co*-acrylonitrile)-Polyaniline Dodecylbenzenesulfonate [NBR-PAni.DBSA] Blends prepared by Thermo-Mechanical Mixing

4.1 Introduction

For practical commercial applications, all rubber compounds (either natural or synthetic ones) which have been mixed and shaped into blanks for further processing (e.g. moulding, calendering and extruding) must be vulcanised by one of many systems [1-10]:

i. Sulphur vulcanisation [1-3]
ii. Sulphurless vulcanisation (e.g. by use of selenium, tellurium or thiuram disulfide compounds as accelerators) [4]
iii. Resin (e.g. phenolic and epoxy resins) vulcanisation [5]
iv. Peroxide vulcanisation (for saturated rubbers that cannot be crosslinked by sulphur or accelerators) [6-7]
v. Irradiation vulcanisation (e.g. electron beam, gamma and X-ray radiation) [8-9]
vi. Other systems, e.g. metal oxides for neoprene and dinitrobenzene for butyl rubber [10]

During vulcanisation, the following changes of rubber happen [11-14]:

i. The long chains of the rubber molecules become crosslinked by reactions with the vulcanisation agent to form three-dimensional structures. This reaction transforms the soft, weak viscous material into a strong elastic product.
ii. The rubber also loses its tackiness and becomes insoluble in solvents and is more resistant to deterioration normally caused by heat, light and ageing processes.

NBR can be vulcanised by sulphur, sulphurless, peroxide or irradiation methods [14]. The irradiation method would be the most costly one, although it is the 'cleanest' method, not involving any chemical additives. A non-sulphur system, i.e. the peroxide one, has some advantages over those involving sulphur. Peroxide-vulcanised nitrile rubber has excellent ageing properties, and is shiny, bloom-free, with a low compression set. Because of the complete lack of sulphur, it does not stain silver nor discolour in the presence of lead, and peroxide can vulcanise blends of NBR and other polymers that would not normally vulcanise with the same system [14]. There is no atom the joining peroxide-vulcanised NBR chains (e.g. the sulphur-sulphur bridges as formed in the sulphur vulcanisation), but only single chemical bonds, i.e. carbon-carbon bonds. The peroxide system can also be cheaper than irradiation, since only small amounts of peroxide vulcanising agent (i.e. 2.4-4.1 p.h.r. of dicumyl peroxide [15]) are used for achieving an optimum vulcanising level.

Hence, in this part of the present work, the peroxide vulcanising system (i.e. by using dicumyl peroxide, shown in Figure 4.1) was selected. Organic peroxides act as free-radical sources; their thermal decomposition generates very active free radicals able to abstract hydrogen atoms from the backbone of both unsaturated and saturated rubbers. Two macro-radicals can then recombine to create a direct carbon-carbon bond between adjacent molecular chains (see Figure 4.2 for a typical mechanism of reaction [16]).

Figure 4.1: Molecular Structure of Dicumyl Peroxide (DCP)

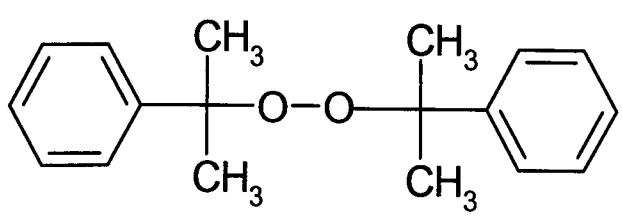

Figure 4.2: Mechanism of Peroxide-Free Radical Crosslinking (where ROOR = organic peroxide; P = unsaturated rubber)

ROOR (heated)	→	2RO*	Peroxide decomposition
RO* + P	→	ROP*	Initiation
ROP* + P	→	ROP-P*	Propagation
ROP-P* + PH	→	ROP-PH + P*	Alternative chain reaction (i)
P* + P	→	P-P*	Alternative chain reaction (ii)
P-P* + P	→	P-P-P*	Alternative chain reaction (iii)
2P*	→	P-P	One example of termination

Note: All the above propagation, chain and termination reactions produce crosslinkings, so that peroxide vulcanisation of butadiene-based rubbers is very efficient.

The aim of this part of the work was to study electrically conductive DCP-vulcanised blends produced by combining NBR [48.2 wt% acrylonitrile (ACN) content] with different amounts of PAni.DBSA. Characterisation of the resulting blends is also reported here, using differential scanning calorimetry (DSC), infrared spectroscopy, morphological study by both optical and electron microscopy, determination of the electrical conductivity and some basic mechanical properties of both raw materials and blends. The effect of realignment of the conductive filler particles on the mechanical and electrical properties of the peroxide-vulcanised blends was also studied in this part of the work. It was decided to produce the DCP-vulcanised blends by thermo-mechanical mixing, i.e. by using a temperature-controllable internal mixer (Brabender Plasticorder, PL 2000E). In the view of the high conductivities observed for NBR-PAni.DBSA blends prepared by solution mixing (Chapter 2), it was hoped that good results could also be achieved by suitable condition of mixing, temperature and vulcanisation for the thermo-mechanically prepared blends described later in this chapter.

An internal mixer is a closed mixing device. The model of an internal mixer shown in Figure 4.3 has a pair of counter-rotating rotors and a moveable steel ram (to force compound ingredients into the rotors' grasp) in order to perform the mixing. The rotors are encased by a heavy metal jacket with a hopper at the top

to feed in the ingredients, and a door at the bottom (underneath the rotors) to let the mixed materials out. There are also drilled channels in the walls of the mixing chamber and in the cores of both rotors, where water can pass through to control the mixing temperature. Mixing can occur between the rotors or between the mixing chamber walls and the rotors.

Figure 4.3: Basic Structure of an Internal Mixer [reproduced from Reference 14]

Both basic- (using a two roll-mill, at temperature ≤60°C) and thermo-mechanical (using an internal mixer or extruder, at temperature ≥100°C) mixings [17-34] are the most popular types of method used for preparing electrical conductive elastomeric blends. However, both non-vulcanised and vulcanised blends of NBR with PAni based conductive filler have never been produced by thermo-mechanical mixing. Non-vulcanised SBS copolymer-PAni.DBSA blends were prepared by using an internal mixer [28], and they reached conductivities in the order of 10^{-2}S.cm^{-1} for blends with 5 wt% of conductive polymer. Metal oxide-

(MgO and ZnO) vulcanised blends of polychloprene with different acid doped-(HCl and ρ-TSA) PAni were produced with a two roll-mill [29] and they all had low conductivies (10^{-9}S.cm^{-1} or less) even when loaded with 50 wt% of conductive polymer. Peroxide-vulcanised EPDM-PAni.p-TSA blends have been prepared by using an internal mixer [30], and the produced blends had low electrical conductivity thresholds, i.e. about 1 wt% of added conductive polymer.

Sulphur-vulcanised NBR-PAni.DBSA blends were prepared [31] by using a two-roll mill, but all the blends showed poor electrical conductivities, ranging from about 10^{-8} to 10^{-12}S.cm^{-1}. Non-vulcanised blends of SBS-PAni.DBSA were also prepared [32] using a two-roll mill and internal mixer respectively, and significantly reported that conductivities were enhanced when blends were formed at higher temperature under intensive mixing in an internal mixer (6 orders of magnitude higher than by two-roll mill). The effects of different vulcanisation methods, i.e. phenolic resin and electron beam irradiation on EPDM-PAni.DBSA blends were studied [33] and the blends were prepared by an internal mixer. It was concluded that those irradiation-vulcanised blends had higher electrical conductivities than the chemically-vulcanised ones. Non-vulcanised blends of polystyrene (PS)-SBS-PAni.DBSA were prepared by a counter-rotating double screw extruder [34] and it was reported that blends with higher proportions of PS had higher electrical conductivities due to an increase in the crystallinity (or molecular orientation of the polymer chains) after processing in the extruder. The increase of conductivity of these blends was attributed to the presence of SBS (as compatibiliser) which promoted a better interaction between the blend components.

4.2 Experimental

4.2.1 Chemicals and Raw Materials

Aniline monomer (99 wt%, Sigma-Aldrich), ammonium persulphate [APS] (98 wt%, Sigma-Aldrich), 36.5-38 wt% HCl solution (GPR), anhydrous ferric chloride [$FeCl_3$] (98 wt%, Sigma-Aldrich), 33 wt% ammonia solution (GPR), 70

wt% DBSA solution in 2-propanol (GPR, Sigma-Aldrich), chloroform (GPR), methanol (GPR). PAni.DBSA with 42% protonation level was prepared by procedures described in Section 2.2.3.2. Commercial grade NBR [Krynac® 50.75 (Bayer)] was used. By ^{1}H NMR analysis of solutions in THF-d8, the actual ACN content for NBR was identified as 48.2±1.0 wt% (see Section 2.3.3 or literature [35]). Dicumyl peroxide (Peroximon DC40 supplied by Elf Atochem with 40 wt% of DCP, 55 wt% of calcium carbonate and 5 wt% of silica gel) was used as the vulcanising agent.

4.2.2 Preparation of Peroxide-Vulcanised NBR-Pani.DBSA Blends

Non-vulcanised NBR-Pani.DBSA blend masterbatches with different compositions of NBR wt%: Pani.DBSA wt% (i.e. 99:1, 97.5:2.5, 95:5, 90:10, 80:20, 70:30, 60:40, 50:50) were first prepared by using an internal mixer (Brabender Plasticorder, PL 2000E). Only NBR with 48.2 wt% of acrylonitrile content was used here due to its having best compatibility with the PAni.DBSA [35]. A fill factor of 0.75 was used here in order to perform the blending in the mixer (with free total volume, 320ml). The starting temperature of each mixing was 140°C and the mixer rotor speed was 100 r.p.m. Stages of each mixing are summarised in Table 4.1.

Table 4.1: Stages of Mixing for NBR-Pani.DBSA Blend Masterbatch by using An Internal Mixer (Brabender Plasticorder, PL 2000E)

Stage of mixing	Timing
1. Addition of raw NBR	0th minute
2. Addition of Pani.DBSA	1st minute
3. Sweeping	2nd minute
4. Dumping	10th minute
	(Total time= 10 minutes)

2.5 p.h.r of total DCP (density=1030kg.m^{-3}) was added manually to each NBR-PAni.DBSA blend masterbatches (with different proportions of both blended polymers) on a slightly pre-warmed (50°C) two roll-mill (with gap distance adjusted to about 3mm). The masterbatch was removed from the two-roll mill in sheet form after about 3 minutes of mixing. Prolonged mixing might lead to the problem of premature vulcanisation (hardening and reducing the processability of the material) due to the heat energy generated through surface friction between the material and mill. The highest safe processing temperature of DCP is about 130°C according to literature [15].

4.2.3 Measurement of Vulcanisation Behaviour of Peroxide-Vulcanised NBR-PAni.DBSA Blends

A moving die type rheometer was used (see Figure 4.4) in this work. It is a modification of the Mooney viscometer, but unlike the Mooney, the non-vulcanised sample is compressed between two heated platens (forming a sealed cavity) and by an applied oscillating force. In this way, the platens are maintained at a desired vulcanisation temperature while one platen oscillates (frequency of rotary oscillation was 1.7Hz). The stationary platen is equipped with a torque transducer, which records the induced torque as time and vulcanisation progress. The sample is thus subjected to an oscillatory shearing action of constant amplitude. Oscillation of the platens does not result in the destruction of the sample. As vulcanisation proceeds, the torque required to shear the rubber increases and a curve of torque versus cure time is generated. Since the platens are straining the rubber, the torque value is directly related to the shear modulus of the rubber. Some of the vulcanisation characteristics (as recommended by ISO 3417[36]) of the test compound can be determined directly, as listed below:

M_L = minimum torque

M_H = highest torque value attained where no constant or maximum value is obtained

$t_{s(x)}$ = scorch time to (x) units of torque increase above minimum torque

$t_{c(x)}$ = cure time to (x) percent of maximum torque development

Figure 4.4: A Monsanto Moving Die Rheometer

The vulcanisation behaviour of dicumyl peroxide-vulcanised NBR-PAni.DBSA blends, containing 2.5 wt%, 20 wt% and 50 wt% of PAni.DBSA were measured by using a Monsanto moving die rheometer (MDR 2000E) at temperature of 150°C and duration of 60 minutes. Information obtained from this test was used as a guideline for the vulcanisation of NBR-PAni.DBSA blend test pieces with hot-press moulding.

4.2.4 Preparation of Peroxide-Vulcanised Test Pieces

The dicumyl peroxide-containing NBR-PAni.DBSA blend sheet as prepared by the two-roll mill was immediately used as it was still warm. The flow direction of

passage through the mill was marked on each sheet in order to study the effect of molecular orientation on its mechanical properties. Appropriate amounts of each blend were cut from the sheet and fed into a 2mm thick rectangle (130mm x 100mm) mould while it was still warm and soft. The mould together with the blend was sent for hot pressing (with a Bradley & Turton hot press) and curing (with temperature 150°C, pressure 60psi and duration 38 minutes, based on the t_{c95}). In the middle of the hot-pressing process, the press was reopened for about 10s in order to release air that might be trapped (this was important to avoid forming air bubbles inside the moulded sheet). Flashes produced as a result of extra feed material were trimmed.

Test pieces for the tensile strength (BS ISO 37 [37]), elongation at break (BS ISO 37 [37]), crescent tear strength (BS ISO 34-1 [38]) and tension set (BS ISO 2285 [39]) were cut out from these moulded sheets for directions parallel and perpendicular to the marked flow. Test pieces in disc shape (with thickness 6.3 mm and diameter 13 mm) that were needed for compression set (BS 903-A6 [40]) and hardness measurement (BS 903-A26 [41]) were prepared by feeding the disc-shaped mould with layers of blended material direct from the two roll-mill (without taking count the flow direction). So, a random molecular orientation was assumed for test pieces prepared for compression set and hardness measurement. Test pieces were also prepared from the pure NBR for all testing for the control purposes. It was not possible to prepare the pure Pani.DBSA test piece by using this hot press-moulding method due to its glassy behavior (which could lead to the shrinkage of test piece).

4.2.5 Mechanical Property Tests

All the basic mechanical properties tests were performed according to international standardised procedures (BS or BS ISO) as introduced by the British Standards Institution. All tests (except the compression set one) were carried out in a controlled atmosphere with room temperature 23 ± 2°C and relative humidity 50 ± 5%. Six test pieces of each raw material or blend were used to repeat each

test in order to define the final result as the mean value of a total of six measurements.

4.2.5.1 IRHD Hardness Measurement

IRHD (International Rubber Hardness Degrees) testing provides four methods for the determination of the hardness of vulcanised or thermoplastic rubber surfaces (N-normal, H-high, L-low and M-micro) and four methods for the determination of the apparent hardness of curved surfaces (CN, CH, CL and CM).

The conventional technique consists of measuring the difference between the depths of indentation of a ball probe into a rubber surface under a small initial contact force followed by a large total test force. The methods differ primarily in the diameter of the indenting ball and the magnitude of the indenting force selected according to the hardness of the rubber [41]. From the difference in indentation depth and using the relevant 'look-up' curve, the IRHD value can be read.

However in this work, the IRHD measurement was performed according to BS 903-A26 [41] by using a modern Wallace H14 measuring meter, where the values could be read directly from the meter. Cylindrical test pieces as prepared for the compression set testing were also used for the IRHD measurement.

4.2.5.2 Tensile Properties Measurement

Two tensile properties, i.e. tensile strength and elongation at break were determined according to BS ISO 37 [37] by using a tensile tester (Instron 5567) with a constant straining rate (500mm/min). Test pieces in standard dumb-bell shape were used here. According to BS ISO 37 [37], tensile strength is defined as the maximum tensile stress recorded in extending the test piece to breaking point, and elongation at break is defined as tensile strain (expressed as a percentage increase of the test length, produced by tensile stress) at the breaking point.

4.2.5.3 Crescent Tear Strength Measurement

The crescent tear strength measurement was performed according to BS ISO 34-1 (Method C) [38]. The crescent tear strength is defined as the minimum force required to cause a nick cut in a crescent-shaped test piece (prepared using an I.C.I. Tear Cutter) to extend by tearing the rubber, divided by the thickness of the test piece, where the force acting in a direction substantially normal to the plane of the nick [38].

The tearing force was applied by means of a tensile testing machine (Instron 5567), operated without interruption at a constant rate (500mm/min) of traverse until the test piece broke. The median force achieved was used to calculate the tear strength. The tear strength T_s, expressed in kilonewtons per metre of thickness, is given by the Equation 4.1.

$$T_s = \frac{F}{d} \qquad \text{(Equation 4.1)}$$

where F is the median force (newtons) and d is the median thickness (mm) of the test piece.

4.2.5.4 Compression Set Measurement

Compression set testing is used to determine the ability of elastomeric materials to maintain elastic properties after prolonged compressive stress. The test measures permanent deformation of the specimen after it has been exposed to compressive stress for a set time period. This test is particularly useful for applications in which elastomers would be in a constant pressure or release state. The compression set of pure PAni.DBSA was not measured here since it is not an elastomeric material.

In this part of the work, all compression sets were measured according to BS 903-A6 [40] by using type B test pieces (cylindrical discs of diameter 13mm

and thickness 6.3mm). Test conditions used here were 25% compression, 23°C test temperature, 24h test duration and 30 min recovery time. The compression force was applied by means of an in-house designed compressor.

The compression set *C*, expressed as a percentage of the initial compression, is given by Equation 4.2.

$$C = \frac{h_0 - h_1}{h_0 - h_s} x\ 100 \qquad \text{(Equation 4.2)}$$

where h_0 is the initial thickness (mm) of test piece, h_1 is the thickness (mm) of test piece after recovery and h_s is the height (mm) of the spacer of compressor.

4.2.5.5 Tension Set Measurement

According to BS ISO 2285 [39], the tension set test is intended to measure the ability of rubbers or thermoplastic elastomers to retain their elastic properties after extension, at a standard temperature, to a specified strain which is maintained for a specified time at a specified temperature, and then released at the test temperature or at the standard temperature.

The tension set measurement was carried out according to BS ISO 2285 by using strip test pieces with enlarged ends as specified by the BS ISO 2285 [39]. Test conditions used here were 100% strain, 23°C test temperature, 22h test duration and 30 min recovery time. The straining force was applied by means of a tension set instrument (Wallace Test Equipment).

The tension set, T_{set} as a percentage of initial strain can be calculated using Equation 4.3.

$$T_{set} = \frac{l_1 - l_0}{l_s - l_0} x\ 100 \qquad \text{(Equation 4.3)}$$

where l_0 is the original unstrained reference length (mm), l_s is the strained reference length (mm) and l_1 is the reference length (mm) after recovery.

4.2.6 Morphological Studies (Optical Microscopy and TEM)

All peroxide-vulcanised NBR-PAni.DBSA blends prepared in this part of the work, were studied with a Nikon OPTIPHOT-2 optical microscope (magnification 200 times) and a TEM (Philips CM12 at accelerating voltage, 80kV) respectively. All observed images were captured digitally. Films with thickness ~6.0μm for optical microscopy were prepared by using a Bradley & Turton hot press at 150°C for 5 minutes. Ultra-thin samples (~150nm) for TEM were obtained by sectioning with an RMC MT7000 microtome. Samples for optical microscopy and TEM were collected on glass slides and standard copper grids respectively.

Transparent films (1cm width x 1cm length x 100μm thickness) were also prepared by using a hot press (at 150°C, 5 minutes) for all the peroxide-vulcanised blends (after passing through the two roll-mill) in order to study the effect of stretching on the alignment of PAni.DBSA polymer chains within the rubber host matrix by optical microscopy (magnification 200 times). Stretching of the sample (up to 30% elongation before it got torn) was performed manually using an in-house designed metal jig.

4.2.7 FT-IR Spectroscopy

Infra-red spectra of PAni.DBSA, peroxide-vulcanised NBR and peroxide-vulcanised NBR-PAni.DBSA blends were recorded on a Perkin-Elmer FT-IR Spectrometer PARAGON 100. A small amount of each solid sample was hot-pressed (with a Bradley & Turton hot press at 150°C, 5 minutes) in order to obtain a thin (6.0μm), transparent film before it was put onto a KBr window (as the substrate) for characterisation.

Thicker transparent films (1cm width x 1cm length x 100μm thickness) were also prepared by using a hot press (at 150°C, 5 minutes) for all the

peroxide-vulcanised blends (after passing through the two roll-mill) in order to study the effect of stretching on the alignment of PAni.DBSA polymer chains within the NBR host matrix. The stretching of sample (up to 30 % elongation) was performed manually using an in-house designed metal jig.

4.2.8 Thermal Analysis

PAni.DBSA, peroxide-vulcanised NBR and peroxide-vulcanised NBR-PAni.DBSA blends were characterised by a Perkin-Elmer Pyris Diamond differential scanning calorimeter (DSC). For above-ambient temperature (30 to 400°C), a heating rate of 20°C/minute was used, and for sub-ambient temperature (-60 to 0°C), the heating rate was 10°C/minute.

Each sample was sealed in a 40μL aluminium pan and was analysed under N_2 atmosphere. An empty pan was used as the reference. Each thermal analysis was repeated twice, and the error for all the results was believed to be ±1.5°C. The definitions described in Section 2.2.8 for the onset temperature of the major exotherm and for the glass transition (Tg) were also used in this part of work.

4.2.9 Electrical Conductivity Measurement

The dc electrical conductivity values for PAni.DBSA, peroxide-vulcanised NBR 48.2 ACN wt% and peroxide-vulcanised NBR-PAni.DBSA blends were calculated from electrical "resistance" (voltage/current) values measured by 2- or 4-probe techniques. The dc electrical conductivity values for both non-vulcanised NBR 48.2 ACN wt% and NBR-PAni.DBSA blends were calculated here, in order to make comparison with the peroxide-vulcanised ones. The non-vulcanised blends were prepared by using an internal mixer with the same procedures described in Table 4.1. The effect of addition of the vulcanising agent (i.e. DCP) on the electrical conductivities of NBR-PAni.DBSA blends was studied here by comparing the measured values for the non-vulcanised and vulcanised materials.

The same electrical "resistance" measurement equipment and conditions described in Section 2.2.9 were employed here. Hot-press moulded samples (Bradley & Turton hot press at 150°C, 38 minutes) of all materials with dimensions, 25mm (length) x 25mm (width) x 2mm (thickness) were used in this part of work. The van der Pauw 4-probe method and the 2-probe method were used in order to measure all samples with electrical conductivities $\geq 10^{-7} S.cm^{-1}$ and $< 10^{-7} S.cm^{-1}$ respectively. All measurement set-ups were exactly the same as those used for cast-film samples (see Section 2.2.9), except that no microscope slides were used here since all prepared test pieces were thick enough to support themselves. For the samples measured by the 4-probe technique, the van der Pauw equation (Equation 2.8) configuration was used. Electrical conductivities were calculated from the Equation 2.9 configuration for the samples measured by the 2-probe method.

The effect of strain (elongation in length of sample) on the peroxide-vulcanised blends' electrical conductivities (prepared parallel and perpendicular to the flow direction when passed through the two roll-mill) were also studied. For each blend, three test pieces (in strip form with dimensions 80mm x 20mm x 1mm) were prepared using a hot press (150°C, 5 minutes) in order to obtain a mean value. Each of the test pieces was strained at a constant rate of 100 mm/min. Three cycles of strain loading and unloading process were carried out for all the blends. The electrical "resistance" measurement set-up in this part of work is shown in Figure 4.5 (based on the 2-probe method and Equation 2.9 as described in Section 2.2.9). Both opposite faces and edges of each test piece were coated with a large area of quick-drying silver paint (Acheson Electrodag 915) in order to minimise the effect of contact resistance. A fine copper wire with length 5 cm was stuck to the middle of each side of these silver paint coated-areas for connection to the ohm meter. All the contacting surfaces between the tensile tester and the test piece were properly insulated by a layer of PTFE sheet (~1.0mm thick). All readings were made at 10s after each elongation step in order to standardise the effect of stress relaxation. The new length (L_i) and thickness (d_i) values of each

test piece were also measured after each elongation step in order to calculate the new values of cross-sectional area (A_i).

Figure 4.5: Electrical Measurement Setup (2-Probe Method) for the Study of Straining Effect on the Peroxide-Vulcanised NBR-PAni.DBSA Blends

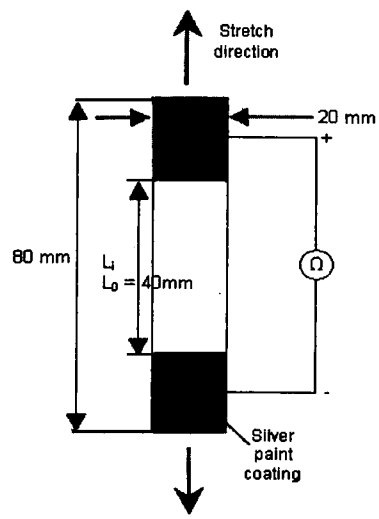

4.3 Results & Discussion

4.3.1 Measurement of Vulcanisation Behaviour of Peroxide-Vulcanised NBR-PAni.DBSA Blends

Results from the rheometer curves (see Figure 4.6 for example) are summarised in Table 4.2. The slowest cure time (t_{95}) was identified as about 38 minutes for Blend 1 with 2.5 wt% of added PAni.DBSA. A 38 minute vulcanisation time was therefore used for all blends as a reference, in order to achieve a vulcanising level of 95% or above. It was observed that the vulcanising times of all blends slightly decreased with increasing the proportion of PAni.DBSA. This is likely there were some extra crosslinkings on the NBR, which contributed by the free radicals released by the PAni.DBSA itself (apart from the peroxide-vulcanising agent) during the high temperature heating process (150°C).

Figure 4.6: Rheometer Curve of Peroxide-Vulcanised NBR-PAni.DBSA Blends (97.5 wt% NBR : 2.5 wt% PAni.DBSA)

Testcode: 41000 Descr.: Rheometer with curves ISO 3417

Variable		Value	Unit
Test temp		150	°C
Test time		60	min
ML		0.81	dNm
MH		8.96	dNm
ts1		2:54	min:sec
ts2		5:16	min:sec
tML		0:27	min:sec
tMH		51:58	min:sec
S*@ML		0.77	dNm
S*@MH		0.42	dNm
t10		2:28	min:sec
t30		6:23	min:sec
t50		11:26	min:sec
t70		18:55	min:sec
t90		32:01	min:sec
t95		37:46	min:sec
Rh		0.48	dNm/min
tRh		2:18	min:sec
MH-ML		8.15	dNm
MachineID		MDR1	

Testdate	23/08/2006 11:13 MKR
Validated by	
Limit version	0
Limits	Not found
Limits remark 1	
Limits remark 2	
Remark 1	
Remark 2	
Production date	23/08/2006
Technologist	YKC
Last changed	23/08/2006 MKR

Status: **Tested**

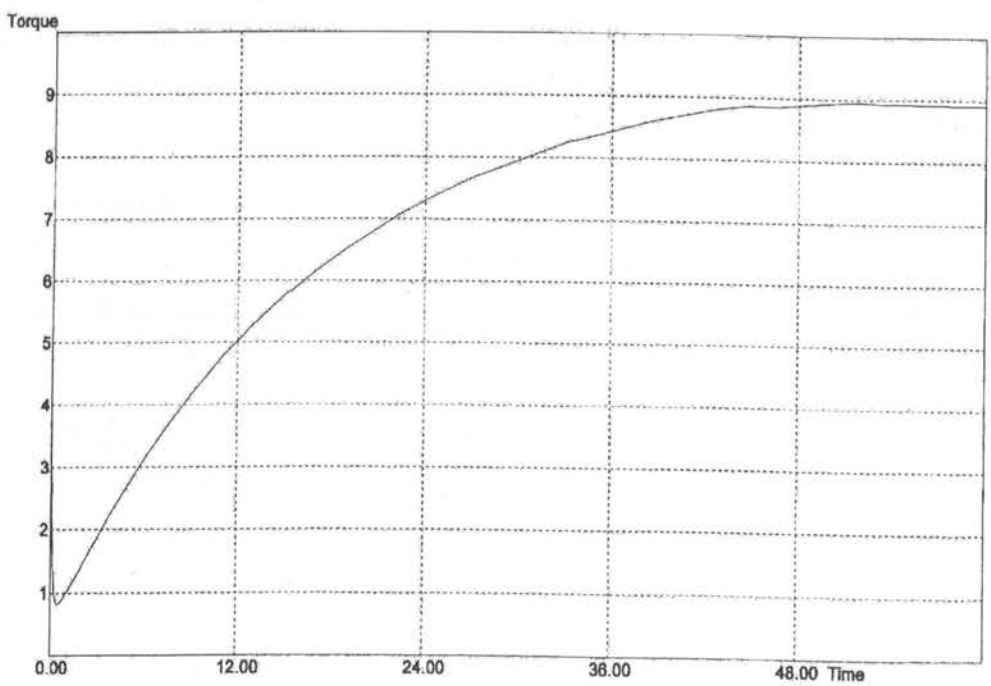

Table 4.2: Vulcanisation Behaviour of Dicumyl Peroxide-Vulcanised NBR-PAni.DBSA Blends

Rheometer curve value	Blend 1 (with 2.5 wt% PAni.DBSA)	Blend 2 (with 20 wt% PAni.DBSA)	Blend 3 (with 50 wt% PAni.DBSA)
Minimum torque (M_L), dNm	0.81	0.83	0.80
Maximum torque (M_H), dNm	8.96	8.99	8.97
Scorch time (t_{S2}), minutes	5	4	4
Cure time (t_{c95}), minutes	38	37	35

It was found that each rheometer curve (see Figure 4.6 for example) also showed a constant value after its maximum torque. It is suggested that all blends reached their maximum vulcanisation level within the chosen test period, i.e. 60 minutes.

4.3.2 Mechanical Property Tests

4.3.2.1 IRHD Hardness Measurement

Results (error ± 1° hardness) of the IRHD measurement are summarised in Figure 4.7. Generally, the degree value of hardness of blend (IRHD) increased with increasing proportion of added PAni.DBSA. This was due to the glassy nature of PAni.DBSA [42] and the increased stiffness of blend as the content of conductive polymer increased. The higher the IRHD value, the stiffer the prepared material. Both of these two parameters could be linearly related with a slope of 0.4734 and intercept of 50.804 as shown in Figure 4.7.

Figure 4.7: IRHD of the Peroxide-Vulcanised NBR and Peroxide-Vulcanised NBR-PAni.DBSA Blends prepared by Thermo-Mechanical Mixing

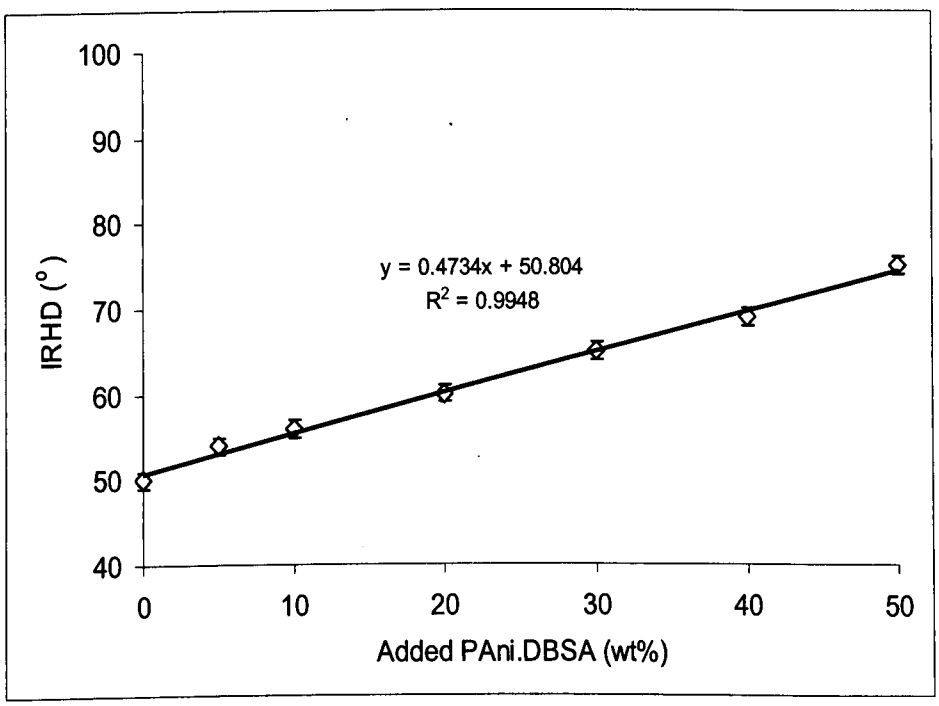

4.3.2.2 Tensile Properties Measurement

Results (error ± 0.05MPa) of the tensile strength experiments are shown in Figure 4.8. For test pieces cut and strained parallel to the flow direction, PAni.DBSA acted as a reinforcing agent, so their tensile strength increased with the proportion of PAni.DBSA (5-30 wt%). The tensile strength decreased for blends with ≥40 wt% of PAni.DBSA (due to the increase of phase-separated PAni.DBSA regions). For test pieces stretched perpendicular to the flow direction, it was observed that there were some smaller reinforcing effects for blends up to 30 wt% of PAni.DBSA, by comparing to test pieces stretched parallel to the flow direction. Both sets of tensile strength vs. concentration data (strained parallel and perpendicular to the flow direction) could be modelled by quadratic equations (correlation coefficients, ~0.99) as shown in Figure 4.8.

Figure 4.8: Tensile Strength of Peroxide-Vulcanised NBR and Peroxide-Vulcanised NBR-PAni.DBSA Blends (Test Pieces stretched Parallel and Perpendicular to the Flow Direction when passing through the Mill)

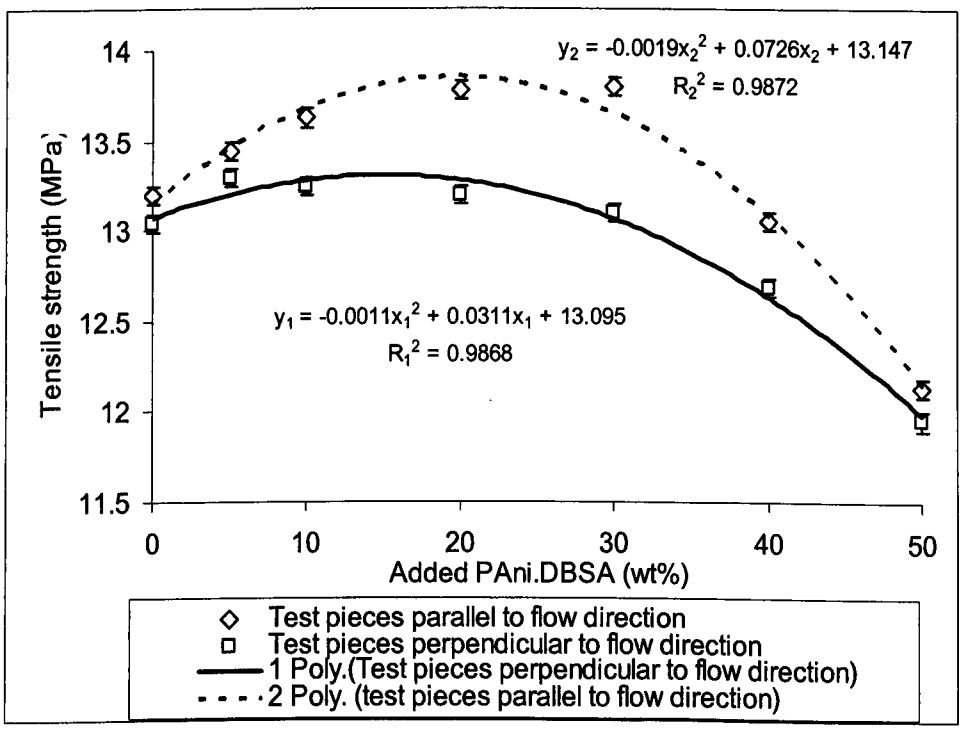

Results (error ±5 %) of the elongation percentage at break (EB%) measurement are summarised in Figure 4.9. For test pieces stretched parallel to the flow direction, the EB% values increased with the proportion of PAni.DBSA (5-30 wt%). The EB% was reduced for blends with >30 wt% of PAni.DBSA. For test pieces stretched perpendicular to the flow direction, it was observed that the EB% also increased with increasing proportion of PAni.DBSA up to 30 wt% of PAni.DBSA. However their EB% values were lower than the values obtained for test pieces stretched parallel to the flow direction. Both of these data sets (stretched parallel and perpendicular to the flow direction) could be modelled by equations (correlation coefficients, ~0.99) as shown in Figure 4.9.

Figure 4.9: Elongation Percentage at Break (EB%) of Peroxide-Vulcanised NBR and Peroxide-Vulcanised NBR-PAni.DBSA Blends (Test Pieces stretched Parallel and Perpendicular to Flow Direction when passing through the Mill)

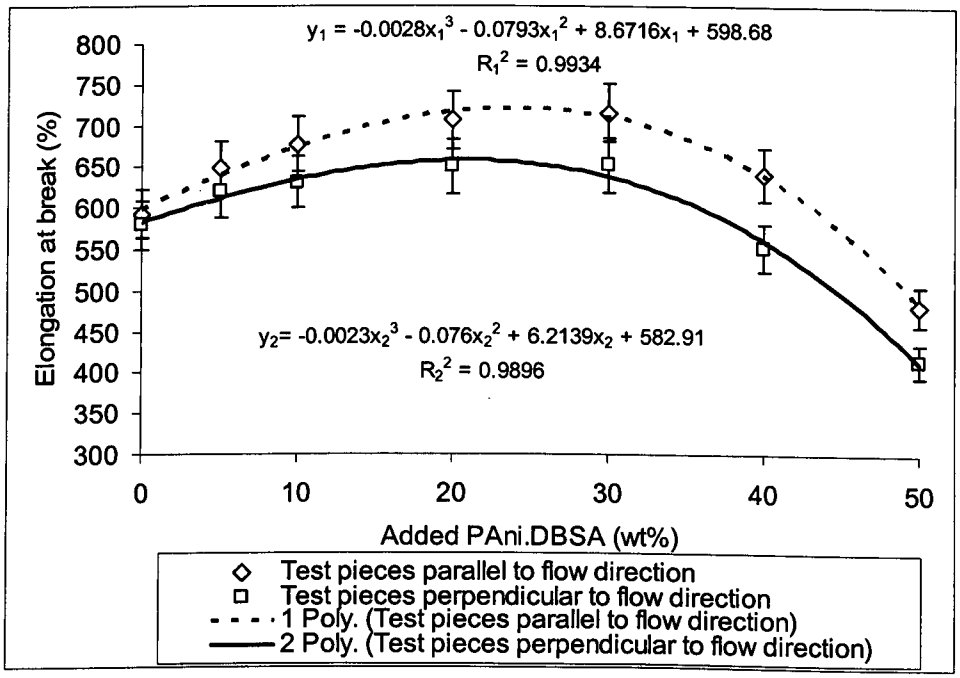

When a test piece with PAni.DBSA contents up to 30 wt% was extended by a tensile force (stretched parallel to the flow direction), it is proposed that the reinforcing effect observed was due to the elongation and alignment of the PAni.DBSA polymer chains that moved closer to each other (as illustrated by Figure 4.10). As a result, they attracted each other more strongly and possibly para-crystallised. Test pieces stretched perpendicular to the flow direction (with ≤ 30 wt% PAni.DBSA) showed smaller reinforcing effects compared to those stretched parallel to the flow direction. This was likely attributable to the higher proportions of well-blended regions (involving some very small and well-dispersed PAni.DBSA particles) produced for those samples (see Section 4.3.3). For test pieces with PAni.DBSA content ≥40 wt% (either stretched parallel or perpendicular to the flow direction), it is proposed that phase-separated PAni.DBSA regions (see Figure 4.15) had started to determine the blends' mechanical properties, making the tensile values decrease and approach those of pure PAni.DBSA [31].

Figure 4.10: 2-Dimensional Illustrations of the Majority Alignment of PAni.DBSA Polymer Chains for a Tensile Test Piece during the Stretching Process; (a) Test Piece stretched Parallel to the Flow Direction when passed through the Two Roll-Mill, and (b) Test Piece stretched Perpendicular to the Flow Direction

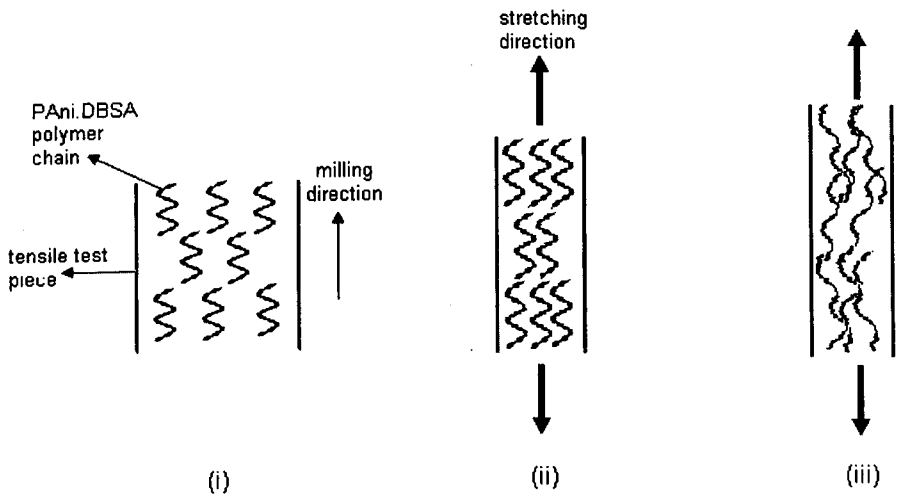

(i) A non-stretched tensile test piece with PAni.DBSA polymer chains aligned rather parallel to the flow direction when passed through two-roll mill.
(ii) Test piece elongated 10% in length, the PAni.DBSA polymer chains are somewhat elongated and move closer to each other.
(iii) Test piece elongated 30% in length, further alignment and elongation of the PAni.DBSA polymer chains. They move closer to each other and hence form stronger secondary bonds.

(a)

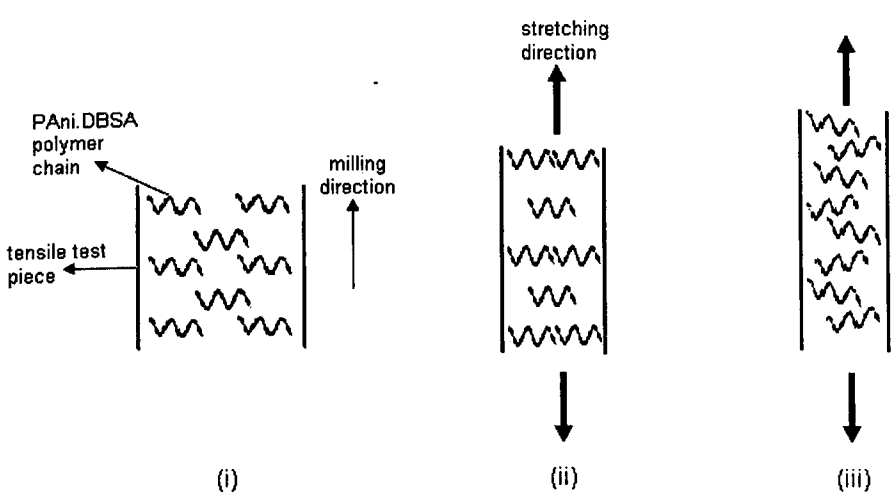

(i) A non-stretched tensile test piece with PAni.DBSA polymer chains aligned rather perpendicular to the flow direction when passed through two-roll mill.
(ii) Test piece elongated 10% in length, bigger gap created between the PAni.DBSA polymer chains.
(iii) Test piece elongated 30% in length, some increased separation of the PAni.DBSA polymer chains and hence reduced inter-chain attractions.

(b)

4.3.2.3 Crescent Tear Strength Measurement

Results (error ±0.2kN/m) for crescent tear strength are summarised in Figure 4.11. For test pieces stretched parallel to the flow direction, the PAni.DBSA was acting as a reinforcing agent, and so the crescent tear strength values increased with the proportion of PAni.DBSA (up to 30 wt%). For test pieces stressed perpendicular to the flow direction, their crescent tear strength values were lower than the ones obtained by stretching parallel to the flow direction. This phenomenon can be described with the simple 2D models as illustrated by Figure 4.12. The cubic equations (with correlation coefficients, ~0.99) shown in Figure 4.11, successfully fit both of these two data sets (parallel and perpendicular to the flow direction).

Figure 4.11: Crescent Tear Strength of Peroxide-Vulcanised NBR and Peroxide-Vulcanised NBR-PAni.DBSA Blends (Test Pieces stretched Parallel and Perpendicular to the Flow Direction)

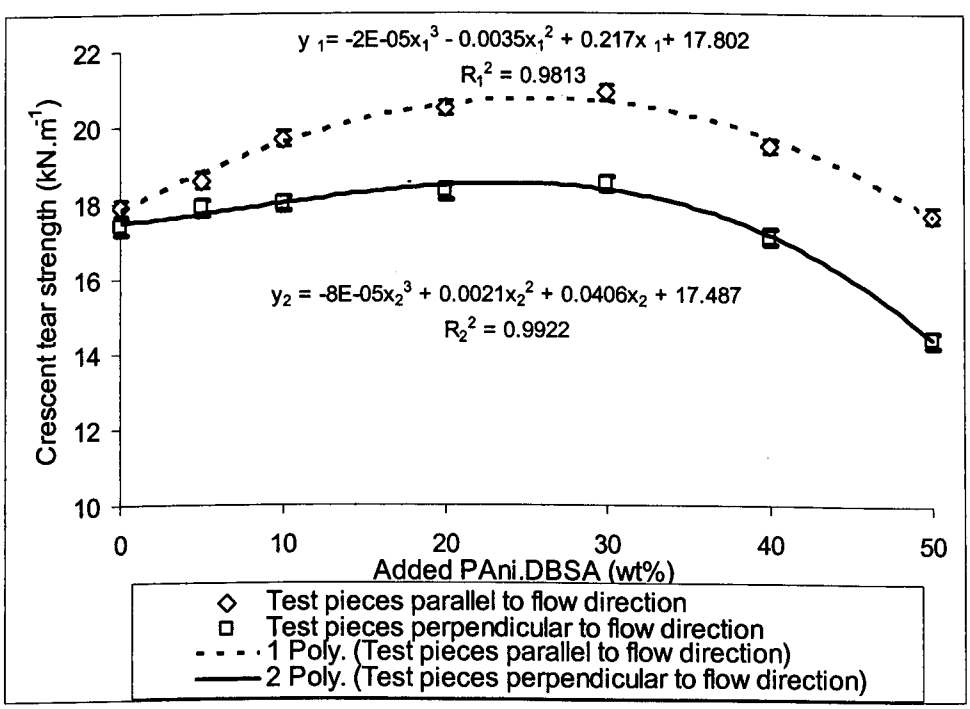

Figure 4.12: 2-Dimensional Illustrations of the Majority Alignment of PAni.DBSA Polymer Chains for a Test Piece during Crescent Tear Strength Test; (a) Test Piece stretched Parallel to the Flow Direction when passed through the Two Roll-Mill, and (b) Test Piece stretched Perpendicular to the Flow Direction

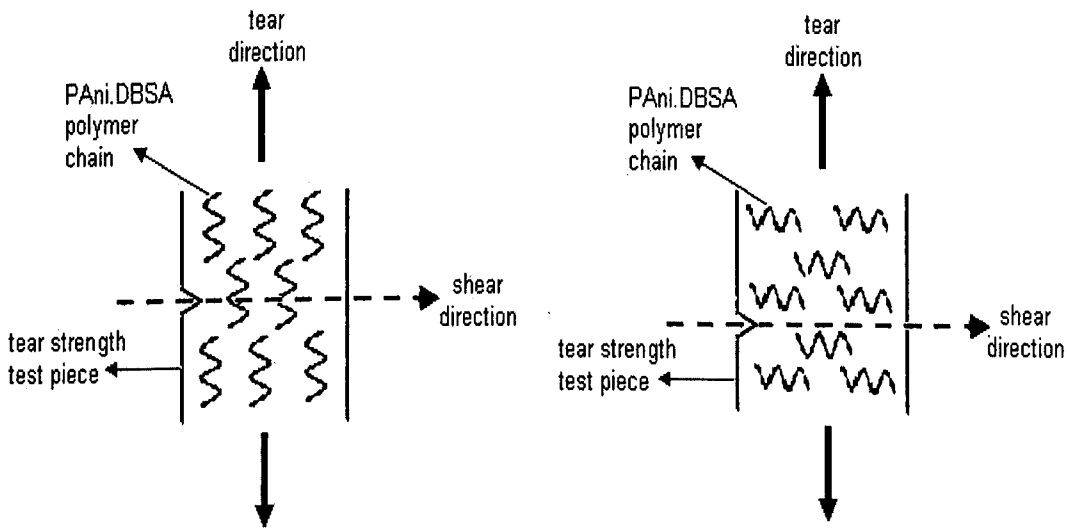

(a) Higher energy (force) needed in order to shear through the test piece in direction that perpendicular with the PAni.DBSA polymer chains alignment
(b) Less energy (force) needed in order to shear through the test piece in direction that parallel with the PAni.DBSA polymer chains alignment

4.3.2.4 Compression Set Measurement

Results (error ±1%) of the compression set measurement are summarised in Figure 4.13. There was no measurement conducted for pure PAni.DBSA because it is not an elastomeric material. Generally, the compression set values increased with the proportion of PAni.DBSA due to the latter's glassy behaviour. A cubic equation (correlation coefficient, ~1.00) as shown in Figure 4.13 fit the data well.

Figure 4.13: Compression Set of Peroxide-Vulcanised NBR and Peroxide-Vulcanised NBR-PAni.DBSA Blends prepared by Thermo-Mechanical Mixing

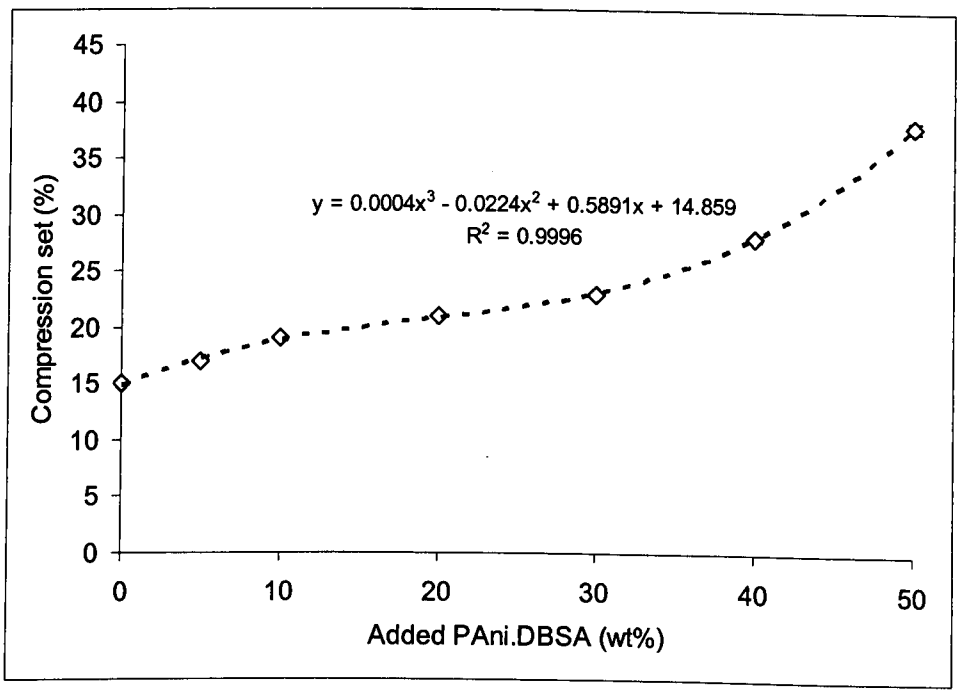

4.3.2.5 Tension Set Measurement

Results (error ±1%) from the tension set measurements are summarised in Figure 4.14. No measurement was again conducted for pure PAni.DBSA, again because it is not an elastomeric material.

Generally, the tension set values increased with increasing proportion of added PAni.DBSA for both sets of prepared test pieces due to its glassy nature. However, the elastomeric behaviour of the blends were reduced more obviously by the PAni.DBSA for the set of test pieces stretched perpendicular to the flow direction if compared to the parallel one, attributed to the different alignment of PAni.DBSA polymer chains (see Figure 4.10). Both of these sets of data (parallel and perpendicular to the flow direction) could again be empirically fit by cubic equations (correlation coefficients, ~1.00) as shown in Figure 4.14

Figure 4.14: Tension Set of Peroxide-Vulcanised NBR and Peroxide-Vulcanised NBR-PAni.DBSA Blends (Test Pieces stretched Parallel and Perpendicular to the Flow Direction when passing through the Mill)

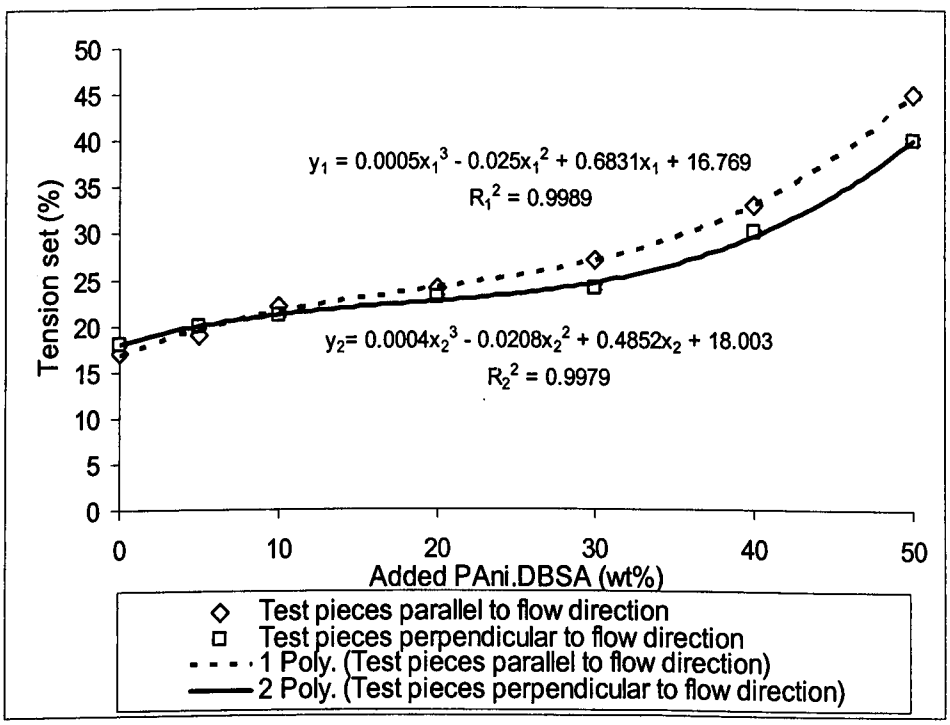

4.3.3 Morphological Studies (Optical Microscopy and TEM)

Optical microscopy was used to study all the peroxide-vulcanised NBR-PAni.DBSA blends, but only images of blends containing 5, 20, 30 and 40 wt% of PAni.DBSA are shown here (Figure 4.15). For all the micrographs, two distinct coloured regions were again observed, i.e. the pale-green ones and the dark-green ones. The dark-green regions (rich in PAni.DBSA) showed some large conductive particles and their agglomerates, which related to some degree of phase-separation. The well-blended regions of PAni.DBSA and NBR were shown as pale-green colour (rich in NBR); they became denser in colour when the concentration of PAni.DBSA was increased. As discussed in Chapter 2, on increasing the proportion of PAni.DBSA, the total area of the dark green-region will increase. For all the optical micrographs, some large, isolated particles could be observed (see Figure 4.15). However, it is strongly believed that the two

blended polymers are significantly compatible, based on the results obtained from the FT-IR spectroscopy and DSC thermal analysis.

Figure 4.15: Optical Micrographs (200 x Magnification) for the Peroxide-Vulcanised Blends of NBR-PAni.DBSA prepared by Thermo-Mechanical Mixing. Blends contain (a) 60:40 (b) 70:30 (c) 80:20 and (d) 95:5 wt% NBR:wt% PAni.DBSA

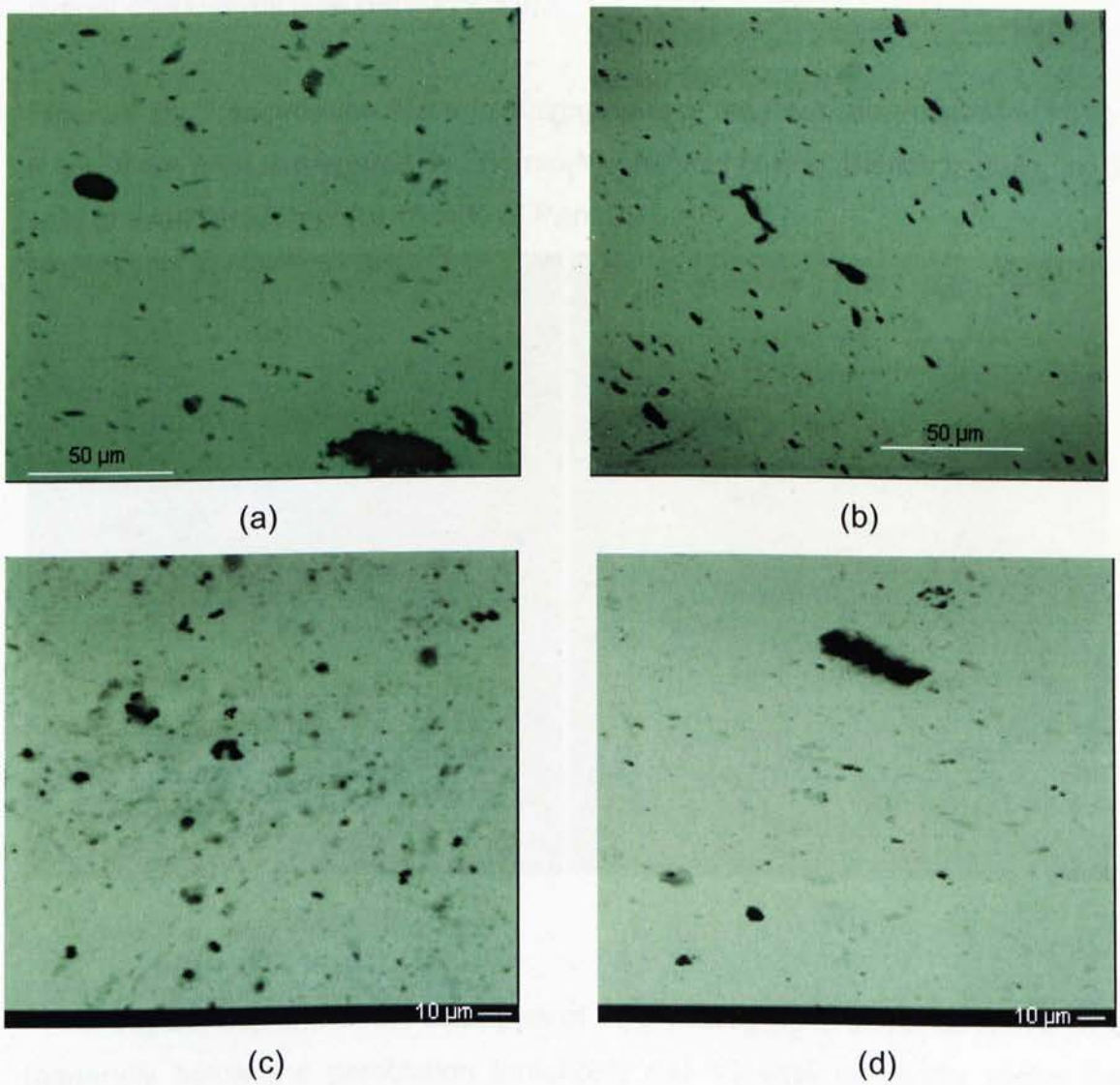

Preparation of NBR-PAni.DBSA blends by using the internal mixer at high temperature produced numerous well-blended regions of NBR and PAni.DBSA (pale-green regions in Figure 4.15). It is likely that most of the electrical

conductivity of these thermo-mechanically mixed blends was contributed by the conducting polymers in these well-blended regions [see Figures 4.15(a) and (b)]. This is in contrast with the same type of blend prepared by solution mixing at room temperature, where it is suggested that the built-up networks or pathways of large phase-separated PAni.DBSA particles had played important role in the overall conductivity [see Section 2.3.4].

Figure 4.16: Transmission Electron Micrographs of the Peroxide-Vulcanised NBR-PAni.DBSA Blends prepared by Thermo-Mechanical Mixing. Blends contain, (a) 5 wt% of PAni.DBSA and (b) 10 wt% of PAni.DBSA

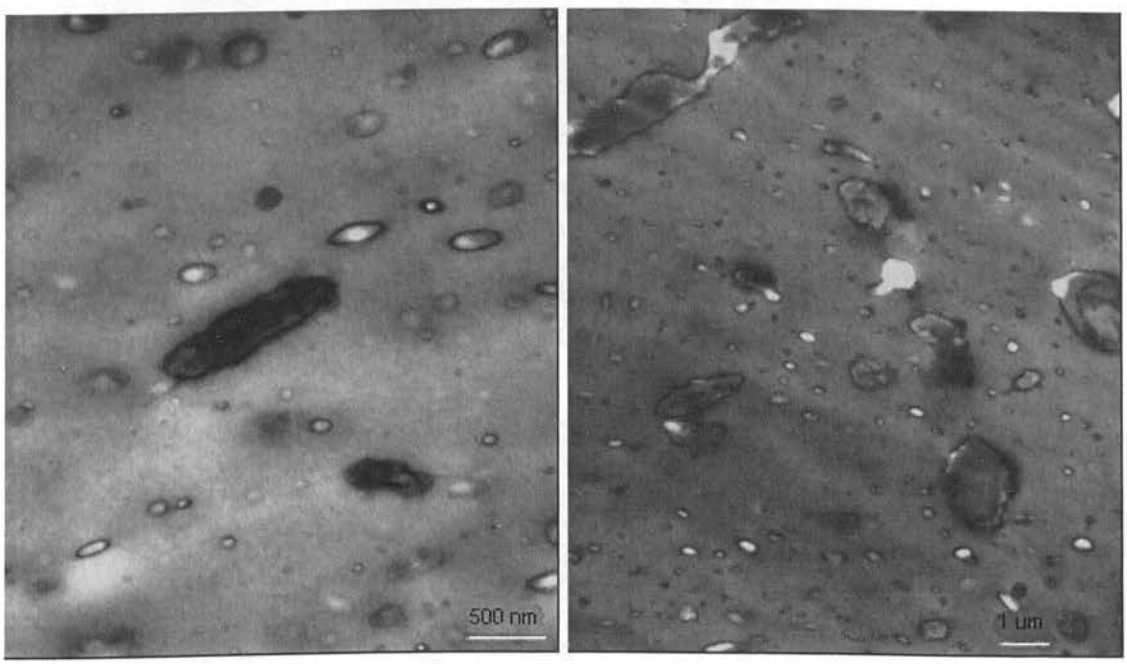

(a) (b)

Figure 4.16 shows the examples of TEM micrographs of blends with 5 wt% (generally below the percolation threshold) and 10 wt% (generally above the percolation threshold) of added PAni.DBSA. The dark regions in both TEM micrographs relate to the large conductive PAni.DBSA particles in a lighter NBR matrix. The TEM also successfully revealed some very small particles of PAni.DBSA (of colloidal dimensions, 50-1000nm). As reported in Chapter 2, all these small PAni.DBSA particles had also contributed to the electrical conductivity

of blends prepared in this part of work, especially the ones that were below the main percolation threshold.

Figure 4.17: Optical Micrographs (200 x Magnification) for the Peroxide-Vulcanised NBR-PAni.DBSA Blends (70 wt%:30 wt%) prepared by Thermo-Mechanical Mixing. Samples are (a) Non-Stretched but aligned Parallel to the Flow Direction when passed through the Two Roll-Mill, (b) 30% Elongation Parallel to the Flow Direction, (c) Non-Stretched but aligned by the Flow Direction as before and (d) 30% Elongation Perpendicular to Flow Direction

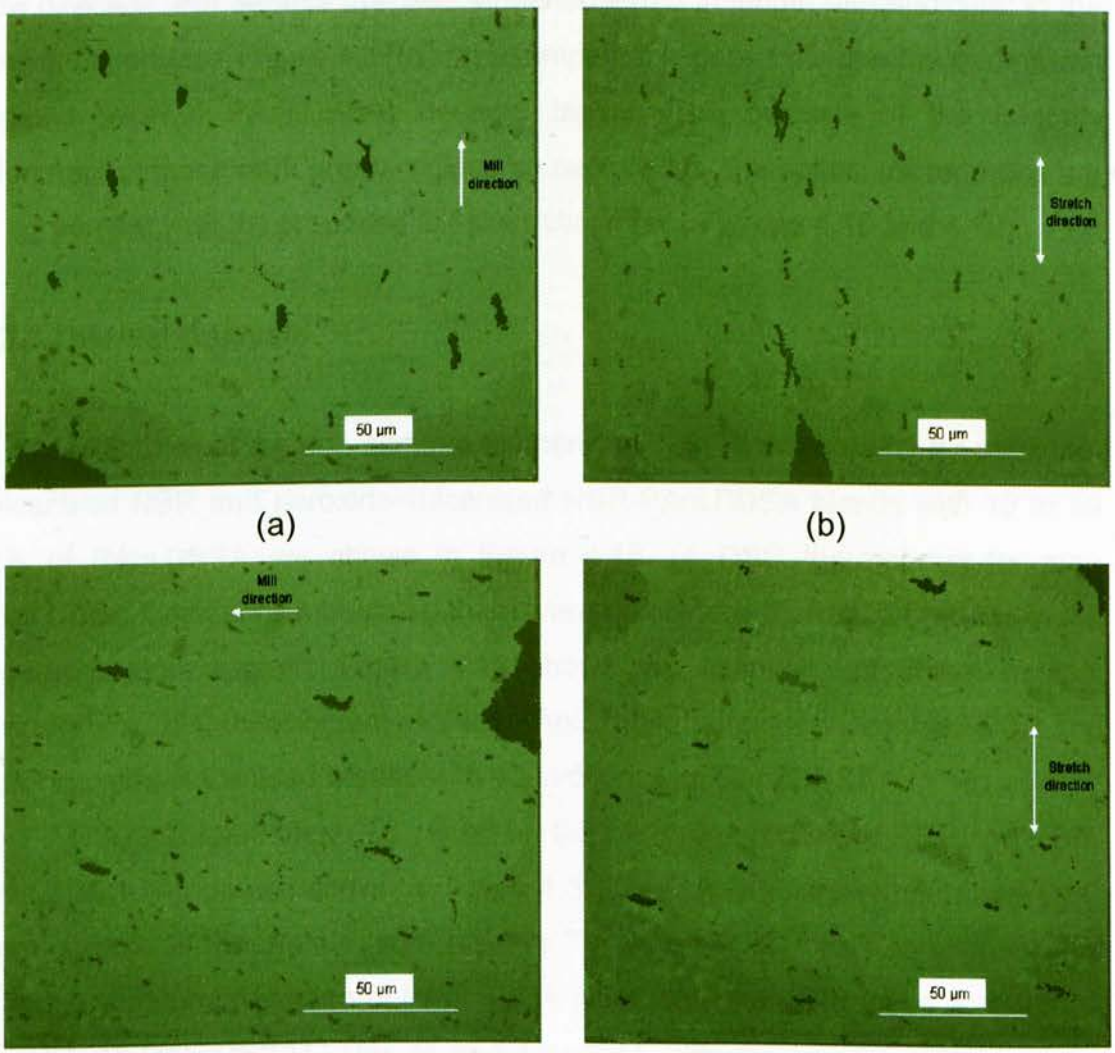

The effect of stretching on the alignment of PAni.DBSA polymer chains within the NBR host matrix was also studied by optical microscope. Figure 4.17

shows the example of optical micrographs for blends with 30 wt% of PAni.DBSA. All micrographs showed the two classic regions, i.e. dark-green ones (rich in PAni.DBSA) and pale-green ones (rich in NBR). As observed from Figure 4.17, majority of the isolated dark-green regions were aligned rather to the flow direction when passed through the two roll-mill.

Some elongated dark-green regions were observed for sample that was stretched ≥10% in length [see Figure 4.17(b) for example] parallel to the original flow direction. For sample that was stretched ≥10% in length perpendicular to the flow direction [see Figure 4.17(d) for example], the gaps between the dark-green regions (rich in PAni.DBSA) became bigger. The patterns of the majority alignment of these dark green-regions as captured by the optical micrographs are in agreement with the proposed 2D-illustrations (see Figures 4.10 and 4.12).

4.3.4 Thermal Analysis

Examples of the sub-ambient temperature DSC thermograms for peroxide-vulcanised NBR and peroxide-vulcanised NBR-PAni.DBSA blends with 10 to 50 wt% of PAni.DBSA are shown in Figure 4.18. (A DSC thermogram for pure PAni.DBSA is not shown because there were no obvious thermal processes in the low-temperature region). Figure 4.19 shows the examples of above-ambient temperature DSC thermograms for the PAni.DBSA, peroxide-vulcanised NBR and their peroxide-vulcanised blends with 10 to 50 wt% of PAni.DBSA.

The calculated mean Tg values for the peroxide-vulcanised NBR and NBR-PAni.DBSA blends are shown in Table 4.3. The sub-ambient temperature DSC thermograms of the blends have positive Tg shifts for the NBR component that increase with the proportion of PAni.DBSA (with maximum shift value achieved at 30 wt% of PAni.DBSA). This is in agreement with the results obtained from Section 4.3.3, which reported that the higher amounts of phase-separated regions could be obtained at the higher contents of PAni.DBSA (≥40 wt%).

Figure 4.18: Sub-Ambient Temperature DSC Thermograms for Peroxide-Vulcanised NBR-PAni.DBSA Blends of Different Composition (wt% NBR:wt% PAni.DBSA*)

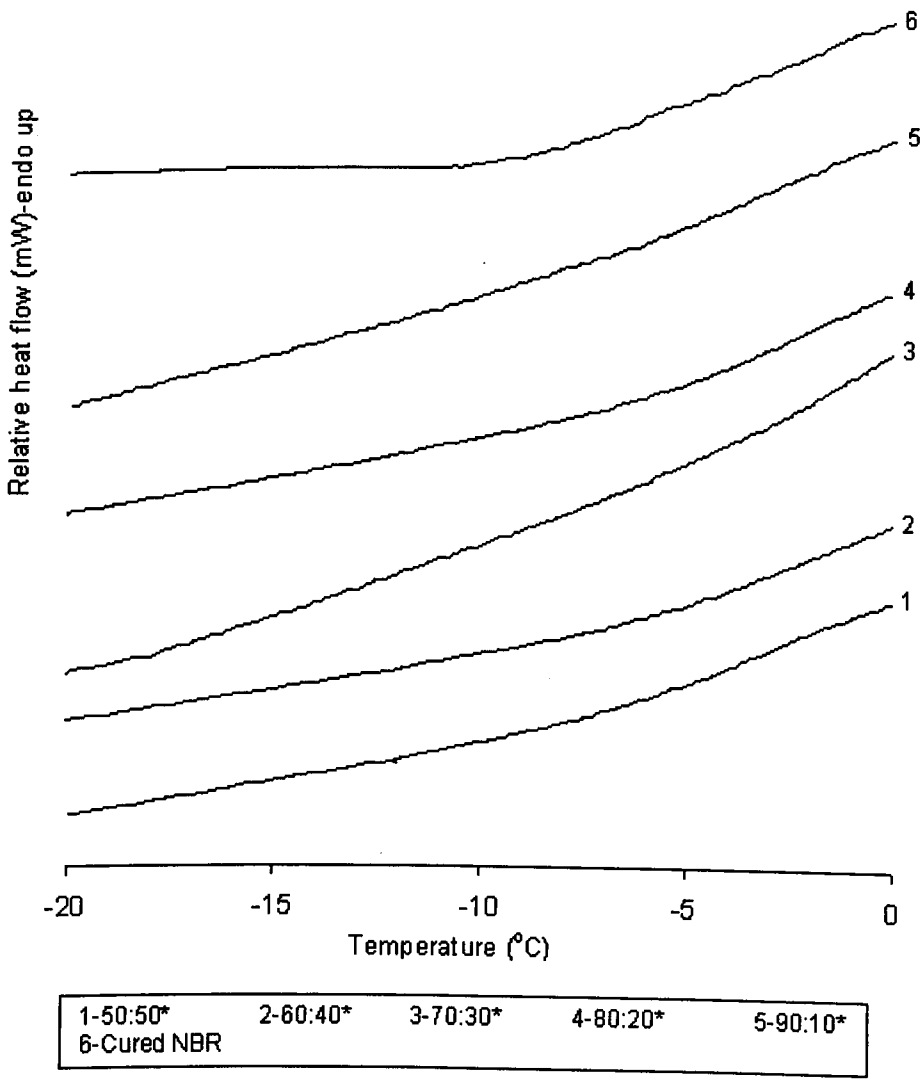

Figure 4.19: Above-Ambient Temperature DSC Thermograms for PAni.DBSA, Peroxide-Vulcanised NBR and Different Compositions (wt% NBR:wt% PAni.DBSA*) of Peroxide-Vulcanised NBR-PAni.DBSA Blends

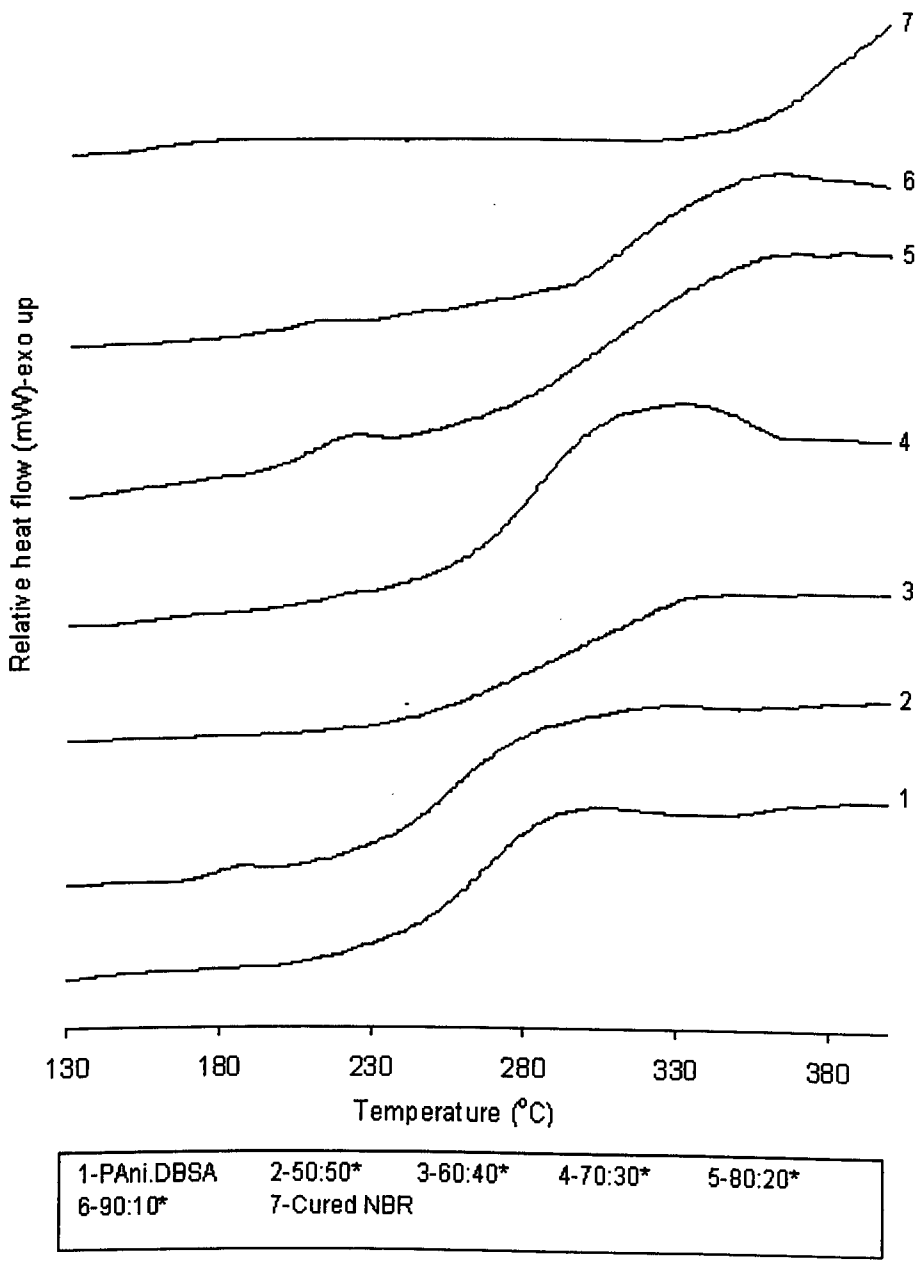

Table 4.3: The Mean Glass Transition Temperature (Tg) Values for Peroxide-Vulcanised NBR and Peroxide-Vulcanised NBR-PAni.DBSA Blends

Composition (wt% NBR : wt% PAni.DBSA*)	Glass transition temperature (Tg), °C
Vulcanised NBR (48.2 wt% ACN)	-10
Vulcanised blend	
90:10*	-7
80:20*	-7
70:30*	-5
60:40*	-8
50:50*	-8

The vulcanised NBR was found (see Table 4.4) to be thermally stable up to about 354°C (which is 23°C higher than the non-vulcanised one discussed in Chapter 2, due to its more rigid crosslinked structure [12]). The PAni.DBSA had good thermal stability up to about 233°C (same value as found in Chapter 2). The thermal processes that were combinations of events recorded for the two raw materials could be observed from all the above-ambient temperature DSC thermograms. However, the detailed examination successfully revealed that the events also showed some degrees of temperature shift related to the corresponding processes in the raw materials.

For the above-ambient temperature DSC analysis, the larger the onset temperature shifts of the blend from the constituent materials, the better the compatibility between the two blended polymers using this high temperature mixing method. From Table 4.4, it was found that the blends containing low to moderate amounts of PAni.DBSA (≤30 wt%) showed larger shifts in the onset temperature of the major exotherm (with respect to the pure PAni.DBSA). However, only smaller shifts in the onset temperature of the major exotherm were observed for the blends with high contents of PAni.DBSA (≥40 wt%). This is again in agreement with the results obtained from Section 4.3.3, where more phase-

separated (dark-green) regions could be found for the blends with ≥40 wt% of PAni.DBSA attributed to the lower level of compatibility between the two constituent polymers.

Table 4.4: The Mean Onset Temperature Values of Major Exotherms for the Above-Ambient Temperature DSC Thermograms of PAni.DBSA, Peroxide-Vulcanised NBR and Peroxide-Vulcanised NBR-PAni.DBSA Blends

Composition (wt% NBR : wt% PAni.DBSA*)	Onset temperature of major exotherm, °C
Vulcanised NBR (48.2 wt% ACN)	354
Vulcanised blend	
90:10*	297
80:20*	276
70:30*	252
60:40*	239
50:50*	229
PAni.DBSA	233

4.3.5 FT-IR Spectroscopy

Examples of FT-IR spectra for PAni.DBSA, peroxide-vulcanised NBR and their peroxide-vulcanised blends (i.e. with 10 wt% and 40 wt% of PAni.DBSA) are shown in Figure 4.20. FT-IR spectrum for the hot-pressed film of peroxide-vulcanised NBR shows its characteristic absorptions at 2238cm^{-1} (-C ≡ N stretching), 1630cm^{-1} (C=C stretch) and 1440-1445cm^{-1} (out of plane C-H wagging). The spectrum of PAni.DBSA has characteristic absorptions at 3448 cm^{-1} (=N-H stretching), 1559cm^{-1} (N=quinoid=N), 1478cm^{-1} (N-benzoid-N), 1295cm^{-1} (quinoid=N-benzoid), 1240cm^{-1} (C aromatic-N stretching) and 1030cm^{-1} (S=O stretching).

Figure 4.20: FT-IR Spectra of PAni.DBSA, Peroxide-Vulcanised NBR and Peroxide-Vulcanised NBR-PAni.DBSA Blends. (a) 1000 to 1650cm^{-1}, (b) 2150 to 2300cm^{-1} and (c) 3400 to 3470cm^{-1}

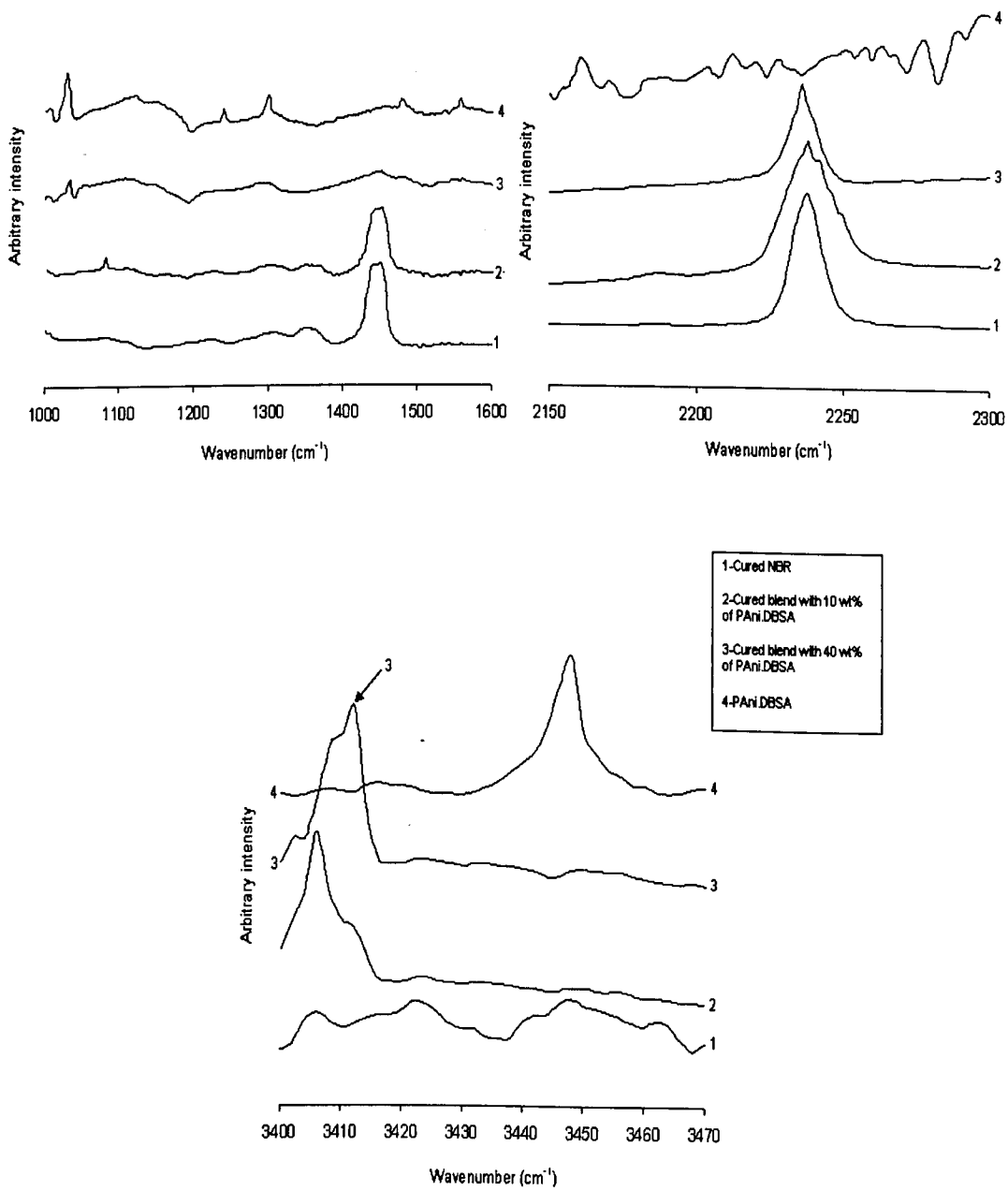

For all the peroxide-vulcanised blends with low contents of PAni.DBSA (i.e. ≤30 wt%), their infrared spectra showed a predominance of NBR absorption bands. There was a predominance of PAni.DBSA absorption bands in all the infrared spectra of peroxide-vulcanised blends with higher levels of PAni.DBSA (i.e. ≥40 wt%). However, some significant shifts of certain characteristic peaks were successfully found through some detailed examination and the mixing efficiency of the two blended polymers was assessed by studying some of these infrared peak shifts (see Table 4.5).

Table 4.5: Characteristic Infrared Absorption Peaks for PAni.DBSA, Peroxide-Vulcanised NBR and Peroxide-Vulcanised NBR-PAni.DBSA Blends

Pure material or blend (wt% NBR: wt% PAni.DBSA*)	Peak assignment, cm^{-1} Indication of peak intensity: W=weak; M=medium		
	=N-H stretching	S=O stretching	-C≡N stretching
PAni.DBSA	3448W	1030M	-
Vulcanised NBR	-	-	2238M
Vulcanised blend			
90:10*	3406W	1081W	2238W
80:20*	3406W	1081W	2237W
70:30*	3406W	1081W	2236W
60:40*	3412W	1033W	2236W
50:50*	3430W	1032W	2236W

The bands at 3448cm^{-1} (N-H stretching) and 1030cm^{-1} (S=O stretching) are solely attributed to the PAni.DBSA, while that at 2238cm^{-1} is derived from the peroxide-vulcanised NBR. From the spectra of all peroxide-vulcanised blends, all these bands were found to have intensities comparable to those for the raw material ones. However, two large peak shifts were successfully found, i.e. a decrease to 3406cm^{-1} for the N-H stretch and an increase to 1081cm^{-1} for the S=O stretch, attributed to the changes of intermolecular interactions. Section 2.3.5 has already discussed this phenomenon.

Both of the Tables 4.6 and 4.7 summarise the characteristic IR absorption peaks of all the non-stretched and stretched peroxide-vulcanised blends that were passed through the two roll-mill. Figure 4.20 shows the example of FT-IR spectra for the peroxide-vulcanised blend with 30 wt% of PAni.DBSA, stretched parallel to the flow direction. The effect of stretching on the alignment of PAni.DBSA polymer chains within the NBR host matrix was studied in terms of the peak shifts and the changes of peak absorption intensity of recorded FT-IR spectra (based on the two characteristic functional groups of PAni.DBSA, i.e. =N-H and S=O). The peak assigned to NBR functional group (-C≡N) had no obvious shift attributed to its strong and stable triple bond.

The effect of stretching was not obvious (in terms of peak shift and absorbance intensity) for the blends with low proportion of PAni.DBSA (10 wt% or below) and this is almost certainly due to the reasonably high compatibility between the two mixed components as this level (less separated phases as observed by microscopy). This phenomenon explains why the mechanical properties (see Figures 4.8, 4.9, 4.11 and 4.14) of both sets of test piece (either stretched parallel or perpendicular to the flow direction) at these levels of added PAni.DBSA are very similar.

Greater peak shifts (both of the =N-H and S=O functional groups) towards the values of pure PAni.DBSA and absorbance intensity changes (see Figure 4.21 for example) were observed for blends (≥20 wt% of PAni.DBSA) stretched parallel to the flow direction, as the elongation of their samples increased. It is likely that this was due to the existence of higher levels of interaction (e.g. secondary bonding) among the elongated PAni.DBSA polymer chains as observed from the optical micrographs [see Figure 4.17(b) for example]. However, no obvious peak shifts and changes of peak absorption intensities were observed for the blends stretched perpendicular to the flow direction. This was attributed to the decreased level of intermolecular interaction and different alignment of the PAni.DBSA polymer chains as illustrated in Figure 4.10(b).

Table 4.6: Characteristic Infrared Absorption Peaks for Peroxide-Vulcanised NBR and NBR-PAni.DBSA Blends stretched Parallel to the Flow Direction when passing through the Two Roll-Mill

Pure material/ blend (wt% NBR: wt% PAni.DBSA*)	Peak assignment, cm^{-1} Indication of peak intensity: W=weak; M=medium		
	=N-H stretching	S=O stretching	-C≡N stretching
Non-stretched			
Pure NBR	-	-	2238W
95:05*	3407W	1081W	2237W
90:10*	3407W	1081W	2237W
80:20*	3407W	1081W	2237W
70:30*	3406W	1081W	2236W
60:40*	3413W	1034W	2236W
50:50*	3430W	1033W	2236W
10% elongated			
Pure NBR	-	-	2237W
95:05*	3407W	1081W	2237W
90:10*	3407W	1081W	2237W
80:20*	3408W	1081W	2237W
70:30*	3410W	1079W	2236W
60:40*	3416W	1032W	2236W
50:50*	3432W	1031W	2236W
20% elongated			
Pure NBR	-	-	2237W
95:05*	3407W	1081W	2237W
90:10*	3407W	1081W	2237W
80:20*	3408W	1080W	2236W
70:30*	3412W	1078M	2236W
60:40*	3417W	1031M	2236W
50:50*	3433W	1031M	2236W
30% elongated			
Pure NBR	-	-	2237W
95:05*	3407W	1081W	2237W
90:10*	3407W	1081W	2237W
80:20*	3409W	1080W	2236W
70:30*	3414M	1077M	2236W
60:40*	3420M	1031M	2236W
50:50*	3434M	1031M	2236W

Table 4.7: Characteristic Infrared Absorption Peaks for Peroxide-Vulcanised NBR and NBR-PAni.DBSA Blends stretched Perpendicular to the Flow Direction when passing through the Two Roll-Mill

Pure material/ blend (wt% NBR: wt% PAni.DBSA*)	Peak assignment, cm^{-1} Indication of peak intensity: W=weak; M=medium		
	=N-H stretching	S=O stretching	-C≡N stretching
Non-stretched			
Pure NBR	-	-	2238W
95:05*	3407W	1081W	2238W
90:10*	3407W	1081W	2237W
80:20*	3407W	1081W	2237W
70:30*	3406W	1081W	2236W
60:40*	3413W	1034W	2236W
50:50*	3432W	1032W	2236W
10% elongated			
Pure NBR	-	-	2238W
95:05*	3407W	1081W	2237W
90:10*	3407W	1081W	2237W
80:20*	3407W	1081W	2236W
70:30*	3406W	1081W	2236W
60:40*	3413W	1034W	2236W
50:50*	3432W	1032W	2236W
20% elongated			
Pure NBR	-	-	2238W
95:05*	3407W	1081W	2237W
90:10*	3407W	1081W	2237W
80:20*	3407W	1081W	2236W
70:30*	3406W	1081W	2236W
60:40*	3413W	1033W	2236W
50:50*	3432W	1032W	2236W
30% elongated			
Pure NBR	-	-	2238W
95:05*	3407W	1081W	2237W
90:10*	3407W	1081W	2237W
80:20*	3407W	1081W	2236W
70:30*	3406W	1081W	2236W
60:40*	3413W	1033W	2236W
50:50*	3432W	1032W	2236W

Figure 4.21: FT-IR Spectra of Non-Stretched and Stretched Peroxide-Vulcanised NBR-PAni.DBSA Blends (70 wt%:30 wt%) stretched Parallel to the Flow Direction when passing through the Two Roll-Mill. (a) 1000 to 1650cm^{-1}, (b) 2150 to 2300cm^{-1} and (c) 3400 to 3470cm^{-1}

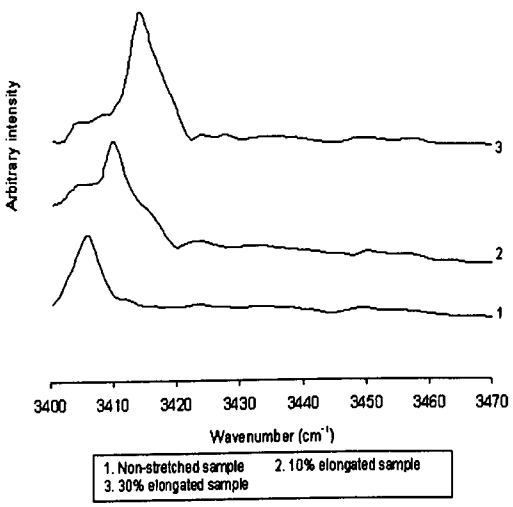

(a)

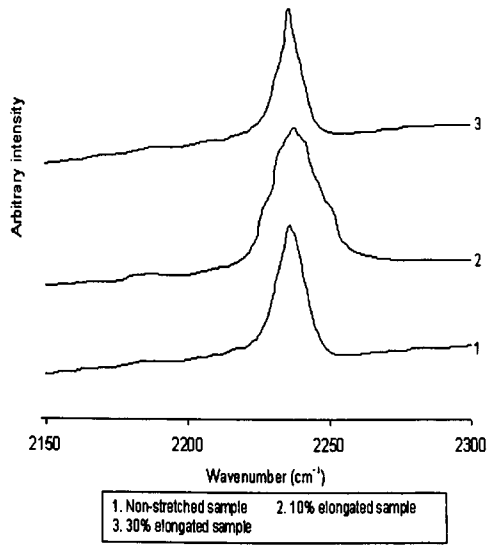

(b)

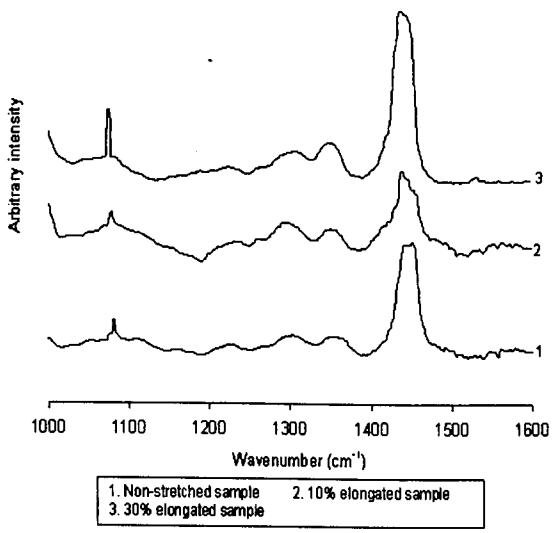

(c)

4.3.6 Electrical Conductivity Measurement

Figure 4.22 shows the electrical conductivities of PAni.DBSA, non-vulcanised NBR and non-vulcanised NBR-PAni.DBSA blends. The calculated electrical conductivity values for the peroxide-vulcanised ones are shown in Figure 4.23.

Both non-vulcanised and peroxide-vulcanised NBR showed conductivities of the order of 10^{-14}S.cm^{-1}. Pure PAni.DBSA had a high electrical conductivity of 1.4 ± 0.5S.cm^{-1}, comparable with literature ones for pressed pellet samples [35, 42]. The electrical conductivity of all blends (both vulcanised and non-vulcanised) increased with the proportion of PAni.DBSA, as observed in several studies of different PAni.DBSA blends [31, 33, 35]. Both vulcanised and non-vulcanised blends reached plateau electrical conductivity of the order of 10^{-2}S.cm^{-1} with about 40 wt% PAni.DBSA loading.

The data from Figure 4.22 were fitted to a simple percolation model as defined by Equation 2.12 [43-44] in order to estimate the conductivity percolation threshold for the non-vulcanised blends. The data were also fitted to a plot of log electrical conductivity (σ) versus log (f-f_p) in order to estimate the values of critical exponent (t) and correlation coefficient (R) for each case (see Figure 4.24a). The estimated electrical conductivity percolation threshold for the non-vulcanised blends is 6.0 wt% (or 5.4 volume %) of PAni.DBSA (with t = 3.8 and R = 0.99).

The conductivity percolation threshold for peroxide-vulcanised NBR-PAni.DBSA blends was also estimated by fitting the data from Figure 4.23 to the simple percolation model as defined by Equation 2.12 [43-44]. Again, it was possible to estimate the values of t and R for each case by fitting the data to a plot of log electrical conductivity (σ) versus log (f-f_p) (see Figure 4.24b). The estimated electrical conductivity percolation threshold for the peroxide-vulcanised NBR-PAni.DBSA blends is 6.0 wt% (or 5.4 volume %) of PAni.DBSA (with t = 3.7 and R = 0.99).

Figure 4.22: Electrical Conductivities for the Non-Vulcanised NBR-PAni.DBSA Blends as a Function of PAni.DBSA Content (wt%)

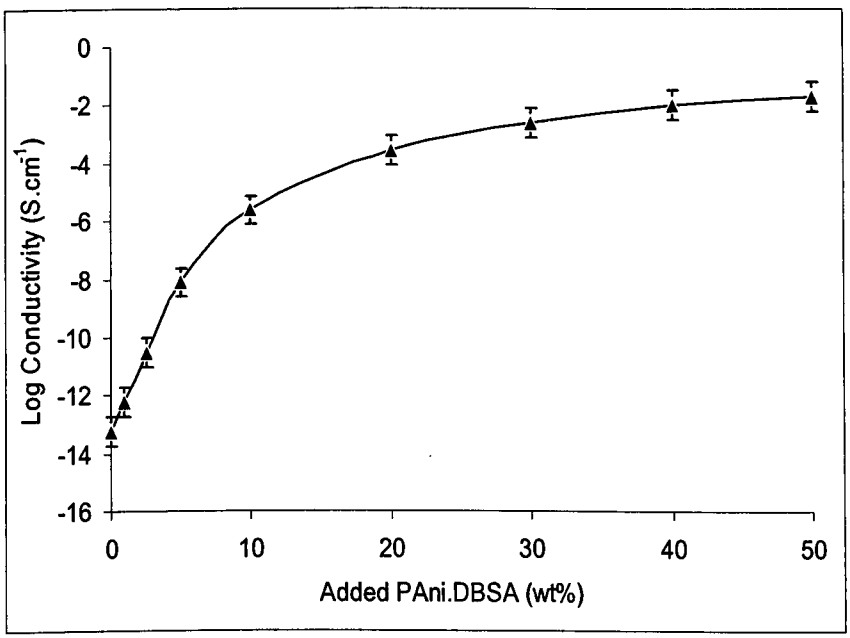

Figure 4.23: Electrical Conductivities for Peroxide-Vulcanised NBR-PAni.DBSA Blends as a Function of PAni.DBSA Content (wt%)

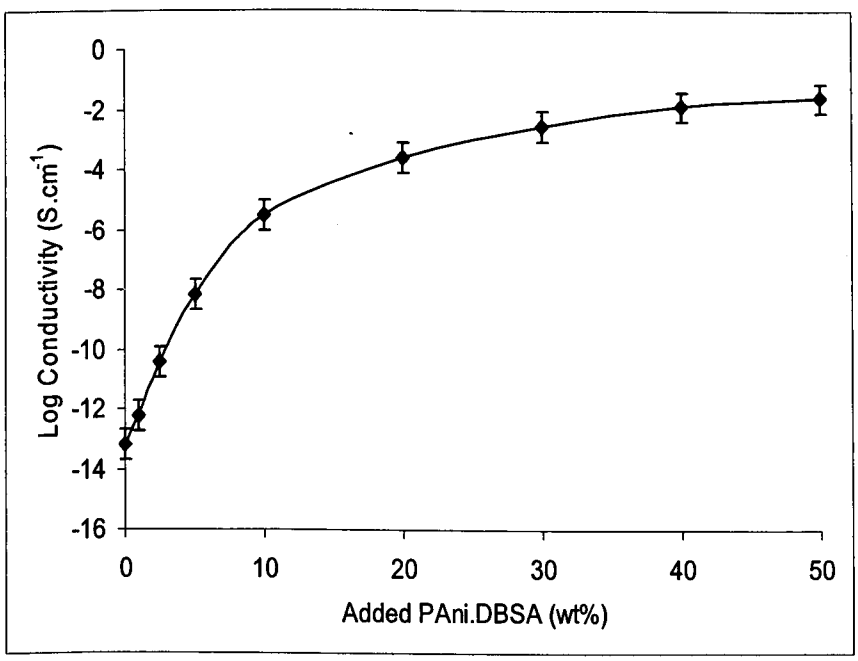

Figure 4.24: Log Electrical Conductivity (σ) vs. Log (f-f_p) Charts for Thermo-Mechanical Mixed NBR 48.2 ACN wt%-PAni.DBSA Blends; (a) Non-Vulcanised Blends and (b) Dicumyl Peroxide-Vulcanised Blends

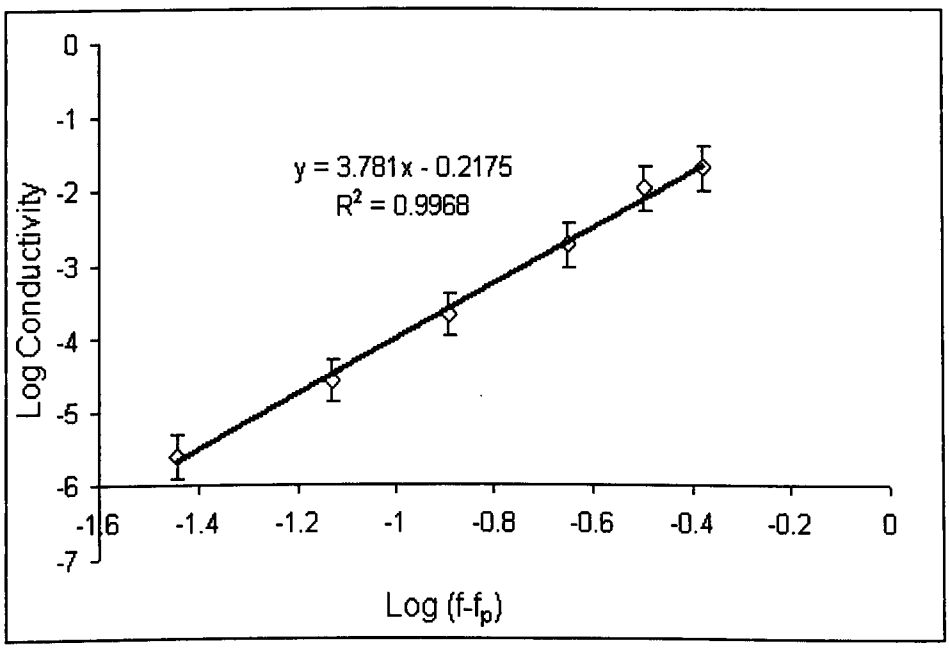

(a)

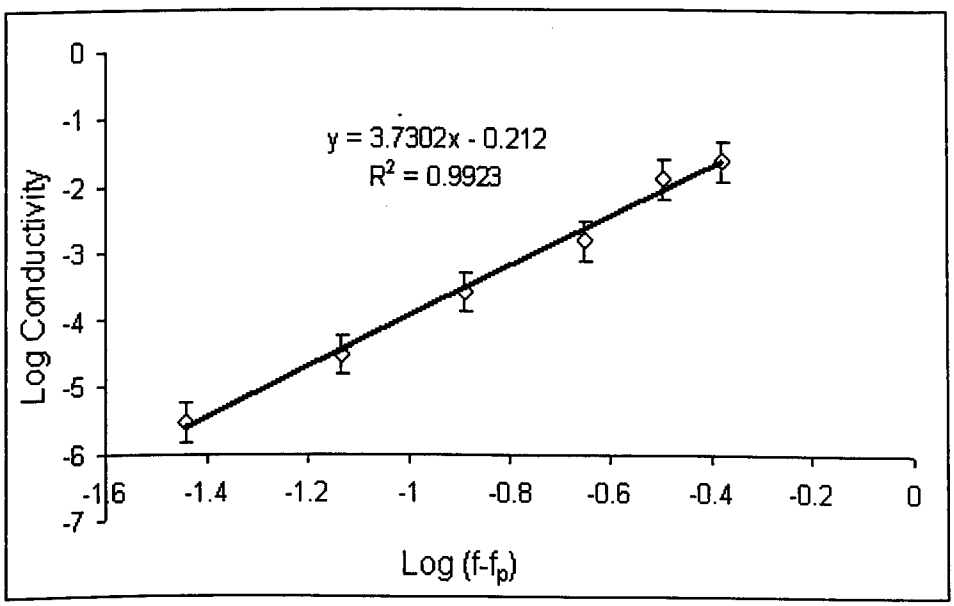

(b)

The values of *t* here for both the non-vulcanised and vulcanised blends are in the range between 2 and 4, which can be explained by a single-percolation model. There was no evidence for a second stage of percolation for these high temperature prepared blends. It is likely due to the more homogeneous mixings obtained from the thermo-mechanical method. So, the contact between the large particles makes very little contribution to the changing of electrical conductivities.

It was found that electrical conductivities of the NBR-PAni.DBSA blends were not much affected by the presence of DCP as vulcanising agent since both the non-vulcanised and vulcanised blends had very close conductivity values at the same levels of PAni.DBSA content. As explained in Section 4.1, only carbon-carbon bonds are formed among the NBR chains in the peroxide vulcanising system and this has the same effect as using the chemical-free irradiation method [12, 14]. As a result, this will minimise the disruption on the PAni.DBSA molecular structure and will also help to retain its good electrical properties.

The charts of log electrical conductivity versus strain (for first, second and third cycle of strain loading and unloading process) for the examples of peroxide-vulcanised NBR-PAni.DBSA blends (i.e. 10 wt%, 30 wt% and 50 wt% of added PAni.DBSA) stretched parallel and perpendicular to the flow direction are shown in Figures 4.25 to 4.30. It is proposed that the realignment of PAni.DBSA polymer chains in the phase-separated regions gave rise to the measured electrical conductivities for all these blends. As a result, the effect of strain on the electrical conductivities was less obvious for blends with low content of PAni.DBSA (≤10 wt%) which had relatively good compatibility.

For the peroxide-vulcanised blends stretched parallel to the flow direction (see Figure 4.25), the electrical conductivities increased when the percentage of strain increased (≥50% of straining for blends with ≤10 wt% PAni.DBSA and ≥10% of straining for blends with ≥20 wt% PAni.DBSA). It is likely that this was attributed to the alignment and the increasing of interactions (e.g. secondary bonding) between the conductive filler particles in the phase-separated regions (as reported in the literature [45-46] and as shown by Figure 4.10). It was observed that all the blends cut and stretched parallel to the flow direction had

good historical memory in terms of their electrical conductivities during the strain unloading process, where they had at least equal or slightly higher electrical conductivity values compared to the original ones.

The blends stretched perpendicular to the flow direction had smaller changes of electrical conductivity with strain than those stretched parallel to the flow direction. This is believed to be due to the lower levels of inter-chain interaction formed among the elongated PAni.DBSA polymer chains (consistent with the results obtained using both optical microscopy and FT-IR spectroscopy). As a result, the electrical conductivities measured during the strain-unloading process were also slightly lower than those measured during the strain loading.

The effect of strain on the peroxide-vulcanised blends prepared by thermo-mechanical mixing was very small since the changes of the measured electrical conductivities were observed to be within the same order. This was attributed to the morphology nature of these high temperature-produced blends, where more well-blended regions (which involved mixing on the nano-scale level that was not easily affected by the alignment effect) between the two polymers were obtained (see Figure 4.16).

After the third cycle of straining, all the peroxide-vulcanised blends prepared by thermo-mechanical mixing retained at least 99% of their original electrical conductivities. This was again due to the large amounts of well-blended region produced for all these blends. For the blends stretched parallel to the flow direction, the flexibility of the conductive networks build-up by the elongated PAni.DBSA particles within the phase-separated regions [see Figure 4.17(b)] probably also contributed to the good historical memory in terms of their electrical conductivities during the cycles of strain.

Figure 4.25: Charts of Log Electrical Conductivity versus Strain (1st Cycle of Straining Process) for the Peroxide-Vulcanised NBR-PAni.DBSA Blends stretched Parallel to the Flow Direction when passed through the Two Roll-Mill; (a) Blend with 10wt% PAni.DBSA, (b) Blend with 30 wt% PAni.DBSA and (c) Blend with 50 wt% PAni.DBSA

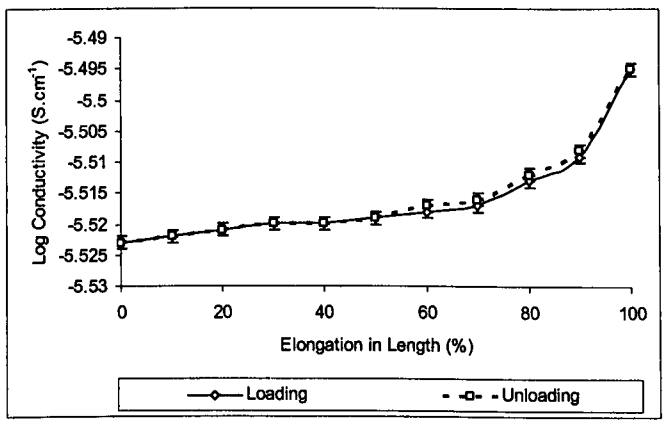

(a)

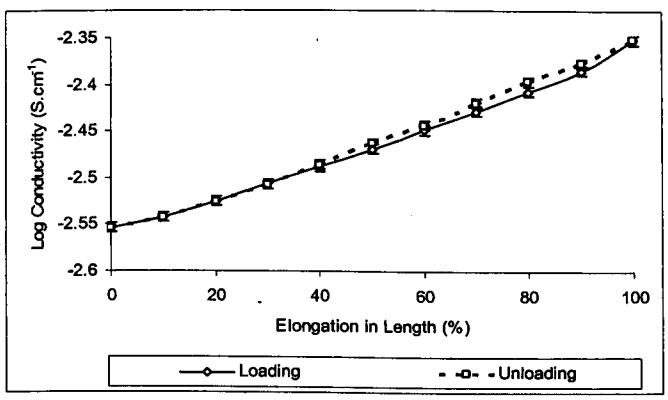

(b)

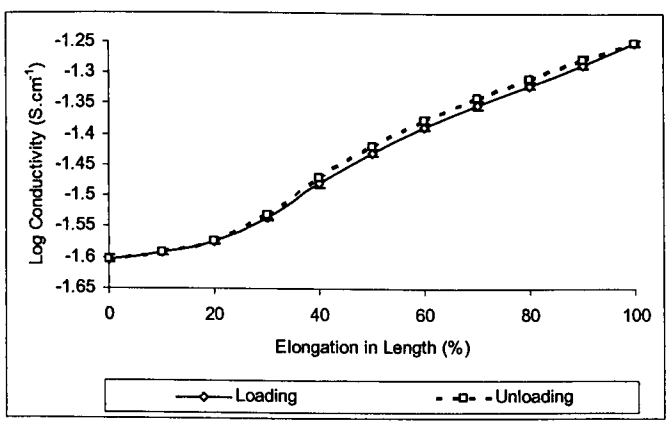

(c)

Figure 4.26: Charts of Log Electrical Conductivity versus Strain (1st Cycle of Straining Process) for the Peroxide-Vulcanised NBR-PAni.DBSA Blends stretched Perpendicular to the Flow Direction when passed through the Two Roll-Mill; (a) Blend with 10wt% PAni.DBSA, (b) Blend with 30 wt% PAni.DBSA and (c) Blend with 50 wt% PAni.DBSA

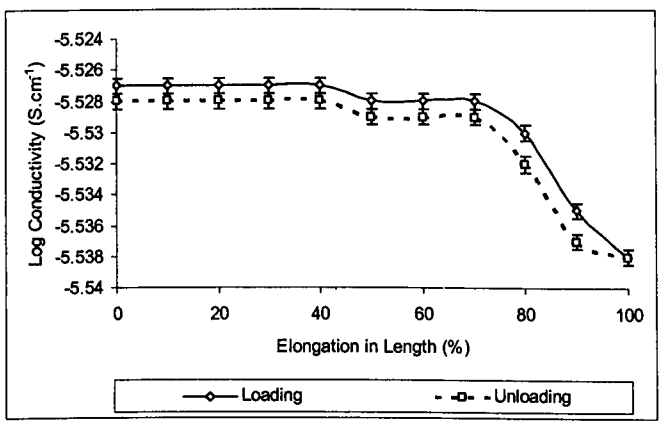

(a)

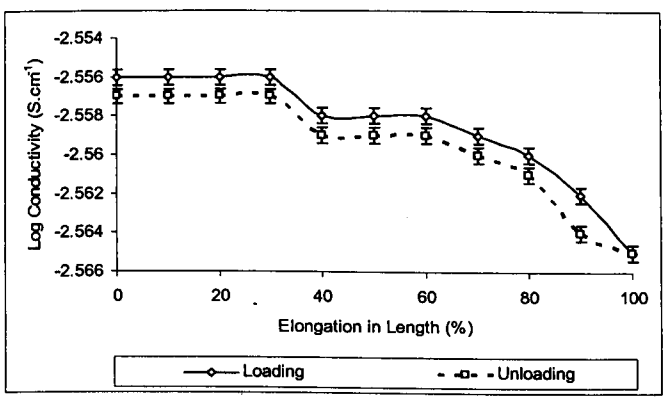

(b)

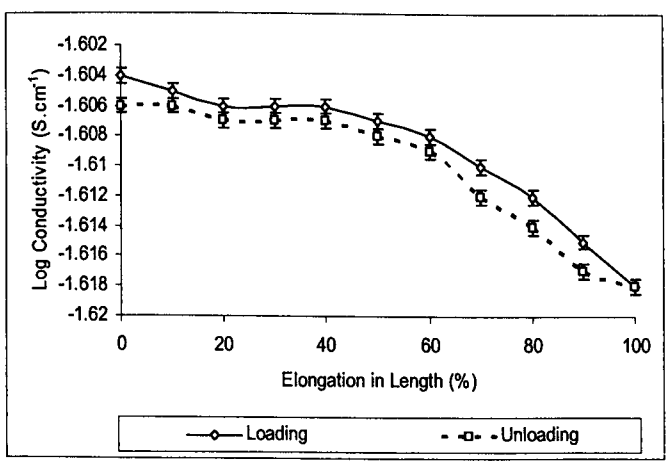

(c)

Figure 4.27: Charts of Log Electrical Conductivity versus Strain (2nd Cycle of Straining Process) for the Peroxide-Vulcanised NBR-PAni.DBSA Blends stretched Parallel to the Flow Direction when passed through the Two Roll-Mill; (a) Blend with 10wt% PAni.DBSA, (b) Blend with 30 wt% PAni.DBSA and (c) Blend with 50 wt% PAni.DBSA

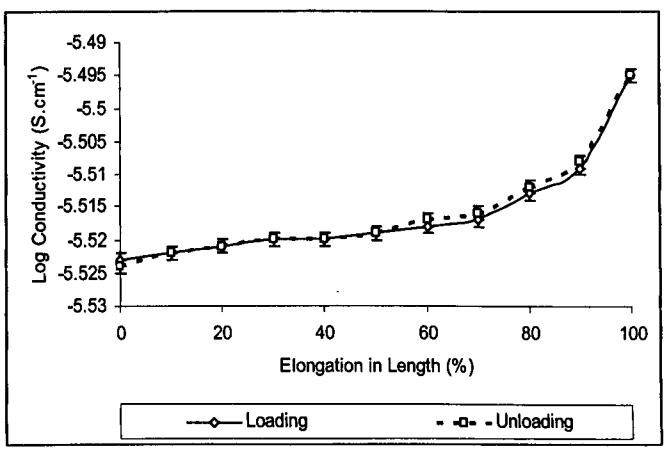

(a)

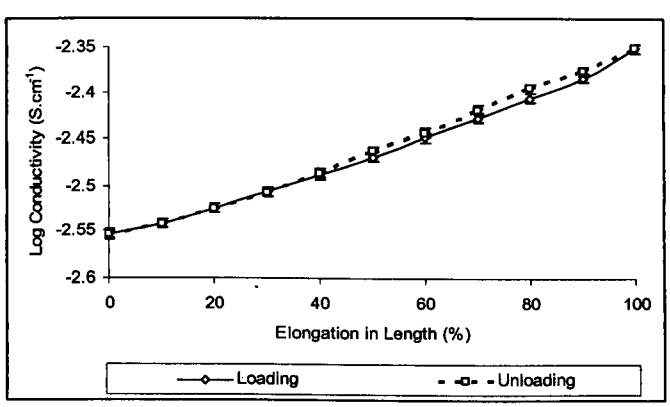

(b)

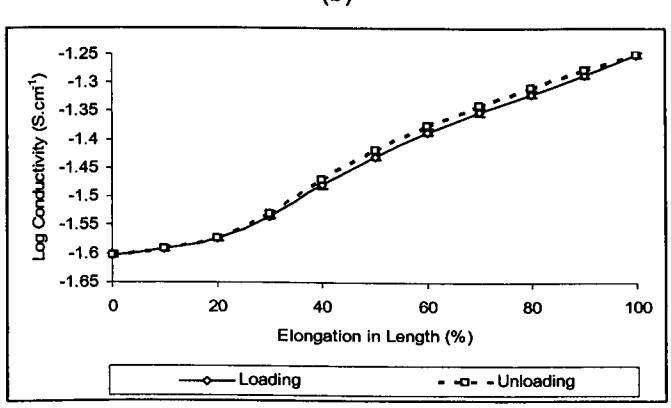

(c)

Figure 4.28: Charts of Log Electrical Conductivity versus Strain (2nd Cycle of Straining Process) for the Peroxide-Vulcanised NBR-PAni.DBSA Blends stretched Perpendicular to the Flow Direction when passed through the Two Roll-Mill; (a) Blend with 10wt% PAni.DBSA, (b) Blend with 30 wt% PAni.DBSA and (c) Blend with 50 wt% PAni.DBSA

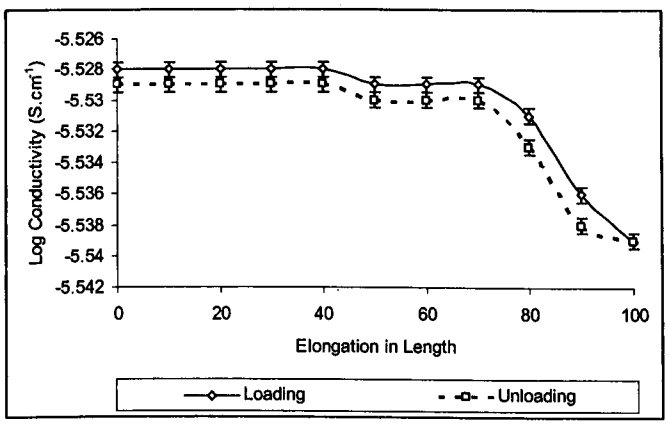

(a)

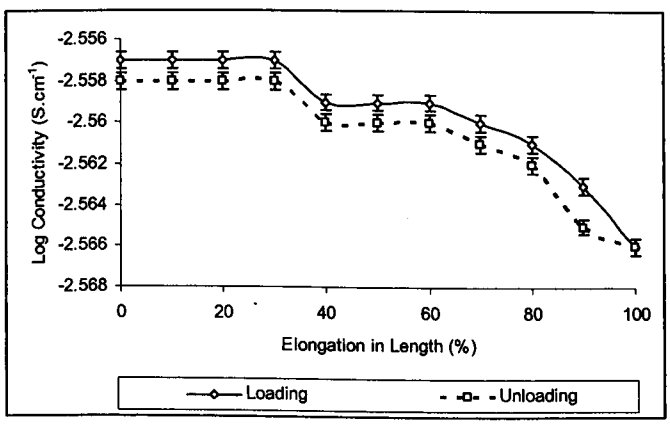

(b)

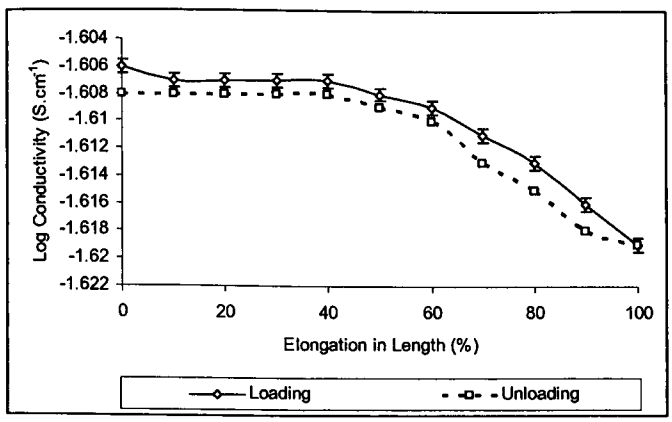

(c)

Figure 4.29: Charts of Log Electrical Conductivity versus Strain (3rd Cycle of Straining Process) for the Peroxide-Vulcanised NBR-PAni.DBSA Blends stretched Parallel to the Flow Direction when passed through the Two Roll-Mill; (a) Blend with 10wt% PAni.DBSA, (b) Blend with 30 wt% PAni.DBSA and (c) Blend with 50 wt% PAni.DBSA

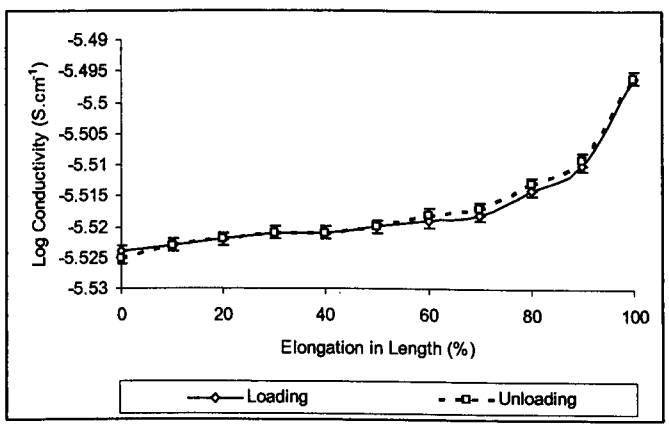

(a)

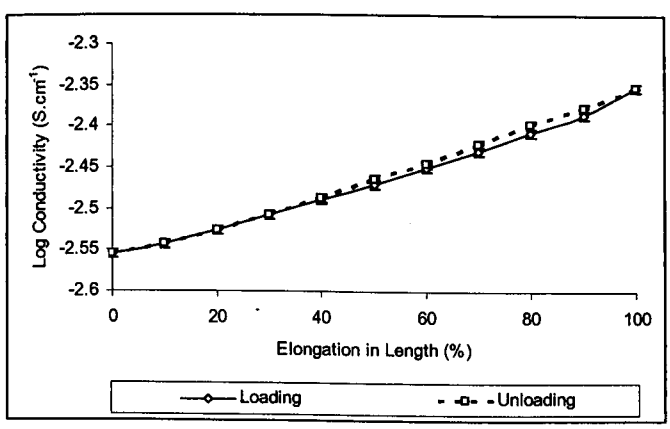

(b)

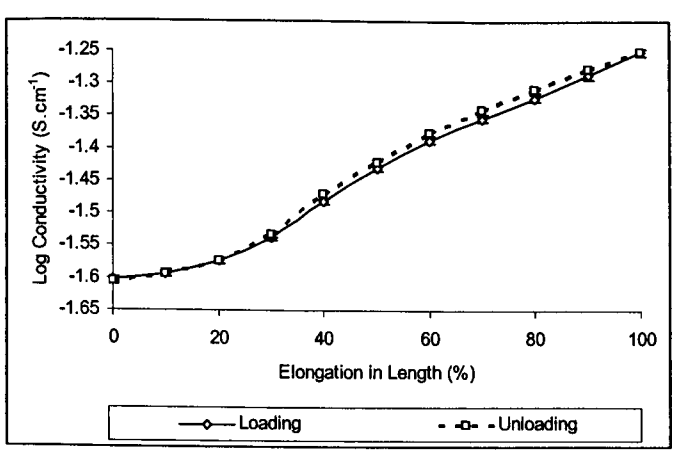

(c)

Figure 4.30: Charts of Log Electrical Conductivity versus Strain (3rd Cycle of Straining Process) for the Peroxide-Vulcanised NBR-PAni.DBSA Blends stretched Perpendicular to the Flow Direction when passed through the Two Roll-Mill; (a) Blend with 10wt% PAni.DBSA, (b) Blend with 30 wt% PAni.DBSA and (c) Blend with 50 wt% PAni.DBSA

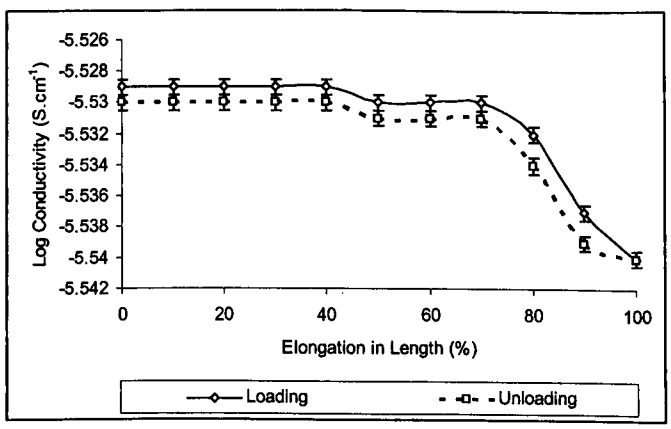

(a)

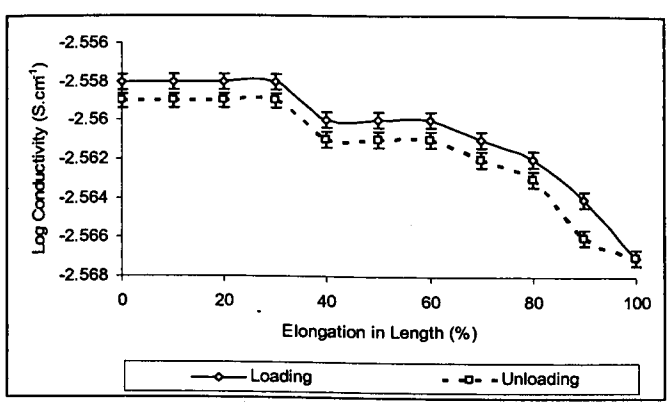

(b)

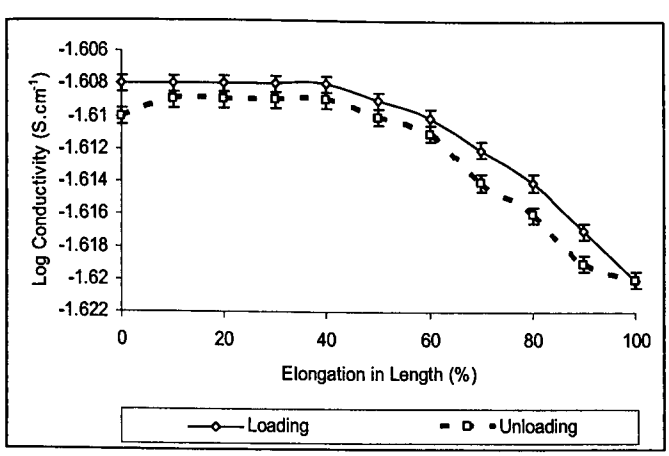

(c)

The electrical properties of all the peroxide-vulcanised blends prepared in this part of work were in contrast with those of the blends prepared with the commonest conventional conductive filler, i.e. carbon black. According to the literature [47], the electrical conductivities of test pieces prepared from the natural rubber-carbon black composites decreased permanently during the first cycle of strain (see Figure 4.31). This was attributed to the high levels of phase separation between the two constituent materials and also the destruction of conductive carbon black networks within the phase-separated regions. The carbon black particles were reported [47] to be spherical in shape rather than the elongated one observed for PAni.DBSA in this work.

Figure 4.31: Electrical Resistivity (ρ) as A Function of the Extension Ratio (λ) during the 1st Cycle of Strain for Natural Rubber (SMR CV60)-Carbon Black (Grade N330-HAF) Blends; where NR50 is the Blend with 50 p.h.r. of Carbon Black and NR70a is the Blend with 70 p.h.r. of Carbon Black [Figure reproduced from Reference 47]

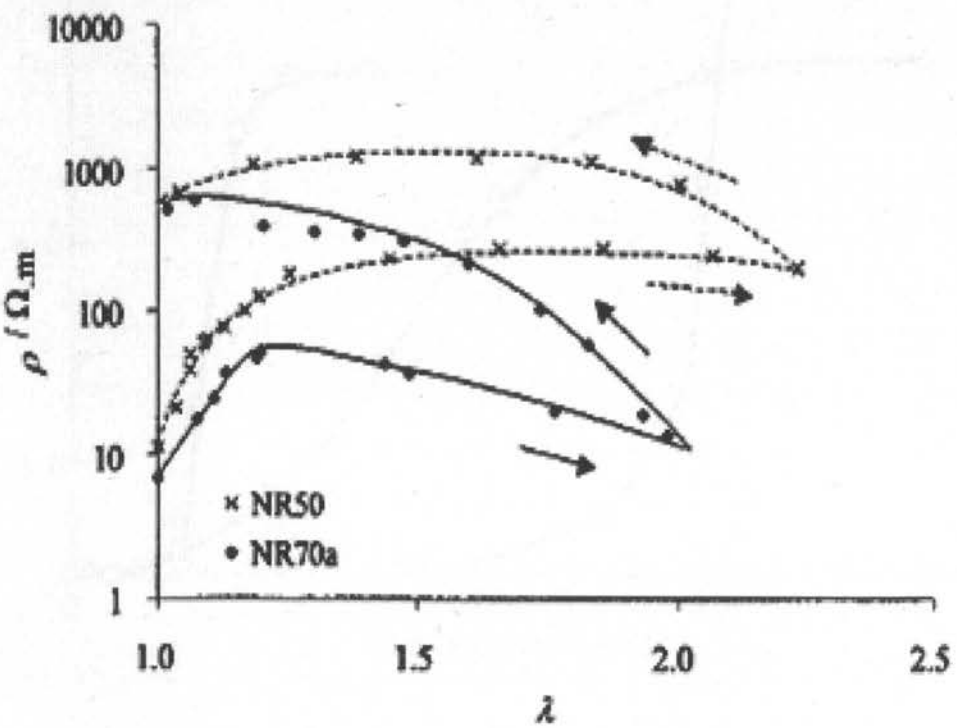

Kathirgamanathan [48] compared the volume conductivities (measured with 4-probe method) of epoxy systems loaded with PAni.p-TSA, carbon black and silver-coated nickel flakes. It was reported that carbon black percolated at a low volume loading of about 5 volume%, PAni.p-TSA at about 10 volume% and silver-coated nickel flakes at about 26 volume%. It was observed that while the percolation curves for carbon black and silver-coated nickel flakes were steep, the percolation curve for PAni.p-TSA was very shallow and the transition was gradual (see Figure 4.32). This phenomenon could be explained on the basis of molecular level interaction of the PAni.p-TSA with the epoxy resin [48].

Figure 4.32: Volume Conductivity vs. Volume Loading for Epoxy Systems loaded with: Δ, PAni.p-TSA; O, Carbon Black; □, Silver-Coated Nickel [Figure reproduced from Reference 48]

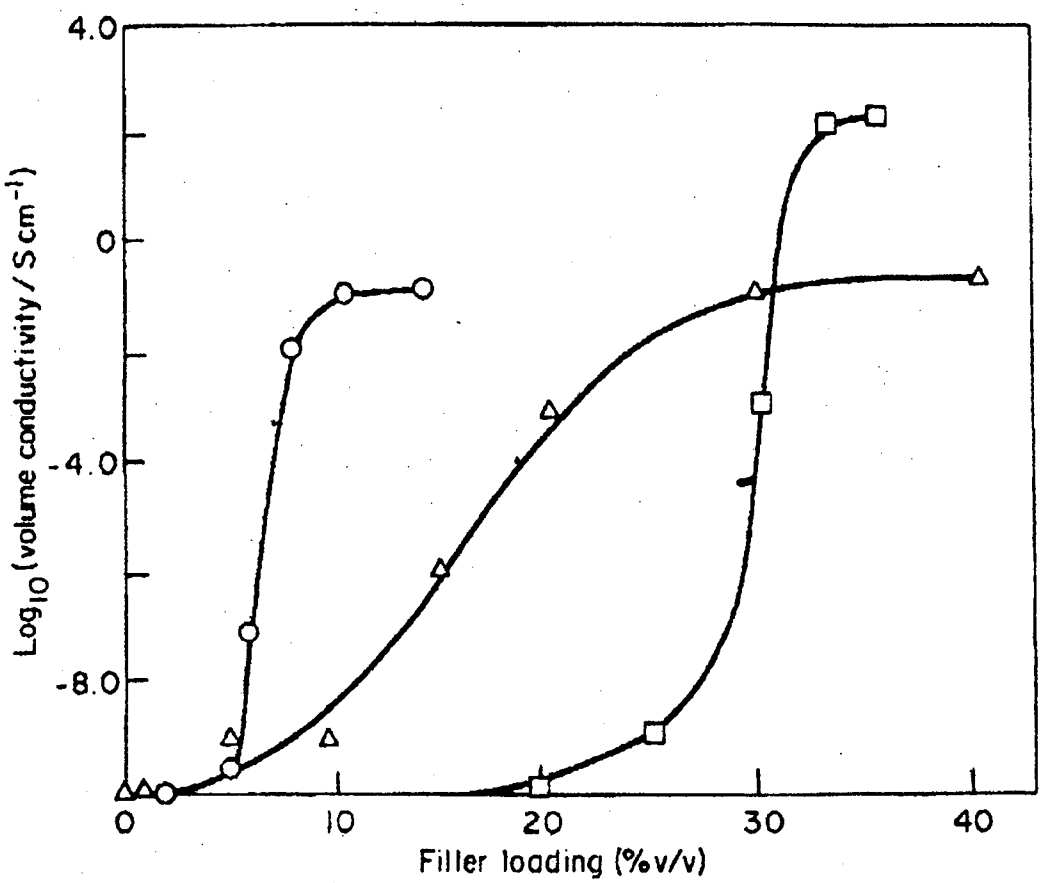

4.4 Conclusion

Peroxide-vulcanised NBR-PAni.DBSA blends with useful electrical conductivities (up to 10^{-2} S.cm^{-1}, with estimated electrical conductivity percolation threshold 6.0 wt%/5.4 volume % of PAni.DBSA) were successfully prepared for the first time by thermo-mechanical mixing. The effect of crosslinking with dicumyl peroxide as vulcanising agent was proved not to affect the electrical properties of NBR-PAni.DBSA blends. All the peroxide-vulcanised blends prepared and strained parallel to the flow direction had their electrical conductivities enhanced with increasing strain, as a result of the alignment and increasing of interactions (e.g. secondary bonding) among the elongated PAni.DBSA chains in the phase-separated regions (as shown by the optical micrographs and peak shifts of FT-IR spectra). All the peroxide-vulcanised blends also had good historical memory in term of their electrical conductivities during three cycles of straining and this was thought to be due to the high levels of well-blended region produced in all these blends.

The FT-IR spectra of PAni.DBSA and peroxide-vulcanised NBR corresponded well with those reported in the literature [35, 44-45]. Although the hot-pressed films of all the peroxide-vulcanised blends resembled a superposition of the spectra of their raw materials, but some significant characteristic peak shifts were successfully found and provided the evidence of bonding interaction between the two polymers. Peroxide-vulcanised NBR-PAni.DBSA blends with the largest temperature shifts for their thermal events as recorded by the low and high temperature DSC thermograms (i.e. those with ≤30 wt% of PAni.DBSA) were the ones with the best compatibility. Results from the FT-IR spectroscopy and DSC thermal analysis studies were consistent with those obtained from the morphological studies (optical and electron microscopy); where more well-blended (pale-green) regions were found for the blends with ≤30 wt% of PAni.DBSA. The morphological studies also showed that the thermo-mechanical mixing method (with high temperature and high shearing conditions) had reduced the amounts of phase separation in the NBR-PAni.DBSA blends. It was likely that

the high mixing efficiency of this method could help to reduce the particle size of the PAni.DBSA, and subsequently created some better-dispersed region of this conductive filler within the NBR host matrix.

Tensile properties and tear strengths of these blends were enhanced by higher loading of PAni.DBSA (up to 30 wt%). The hardness, compression set and tension set of these blends also increased with increasing proportion of PAni.DBSA. Samples stretched parallel to the flow direction when passed through the two roll-mill also had better mechanical properties (i.e. higher tensile strength, higher elongation at break, higher tear strength and lower tension set) compared to the "perpendicular" ones, due to the different levels of interaction and alignment of PAni.DBSA polymer chains within the rubber host.

References

1. Basfar, A. A., Abdel-Aziz, M. M. and Mofti, S. *Radiation Phys. Chem.*, **63(1)**, 81 (2002).

2. Hernandez, L. G., Rueda, L. I., Diaz, A. R. and Anton, C. C. *Polymer*, **33(17)**, 3635 (1992).

3. Varughese, S. and Tripathy, D. K. *Polym. Degrad. Stabil.*, **38(1)**, 7 (1992).

4. Scott, G. and Smith, K. V. *European Polym. J.*, **14(11)**, 905 (1978).

5. Dutta, N. K. and Tripathy, D. K. *Polym. Degrad. Stabil.*, **36(1)**, 73 (1992).

6. Sirisinha, C., Phoowakeereewiwa,t S. and Saeoui, P. *European Polym. J.*, **40(8)**, 1779 (2004).

7. Agarwal, K., Setua, D. K. and Sekhar, K. *Polym. Testing*, **24(6)**, 781 (2005).

8. Nasr, G. M., Badawy, M. M. and Ateia, E. *Polym. Degrad. Stabil.*, **60**, 333 (1998).

9. Gwaily, S. E., Nasr, G. M. and Badawy, M. M. *Egypt. J. Sol.*, **24(2)**, 193 (2001).

10. Mondal, U. K., Tripathy, D. K. and De, S. K. *Polymer*, **34(18)**, 3832 (1993).

11. Windspear, G. G (Editor). *The Vanderbilt Rubber Handbook*. R. T. Vanderbilt Co. Inc., (1968).

12. Alliger, G. and Sjothun, I. J. *Vulcanization of Elastomers*. New York: Reinhold Publishing Corporation, (1964).

13. LeBras, J. *Rubber: Fundamentals of Its Science and Technology*. New York: Chemical Publishing Co., (1957).

14. Morton, M. (Editor). *Rubber Technology (2nd Edition)*. New York: Van Nostrand Reinhold Company, pp. 27, 310-311, (1973).

15. Akzo Nobel Polymer Chemicals. *Catalogue-Crosslinking Peroxides and Polymer Additives*, (June 2006).

16. Kovacic, P. *Rubb. Chem. Technol.*, **74**, 452 (1997).

17. Luheng, W., Tianhua,i D. and Peng, W. *Sensors and Actuators A: Phys.*, **135(2)**, 587 (2007).

18. Carrillo, A., Martín-Dominguez, I. R., Glossman, D. and Marquez, A. *Sensors and Actuators A: Phys.*, **119(1)**, 157 (2005).

19. Sun, Y., Luo, S., Watkins, K. and Wong, C. P. *Polymer Degrad. Stabil.*, **86(2)**, 209(2004).

20. Das, N. C., Chaki, T. K. and Khastgir, D. *Carbon*, **40(6)** 807 (2002).

21. Das, N. C., Khastgir, D., Chaki, T. K. and Chakraborty, A. *Comp. Part A: Appl. Sci. and Manuf.*, **31(10)**, 1069 (2000).

22. Nasr, G. M., Osman, H. M., Abu-Abdeen, M. and Aboud, A. I. *Polym. Testing*, **18(7)**, 483 (1999).

23. Sau, K. P., Chaki, T. K. and Khastgir, D. *Polymer*, **39(25)**, 6461 (1998).

24. Sau, K. P., Chaki, T. K. and Khastgir, D. *Comp. Part A: Appl. Sci. and Manuf.*, **29(4)**, 363 (1998).

25. Badawy, M. M. and Nasr, G. M. *Polymer Testing*, **16(2)**, 155 (1997).

26. Pramanik, P. K., Khastgir, D. and Saha, T. N. *Composites*, **23(3)**, 183 (1992).

27. Job, A. E., Oliveira, F. A., Alves, N., Giacometti, J. A. and Mattoso, L. H. C. *Synthetic Met.*, **135**, 99 (2003).

28. Davies, S. J., Ryan, T. G., Wilde, C. J. and Beyer, G. *Synthetic Met.,* **69**, 209 (1995).

29. Pinho, M. S., Gorelova, M. M., Dezzoti, M., Soares, B. G. and Pertsin, A. J. *J. Appl. Polym. Sci.,* **70**, 1543 (1998).

30. Faez, R., Gazotti, W. A. and De Paoli, M.-A. *Polymer*, **40**, 5497 (1990).

31. Vallim, M. R., Felisberti, M. I. and De Paoli, M.-A. *J. Appl. Polym. Sci.,* **75**, 677 (2000).

32. Leyva, M. E., Barra, G. M. O, Gorelova, M. M., Soares, B. G. and Sens, M. *J. Appl. Polym. Sci.,* **80(4)**, 626 (2001).

33. Faez, R., Schuster, R. H. and De Paoli, M.-A. *European Polym. J.,* **38(12)**, 2459 (2002).

34. Martins, C. R. and De Paoli, M.-A. *European Polym. J.*, **41(12)**, 2867 (2005).

35. Yong, K. C., Foot, P. J. S., Morgan, H., Cook, S. and Tinker, A. J. *European Polym. J.*, **42(8)**, 1716 (2006).

36. ISO 3417. *Rubber-Measurement of Vulcanization Characteristics with the Oscillating Disc Curemeter.* The International Organization for Standardization, (1991).

37. BS ISO 37. *Rubber, Vulcanised or Thermoplastic-Determination of Tensile Stress-Strain Properties.* British Standards Institution, (2005).

38. BS ISO 34-1. *Rubber, Vulcanised or Thermoplastic-Determination of Tear Strength, Part 1: Trouser, Angle and Crescent Test Pieces.* British Standards Institution, (2004).

39. BS ISO 2285. *Determination of Tension Set at Normal and High Temperatures.* British Standards Institution, (2001).

40. BS 903-A6. *Method for Determination of Compression Set at Ambient, Elevated or Low Temperatures.* British Standards Institution, (1992).

41. BS 903-A26. *Method for Determination of Hardness (Hardness between 10 IRHD and 100 IRHD).* British Standards Institution, (1995).

42. Poussin, D., Morgan, H. and Foot, P. J. S. *Polym. Int.*, **52**, 433 (2003).

43. Stauffer, D. *Introduction to Percolation Theory.* London: Taylor and Francis, (1985).

44. Leyva, M. E., Barra, G. M. O. and Soares, B. G. *Synthetic Met.,* **123**, 443 (2001).

45. Balberg, I., Anderson, C. H., Alexander, S. and Wagner, N. *Phys. Rev. B.,* **30(7)**, 3933 (1984).

46. Suzuki, Y. Y., Heeger, A. J. and Pincus, P. *Macromolecules*, **23(21)**, 4730 (1990).

47. Yamaguchi, K., Busfield, J. J. C. and Thomas, A. G. *J. Appl. Polym. Sci. Polym. Phys.*, **41**, 2079 (2003).

48. Kathirgamanathan, P. *Polymer*, **34(13)**, 2907 (1993).

Chapter 5: Conclusion

This chapter summarises the principal findings of this PhD. research degree project and also outlines some potential future work related to it.

5.1 NBR-PAni.DBSA Blends prepared by Solution Mixing

i. Non-vulcanised NBR-PAni.DBSA blends (based on NBR with 25.7, 33.1, 41.4 and 48.2 wt% ACN), with electrical conductivities up to 10^{-2}S.cm^{-1} have been successfully prepared by solution mixing for the first time in this part of work. The conductivities of all these blends were much higher than those of comparable materials reported previously due to reasonably good compatibility between the two polymers. Blends prepared using NBR with 48.2 wt% ACN showed the best electrical properties (with the lowest percolation threshold of 6.0 wt%/5.4 volume% of PAni.DBSA) due to its having the best compatibility with PAni.DBSA (in terms of solubility parameter values). All blends prepared by the solution mixing also showed a clear second stage of percolation with higher loading of PAni.DBSA which corresponded to contact between the micron-scale PAni.DBSA particles in the separated phases.

ii. Two distinct regions, i.e. the dark green ones (rich in PAni.DBSA) and pale green ones (rich in NBR) were observed by optical microscopy for NBR-PAni.DBSA blends prepared by solution mixing. The dark ones corresponded to the regions with high level of phase separation between the polymers, and the pale ones corresponded to well-mixed polymers. The higher the content of PAni.DBSA, the more phase separation was observed. The electrical conductivity networks for these blends were observed to be clearly built-up by the PAni.DBSA-rich (dark-coloured) regions. Some small PAni.DBSA particles (of colloidal dimensions, 50-1000nm) were revealed by the TEM and they were believed to have made

a contribution to the electrical conductivities of these blends (especially for those that were below their main percolation thershold).

iii. The FT-IR spectra of all NBR-PAni.DBSA blends (as cast films) resembled a superposition of the spectra of their constituent materials. However, some notable shifts were successfully found for the characteristic peaks assigned to both blended polymers. This is proposed as direct evidence for secondary bonding interaction between the two blended polymers.

iv. NBR (48.2 wt% ACN)-PAni.DBSA blends (with up to 30 wt% PAni.DBSA), prepared via solution mixing showed the largest temperature shifts for their thermal events in both sub- and above-ambient temperature DSC thermograms. The larger the temperature shift, the better the compatibility between the two blended polymers, and also the stronger the intermolecular forces as indicated by the FT-IR data.

5.2 ENR 50-PAni.DBSA Blends prepared by Solution Mixing

i. ENR 50 was found to have a 47.2 mole % epoxidation level by using NMR spectroscopy. ENR 50-PAni.DBSA blends with useful electrical conductivities (up to x 10^{-3}S.cm^{-1}) were successfully prepared for the first time by solution mixing in this part of work due to appreciable compatibility between the two constituent polymers.

ii. Two distinct regions, i.e. dark- and light-green, were observed for the ENR 50-PAni.DBSA blends. The dark regions corresponded to phase separation between the two blended polymers and the light regions corresponded to well-mixed regions. It was observed that the higher the content of PAni.DBSA, the more phase separation was found. TEM micrographs showed some very small particles of PAni.DBSA (of colloidal dimensions,

20-100nm) and it is likely they could also form some conductive networks (similar to the case of NBR-PAni.DBSA blends as studied in Chapter 2).

iii. Two stages of electrical percolation were observed for these blends. The first threshold (2.9 wt%/2.5 volume% of PAni.DBSA) corresponded to percolation in the well-blended regions (pale colour as seen in both optical and electron micrographs) and the second one (5 wt%/4.4 volume% PAni.DBSA) corresponded to the phase-separated regions (dark colour in optical and electron micrographs).

iv. Both the NMR and FT-IR spectroscopy results revealed that significant ring opening of the ENR 50 occurred in blends with a high loading of PAni.DBSA (30 wt% or above). This was attributed to the sensitivity of the epoxide group of the rubber to the acidic conditions (caused by some small amount of doping acid residues). It was however observed that the ring opening did not seriously affect the electrical properties of these blends.

v. Progressive temperature shifts were observed for all ENR 50-PAni.DBSA blends for both sub- and above-ambient temperature DSC thermograms. The higher the content of PAni.DBSA, the bigger the temperature shifts of these recorded thermal events (especially the Tg values). It is proposed that this was at least partly due to the further ring opening of the epoxide group of ENR. Hence, the tolerable amount of PAni.DBSA to be used with the ENR 50 is recommended ≤30 wt%.

5.3 NBR-PAni.DBSA Blends prepared by Thermo-Mechanical Mixing

i. Peroxide-vulcanised NBR-PAni.DBSA blends (based on NBR with 48.2 wt% of ACN) have been successfully prepared for the first time using thermo-mechanical mixing and the electrical conductivity values were comparable with the non-vulcanised ones prepared by solution mixing in

this work. The electrical conductivities were proven to be hardly affected by crosslinking with dicumyl peroxide (by comparing with the values of the non-vulcanised blends prepared in the same way and at the same level of PAni.DBSA). In contrast with blends prepared by solution mixing, all blends prepared by thermo-mechanical mixing did not show an obvious second stage of percolation (with higher loading of PAni.DBSA). This was thought to be due to the higher proportion of well-blended regions (as shown in the optical and electron micrographs) that were present. The high mixing efficiency and well-optimised mixing conditions of this method were believed to have been important in producing this.

ii. It was found that the electrical conductivities of all peroxide-vulcanised blends were increased, when they were strained along the orientation axis of the PAni.DBSA particles (parallel to the flow direction when the blends were passed through the two-roll mill). It is proposed that this was caused by the alignment and increasing of interactions between the large and elongated PAni.DBSA particles (as revealed by the optical micrographs and the peak shifts of FT-IR spectra respectively). All the peroxide-vulcanised blends prepared by thermo-mechanical mixing had good historical memory in terms of their electrical conductivities (99% retention of the original non-strained sample's value) during the three cycles of straining. It is likely that this can also be attributed to the high proportion of well-blended regions in all these blends.

iii. The FT-IR spectra showed a predominance of NBR absorption bands for the peroxide-vulcanised blends with low contents of PAni.DBSA (i.e. 30 wt% or less). There was a predominance of PAni.DBSA absorption bands in the FT-IR spectra of the peroxide-vulcanised blends with higher contents of PAni.DBSA (i.e. ≥40 wt%). Detailed examination revealed some notable characteristic IR peak shifts, which provided direct evidence for the existence of bonding interaction between the two constituent components.

iv. The peroxide-vulcanised blends prepared via thermo-mechanical mixing with PAni.DBSA content up to 30 wt%, showed the largest temperature shifts for their thermal events in both sub- and above-ambient temperature DSC thermograms. It is proposed that this was attributed to the good compatibility between the two blended polymers.

v. Two regions, i.e. the dark-green ones (rich in PAni.DBSA) and the pale-green ones (rich in NBR) were again observed for all peroxide-vulcanised blends. The higher the content of PAni.DBSA, the more of dark-green phase was observed. However, the thermo-mechanically mixed blends, which involved a high temperature (at 140°C) and high shearing mixing conditions had produced higher proportions of well-blended region even at a high level of PAni.DBSA content (≥40 wt%). TEM micrographs of all these blends showed many very small particles of PAni.DBSA (of colloidal dimensions, 20-1000nm). It was likely that the high mixing efficiency by using this type of mixing method could reduce the conductive filler's particle size and enhanced their dispersion level within the rubber host matrix. Most of the electrical conductivities of the thermo-mechanically mixed blends at high levels of PAni.DBSA (≥30 wt%), are thought to be contributed by the conducting polymer within these well-blended regions. This is in contrast with the solution-mixed blends, where the build-up of electrical conductivity networks was clearly observed within the phase-separated (dark-green) regions.

vi. It was found that PAni.DBSA acts as a mechanical property reinforcing agent in NBR-PAni.DBSA blends with contents ≤30 wt%. Both tensile properties and tear strength of the peroxide-vulcanised blends prepared by thermo-mechanical mixing were enhanced by increasing the loading of PAni.DBSA (up to 30 wt%). The hardness, compression set and tension set of these blends were also increased with increasing proportion of

PAni.DBSA. However, it was concluded that the higher the level of phase separation, the poorer the mechanical properties of the blends.

vii. Samples prepared and strained parallel to the flow direction when passing through a two roll-mill had better mechanical properties (i.e. higher tensile strength, higher elongation at break, higher tear strength and lower tension set) compared to the blends stretched perpendicular to the flow direction. This was likely to be due to the different alignment (shown by the optical micrographs) of the elongated PAni.DBSA polymer particles within the NBR host matrix; also from the higher levels of inter-chain interaction (revealed by the FT-IR spectra peak shifts) between the conductive polymers.

From the literature, most of the elastomer-conductive polymer blends prepared previously by using a conventional mechanical mixer (e.g. a two-roll mill), had poor mechanical properties and low electrical conductivities (even at high conductive polymer loading). This is partly due to the incompatibility of the polymer properties in some cases, but it is also due to the simple and low mixing-efficiency design of the equipment which is normally used for basic and fundamental mixing studies. Higher mixing efficiency can be achieved by preparing the elastomer-conductive polymer blend with a modern mechanical mixer such as an internal mixer, which has more sophisticated mixing designs, e.g. high efficiency internal mixing structures, the ability to provide a high temperature and pressure processing environment and the high accuracy by using the computerised mixing conditions etc.

5.4 Future Work

i. Some future research work should be carried out in order to further improve the compatibility between NBR and PAni.DBSA. It is likely that compatibility between the various grades of pure NBR (even for the lower ACN contents) and the PAni.DBSA could be enhanced by introducing a coupling agent into the blend system. The coupling agent could be incorporated directly as one of the system additives, or indirectly by using a chemically modified NBR grade (e.g. carboxylated NBR) as the elastomeric host.

ii. While acid-doped PAni may be used as a blend partner for ENR in terms of electrically conductive blend preparation, some useful research work could also be carried out in order to investigate the possibility of using of PAni emeraldine base as a thermal ageing-antioxidant for natural rubber (see Chapter 3: Reference 30 for some basic studies regarding to this potential usage).

iii. Although vulcanised conductive elastomeric compounds have been successfully prepared with acid-doped PAni by different methods, the presence of acidic conditions (due to the residues of doping acid) is believed could affect the efficiency of some chemical crosslinking agents, e.g. sulphur, resins and peroxide. To avoid this problem, the possibility of using of irradiation-induced crosslinking for this type of blend (by exposing the blends to different irradiation sources, e.g. electron beam, gamma, X-ray etc.) might be investigated.

iv. An electrically conductive thermoplastic rubber vulcanizate could be prepared as a tertiary blend system consisting of a vulcanised rubber, a thermoplastic and an intrinsic electrically conductive polymer (as the conductive filler). It is expected that beneficial characteristics could be

created with this type of blend, where the good elastic property (from the vulcanised rubber), good processability (from the thermoplastic) and good electrical property (from the conductive filler) may be optimised. The blend could also be recycled and reused just like a conventional thermoplastic. Some research work relating this particular subject should be encouraged, since the outcomes are believed to have significant commercial potential.

Appendices

Appendix 2.1: NMR Spectrum of Methanol washed-NBR Krynac®27.50

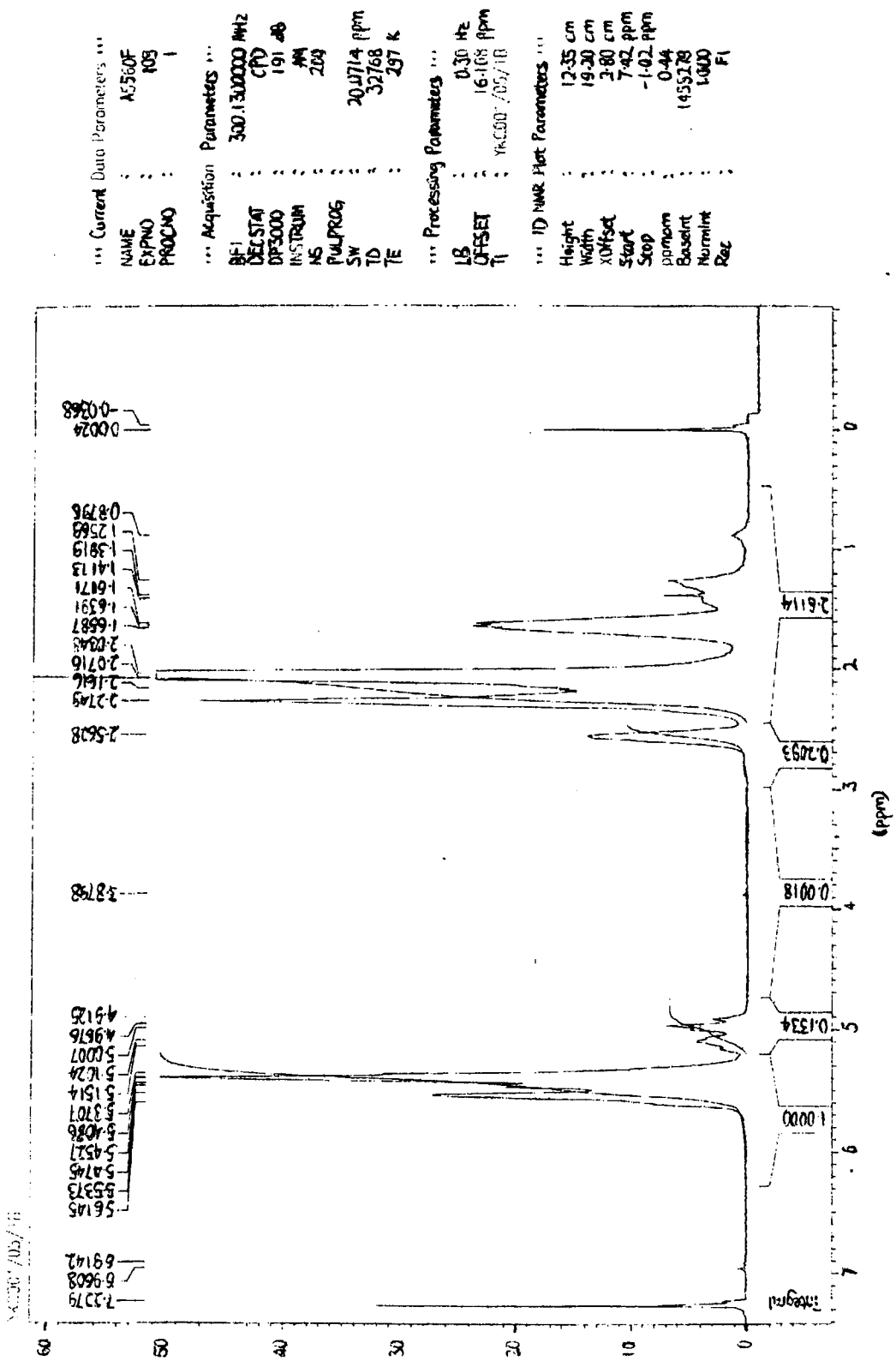

Appendix 2.2: NMR Spectrum of Methanol washed-NBR Krynac®34.50

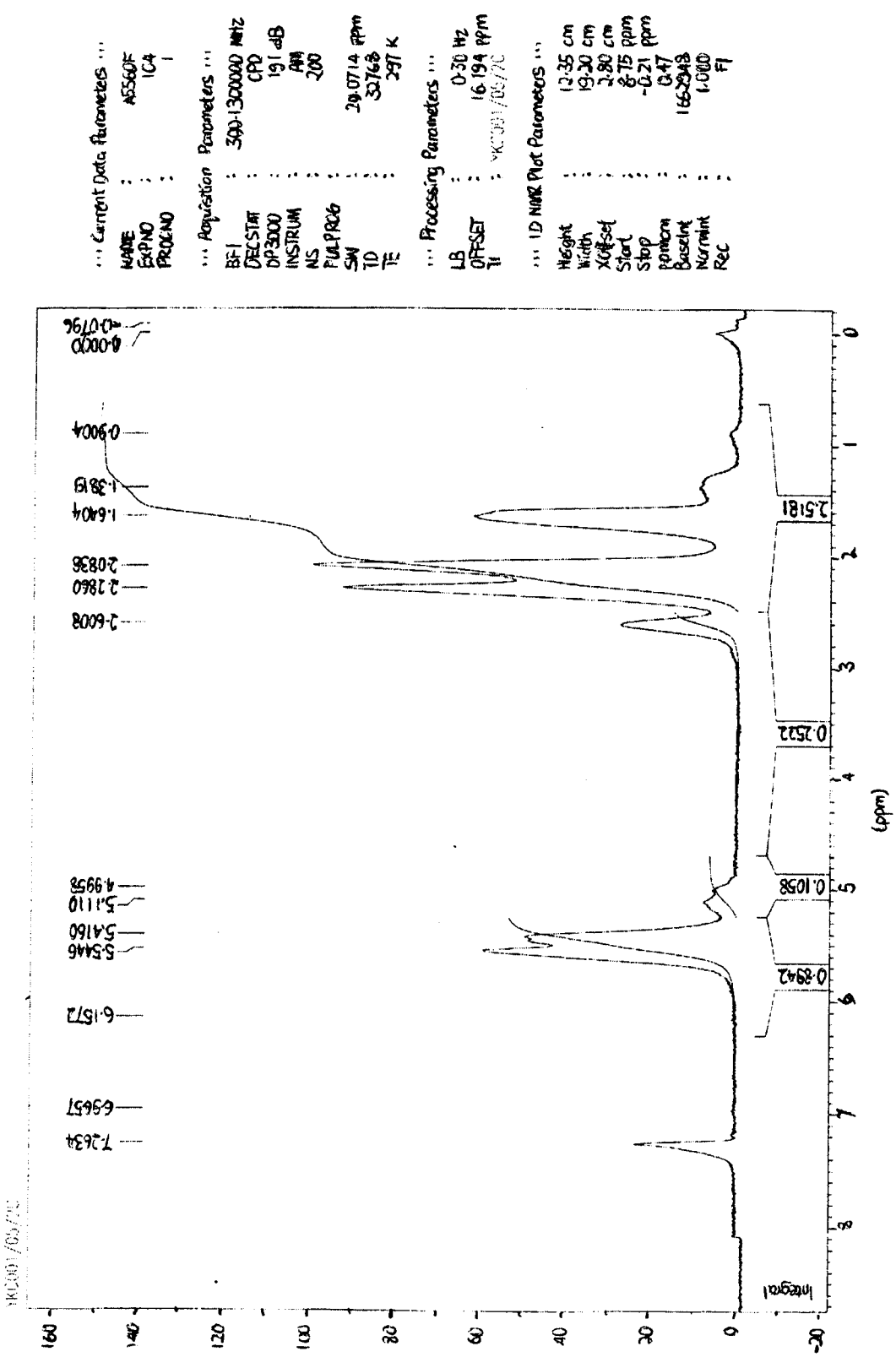

Appendix 2.3: NMR Spectrum of Methanol washed-NBR BreonN41C45

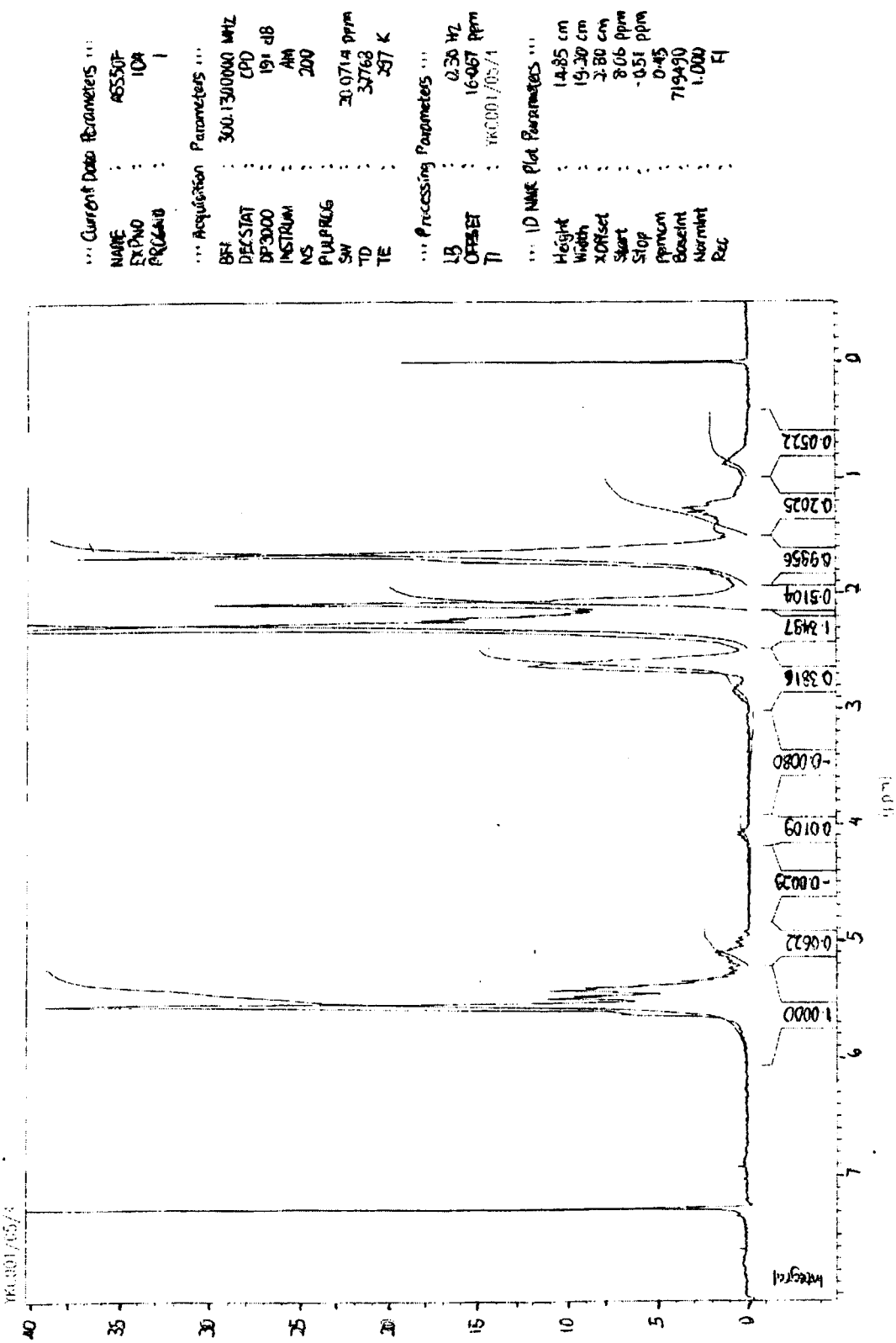

Appendix 2.4: NMR Spectrum of Methanol washed-NBR Krynac®50.75

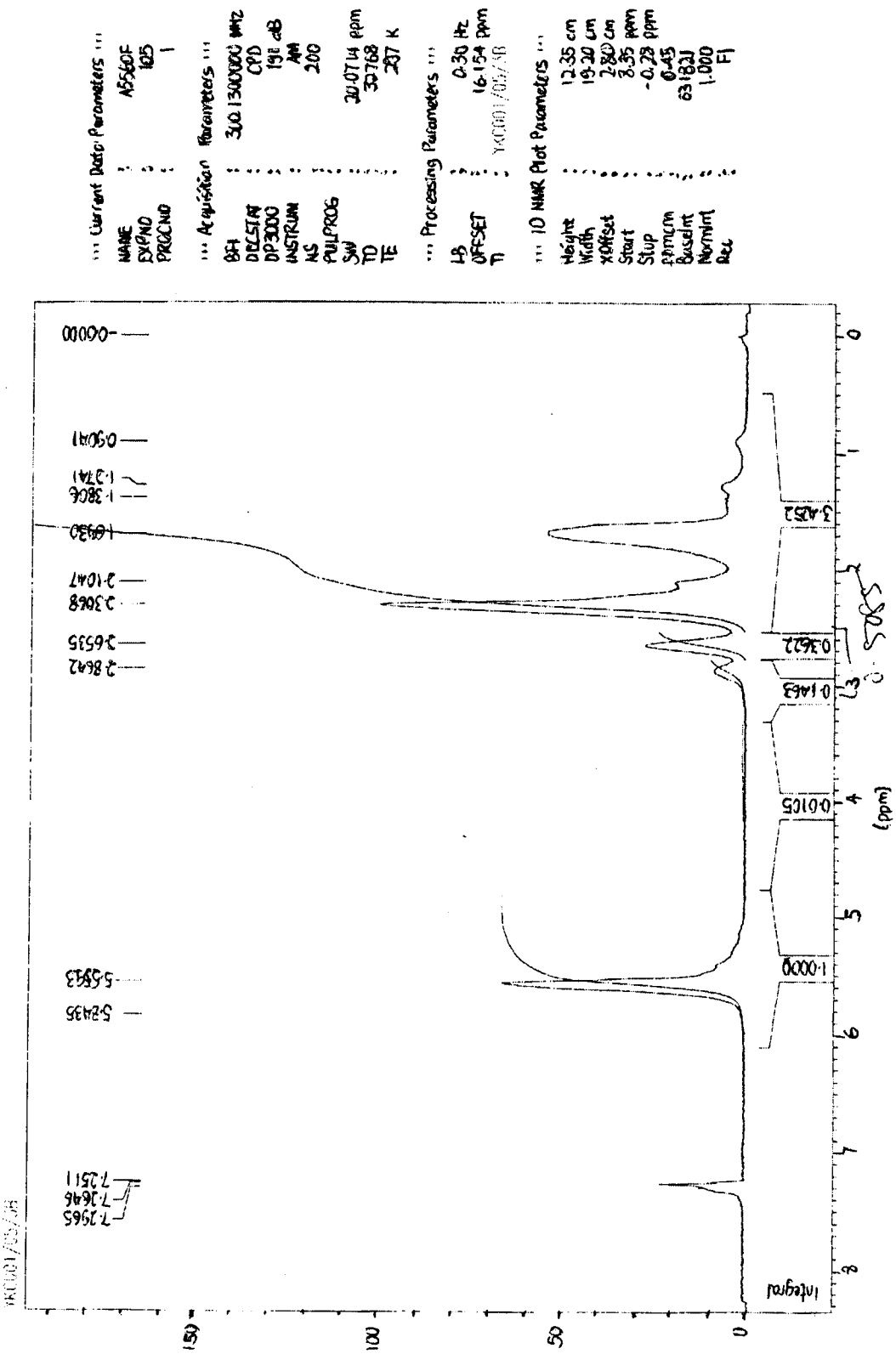

Appendix 3.1: NMR Spectrum of ENR-PAni.DBSA Blend (90 wt%:10 wt%)

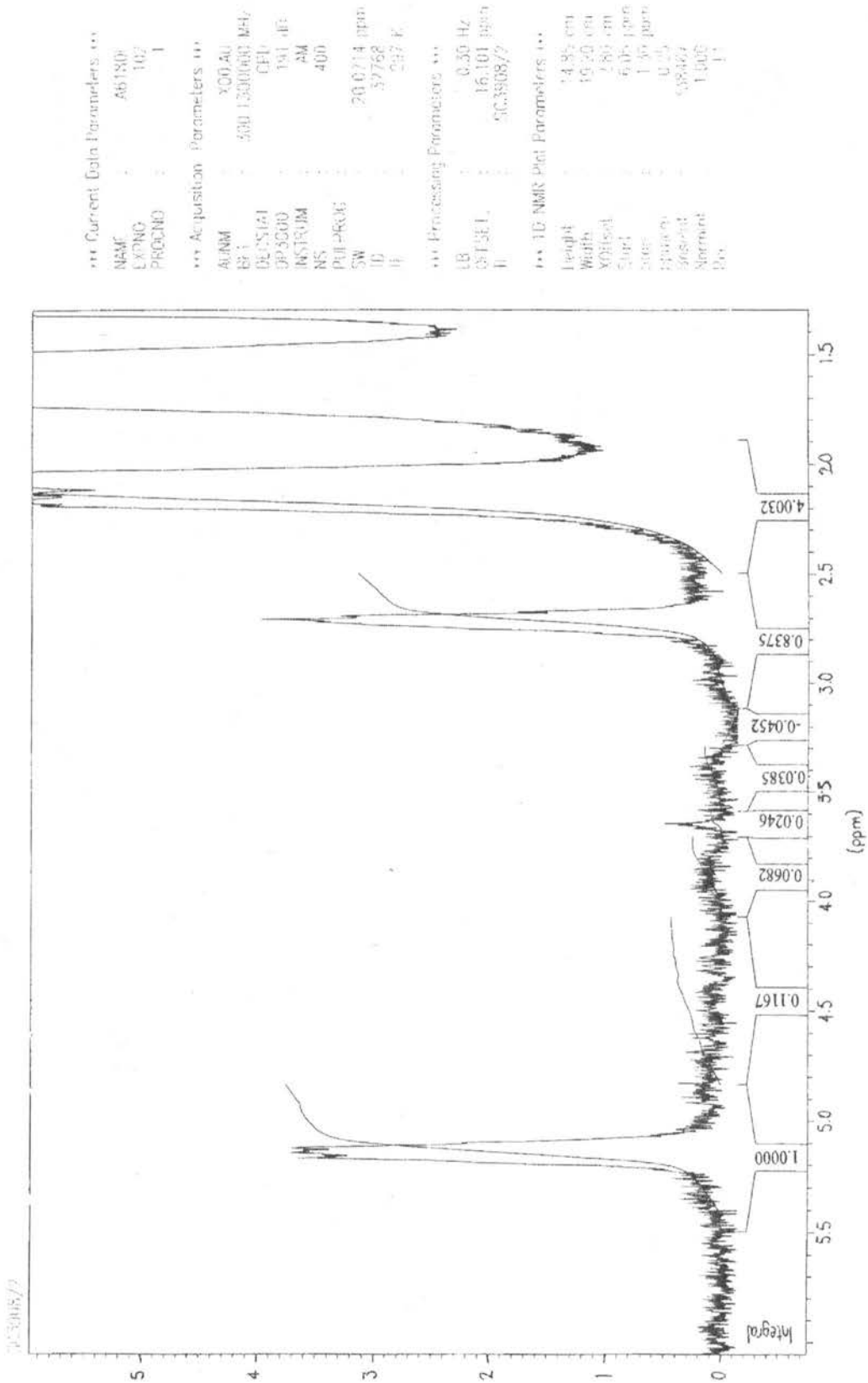

Appendix 3.2: NMR Spectrum of ENR-PAni.DBSA Blend (80 wt%:20 wt%)

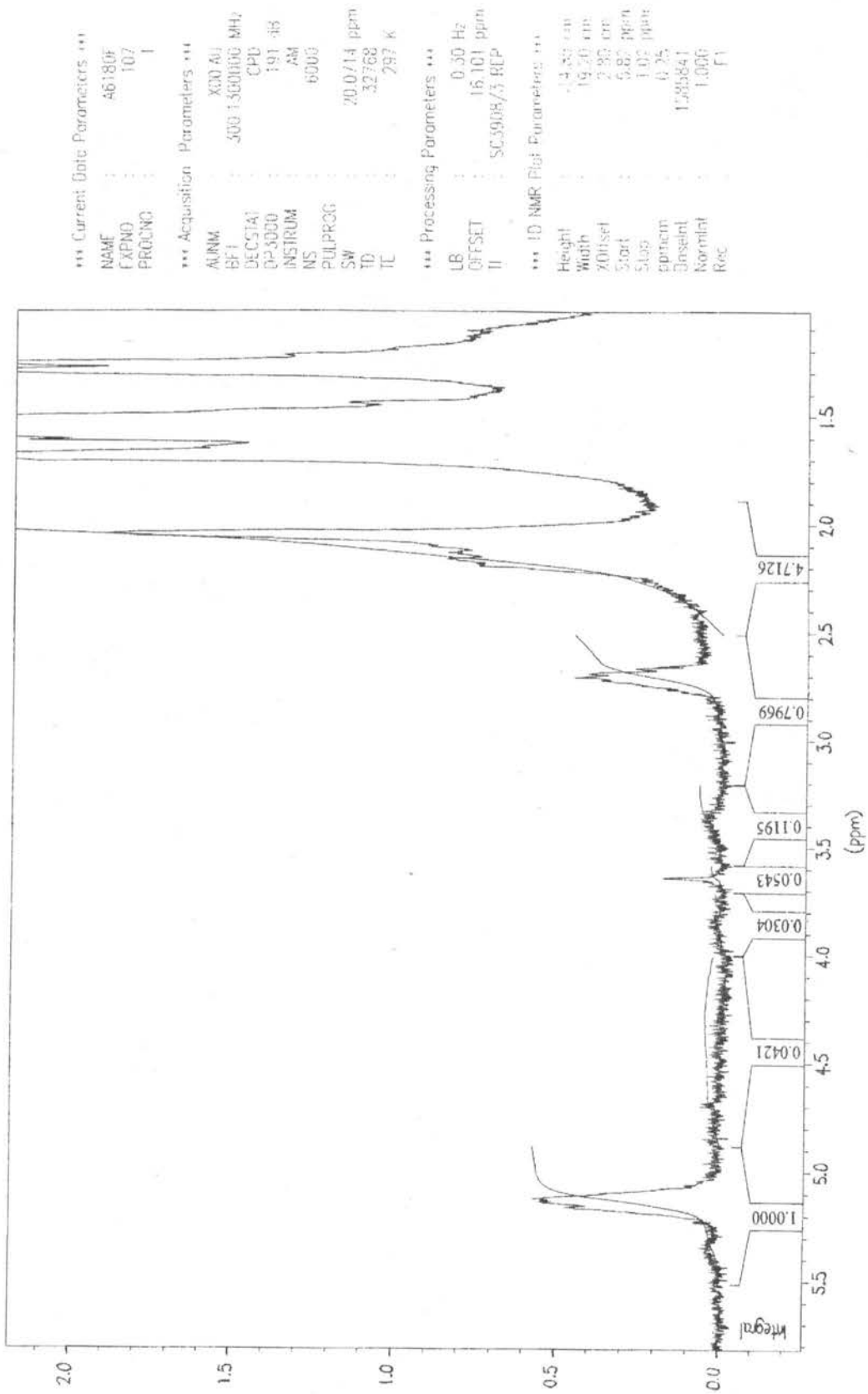

Appendix 3.3: NMR Spectrum of ENR-PAni.DBSA Blend (70 wt%:30 wt%)

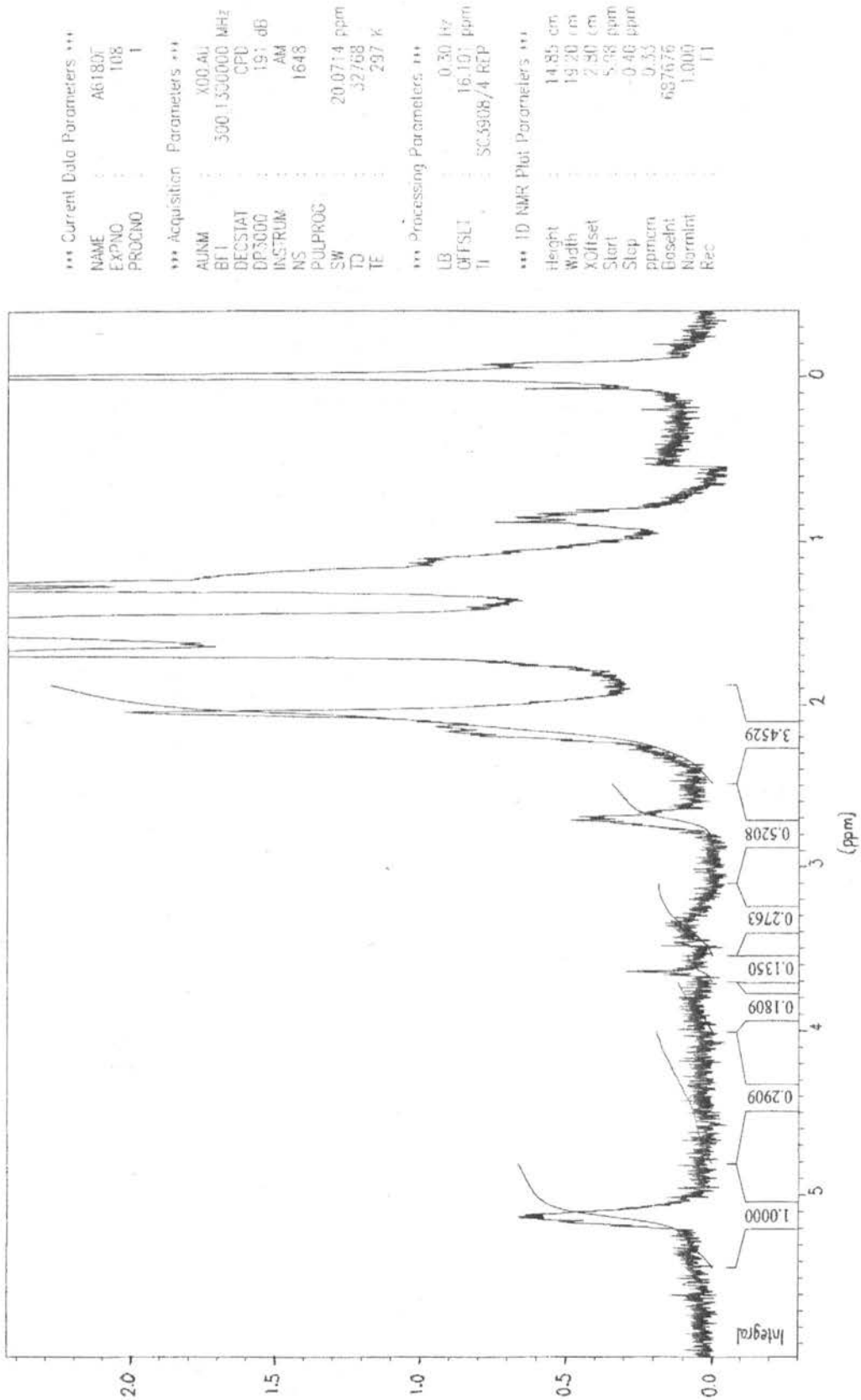

Appendix 3.4: NMR Spectrum of ENR-PAni.DBSA Blend (60 wt%:40 wt%)

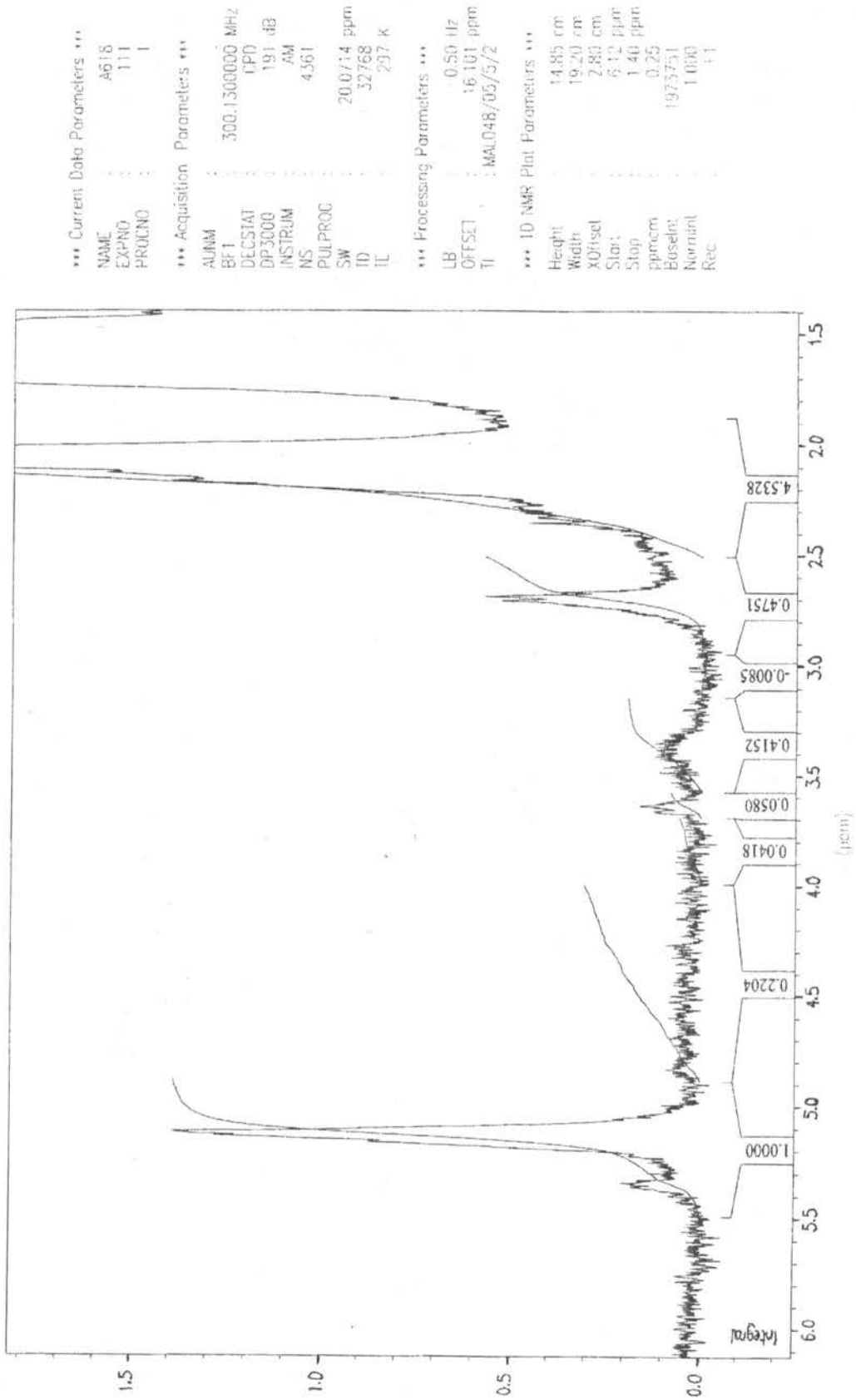

Appendix 3.5: NMR Spectrum of ENR-PAni.DBSA Blend (50 wt%:50 wt%)